Institute of Child Health

Department of Women and Children's Health and

Department of Clinical Infection Microbiology and Immunology

Regulatory Immune Cytokines in RSV infection

Thesis submitted in accordance with

the requirements of the University of Liverpool

for the degree of Doctor in Philosophy

by

Wael Hamoud Alturaiki

December 2014

List of contents

Abstract

Antibody production in the lungs is an essential defence mechanism against respiratory pathogens. However, little is known about the local activation of B cells in the lung.The production of BAFF and APRIL by airway epithelial cells could contribute to local recruitment, activation, class switch recombination and antibody production by B cells in the lung.

In vitro, BEAS-2B cells were used to characterize BAFF and APRIL production simulated either by RSV infection or addition of cytokines. RSV and IFN-β significantly induced expression of BAFF mRNA and protein but not APRIL. BAFF mRNA reached significantly high levels at 12h and declined at 48h after either RSV infection or IFN-β stimulation. Western blot analysis of resting epithelial cells showed that membrane BAFF was expressed by resting cells. On RSV infection or IFN-β stimulation, expression of membrane BAFF increased at 12 and 24hours and disappeared at 48h, which suggests soluble BAFF was cleaved from the membrane and released into the culture supernatant by 48h, where it was measured by ELISA. When BEAS-2B cells were infected with RSV after pre-incubation with anti-IFN β, expression of BAFF was blocked, which indicates that airway epithelial cells can produce BAFF in an interferon dependent manner. BEAS-2B cells did not express CXCL12, CXL13, CCL19 or CCL21, which indicates there are other potential sources that express these chemokines during RSV infection rather than the airway epithelium.

A murine model of RSV infection was used to examine expression of BAFF, APRIL and of the chemokines CXCL12, CXCL13, CCL19 and CCL21. Cytokine mRNA and RSV N gene expression were measured by Taqman PCR in lung tissue from control mice at day 0 and mice challenged with RSV (A2 strain) or control UV-treated RSV at days 1, 2, 4, 7, 8, 10, 14 and 21 days after RSV infection by ELISA. RSV N RNA was significantly detected at day 1, 2 and 4 after RSV infection compared to UV RSV control. BAFF mRNA expression was increased significantly after RSV infection on day 1 ,7 and 8 in comparison to UV treated RSV control at the same time points. Equally, BAFF protein was also elevated significantly after RSV infection at days 1, 2, 4, 7 and 8 in comparison to UV- RSV control at the same time points.

CXCL13 mRNA expression was increased significantly after RSV infection on day 1 and 7 in comparison to UV-RSV control at the same time points. Moreover, CXCL13 protein was increased significantly after RSV infection at day 1, 2 and 7 in comparison to UV RSV control at the same time points. CXCL12, CCL19 and CCL21 mRNA and protein levels were not increased significantly after RSV infection, which may indicate they are not active during RSV infection.
Examination of mouse lung sections showed strong positive staining of B cells (CD20) following RSV infection at day 1, 2, 4, 7 and 8 and FACS analysis B cells numbers were increased significantly at day 6 and 8 following RSV infection relative to UV-RSV control.

RSV infection results in up-regulated BAFF and CXCL13 expression, consistent with a role for CXCL13 in recruiting B cells and BAFF in promoting airway B cell survival or differentiation. Collectively, these results suggest that the airway epithelial could help recruit and support B cell growth and development and Ab production in the lung.

Declaration

No part of the work referred to in this thesis has been submitted in support of an application for another degree or qualification at this or any other university, or other institution of learning. All laboratory experiments described here have been carried out by the author, in the Division of Immunology, Duncan building, University of Liverpool or the Department of Women and Children's Health, Institute of Child Health, Alder Hey Children's Hospital, University of Liverpool.

Wael Hamoud Alturaiki

December 2014

Acknowledgements

I would like to offer my heartiest gratitude to my supervisor Dr Brian Flanagan for giving me the opportunity to work under his supervision and guiding me throughout the course of my study. His constant motivation and mentoring invaluably contributed to my graduate experience. I would also like to thank my second supervisor Dr Paul McNamara, who was always encouraging and to Dr Steve Christmas, who was inspirational during my study.

Very special thanks to the Saudi Cultural Bureau in the UK and Majmaah University for sponsoring me. Without their generous support I would not be able to complete my studies here.

I would like to express my gratitude to Mr Graham Jeffers, Rachael Corkhill, Dr Angela Midgley, Dr Debbie Howarth, Dr Mohamad Ahmad and Ms Caroline Broughton for providing me the technical support in the laboratory and helping to build confidence to perform new experimental techniques.

I am also grateful to Ms Helen Nelson and Moira Saphier for their general advice, support and encouragement. I must acknowledge all other academics, members of the staff and researchers in the Department of Clinical Infection, Microbiology and Immunology and institute of Child Health, University of Liverpool, for being so nice and supportive during my course of studies. In addition, I want to thank my childhood friend Mr A. Alromi for his support and communication during my study.

Also, I would like to thank Prof Jurgen Schwarze and Miss Amanda McFarlane who work at Queens Medical Research Institute at the University of Edinburgh for their help with the animal work and some analysis.

I would like to extent special thanks to my parents. All my successes would not have been possible without the prayers of my mother and support given by my father. I could not possibly thank him/her enough for everything in my life and for the sacrifice she and he had to make for my studying here. I am grateful to my brothers and sisters for supporting and encouraging me all my life. My unlimited thanks go to my beloved wife Anhar for her patience, support and inspiration through the good times and the bad. Finally, massive thanks to my son Eyad for enduring with a daddy who is always busy rather than playing with him.

List of Figures

Chapter 1

Page

Chapter 2

Chapter 3

Chapter 4

Chapter 5

Chapter 6

List of Tables

Chapter 1 **Page**

Chapter 2

Chapter 3

Chapter 4

Chapter 5

List of Abbreviations

AA	Amino acids
Ab	Antibody
Ag	Antigen
ANOVA	Analysis of variance
APCs	Antigen presenting cells
APRIL	A proliferation inducing ligand
ASCs	Antibody secreting cells
B cell	B-lymphocyte cells
BAFF-R	B cells activation Factor receptor
BALF	Broncho-alveolar lavage Fluid
BCA	Bicinchoninic acid
B-CLL	B-cells Chronic lymphocytic leukaemia
BCMA	B-cell Maturation Antigen
BCR	B-cell receptor
BDs	β-defensins
BLyS	B-lymphocyte stimulator
BM	Bone marrow
bp	Base pairs
BSA	Bovine Serum Albumin
CC	Chemokine (C-C motif)
CCL2	Chemokine (C-C motif) ligand 2
CCL3	Chemokine (C-C motif) ligand 3
CCL4	Chemokine (C-C motif) ligand 4
CCL5	Chemokine (C-C motif) ligand 5
CCL7	Chemokine (C-C motif) ligand 7
CCL11	Chemokine (C-C motif) ligand 11
CCL19	Chemokine (C-C motif) ligand 19
CCR21	Chemokine (C-C Motif) Receptor 21
CD	Cluster of differentiation
CD20	B cells marker
CD3	T cells marker
CD4 T	T subset helper
CD40L	CCD40 ligand
CD8	Cytotoxic T cells
cDNA	Complementary DNA
CF	Cystic fibrosis
CLTs	Cytotoxic T lymphocytes
COOH	Carboxyl-terminus
CSR	Class switch recombination
CX3C	chemokine (C-X3-C motif)
CXC	C-X-C motif chemokine
CXCL10	C-X-C motif chemokine 10
CXCL12	C-X-C motif chemokine 12
CXCL13	C-X-C motif chemokine 13
CXCL8	The chemokine (C-X-C motif) ligand 8
CXCR3	The CXC chemokine receptor 3
CXCR4	The CXC chemokine receptor 4

CXCR5	The CXC chemokine receptor 5
DAPI	4',6-diamidino-2-phenylindole
DCs	Dendritic cells
DMEM	Dulbecco's Modified Eagle Medium
DNA	Deoxyribonucleic Acid
dNTP	Deoxyribonucleotide triphosphate
dsRNA	Double Stranded RNA
DTT	Dithiothreitol
EBV	Epstein Barr virus
ECL	Enhanced chemiluminescence
EDTA	Ethylene diamine tetra acetate
ELISA	Enzyme-linked immunosorbent assay
F	RSV Fusion protein
FACS	Fluorescence activated cell scanner
FasL	Fas ligand
FBS	Foetal Bovine Serum
FCS	Foetal Calf Serum
FDC	Follicular dendritic cells
FI-RSV	Formalin-inactivated RSV formulation
FITC	Fluorescein isothiocyanate
G	Attachment protein
GC	Germinal centre
G-CSF	Granulocyte-colony stimulating factor
h	Hour(s)
H1N1	Influenza A virus subtype H1N1
H2SO4	Sulphuric acid
HCV	Hepatitis C virus
HEp-2	Human epithelial type 2
HEVs	High endothelial venules
HIV	human immunodeficiency virus
HRP	Horseradish peroxidase
HSPG	Heparansulfate proteoglycans
i.n.	Intra-nasal
ICAM-1	Intercellular adhesion molecule-1
IFN	Interferon
IFN-α	Interferon alpha
IFN-β	Interferon beta
IFN-γ	Interferon gamma
Ig	Immunoglobulin
IgA	Immunoglobulin A
IgE	Immunoglobulin E
IgG	Immunoglobulin G
IgM	Immunoglobulin M
IL-17A	Interleukin 17 A
IL-1β	Interleukin-1 beta
IL-2	Interleukin 2
IL-6	Interleukin 6
IRF	Interferon regulatory factor
Kb	Kilobase
kDa	Kilodalton

L	Large polymerase subunit
LF	Lactoferrin
LPS	Lipopolysaccharide
LRTI	Lower respiratory tract infection
M	Respiratory syncytial virus matrix protein
M2-1	Respiratory syncytial virus anti-termination factor
M2-2	Respiratory syncytial virus RNA regulatory protein
mAb	Monoclonal antibody
MCP	Monocyte chemotactic protein
MCP-1	Monocyte chemoattractant protein-1
medLN	mediastinal lymph node
mg	Milligram
MHC	Major Histocompatibility Complex
MIP	Macrophage inflammatory protein
MIP-1α	Macrophage inflammatory protein -1 alpha
MLR	Mixed lymphocyte reaction
MOI	Multiplicity of infection
mRNA	Messenger RNA
MTT assay	Methyl thiazol Tetrazolium Assay
MVECs	Multinucleated variant endothelial cells
MyD88	Myeloid differentiation factor 88
MZ	Marginal zone
N	Nucleocapsid protein
NaCl	Sodium chloride
NF-κB	Nuclear factor kappa B
Ng	Nanogram
NH3	Amino-terminus
NK	Natural killer cells
NO	Nitric oxide
NS1	Respiratory syncytial virus nonstructural protein 1
NS2	Respiratory syncytial virus nonstructural protein 2
NZB	New Zealand Black mice
OD	Optical density
P	P respiratory syncytial virus phosphoprotein
PAMPs	Pathogen associated molecular patterns
PBMC	Peripheral blood mononuclear cells
PBS	Phosphate buffered saline
PFU	Plaque-forming units
Pg	Picogram
Poly (I:C)	Polyinosinic:polycytidylic acid
PRRs	Pattern recognition receptors
RANTES	Regulation upon activation, normal T cell expressed, and secreted
rBAFF	Recombinant BAFF
RLT	RNA lysis buffer
RNA	Ribonucleic Acid
RPE	RNA wash buffer
rpm	Revolutions per minute

RSV	Respiratory syncytial virus
RSV F	RSV fusion protein
RSV G	RSV attachment protein
RSV SH	RSV small hydrophobic protein
RT	Room temperature
RT-PCR	Real time polymerase chain reaction
RWI	RNA wash buffer
SD	Standard Deviation
SDS	Sodium dodecyl sulfate
SP	Surfactant Proteins
T1	Transitional type-1
T2	Transitional type-2
TACI	Transmembrane Activator and Calcium modulator and Cyclophylin ligand Interactor
TALL-1	TNF- and ApoL-related leucocyte-expressed ligand-1
TALL-2	Related death ligand-2
TBST	Tris Buffered Saline with Tween
TGF-β	transforming growth factor beta
Th1	T cell helper 1
Th17	T cell helper 17
Th2	T cell helper 2
THANK	TNF homologue that activates apoptosis, nuclear factor-κB and c-jun N-terminal kinase
THD	TNF Homology Domain
TLR	Toll-like receptor
TMB	Tetra-Bethyl Benzidine
TNF	Tumour Necrosis factors
TNFR1	Tumor necrosis factor receptor-I
TNFSF13	TNF superfamily member 13
TNFSF13B	TNF superfamily member 13B
TRDL-1α	TNF-related death ligand-1α
Treg	T–regulatory cells
TRIF	TIR-domain-containing adapter-inducing interferon-β
Tween-20	Polyoxyethylenesorbitan monolaurate
TWE-PRIL	TWEAK and APRIL
URTI	Upper respiratory tract infection
UV-RSV	Ultraviolet irradiated respiratory syncytial virus
VLPs	Virus-like particles
WT	Wild type
XC	XC chemokine receptor-1
Δ4BAFF	Delta 4 BAFF transcript
ΔBAFF	Delta BAFF transcript
µg	Microgram
µl	Microliter
Ψ BAFF	Pseudo BAFF transcript

CHAPTER 1: INTRODUCTION

RSV is a common pathogen of the human respiratory tract. The work described in this thesis focuses on the response of the airway epithelium to RSV infection. Specifically, how the innate response of the epithelium to infection may influence induction of the adaptive immune response through production of B cell growth factors. Here the characteristics of RSV itself are first described, followed by a discussion of how this virus causes airway disease, particularly bronchiolitis, in infants. This is followed by an explanation of how the immune response is known to respond to RSV and of the role of two growth factors BAFF and APRIL in the immune system. Finally, the aims and objectives of this study, which include both an analysis of the human airway epithelial response to infection and experiments using a murine model of RSV infection to examine these responses, are presented.

1.1. Respiratory syncytial virus (RSV)

RSV was first described in 1956 in samples from the upper respiratory tract of a chimpanzee with an acute respiratory illness characterized by coughing, sneezing, and mucopurulent nasal discharge and named chimpanzee coryza agent (Blount, Morris & Savage 1956). Subsequently, in 1957, this virus was also isolated from an infant with acute lower respiratory tract disease (Chanock, Roizman & Myers 1957). Its name is derived from a characteristic cytopathic effect, the formation of multinucleated giant cells or syncytia observed in infected airway epithelial cell culture (Chanock, Roizman & Myers 1957; Prober & Sullender 1999). RSV is one of the paramyxoviridae, subfamily of pneumovirinae genus pneumovirus (Borchers *et al.* 2013; Collins & Graham 2008). RSV is divided into two serological groups, A and B, based on their antigenic and genetic characteristics (Anderson *et al.* 1985; Oliveira *et al.* 2008). It is the most common cause of acute respiratory tract infection in newborn infants and young children (Hall *et al.* 2009). RSV also causes upper and lower respiratory tract infection in elderly or immunocompromised people (Falsey *et al.* 2005; Falsey & Walsh 2005).

1.1.2. Epidemiology

In temperate regions RSV outbreaks occur in late autumn or at the beginning of winter and typically peak between mid-December and early February. In tropical regions RSV infection occurs during the rainy season and can peak twice in spring and autumn (Borchers *et al.* 2013). Duration of the RSV epidemic varies from one year to another (Figure 1.1), but on average the duration of the outbreak is 22 weeks (Bricks 2001). Humans are the only host for RSV and viral infection is highly contagious and can transfer from person to person either by contact directly with contaminated secretions, droplets or fomites or through self-inoculation of eyes and nose (Collins & Graham 2008). Self-inoculation with contaminated hands is considered to be source of infection as the virus can survive in contaminated hands for more than half hour and on the surface of contaminated objects, for several hours (Bricks 2001).

Several factors are thought to contribute to the pathogenesis of RSV infection. The age of infants at the start of the RSV infection is a high risk factor, infants < 3-6 months are more susceptible to RSV infection. Other risk factors include smoking by family members in the household, a previous stay in hospital, daycare attendance both of which might enhance the risk of exposure and developing an infection with RSV (van Drunen Littel-van den Hurk & Watkiss 2012). Viral load correlates with the risk of developing severe infection and has been associated with the severity of RSV disease (DeVincenzo *et al.* 2010). Other risk factors that may increase the risk of developing RSV infection relate to the host, such as the premature infant, chronic lung disease of prematurity, incomplete development or damage to the airway, immunodeficiency, immunosuppression or old age that could extend viral replication, male gender, low birth weight, multiple births and low titre of RSV-specific maternal antibodies (Groothuis, Hoopes & Jessie 2011; van Drunen Littel-van den Hurk & Watkiss 2012).

RSV is also a major cause of morbidity and mortality in elderly people and immunocompromised patients (Falsey *et al.* 2005). Worldwide, RSV infects 34 million people and causes 200,000 deaths yearly (Nair *et al.* 2011). Although RSV has a single serotype, primary infection results in moderate levels of antibody that do provide lasting protection, reinfection can occur throughout life again (Glezen *et al.*

1986; Trento *et al.* 2006). So far there is no safe and effective vaccine available against RSV (Jorquera, Oakley & Tripp 2013). However, during each epidemic season infants at high risk of developing bronchiolitis, such as premature infants and those with congenital heart disease can receive a prophylactic treatment Palivizumab (Synagis), which is a humanized monoclonal antibody that can neutralize RSV.

Treatment with this antibody reduces RSV incidents up to 55% (Cardenas, Auais & Piedimonte 2005). Globally, morbidity and mortality due to cases of RSV in infants, the immunocompromised, and elderly continue to increase. Thus, better understanding of the mechanism of RSV pathogenesis and methods of prevention are required (van Drunen Littel-van den Hurk & Watkiss 2012).

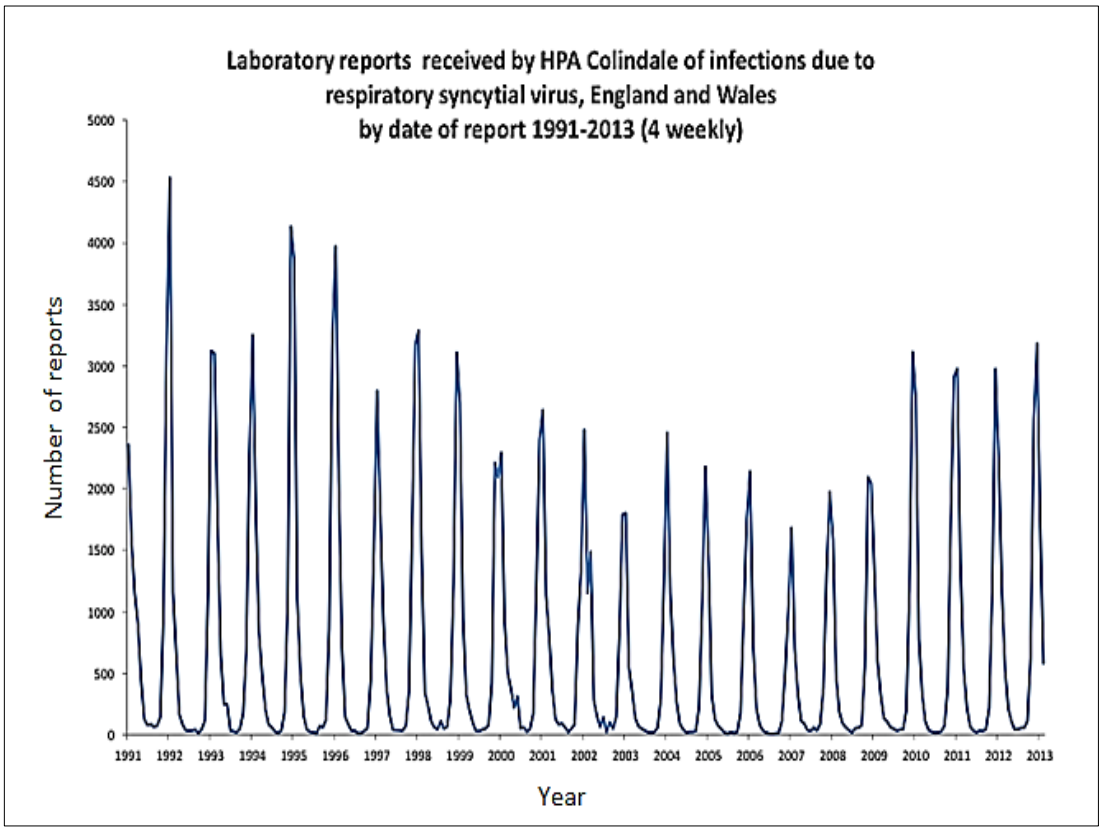

Figure 1.1. Laboratory reports of RSV infection from 1991 to 2013, 4 weekly in England and Wales

The seasonal and yearly variation of RSV bronchiolitis. Taken from (Agency HP. Laboratory reports received by HPA Colindale of infections due to respiratory syncytial virus, England and Wales 2013).

1.1.3. RSV structure

The genome of RSV is a non–segmented single stranded negative sense RNA (15.2 kb) (Domachowske & Rosenberg 1999) (Figure 1.2). The genome is located in the helical nucleocapsid and encodes for 11 proteins, including both structural and non-structural proteins. The virus is enveloped with a lipid bilayer derived from the host plasma membrane. RSV has three surface viral glycoproteins, attachment protein G, fusion protein F, and the small hydrophobic or SH protein. G glycoprotein facilitates RSV attachment to the infected cell (Teng, Whitehead & Collins 2001). RSV F protein mediates fusion between the virus and the host plasma membrane of the cell (Gonzalez-Reyes *et al.* 2001). Unlike the F and G proteins, the role of the SH protein in RSV replication and pathogenesis is not fully understood. However, it has been shown that SH protein can act to inhibit production of the inflammatory cytokine TNF-α and this may lead to enhanced viral replication *in vivo* (Li *et al.* 2011).

The Nucleocapsid is surrounded by the M protein situated in the inner layer of the lipid bilayer and which has been found to play a key role in the assembly of the viral particles (Lay *et al.* 2013). The RSV nucleocapsid has a helix shape and is surrounded by four nucleocapsid proteins, including (N), (P), (M2-1), and (L) (Lay *et al.* 2013). RSV (N) protein and (P) protein are essential for transcriptional activity (Hacking & Hull 2002). The (L) protein initiates viral transcription on infection after which replication proceeds (Fearns & Collins 1999; Oshansky *et al.* 2009). The M2-1 is a transcription elongation factor, whereas M2-2 regulates viral transcription (Hacking & Hull 2002). Non-structural proteins including NS1 and NS2 are involved in altering the host response to infection by interrupting Interferon signaling (anti-alpha and anti –beta activity) (Spann, Tran & Collins 2005).

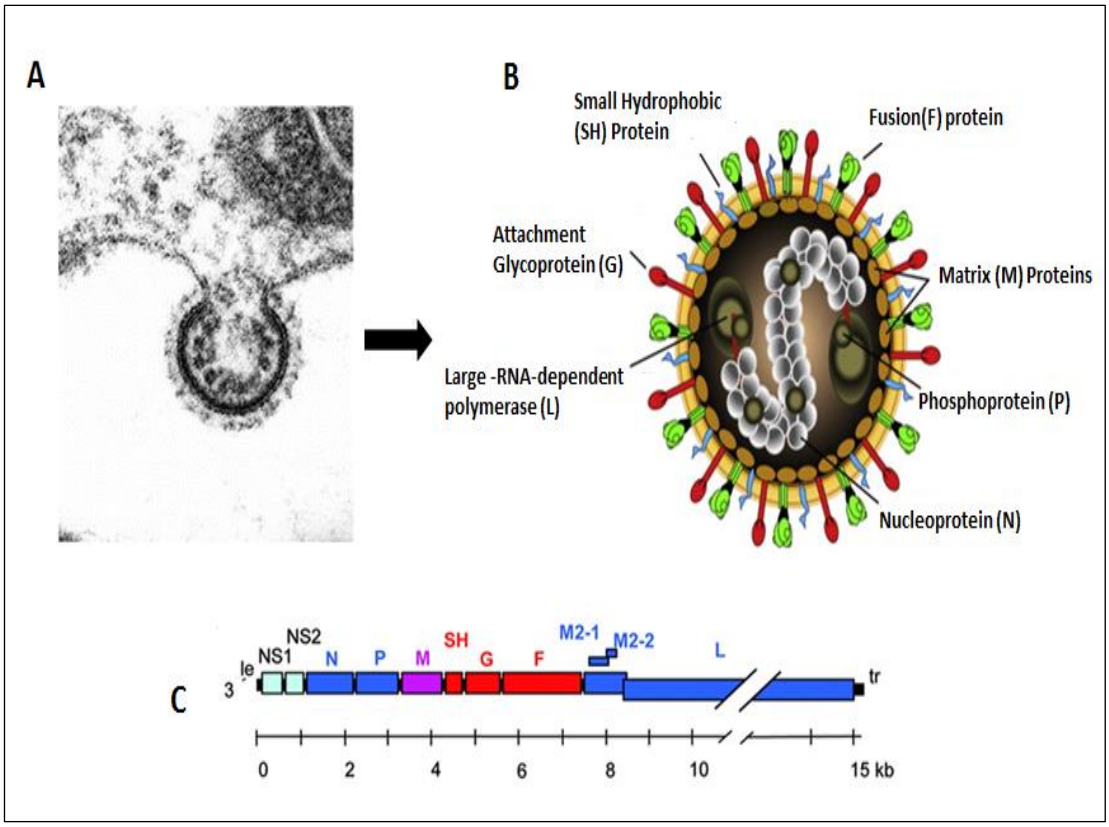

Figure 1.2. Structure and genome organization of RSV

In (A) - electron micrograph of RSV at the cell membrane of an infected cell. In (B)- a cartoon diagram shows the mains parts of RSV, the nucleocapsid is surrounded by M, matrix protein and an envelope containing host cell membrane and viral glycoproteins: G, attachment glycoprotein; F, fusion glycoprotein; and SH, small hydrophobic. In (C) the genome of RSV is non-segmented RNA, negative sense, (strain A2), 15.2 kb, which is associated with viral polymerase proteins and contained within a helical nucleocapsid composed of: N, nucleoprotein; P, phosphoprotein; L, large RNA-dependent-RNA-polymerase; M2-1; M2-2; NS1, non-structural protein-1; and NS2, non-structural protein-2. Taken and modified from (Electron micrograph of respiratory syncytial virus (RSV) virion at a cell membrane 2014; Collins & Graham 2008; Lay et al. 2013).

1.1.4. Pathogenesis of RSV

After inhalation RSV replicates in the nasopharynx with an incubation period of 4-5 days. This may be followed by spread to the lower respiratory tract over the next days that leads to the development of bronchiolitis, characterized by air trapping, increased airway resistance , mucus production and wheezing (Collins & Graham 2008; Hall 2001; McNamara & Smyth 2002). RSV Infection is primarily restricted to airway epithelial cells (Johnson *et al.* 2006; Welliver *et al.* 2007), lower airway type 1 pneumocytes and ciliated cells of the small bronchioles near the alveoli are reported to be the main sites of RSV infection. Additionally, non-ciliated epithelium cells, intraepithelial DCs and possibly alveolar macrophages can be infected with RSV (Johnson *et al.* 2006).

Infiltration of inflammatory immune cells, such as neutrophils and macrophages that can contribute to pulmonary inflammation, is observed during infection (Aherne *et al.* 1970; Lay *et al.* 2013; Welliver *et al.* 2007). Although RSV infection of respiratory epithelium causes airway damage, the relative contributions of virus-induced inflammation and the host immune response, each of which may contribute to RSV-induced disease severity, remains unclear (Varga & Braciale 2013).

Neutrophil cells are one of the major inflammatory cells present in the airways during RSV bronchiolitis (Everard *et al.* 1994; McNamara & Smyth 2002). In RSV infection of the infant, neutrophils were found to represent a median of 93% and 76 % in the upper and lower airway, respectively (Everard *et al.* 1994; McNamara & Smyth 2002). Moreover, in RSV infection neutrophil chemotaxis is thought to be dependent on the production of the chemokine IL-8 by airway epithelial cells and macrophages. These findings suggest that neutrophils may contribute to the pathological changes that occur during RSV bronchiolitis (McNamara & Smyth 2002; Wang & Forsyth 2000).

Alveolar macrophages are present in the lower respiratory tract; these cells have been reported to be a significant source of pro-inflammatory cytokines such as TNF-α, IL-6 and IL-8 after RSV infection (Becker, Quay & Soukup 1991; Oshansky *et al.* 2009). Depletion of macrophages in BALB/c mice prior to RSV infection significantly inhibited the early production of inflammatory cytokines and resulted in

increased virus titres in the lung (Oshansky *et al.* 2009; Pribul *et al.* 2008), which suggests that macrophages may play a more important role during the earliest time points after RSV infection. Moreover, depletion of alveolar macrophages in BALB/c and NZB mice prior to RSV infection resulted in airway occlusion, which suggests that alveolar macrophages contribute to the control of RSV disease and act to reduce disease severity (Oshansky *et al.* 2009; Reed *et al.* 2008).

Eosinophils may be involved in the pathogenesis of RSV. RSV infected respiratory epithelial cells show expression of eosinophil chemo-attractants including RANTES and MIP-1α (Becker & Soukup 1999; Harrison *et al.* 1999). Furthermore, children who were vaccinated with a formalin-inactivated RSV formulation (FI-RSV) and who died upon subsequent RSV infection (Kapikian *et al.* 1969; Kim *et al.* 1969) showed at post mortem analysis extensive infiltration of Eosinophils cells into the lung, possibly due to the activation of a Th2 response against RSV (Connors *et al.* 1994; Moghaddam *et al.* 2006; Waris *et al.* 1996). This suggests that these cells may contribute to RSV disease. However, their precise role in RSV disease remains unclear and needs to be fully characterized (Rosenberg, Dyer & Domachowske 2009).

NK cells are cells of the innate immune system which have a key role in clearance of virus-infected cells through their natural cytotoxicity. NK cells can recognize infected cells that express low levels of MHC class one (Kärre 2002). However, viruses can escape from recognition by the NK cells through increased expression of MHC class one (Kärre 2002). Furthermore, it has been found that RSV infection of BALB/c mice induced severe lung injury and promoted activation and accumulation of lung NK cells at the early stage (peaked at day 3) that produced significant amounts of IFN-γ secretion, which was responsible for acute lung injury (Li *et al.* 2012). Depletion of NK cells prior to RSV infection resulted in attenuated lung immune injury and reduced infiltration of inflammatory cells and reduced secretion of IFN-γ into the BALF, which suggests that NK cells are involved in the lung immune injury at the early stage of RSV infection through IFN-γ secretion (Li *et al.* 2012).

DCs are APCs that may be considered to link innate and adaptive immune responses. Found in both lymphoid and non-lymphoid tissues, their main function is to take up

antigens and present them to T cells in the context of MHC class I or class II molecules (Trombetta & Mellman 2005). Upon activation, DCs undergo maturation that results in increased phagocytic capacity, surface peptide-major histocompatibility complexes and up-regulated expression of co-stimulatory molecules such as CD80 and CD86 (Trombetta & Mellman 2005).

Efficient immunity against viruses is promoted by DCs, that prime antigen-specific helper and cytotoxic T cells. Therefore, impaired DC function and prevention of the induction of T cell immunity could be an advantage of RSV to induce disease (González *et al.* 2008).

To evaluate whether RSV infection can enhance the capacity of DCs to activate naïve T cells, RSV-infected murine DCs were used to stimulate naïve T cells *in vitro* (González *et al.* 2008). T cell activation was examined by measuring IL-2 secretion in response to increasing numbers of control or RSV-infected DCs. T cells stimulated with RSV-pulsed DCs resulted in a strong inhibition of IL-2 secretion as compared with T cells stimulated with unpulsed or UV-RSV-pulsed DCs, that secreted significant levels of IL-2. In addition, in the presence of RSV neutralizing antibodies, RSV failed to inhibit the capacity of DCs to stimulate T cells. RSV has impaired T cell activation by murine DCs directly through elimination of immunological synapse assembly (González *et al.* 2008). Taken together this showed that RSV is responsible for the observed inhibition of DC function and T cell activation and therefore RSV infection of DCs could contribute to RSV pathogenesis by reducing T cell-mediated virus clearance. Furthermore, direct contact of T cells with RSV F protein has been shown to inhibit T-cell activation (Schlender *et al.* 2002). Thus, it could be possible that RSV-infected DCs expressing F protein may also inhibit T-cell activation by the same mechanism.

1.1.5. The host immune response to RSV

1.1.5.1. Innate immune response

Innate immunity represents the first line of host defence against foreign organisms. It attracts effector molecules and cells to the site of the infection through the release of cytokines. It is characterized by rapid response and lacks immunological memory.

1.1.5.1.1. Airway epithelial cells

The human lung is exposed to a wide range of inhaled microbes and therefore the airway epithelium cells are at the direct interface of the human body with the inhaled environment and represent a primary site for entry of microorganisms. The epithelium forms a physicochemical barrier complemented by the mucociliary escalator mechanism of ciliated cells, mucus production by secretory goblet cells that act as the first line of defence against inhaled microbes (Bals & Hiemstra 2004; Mukherjee & Lukacs 2013). The mucus layer of the airway epithelium is covered with a wide range of peptides, proteins, and organic molecules, including IFNs, lactoferrin (LF), β-defensins (BDs), and nitric oxide (NO) that act as antimicrobial host defence molecules (Figure 1.3) and thus airway epithelium regulates both innate and adaptive immune responses, through production of antiviral substances and production of cytokines and chemokines which recruit and activate immune cells in the submucosa (Vareille *et al.* 2011). LF is member of the transferrin gene family and has been shown to act as antiviral by preventing RSV entry to host cells through interaction with RSV fusion protein (Sano *et al.* 2003). In addition, BDs such as hBD-2 and hBD-3 can inhibit viral replication by interfering with T cells, monocytes and immature DCs, either through inducing cytokine production by epithelial cells or directly binding to certain viruses (Schutte & McCray 2002; Vareille *et al.* 2011). NO has also an important role in the antiviral defence of the airway epithelium through inhibition of viral replication. For example, it has been shown that increased parainfluenza virus 3 replication in CF patients is due to lack of NOS-2 response (Zheng *et al.* 2003).

Notable factors known to be expressed by respiratory epithelial cells that have been shown to play key role in host immune defence and regulation of immune response

in the lung include surfactant proteins (SP), including SP-A and SP-D (LeVine & Whitsett 2001). These proteins can also act as opsonins during RSV infection (Welliver 2008), SP-A can bind with RSV G and F proteins and improves the antigen uptake of RSV by HEp-2 cells (Ghildyal *et al.* 1999; Hickling *et al.* 2000). In addition, it has been found that SP-D binds with RSV G protein and can inhibit RSV infection in vivo and *in vitro* (Hickling *et al.* 1999).

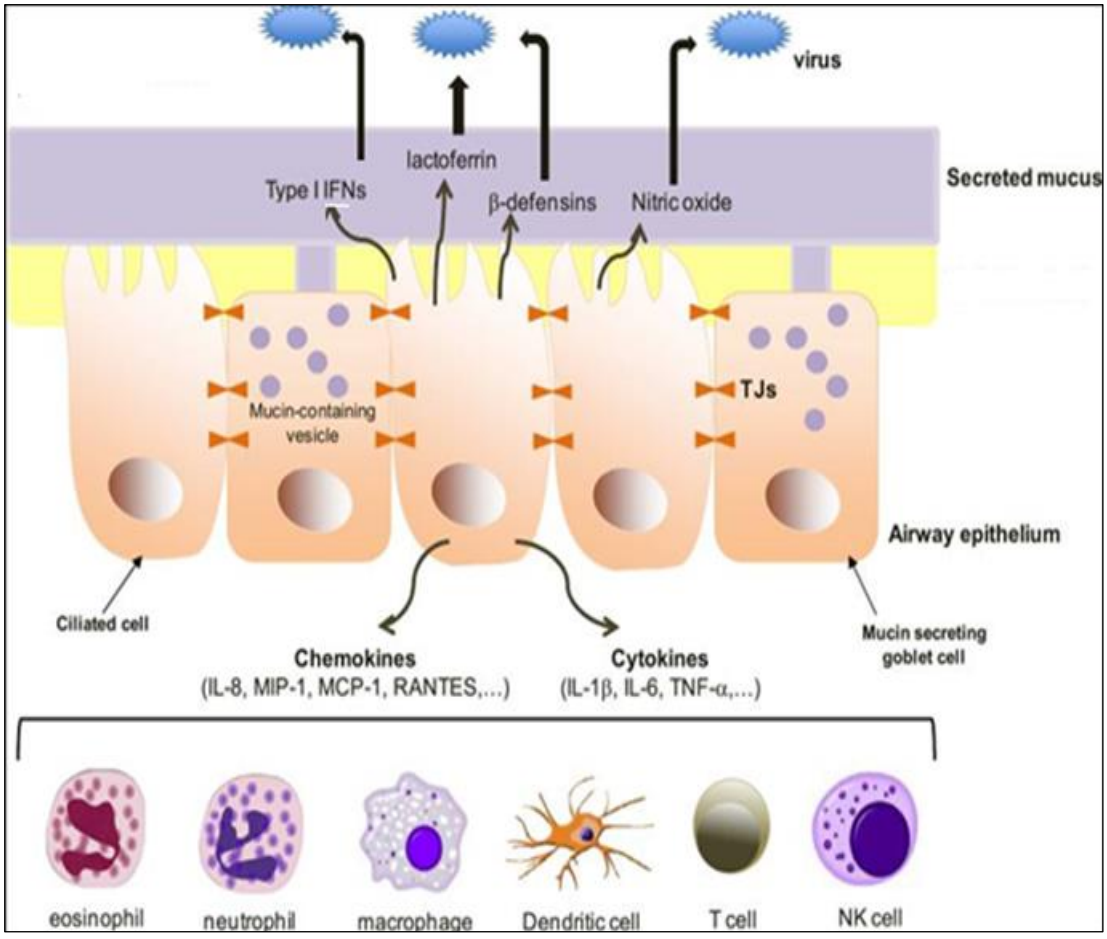

Figure 1.3. Anti-viral defences of the airway epithelium to respiratory viruses

The airway epithelium can regulate both innate and adaptive immune responses by production of antiviral substances such as IFNs, lactoferrin, β-defensins, and nitric oxide in the mucus layer, as well as production of cytokines and chemokines that recruit and activate immune cells response in the submucosa. In addition, mucociliary escalator mechanism of ciliated cells and tight junctions (TJs) provided mechanical, biological, and chemical protection. Taken from (Vareille et al. 2011).

1.1.5.1.2. Recognition of RSV by Toll-Like Receptors (TLRs)

TLRs are PRRs expressed by innate immune cells, which recognize PAMPs associated with groups of pathogens (Kumar, Kawai & Akira 2009). Airway epithelial cells can recognize RSV F protein by TLR4 (Figure 1.4) expressed on the cell surface (Kurt-Jones *et al.* 2000). The outcome of this interaction leads to NF-kB activation and promotes secretion of cytokines including IL-8, IL-10, IL-6 and IFN-β (Kurt-Jones *et al.* 2000; Tulic *et al.* 2007). RSV can also be recognized by intracellular TLR3 on respiratory epithelial cells (Rudd *et al.* 2006). TLR3 can recognize viral products during replication, such as dsRNA. It has been found that after RSV infection mice lacking TLR3 increase production of Th2 cytokines, as well as mucus in the lung in comparison to wild-type mice (Rudd *et al.* 2006). This suggests that TLR3 or signaling from TLR3 may play a key role in regulating the immune environment in the lung, as well as induce expression of IFN-β.

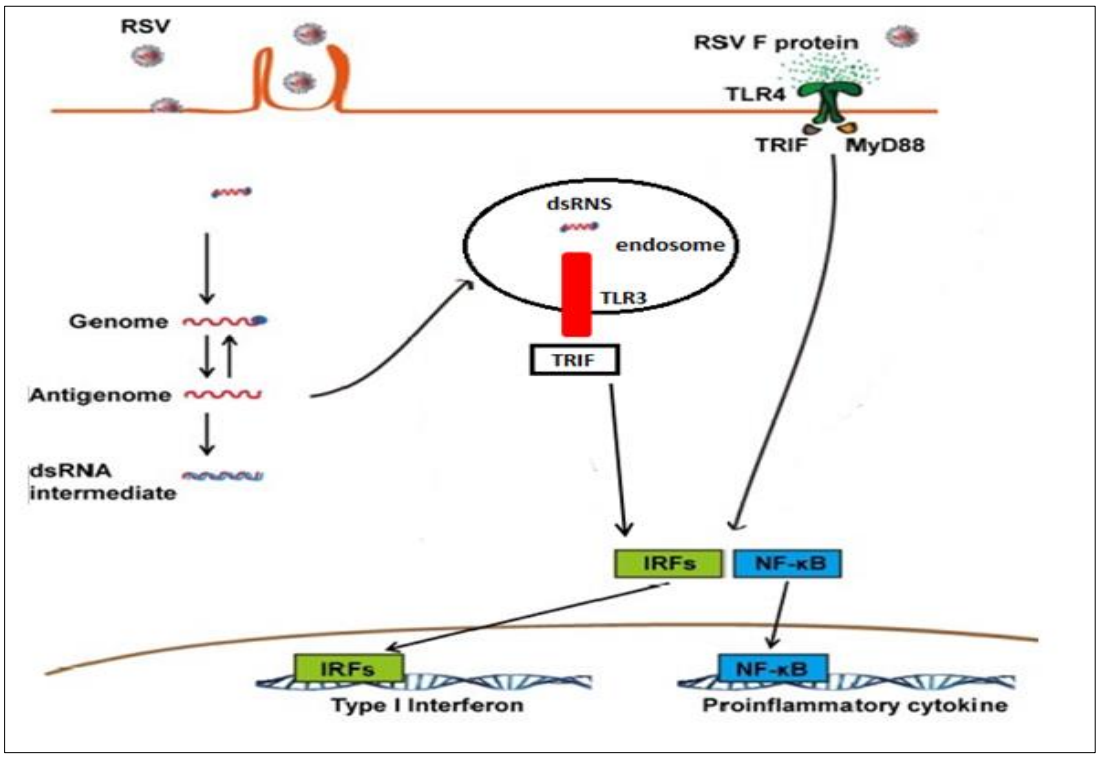

Figure 1.4. Recognition of RSV by TLRs

Activation of TLR4 with RSV F glycoprotein in a TRIF or MyD88-dependent signaling pathway prompts production of type I interferon or proinflammatory cytokines. Endosomal TLR3 can detect dsRNA that is generated during replication of RSV and then induces production of type I interferon or proinflammatory cytokines in a TRIF-dependent signaling pathway. Taken and modified from (Kim & Lee 2014).

1.1.5.1.3. Cytokines during RSV infection

Cytokines are typically secreted regulatory proteins (~5–20 kDa) produced by different cells in response to immune stimuli which enable the cells to communicate with each other. They can act in a paracrine or autocrine manner. Cytokines have important regulatory functions in cell behaviour, including proliferation, differentiation, function and migration. IFNs , TNF, and chemokines are examples of cytokines (Wood 2011).

1.1.5.1.3.1. Interferon type 1

There are two major types of IFN, type I and type II. Type I include IFN-α and IFN-β, type II include IFN-γ. Most cell types, including macrophages, fibroblasts, lymphocytes, endothelial cells and epithelial cells, produce IFN-α and IFN-β (Wood 2011), whereas IFN-γ is mainly produced by lymphocyte cells, including NK cells, T_H1 cells and CD8, as well as activated monocytes (Katze, He & Gale 2002; Yamaguchi *et al.* 2005). IFN-α and IFN-β have an ability to inhibit viral replication in infected cells. It has been shown that deficient IFN-β production may contribute to infection due to the failure of infected host cells to mediate early apoptosis and increased virus replication (Vareille *et al.* 2011; Wark *et al.* 2005). In addition, secretion of Type-1 interferon has several functions (Figure 1.5). First, it can limit the spread of viral infection to the neighbouring cells through induction of the cell-intrinsic antimicrobial states in the infected cells. Second, modulation of the innate immune responses either by promoting antigen presentation and natural killer cell functions or restraining pro-inflammatory pathways and cytokine production. Third, initiate the adaptive immune system though supporting the development of high-affinity antigen-specific T and B cell responses and immunological memory (Ivashkiv & Donlin 2014; Trinchieri 2010).

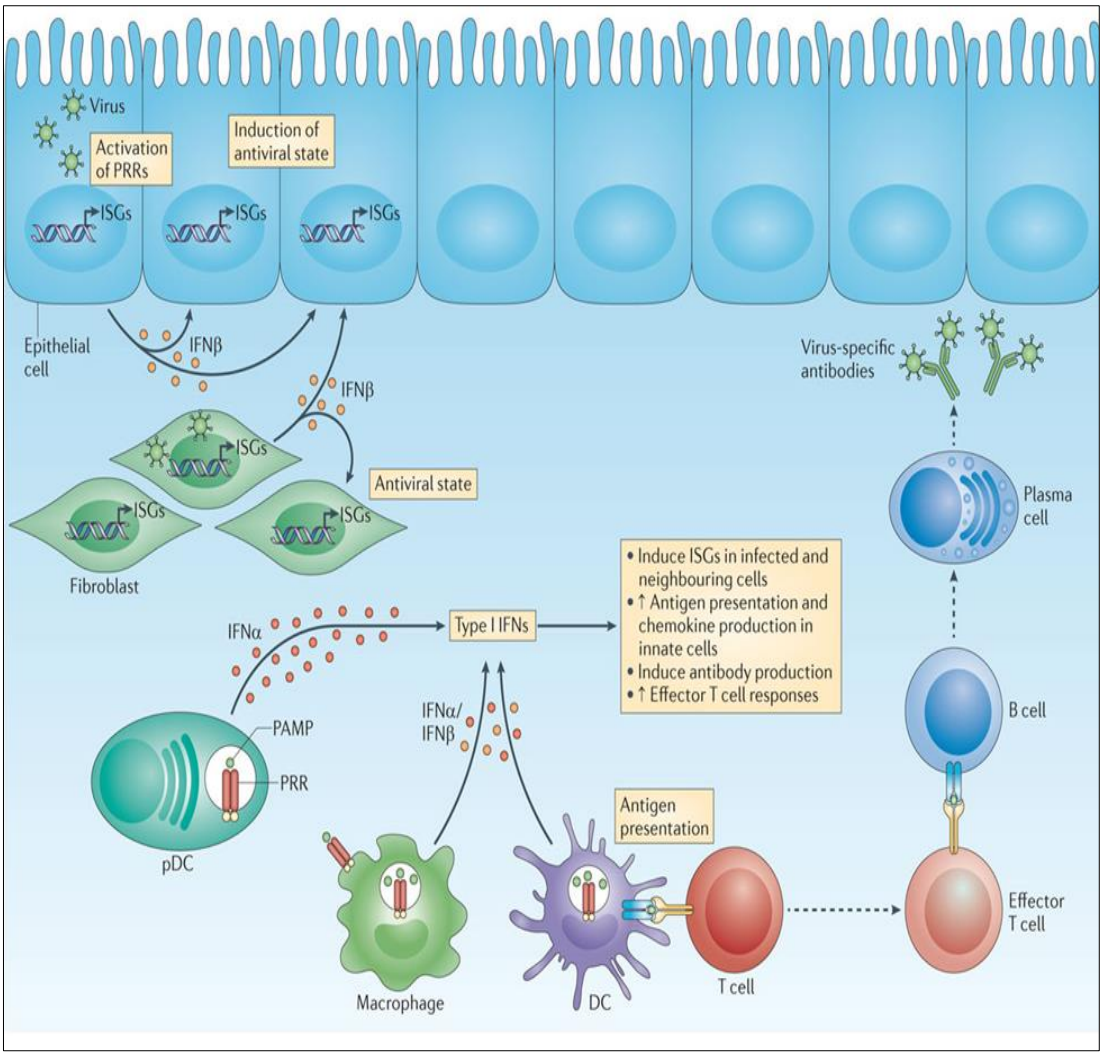

Figure 1.5. Role of Type I interferon in controlling innate and adaptive immunity

Early virus detection can be mediated though PRRs that identify PAMP expressed on various pathogens. Infected cells produce type I interferons. Innate immune cells, such as macrophages and DCs, produce type I IFNs. Cells such as plasmacytoid DCs (pDCs) produce large quantities of IFNα. Non-immune cells, such as fibroblasts and epithelial cells predominantly produce IFNβ. In infected and neighbouring cells, type I IFNs activates expression of IFN-stimulated genes (ISGs), which lead to initiate an intracellular antimicrobial status that limits the spread of infectious agents. Innate immune cells also respond to type I IFNs by enhancing antigen presentation and the production of cytokines and chemokines. Adaptive immunity is also influenced by type I IFNs: for example, type I IFNs can increase antibody production by B cells and amplify the effector function of T cells. Taken from (Ivashkiv & Donlin 2014).

1.1.5.1.3.2. Chemokines

Chemokines are a family of small chemotactic cytokines, their name is derived from their main function which is to induce chemotaxis of immune cells and normal tissue maintenance of the secondary lymphoid tissue. Structurally, chemokines are classified into four subfamilies, CXC, CC, CX3C and XC, according to the positions of conserved cysteine residues that form disulphide bonds. Based on their function, they can be further subdivided into two groups, inflammatory chemokines and homeostatic chemokines. Inflammatory chemokines are produced by immune cells and other cells such as epithelial cells during infection and can induce the migration of leukocytes to the site of infection. These chemokines examples include CXCL8, CCL2, CCL3, CCL4, CCL5, CCL11, and CXCL10 (Fernandez & Lolis 2002). Homeostatic chemokines (section 1.4) direct the trafficking of lymphocytes to lymphoid tissues under non inflammatory conditions and are also involved in immune surveillance and act for example to localize T or B cells with antigen in the lymphatic system (Fernandez & Lolis 2002). These chemokines examples include CXCL12, CXCL13, CCL19 and CCL21.

In vitro, it has been shown that RSV infection of human respiratory epithelial cells and alveolar macrophages induced chemokine expression including IL-8, CCL3, CCL4 and CCL5 (Fiedler, Wernke-Dollries & Stark 1995; Jaovisidha *et al.* 1999; Mellow *et al.* 2004; Thomas *et al.* 1998).

In vivo, RSV infection in BALB/c mice results in chemokine expression including CXCL2, CXCL10, CCL5, CCL11, CCL4, CCL3, CCL2, CCL1 and lymphotactin (Haeberle *et al.* 2001). Furthermore, it has been shown that during severe RSV infection in infants chemokines expressed include, CXCL10, CXCL8, CCL2 and CCL3 in the lower respiratory tract. Thus, these chemokines may contribute to the pathogenesis of RSV disease through directing migration of leucocytes, including neutrophils into the lungs (McNamara *et al.* 2005).

1.1.5.2. Adaptive immune response

Adaptive immunity represents the second line of host defence against pathogens. It is very highly specific, takes a longer time to develop and provides effective response against pathogens. In contrast to innate immunity, it develops immunological memory cells. Adaptive immunity consists of two types, including cell-mediated immunity and humoral immunity.

1.1.5.2.1. Cell-mediated immunity

The cellular immune response has an important role in controlling viral infection, in particular CD8 T cells which are essential in the host defence against viral infection. CD8 T cells can recognize viral peptides in the context of MHC class I molecules. After viral recognition, CD8 T cells mediate death of the infected cell by inducing apoptosis. Multiple pathways involved including released cytotoxic proteins including the granzymes and perforin (Janeway 2001). The granzymes can induce apoptosis, and perforin forms holes in the target-cell membrane through which the granzymes can enter the infected cells. Furthermore, apoptosis can also be induced by a membrane-bound molecule, FasL, which is expressed by CD8 T cells and binds to Fas expressed by target cells. Moreover, CD8 T cells also produce cytokines such as IFN-γ, TNF-α, and TNF-β, which further contribute to host defence. IFN-γ can act as an inhibitor of viral replication and can also induce increased expression of MHC class I, as well as macrophage activation. In addition, TNF-α or TNF-β can synergize with IFN-γ in macrophage activation, and in killing infected cells through their interaction with TNFR-I (Janeway 2001; Zajac & Harrington 2008).

CD4 T cells also known as helper T cells can recognize viral peptides in the context of MHC class II molecules expressed by the antigen presenting cells. Recognition leads to production of a wide range of cytokines. Based on cytokine production, CD4 T cells can be divided into distinct subsets, including Th1, Th2, and T-regs and recently Th17. Th1 cells are characterized by the production of IFN-γ. Th2 cells produce cytokines including IL-4, IL-5, and IL-13. Th17 cells are characterized by the production of cytokines including IL-17, IL-21 and IL-22 (Ouyang, Kolls & Zheng 2008).

T-regs cells are characterized by expression of the transcription factor Foxp3 and production of the suppressive cytokines including IL-10 and TGF-β (Rosendahl Huber *et al.* 2014; Zajac & Harrington 2008).

Children with defective T-cell responses show reduced RSV clearance, which suggests an important role for the adaptive cellular immune response against RSV (Fishaut, Tubergen & McIntosh 1980). Histological analysis of infants with fatal cases of RSV showed few CD4 and CD8 T cells in the lung (Welliver *et al.* 2007). However, another study has detected virus-specific CD8 T cells in the bronchial alveolar lavage and peripheral blood of infants after RSV infection (Heidema *et al.* 2007).

It has been reported that BALB/c mice which lack CD8 T cells have delayed viral clearance, demonstrating the importance of CD8 T cells in clearance during primary RSV infection (Graham *et al.* 1991b). Furthermore, RSV infection of BALB/c mice showed that 30–50 % of specific CD8 T-cell response in the lungs that recognize an immunodominant $M2_{82–90}$ epitope of RSV which mediates viral clearance (Chang & Braciale 2002).

To find out the effector mechanism involved in RSV clearance by specific CD8 cells, RSV-specific memory CD8 T cells deficient in IFN-γ were transferred to naive recipient mice and following subsequent RSV infection these cells failed to provide protection, which suggests the role of IFN-γ produced by RSV-specific CD8 T cells is essential for secondary responses to RSV (Ostler, Davidson & Ehl 2002). Another mechanism for target cell apoptosis is mediated by FasL that is expressed by activated T cells and binds to Fas on target cells. In addition, it has been reported that FasL-deficient mice show delay in the viral clearance in comparison to wild-type controls which is suggests the important of FasL in RSV clearance during acute infection (Rutigliano & Graham 2004). Taken together, these observations indicate the importance of CD8 T cells in the control and elimination of RSV during acute infection.

RSV disease is characterized by wheeze, increased mucus production and airway hyperreactivity, features shared with asthma, which is characterized by induction of Th2 immune responses that produce cytokines including IL-4, IL-5 and IL-13 and, therefore, Th2 responses have been implicated in contributing to the pathogenesis of

RSV during severe infection. Furthermore, the roles of Th2 cytokines including IL-4, IL-5 and IL-13 in the pathogenesis of RSV disease in humans remain controversial. Studies have demonstrated the association between the levels of Th2 cytokines and the severity of RSV disease in young children (Legg *et al.* 2003; Roman *et al.* 1997). On the other hand, other reports did not observe any correlation between the levels of Th2 cytokines and the severity of RSV disease (Brandenburg *et al.* 2000; Garofalo *et al.* 2001). Thus, it could be possible that both of Th1/Th2 cells contribute to the various manifestations of RSV disease. RSV infected BALB/c mice showed that IL-13 production is associated with increased mucus production (Tekkanat *et al.* 2001). RSV infection is most common in infants under 6 months of age when the human immune system is believed to be more Th2 dominant (Varga & Braciale 2013).

It has been shown that DCs isolated from human cord blood produce low levels of IL-12, which is important for differentiation of CD4 T cells into Th1 or IFN-γ secreting cells. Therefore, it could be possible that the Th2 response observed in children during RSV infection may be as a result of functional differences in neonatal-derived DCs that lead to insufficient signals provided by DCs to naïve T cells (Hunt *et al.* 1994). Flow cytometric analysis of DCs isolated from infant cord blood showed significant low levels of intercellular adhesion molecule-1 (ICAM-1; CD54) and (MHC) class I and class II than those on adult blood DCs. Therefore cord blood DCs may not deliver sufficient signals to activate T cells as a result of their low cell surface expression of MHC and cell adhesion molecules (Hunt *et al.* 1994). However, work in mice showed that age influences RSV infection. Mice infected with RSV at early age (e.g 5 days) develop disease and when they are re-challenged again at 8 weeks old they develop Th2 response cytokines ,whereas if the mice were infected for the first time at 4 weeks with RSV and re-infected again at 8 weeks they will develop Th1 response (Openshaw 2013). Moreover, it has been shown that Th17 cells also may contribute to RSV-induced disease severity (Kallal *et al.* 2010). RSV-infected infants has been shown to induce significant levels of IL-17A protein in tracheal aspirate samples and neutralization of IL-17A in mice leads to a significant decline in mucus production after severe RSV infection. Therefore, IL-17 may play an essential role in RSV-induced disease (Mukherjee *et al.* 2011). Mice deficient in T-regs prior to RSV infection have delayed viral clearance as well as

enhanced disease severity (Fulton, Meyerholz & Varga 2010). This suggests that T-reg cells have an important role in regulation of viral clearance during RSV infection and reduce the level of disease.

1.1.5.2.2. Humoral immunity

Antibodies play an important role in preventing re-infection with viruses either by directly neutralizing or enhancing the opsonization of extracellular viral particles. RSV specific neutralizing antibodies bind to (G) and (F) proteins (Varga & Braciale 2013). Mice infected with RSV initially produce virus specific serum IgM followed by IgG (IgG2a) and RSV-specific IgA is present in their BAL fluid (Borchers *et al.* 2013; Kamphuis *et al.* 2012; Singleton *et al.* 2003).

It has been shown that viral clearance is not altered in BALB/c mice deficient in B cells, but severe lung inflammation, increased viral replication and clinical illnesses are more noticeable compared to animals with a complete B cell compartment after re-infection with RSV (Graham *et al.* 1991a),which suggests that viral clearance is mediated by the T cells response during the primary infection.

In young children it has been shown that following acute RSV infection both levels of IgA and IgG antibodies titres rapidly declined. However, in adults lower nasal IgA titres were associated with elevated risk of RSV infection (Walsh & Falsey 2004). In addition, following one year of natural RSV infection 75% of adults showed decrease in serum neutralizing anti-RSV F and anti-RSV G IgG titres compared to uninfected subjects, who remained stable overtime (Falsey, Singh & Walsh 2006). Therefore, this decrease is more likely to allow re-infection with RSV, as increased susceptibility to RSV infection has been associated with lower serum neutralizing antibody titre in the elderly (Falsey & Walsh 1998). Furthermore, it has been shown that maternal antibodies can interact with the immaturity of the immune system and this can lead to reduced antibody responses induced by severe RSV infection (Kasel *et al.* 1987; Murphy *et al.* 1986). It has been reported that 50-70% of children less than six months of age had RSV specific neutralizing antibodies that can be detected following RSV infection (Brandenburg *et al.* 1997; Murphy *et al.* 1986). In addition, it has been found that antibodies produced against RSV have low avidity which may raise the susceptibility of infants and allow re-infection (Meurman, Waris & Hedman 1992).

Moreover, histological tissue of infants who died following severe RSV infection showed prominent presence of B cells and near absence of CD3+ T cells, which suggests that B cell activation in the lungs during severe infection could be T cell-independent (Borchers *et al.* 2013; Reed *et al.* 2009). However, equally it could be possible that those children died because they did not make a proper T cell response.

1.1.6. Modulation of host response by RSV

The RSV nonstructural proteins , including NS1 and NS2 have been reported to inhibit type I IFN production (Ramaswamy *et al.* 2006). Reduced IFN production may enhance viral replication, as well as reduce chemokine production that also could affect the inflammatory response. Thus, this can negatively affect the CD8 T-cells response since CD8 T cell require type 1 IFNs to become activated (Kotelkin *et al.* 2006; Varga & Braciale 2013). Therefore, suppression of the type I IFNs response by viral protein such as NS2 may reduce production of factors important for the activation of CD8 T cells, such as decreased expression of MHC class I molecules whose expression is up-regulated by type 1 IFNs as well as CXCR3 which is regulated by IFN-α /β in CD8, and it is critical for the efficient $CD8^+$ T-cell activation (Ogasawara *et al.* 2002). Furthermore, suppression of the IFN response by the NS2 protein may enhance death of RSV-specific CD8, as incubation of activated $CD8^+$ and CD4 with type I IFNs lead to a strong inhibition of their death (Kotelkin *et al.* 2006; Marrack, Kappler & Mitchell 1999; Varga & Braciale 2013).

The RSV G protein can be found in two forms: a membrane anchored and a soluble secreted form. The soluble form can bind neutralizing antibodies blocking neutralization and opsonization of the virus by antibody acting as an immune decoy for the whole virus. RSV G protein also has structural homology to the CX3C chemokine fractalkine, and once secreted can modify the local inflammatory environment in the lung by varying the infiltrating inflammatory cells that express fractalkine receptor CX3CR1, such as neutrophils and NK cells, which then may show impaired chemotaxis (Tripp *et al.* 2001). Consistent with this, it has been reported that mice infected with RSV G protein resulted in inhibited trafficking of NK cells and dendritic cells into lung compared with mice challenged with RSV lacking of G protein (Harcourt *et al.* 2006; Varga & Braciale 2013).

1.2. Tumor necrosis factor Family (TNF)

TNF cytokine family members control many aspects of the immune system including lymphocyte activation, differentiation and apoptosis (Treml *et al.* 2009). TNF family members are type II transmembrane proteins that can form membrane-bound or released as soluble molecules. The BLyS family of proteins including both BAFF and APRIL are comparatively new additions to the TNF cytokine superfamily (Treml *et al.* 2009). The B-cell activating factor or BAFF was identified independently by different groups. Schneider et al**.** discovered it by sequence homology with the members of the TNF superfamily (Schneider *et al.* 1999) and subsequently named this molecule BLyS due to its ability to induce B lymphocyte proliferation and immunoglobulin production (Moore *et al.* 1999). Other names for BAFF include THANK (Mukhopadhyay *et al.* 1999), TALL-1 (Shu, Hu & Johnson 1999), and TNFSF13B (Gross *et al.* 2000). APRIL, also known as TRDL-1α, TALL-2, or TNFSF13 (Kelly *et al.* 2000), was recognized as a close structural homologue of BAFF (Hahne *et al.* 1998).

1.2.1. BAFF

1.2.1.1. BAFF gene

The human BAFF gene located on chromosome 13q33.3 has 6 exons and 5 introns (39 kb). In mouse, the gene is on chromosome 8 A1.1 and comprises of 7 exons and 6 introns (31 kb) (Lahiri *et al.* 2012). The genomic organization is shown in (Figure 1.6), where the alternative splicing points in associated transcripts are shown, and the name of the resulting protein form indicated.

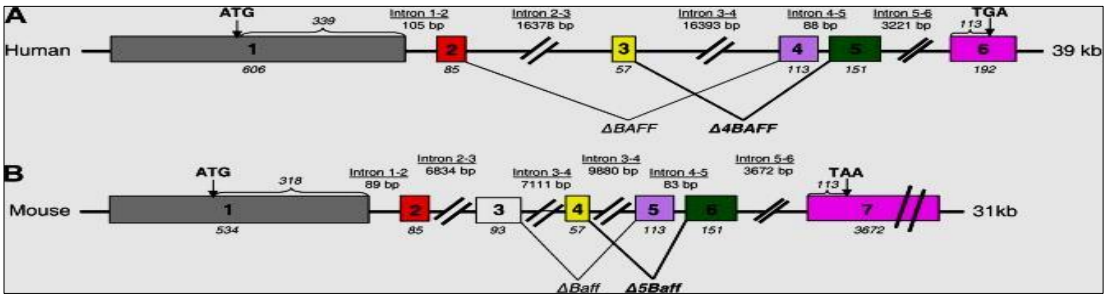

Figure 1.6. Genomic organization of BAFF in humans (A) and mice (B)

Exons are shown as boxes and introns (thin line) are illustrated. Points for alternative splicing are presented, and the name of the predicted protein is indicated. Taken from (Lahiri et al. 2012).

1.2.1.2. BAFF transcripts

There are various forms of BAFF transcript, including ΨBAFF, ΔBAFF and Δ4BAFF (Figure 1.7). Ψ BAFF is a long transcript only identified in humans, formed as a result of incomplete splicing of intron sequences. This isoform seems not able to make BAFF protein. ΔBAFF is identified in both humans and mice. This form lacks exon 3 in humans or exon 5 in mice. The corresponding protein of ΔBAFF has not been detected yet. ΔBAFF is associated with heteromultimers and the soluble form of these molecules binds poorly to receptors relative to homomultimers of BAFF. Therefore, ΔBAFF may suppress BAFF function by competitive co-association and limiting BAFF homotrimerization (Lahiri *et al.* 2012). ΔBAFF and BAFF have different effects on B cell survival and marginal zone B cell numbers. Analysis of ΔBAFF in transgenic mice showed a decreased number of B cells and T cells relative to BAFF (Gavin *et al.* 2005; Lahiri *et al.* 2012). Furthermore, the functional characteristics and patterns of expression for ΔBAFF and Δ4BAFF proteins have not yet been fully defined. The points for alternative splicing and the name of the resulting protein are indicated (Figure 1.6) (Lahiri *et al.* 2012).

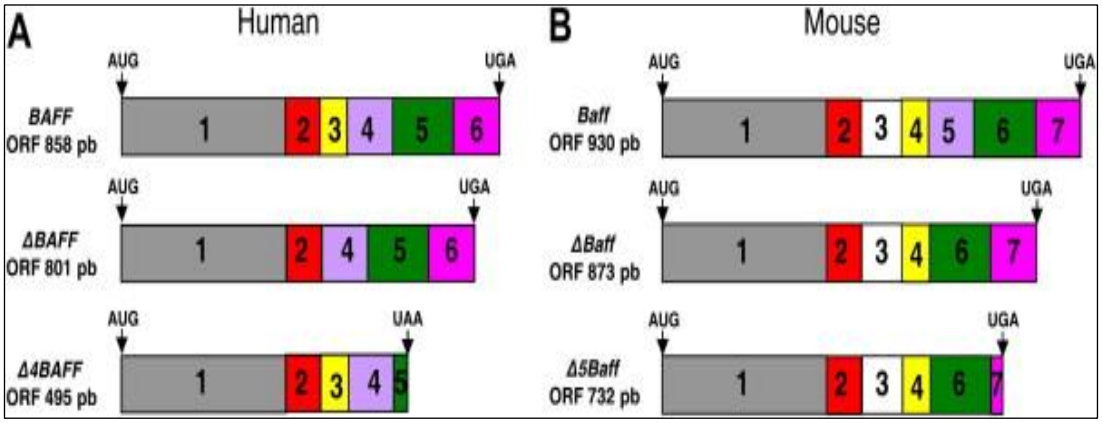

Figure 1.7. Diagram illustration of BAFF transcripts in humans (A) and mice (B)

The number of base pairs (bp) in the open reading frame (ORF) is shown next to each BAFF transcripts, including ΨBAFF, ΔBAFF and Δ4BAFF. *Taken from (Lahiri et al. 2012).*

1.2.1.3. BAFF protein

Human and mouse BAFF are type II transmembrane proteins (Figure 1.8). Type II membrane proteins have their C-terminus (COOH) exposed to the extracellular and have their N-terminus (NH3) on the cytoplasmic side of the cell, while type I membrane proteins have their N-terminus (NH3) exposed to the extracellular and the C-terminus (COOH) portion exposed on the cytoplasmic side. Human BAFF protein contains 285 amino acids (aa) (31.2 kDa), mouse BAFF 309 aa (34.2 kDa). The soluble form results from cleavage of the membrane bound form. In human BAFF the transmembrane domain is encoded by exon 1 (from L^{47} to Y^{67}) and in mouse from L^{48} to Y^{68}). Also, the cleavage site of membrane BAFF where soluble BAFF cleavage is encoded by exon 2 after (R^{133}) and for mouse after (R^{126}). Moreover, for humans the C-terminal domain is encoded by exons (3, 4, 5, and 6), while in mouse (4, 5, 6, and 7). This domain is known as the TNF homology domain (THD), which has an essential role in the organization of protein structure (Lahiri *et al.* 2012). Initially, BAFF is expressed on the cell membrane and can be cleaved by a furin-convertase enzyme and then released as soluble molecule. Soluble Human BAFF contains 152 aa (17.2 kDa) (from A^{134} to L^{285}) and 183 aa (from A^{127} to L^{309}) (20.6 kDa) in mice. The main difference between human and mouse BAFF is the exon 3, which in mice has no matched counterpart to that in humans (Lahiri *et al.* 2012).

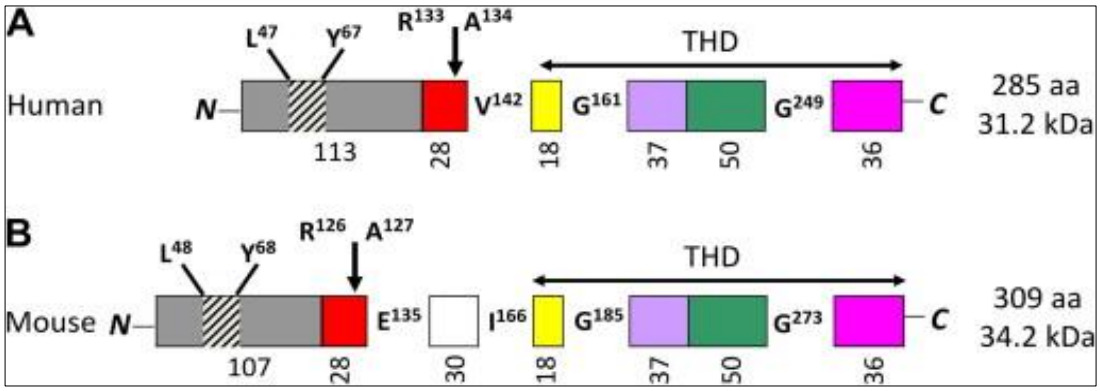

Figure 1.8. Diagram illustration of BAFF protein in humans (A) and mice (B)

Coloured boxes represents exons. The hatched areas represent the transmembrane region. The vertical arrow indicates the cleavage site for furin and the horizontal arrow illustrates the THD. The number of (aa) and expected molecular weight in kilo Daltons (kDa) for each BAFF protein are also described. Taken from (Lahiri et al. 2012).

The biological form of BAFF is a trimers (Zhukovsky *et al.* 2004). This structure consists of layered aromatic residues from three monomers (Figure 1.9). The FLAP region of BAFF is termed due to its shape (Liu *et al.* 2002). It allows trimer–trimer interaction leading to a virus-like assembly of soluble trimmers as an oligomer consisting of 60 monomers or 20-trimers connected to each other by hydrogen and hydrophobic bonds. Indeed, it has been shown that the pH of the environment plays an important role in forming and deforming of different forms of BAFF, including monomers, trimers and oligomers. At pH = 6.0, BAFF is present in a trimeric form. At pH = 6.5, the ratio oligomers/trimers ratio is 1:2 and 1:1 at pH = 7.0. At pH = 7.4, the oligomeric form is predominant (Lahiri *et al.* 2012). Furthermore, BAFF-60 mer can bind to its receptors (Liu *et al.* 2002). While this form has been described only in mice, it remains unclear if it can be or cannot be detected in humans (Vincent *et al.* 2013). Therefore, it could be possible that interaction of BAFF 60-mer with its receptors may act to increase BAFF signalling at a local site and concentrate BAFF on the cell surface more than the BAFF 3 mer does.

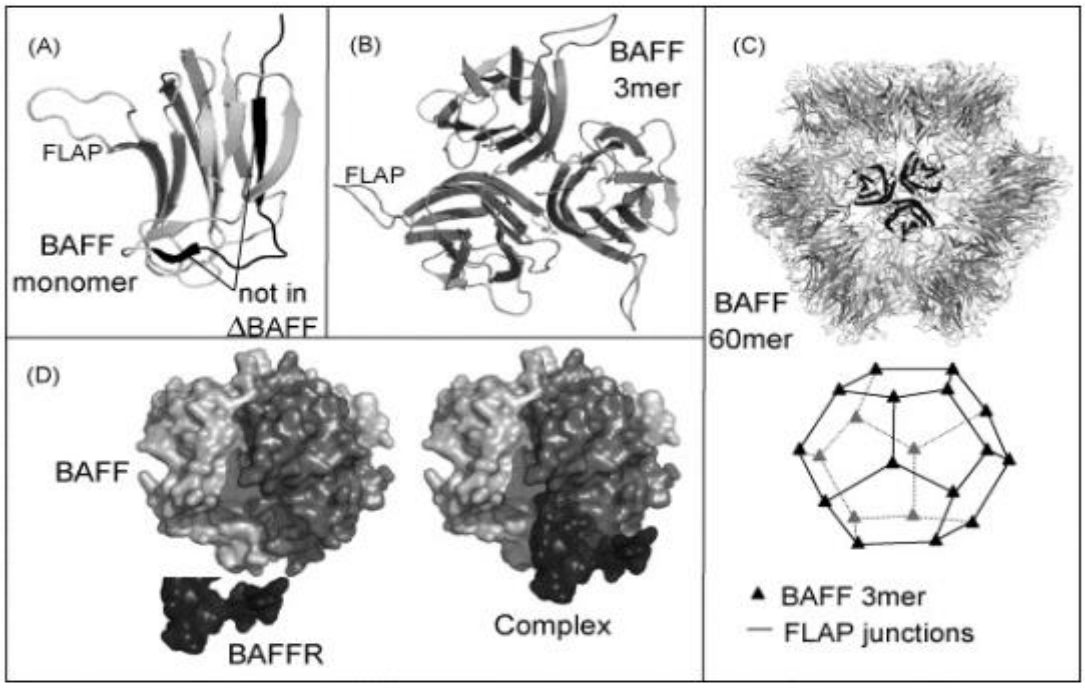

Figure 1.9. Structure of BAFF

BAFF monomer (A). BAFF trimer and FLAP region implicated in 60-mer formation (B). BAFF 60-mer (C). In (D) BAFF trimer and BAFF-R monomer in surface representation, before and after binding. One BAFF trimer can bind three receptors, each contacting a single monomer within the BAFF trimer. Taken from (Bossen & Schneider 2006).

1.2.1.4. Expression of BAFF

BAFF is mainly expressed by PBMCs, low levels of BAFF in tissues including spleen and lymph nodes have been detected. The major immune cells that expressed BAFF are monocytes, macrophages, dendritic cells, neutrophils and activated T cells (Mackay & Ambrose 2003). Moreover, expression of BAFF by B-CLL cells has been demonstrated (Daridon *et al.* 2007; Kern *et al.* 2004). Other cells such as stromal cells from the BM, FDC, synoviocytes, astrocytes, and epithelial cells of the salivary glands have been shown to express BAFF. BAFF expression is regulated by cytokines. Stimulation of monocytes with IFN-α, IFN-γ, IL-10 or CD40L has been shown to increase the expression of membrane BAFF. It has been shown that stimulation of neutrophils with G-CSF and IFN-γ leads to increased secretion of BAFF (Scapini *et al.* 2003). However, neutrophils do not express BAFF on their surfaces. This secretion of BAFF has been blocked by targeting the furin like convertase responsible for cleavage of the membrane form by a specific inhibitor. This suggests that when produced by neutrophils BAFF is processed intracellularly and subsequently secreted by these cells and not cleaved from the membrane. Therefore, the mechanism of BAFF cleavage via the furin protease can occur either intracellularly, at least in neutrophils, or at the cell surface (Lahiri *et al.* 2012).

1.2.2. APRIL

1.2.2.1. APRIL gene

The human APRIL gene is located on chromosome17 (17p13). Seven transcript variants of APRIL have been identified, including APRIL-α [NM_003808.3] which is composed of 6 exons, APRIL-β [NM_172087.2] that is characterized by the deletion of exon 3 and the resulting form of APRIL is quite similar to ΔBAFF , APRIL-γ [NM_172088.2] has seven exons, APRIL-δ [NM_001198622] is characterized by loss of exon 2 and two nucleotides, APRIL-ε [EF_211088.1] has only exon1, APRIL- η [NM_001198624.1] is missing the initial exon 2 as well as the full exon 1 which is replaced by 2 exons of 84 and 239 bp and APRIL-ζ [NM_001198623.1], where the initial exon 2 is missing and the resulting exon 2 contains only 42 bp, as indicated in (Figure 1.10) (Lahiri *et al.* 2012). The molecular significance of these multiple alternate spliced forms has yet to be defined. The major form studied at the protein level is formed from the full length transcript derived from all six exons and shown first in Figure 1.10

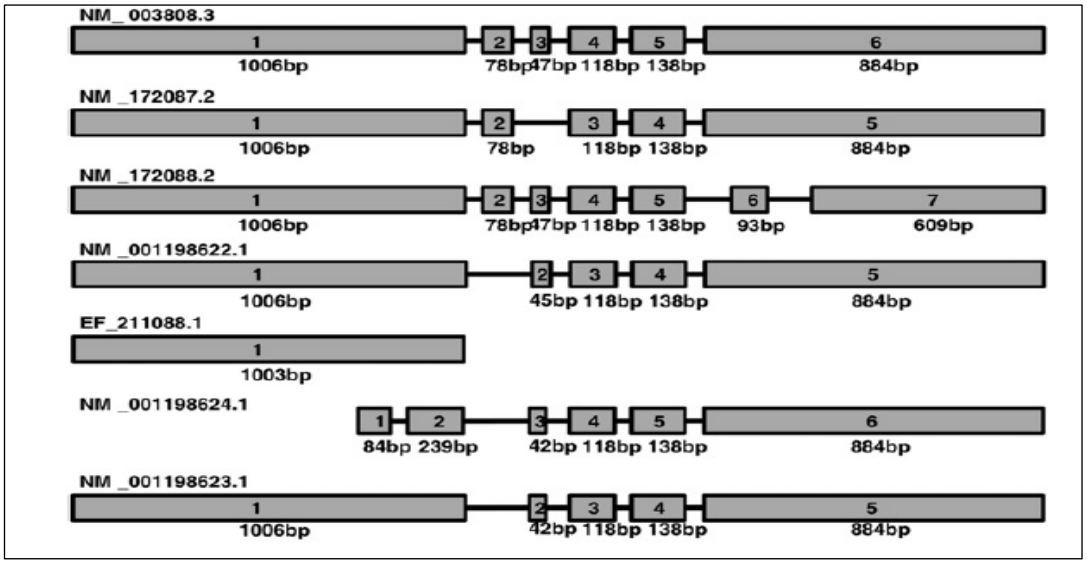

Figure 1.10. Genomic organisation of APRIL transcripts

Exons are represented by grey boxes. The thin line corresponds to introns. Taken from (Lahiri et al. 2012).

1.2.2.2. APRIL protein

At the protein level both human and murine APRIL molecules (Figure 1.11) share about 85% similarity (Hymowitz *et al.* 2005). APRIL is synthesized as type II transmembrane protein (molecular weight 27 kDa). APRIL is expressed by several cells such as dendritic cells, monocytes, neutrophils, macrophages, and activated T cells (Huard *et al.* 2008; Mackay & Ambrose 2003; Stein *et al.* 2002). In addition, non-immune cells such as epithelial cells can express it (Kato *et al.* 2006). Moreover, APRIL is expressed by tumour cells such as CLL (Haiat *et al.* 2006). In contrast to BAFF, APRIL does not have a cell surface membrane bound form and is processed and cleaved in the Golgi apparatus by a furin-convertase enzyme before reaching the cell surface (Daridon, Youinou & Pers 2008) and results in secreted or soluble APRIL (molecular weight 14 kDa) (Dillon *et al.* 2006; Lopez-Fraga *et al.* 2001). Unlike BAFF, APRIL does not from 60-mer complexes (Bossen & Schneider 2006), but can combine with BAFF and to form heterotrimers, which are either formed at the cell surface or inside cells (Golgi apparatus), and increased expression of these heterotrimers complexes has been suggested to occur in autoimmune diseases, although any pathogenic role has yet to be defined (Roschke *et al.* 2002).

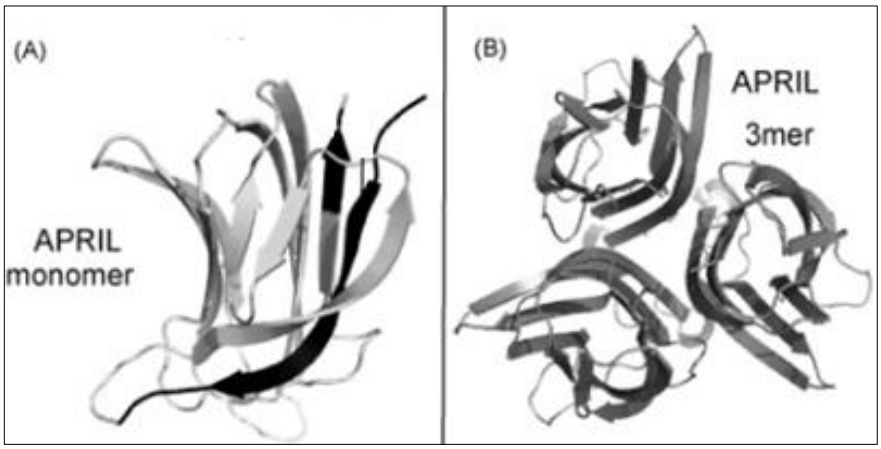

Figure 1.11. Structure of APRIL

APRIL monomer (A). APRIL trimer (B). An APRIL trimer can bind three receptors, each contacting a single monomer within the APRIL trimer. Taken from (Bossen & Schneider 2006).

1.2.3. BAFF and APRIL Receptors

The interaction of BAFF/APRIL with their receptors is both specific and redundant (Figure 1.12). BAFF and APRIL both bind with each of two receptors expressed by B cells, transmembrane activator and calcium modulator and cyclophylin ligand interactor (TACI) and B-cell maturation antigen (BCMA). BAFF binds TACI with higher affinity than it does BCMA, while APRIL interacts with BCMA with higher affinity than TACI. In addition, BAFF also interacts with a third receptor known as B cell-activating factor receptor (BAFF-R). APRIL interacts with heparan sulphate proteoglycans (HSPGs),which form part of the extracellular matrix and are expressed by many cell types including B cells (Mackay & Leung 2006). It has been thought that engagement of APRIL with HSPGs enhances APRIL signalling at a local site and concentrates APRIL on the cell surface (Vincent *et al.* 2013). BAFF and APRIL receptors are mainly expressed on B cells, however their expressions are different from cell to cell (table 1.1). Indeed, BAFF-R is expressed by all peripheral B cells subsets including immature and mature B-cell subsets, marginal zone (MZ), germinal center (GC), follicular ,transitional type-1 (T1), transitional type-2 (T2) and some plasmacytoid B cells and TACI is expressed by stimulated follicular and MZ B cells, while BCMA is expressed by activated memory and plasmacytoid B cells (Schneider 2010).

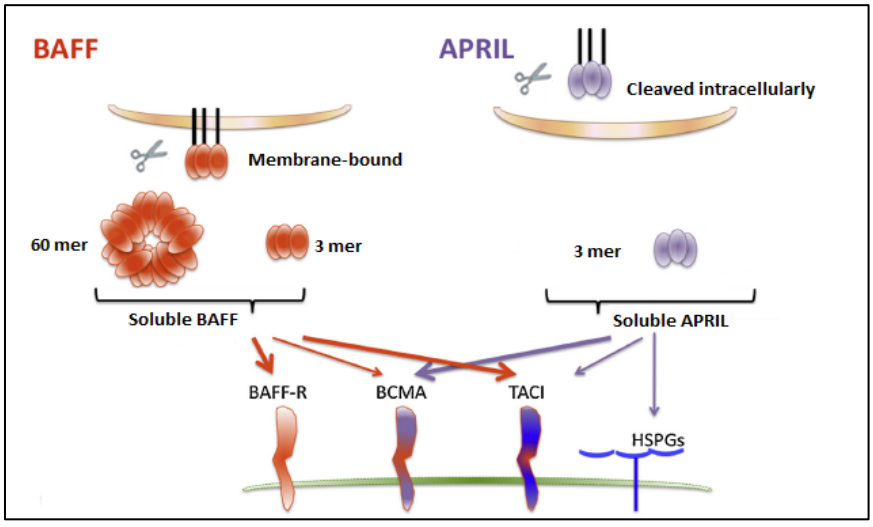

Figure 1.12. Interaction of BAFF and APRIL with their receptors

BAFF can be expressed as a membrane-bound or released into a soluble cytokine after cleavage at a furin protease site. In contrast to BAFF, soluble APRIL is cleaved intracellularly. BAFF only has weak affinity for BCMA. BAFF-R is important for survival and maturation of immature B cells. TACI is critical for T-cell-independent responses of B cells, negative regulation of the size of the B-cell compartment and class-switch recombination. BCMA enhances plasma-cell survival. Taken and modified from (Vincent et al. 2013).

Cell type	Ligands	Receptors
Astrocytes (human primay cells)	BAFF	
Microglia (rat primary cells)	BAFF	BAFF-R, TACI
Immature B cells (human and mouse)		BAFF-R
Mature B cells (human and mouse)	APRIL, BAFF	BAFF-R, TACI
Bone marrow plasma cells (human and mouse)		BCMA
Myeloid precursor cells (human)	APRIL	
Activated T cells (human)	APRIL, BAFF	BAFF-R
NK cells (human blood cells)	BAFF	
pDC (human and mouse)	BAFF	
Neutrophils, Monocytes, Macrophages and Dendritic cells (human and mouse)	APRIL, BAFF	
Intestinal epithelial cells (human)	BAFF	
Adipocytes (human and mouse)	APRIL, BAFF	BAFF-R, BCMA, TACI
Skin keratinocytes (human)	APRIL, BAFF	BAFF-R, BCMA, TACI
Adipose-derived stem cells (human)	APRIL, BAFF	BAFF-R, BCMA, TACI
BM $CD14^+$ cells and osteoclasts (human)	APRIL, BAFF	
Primary CNS lymphoma cells (human)		BAFF-R, BCMA, TACI
CLL stromal microvascular endothelial cells (MVECs) (human)	APRIL, BAFF	
CLL cells (human and mouse)	BAFF APRIL	BAFF-R, BCMA, TACI

Table 1.1. Types of cells expressing BAFF/APRIL and their receptors*. Taken and modified from (Vincent et al. 2013).*

1.2.4. Functions of BAFF and APRIL

1.2.4.1. B cell survival

For many years, it has been thought that functional BCR signals were sufficient for B cell survival (Mackay *et al.* 2010). However, the discovery of BAFF and APRIL changed this view (Figure 1.13).

It has been revealed that mice deficient in BAFF or BAFF-R have a significantly lower number of peripheral B cell compared to control (Mackay & Schneider 2009) and in mice or patients challenged with anti-BAFF this leads to the loss of mature B cells (Dall'Era & Wofsy 2010; Vora *et al.* 2003). This suggests that BAFF mediates an important role in B cell development or maintenance of B cell numbers.

In vitro, it has been reported that APRIL can stimulate proliferation of primary B cells purified from the spleen of normal mice and in *in vivo*, the administration to mice of APRIL daily for 5 days (1mg/kg) resulted in an increase in the size of the spleen and accumulation and increased numbers of splenic B cell (Yu *et al.* 2000). However, a study in APRIL deficient mice showed normal B cells development and normal proliferation *in vitro* (Castigli *et al.* 2004). Taken together, this suggests that APRIL may be less important to some extent in B cell development at the early stages and the possible role of APRIL in maintaining long lived plasma B cell survival through interaction with BCMA (Treml *et al.* 2009).

BAFF can maintain the survival of murine and human B cells at various phases of development and differentiation. BAFF sustains B cell survival by altering expression of pro- and anti-apoptotic molecules. *In vitro*, it has been found that expression of the anti-apoptotic genes including bcl-xL, Mcl-1, Al and bcl-2 increased upon exposure of murine B cell to BAFF (Do *et al.* 2000; Hsu *et al.* 2002; O'Connor *et al.* 2004), whereas the pro-apoptotic molecules including Bak, Blk and Bim were reduced (Amanna *et al.* 2001; Craxton *et al.* 2005; Do *et al.* 2000; Lesley *et al.* 2004). This indicates that BAFF supports the survival of B cells by modifying the balance between pro-survival and pro-apoptotic molecules (Tangye *et al.* 2006).

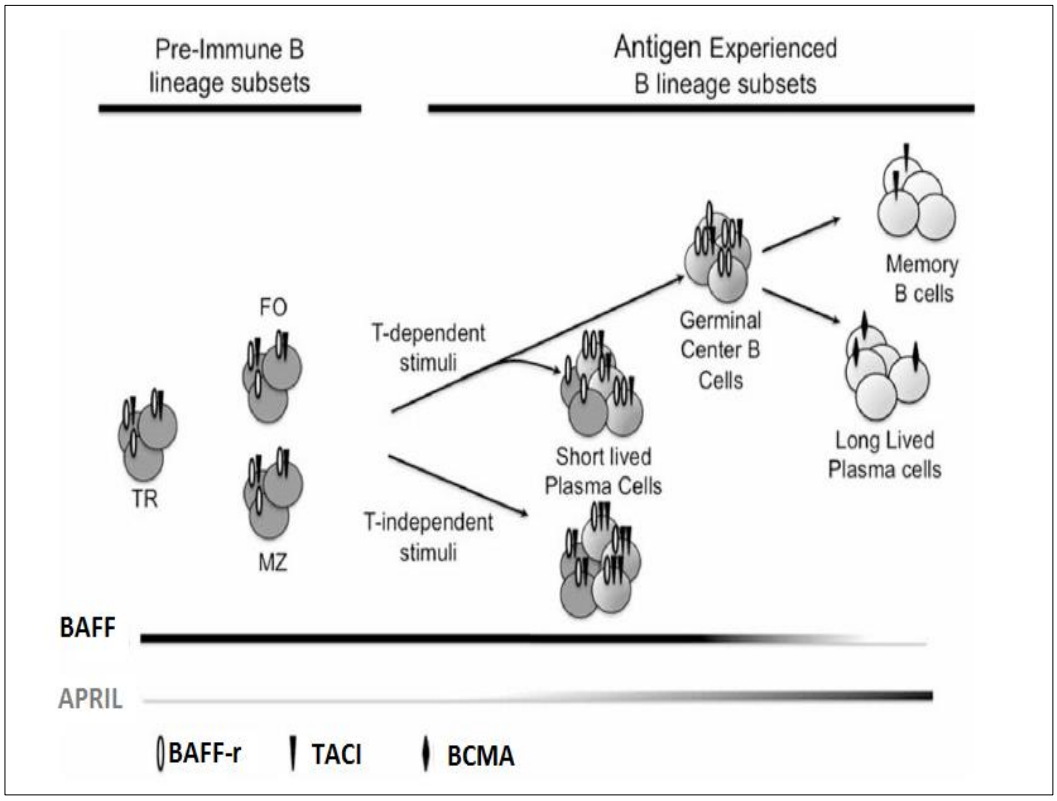

Figure 1.13. Expression of BAFF and APRIL receptors and cytokine dependence

B cells at the early stage (TR; Transitional, FO; Follicular, MZ; Marginal zone) express BAFF-r and TACI, but only BAFF is required for their normal development. Changes of receptor expression are taken place upon antigen stimulation. Thus, T cell dependent stimuli is mediated by BAFF-r expression that resulted in germinal center reactions, whereas T cell independent stimuli is mediated by TACI expression which is resulting in production of short-lived plasma cells. BCMA is expressed on Long-lived bone marrow plasma cells that require APRIL for their normal survival. Memory cells express TACI, but are independent of BAFF and APRIL. Taken from (Treml et al. 2009).

1.2.4.2. Class switch recombination (CSR)

CSR is a genetic process where during antigen driven responses B cells can switch expression of the heavy chain for IgM to produce new class or isotype of antibody such as IgG, IgE and IgA (Chaudhuri & Alt 2004). CSR requires two signals. The first one normally comes by T-cell cytokines including (IL-4, IL-10, IL-13 and TGF-β), and the second signal is mediated by interaction of CD40 on B cells (Stavnezer & Amemiya 2004). BAFF has been recognized to play a role as a second signal for CSR in the absence of T cells or CD40-dependent signalling (Litinskiy *et al.* 2002; Mackay, Silveira & Brink 2007).

BAFF influences this process by engagement with TACI and BAFF-R to enhancing class switching to IgG, IgA or IgE antibodies (Castigli *et al.* 2005b; Kato *et al.* 2009; Stavnezer & Amemiya 2004). Although CSR is generally restricted to lymphoid organs, it has been reported that local immunoglobulin CSR and IgE production also take place in the nasal and airway mucosa of patients who had allergic asthma and allergic rhinitis, in addition to in the oesophageal mucosa of patients with eosinophilic oesophagitis (Kato *et al.* 2009; Vicario *et al.* 2010).

Furthermore, it has been shown *in vitro* that BAFF and APRIL are able to induce CSR in murine B cells also (Castigli *et al.* 2004; Castigli *et al.* 2005b). Stimulation of murine B cells with BAFF or APRIL resulted in production of IgA and IgG1, but for production of IgE, the IL-4 was required in addition to BAFF or APRIL (Castigli *et al.* 2004; Castigli *et al.* 2005b). Furthermore, in mice lacking TACI (–/–TACI mice) both APRIL and BAFF fail to induce IgA secretion by B cells in contrast to mice with B cells expressing a non-functional BAFF-R or which lacked BCMA. This demonstrates the importance of TACI in inducing CSR at least to IgA in response to BAFF or APRIL (Castigli *et al.* 2004; Castigli *et al.* 2005b). TACI is required for APRIL-induced production of IgA by human B cells, but not IgG, while BAFF-R contributes to BAFF-mediated CSR to both IgG and IgA by human B cells. It has been shown that human B cells with mutations in TACI also fail to secrete IgA in response to APRIL or BAFF, which suggests an important role for TACI in CSR to IgA (Castigli *et al.* 2005a; Tangye & Fulcher 2010).

1.2.4.3. T-Cell activation

T-cell production and response to BAFF and APRIL can be considered a controversial issue. BAFF and APRIL were initially suggested to be expressed by activated T cells (Lavie *et al.* 2004). However, other studies were unable to fully confirm this observation and show significant production of BAFF and APRIL (Mackay & Leung 2006). Moreover, TWE-PRIL is a transmembrane protein that consists of a part of the APRIL sequence and the TWEAK gene (Kolfschoten *et al.* 2003), and it has been shown to be expressed on resting and activated primary T cells, which may make detection of APRIL difficult (Mackay & Leung 2006). In addition, expression of BAFF and APRIL receptors (BAFF-R, TACI and BCMA) remains not fully identified. BAFF-R and TACI have been detected on activated T cells (Lavie *et al.* 2008; Wang *et al.* 2001). However, BCMA is not expressed on T cells. It has been reported that BAFF can act as a co-stimulator of T cell activation. Stimulation of human or murine T cells with anti-CD3 mAb in the presence of exogenous BAFF has increased proliferation and cytokine production (Huard *et al.* 2004; Huard *et al.* 2001; Ng *et al.* 2004). Furthermore, *in vitro* it has been reported that BAFF may also be able to improve response of $CD4^{+}$, CD8+, naïve and effector T cells (Huard *et al.* 2001; Tangye *et al.* 2006). In addition, APRIL can also act as co- factor when T cells were stimulated with anti-CD3, and the exactly role of BAFF and APRIL in T cells function and survival remains to be investigated (Mackay & Leung 2006).

1.3. Role of BAFF and APRIL in diseases

1.3.1. Infectious diseases

BAFF can be induced in response to viral infection including hepatitis C virus, human immunodeficiency virus (HIV) RSV and H1N1 influenza (McNamara *et al.* 2013; Rodriguez *et al.* 2003; Toubi *et al.* 2006). Moreover, studies *in vitro* showed that cell lines, including Human umbilical vein endothelial cells (ECs), HL-60 cells and Human erythroleukemia K562 cells infected with Dengue virus, Epstein–Barr virus (EBV), Sendai virus and reovirus-1, respectively, also induce expression of BAFF (Dalrymple & Mackow 2012; He *et al.* 2003; Ittah *et al.* 2011). Furthermore,

APRIL was expressed following RSV infection in humans (Reed *et al.* 2009). However, in our recent study focusing on airway epithelial cell expression both *in vitro* and *in vivo* we did not detect significant up-regulation of APRIL after RSV infection in humans (McNamara *et al.* 2013). Several studies have reported that up-regulation of BAFF following viral infection is IFN-β dependent (McNamara *et al.* 2013; Nardelli *et al.* 2001).

Treatment with type 1 interferon can induce BAFF expression by myeloid cells and epithelial cells. Furthermore, infection of salivary gland epithelial or stimulation with dsRNA, induced BAFF expression (Ittah *et al.* 2009; Ittah *et al.* 2011). In addition, IFN-β expression is also strongly induced by virus infection or dsRNA stimulation of airway epithelial cells (Guillot *et al.* 2005; Ronni *et al.* 1997). BAFF induction by viral infection is a general phenomenon, but the types of viruses and the mechanisms depend on the cell type (Ittah *et al.* 2011). BAFF secretion as a result of infection is thought to play an important role in local immune responses (Ittah *et al.* 2011).

Mice infected with influenza virus for 35 days and later treated for 2 weeks with TACI-Fc that neutralizes both BAFF and APRIL resulted in reduced percentage and total number of antibody secreting cells (ASCs), including virus-specific ASCs, in lungs and bone marrow (BM). This was associated with a significant reduction in antiviral serum IgG, as well as virus-specific IgG and IgA in the BAL (Wolf *et al.* 2011). However, mice treated with anti-BAFF antibody after 36 days of Influenza infection showed no change in protective antiviral antibody titres IgG and IgA in serum or BAL. $CD19^{+}$ B cells were significantly reduced in spleen, lung-draining medLN, and lungs. These observations suggested that blockade of BAFF and APRIL, but not BAFF alone, reduces ASC survival in response to influenza virus infection (Wolf *et al.* 2011). Furthermore, it has been shown that TACI has a significant impact on antiviral Ab responses, TACI deficient mice and WT mice were infected with influenza virus for 0, 8, 18, 32, 33, 60 and 90 days. At the early time of infection there was no difference between TACI deficient and WT strains in the antibody production, IgM peaked at 15 days to 30 days (Wolf *et al.* 2011). However, after 30 days of infection, virus-specific IgG titres in the serum declined significantly in TACI deficient mice in comparison to control, which indicates TACI is required for maintenance of antiviral IgG in the serum. Furthermore, as in the serum, there was no difference in virus-specific IgM in the BAL from WT and

deficient mice on day 8. However, by day 32 virus-specific IgG and IgA were 2- and 10-fold reduced in BAL of TACI deficient mice, respectively. In addition, the concentration of total IgG in BAL was not different, while total IgA was reduced in TACI deficient mice (Wolf *et al.* 2011).

To further understand the mechanism behind this process APRIL alone could be blocked and see if the survival of B cells will be affected or not since the study above targeted BAFF and APRIL or BAFF alone but not APRIL alone.

Moreover, BAFF has been reported to be expressed in response to parasite infections including diseases such as Malaria. *In vivo*, it has been found that malarial infections result in decreased BAFF expression by DCs, which can lead to decrease ability of these DCs to support memory B-cell differentiation of ASCs in addition to the survival of ASCs (Liu *et al.* 2012), and by over-expressing BAFF, malarial-specific antibody secreting cell numbers were increased and mice were protected from infection (Liu *et al.* 2012). Taken together, these observations underline the importance of BAFF and APRIL in providing appropriate long lasting protective responses to infections and therefore increase our understanding of these cytokines during RSV infection and may help us to find out why there is not an effective long lived antibody to RSV.

1.3.2. Cancer

B-CLL is characterized by the slow accumulation in patients of small mature B cells expressing CD5, CD19, CD23 and CD20 markers on their surface. This accumulation results from deficient apoptosis (Haiat *et al.* 2006). *In vitro*, it has been shown that B cells die as result of a lack of essential growth factors in the culture medium (Haiat *et al.* 2006). This rate of B-CLL cell death *in vitro* can be modulated by cytokines such as BAFF (Haiat *et al.* 2006). Recently, it has been reported that BAFF and APRIL can be expressed by B-CLL cells and are able to protect the leukaemic cells against spontaneous and drug-induced apoptosis via autocrine and/or paracrine pathways. This suggests that BAFF and APRIL may be involved in the pathogenesis of B-CLL (Bojarska-Junak *et al.* 2009; Haiat *et al.* 2006). Furthermore, it has been shown that BAFF and APRIL produced by stromal cells such as MVECS enhanced cancer cell survival upon engagement of CD40 on MVECs by CD40L aberrantly expressed on the surface of CLL cells (Cols *et al.* 2012). Thus, as BAFF

and APRIL have key roles in B cell survival this may contribute to expanding the CCL disease especially in patients who are suffering associated infection.

1.3.3. Autoimmune disease

BAFF and APRIL play a central role in the pathogenesis of several autoimmune diseases. BAFF overproduction is often a characteristic of autoimmune diseases, such as systemic lupus erythematosus, Sjögren's syndrome, systemic sclerosis, and rheumatoid arthritis (Lied & Berstad 2011). In addition, it has been shown that patients with systemic lupus erythematosus have higher concentration of APRIL in the serum that seems to correlate with the titre of anti-DNA antibodies (Koyama *et al.* 2005). Furthermore, it has been reported that blockade of APRIL in NZB mice developing lupus spontaneously was associated with reduction of the concentration of auto-antibodies against double-stranded DNA (Huard *et al.* 2012). Moreover, BAFF and APRIL could enhance autoimmune disease such as RA through maintaining the germinal centre - like structure, either by support of the survival of auto-reactive B cells or inducing them to undergo class-switching that results in pathogenic autoantibodies (Tangye & Fulcher 2010).

1.4. Role of homeostatic chemokines in viral infection and iBALT formation

Homeostatic chemokines are commonly expressed in secondary lymphoid organs such as spleen, where they control placement of lymphocytes and DCs (Cyster 1999). Chemokines CXCL13, CCL19, CCL21 and CXCL12 are each homeostatic chemokines that are believed to influence lymphoid tissue structure (Zlotnik, Burkhardt & Homey 2011).

CXCL13 is ligand for CXCR5, whereas CCL19 and CCL21 are ligands for CCR7. CXCL12 is the ligand for CXCR4 (Bleul *et al.* 1996; Zlotnik, Morales & Hedrick 1999). CXCL12 is another B cell chemoattractant. CXCL13 chemokine is expressed in B cell follicles and can attract naive B cells that express CXCR5 (Gunn *et al.* 1998), DCs and activated $CXCR5^+$ T cells (Ansel *et al.* 1999). CXCL13 is also expressed by HEVs, small subsets of normal $CD4^+$ and CD8+ T cells, and skin-derived migratory dendritic cells (Forster *et al.* 1994; Saeki *et al.* 2000; Wang *et al.*

2007; Wu & Hwang 2002; Yu *et al.* 2002), and helps to recruit CXCR5-expressing cells into lymphoid organs (Ebisuno *et al.* 2003).

In contrast to CXCL13, CCL21 and CCL19 are expressed in the T cell zones of the secondary lymphoid organs and they attract naïve T cells that express CCR7 and activated CCR7+ve APC to enter the T cells area. CCR7 is present on activated B cells, naive and central memory T cells, and dendritic cells. Both CCL21 and CCL19 chemokines strongly recruit subsets of T cells, B cells and mature dendritic cells into secondary lymphatic organs (Luther *et al.* 2000; Ngo, Lucy Tang & Cyster 1998). CCL21 is also expressed on HEVs and involved in recruitment of T cells from blood into lymph nodes (Gunn *et al.* 1999). Thus, homeostatic chemokines play an essential role in organizing and maintaining the B and T cell areas of secondary lymphoid organs and contribute to shape the architecture of the secondary lymphoid organs in addition to initiating the interaction of lymphocytes and APCs (Rangel-Moreno *et al.* 2005).

Moreover, recent studies have found that homeostatic chemokines, including CXCL13, CCL19, and CCL21 are expressed in non-lymphoid tissues, such as lungs, after inflammation or infection and can trigger lymphocytes to the side of infection during local immune responses. For example, after influenza infection CXCL13, CCL19, and CCL21 are expressed in the lung including within areas containing B and T cells, and similar to ectopic lymphoid follicles. Accumulation of B and T cells in these areas can be termed iBALT (Figure1.14) (Moyron-Quiroz *et al.* 2004; Rangel-Moreno *et al.* 2007). The iBALT may be formed to initiate and provide an immune response independently from the lymph node.

Within the airway iBALT can be found in areas around the bronchioles and nearby arteries and has been established to be induced in response to different respiratory stimuli such as exposure of neonatal mice to inhaled LPS (Rangel-Moreno *et al.* 2011), toll-like receptor ligands (Luhrmann, Tschernig & Pabst 2002), small proteins (Wiley *et al.* 2009) and cigarette smoke (van der Strate *et al.* 2006). Exposure of the lungs to non-replicative virus-like particles (VLPs) also induces the formation of iBALT (Richert *et al.* 2013; Wiley *et al.* 2009).

Local expression of CXCL13 and CCL21 may contribute to the organization of ectopic lymphoid tissues which are frequently correlated with chronic diseases, such

as rheumatoid arthritis. It has been reported that expressions of ectopic lymphoid tissues promote local immune responses. However, they might also promote or allow activation of abnormal T and B cell responses which could lead to autoimmunity or amplification of chronic inflammation as a result of incorrect organization or structure (Aloisi & Pujol-Borrell 2006; Kato *et al.* 2013).

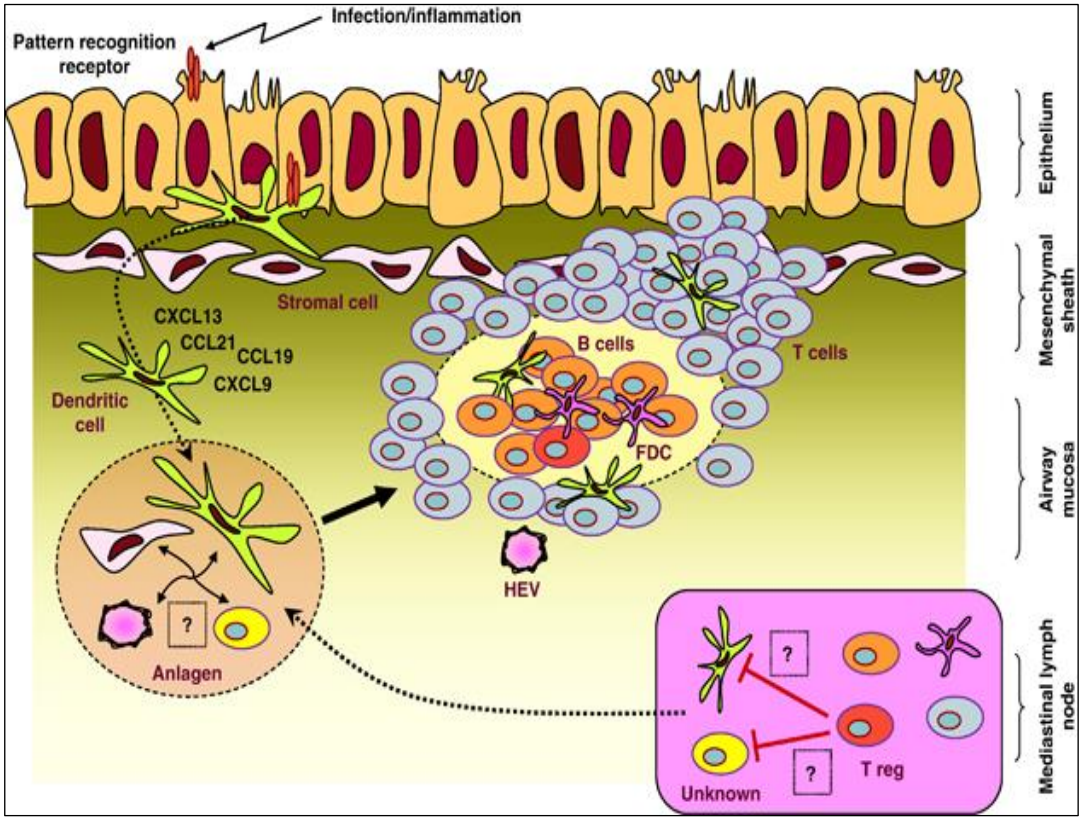

Figure 1.14. Potential mechanism of formation of iBALT during infection

Upon antigen recognition by PRRs (such as TLRs) expressed on epithelial cells or DCs, this leads to immediate early activation that eventually contributes to development of iBALT. The formation of iBALT depends on complex interactions between activated DCs, stromal cells and adhesion molecules on HEVs, results in release of chemokines and cytokines that recruit of T and B cells to the site which are often organized into distinct zones. FDCs are located in B-cell area where they present antigen and co-stimulatory signals to the B cells. Tregs in the draining mediastinal lymph node can attenuate formation of iBALT , however, the mechanism remains unknown, but it could be is possible that Tregs may not fully inhibit cells activation and therefore exit from lumph node and migrate to the lungs to initiate iBALT formation. Taken from (Foo & Phipps 2010).

1.5. Aim of thesis

The main aim of the work described in this thesis was to investigate the ability of airway epithelial cells to support protective immune responses, particularly B lymphocyte responses during RSV infection both *in vitro* and *in vivo*.

BEAS-2B cells, a cultured airway epithelial cell line, were used to characterize expression of BAFF and APRIL, following both RSV infection and cytokine stimulation *in vitro*. The forms of BAFF which epithelial cells can express after RSV infection and the mechanisms that regulating expression BAFF were also examined.

Further aims were to determine if BAFF derived from RSV infected epithelial cells has functional activity influencing B cell survival, and if epithelial cells have the ability to additionally support the adaptive immune response by expression of homeostatic chemokines, including, CXCL13, CCL19, CCL21 and CXCL12. This work is described in chapter three.

To further understand the airway B cell response to RSV infection a murine model of human RSV infection was used to evaluate expression of BAFF and APRIL. In addition, to investigate which forms of BAFF are expressed in murine lungs after RSV infection. Further aims were to examine RSV and BAFF localization in murine lung sections. These experiments are described in chapter four.

Furthermore, local expression of the lymphoid chemokines, including CXCL12, CXCL13, CCL19 and CCL21 which could influence B and T cellrecruitment in to the airway were studied in this model of RSV infection. This work is described in chapter five.

CHAPTER 2: MATERIALS AND METHODS

2.1: Growth of the Human airway epithelial cell line, BEAS-2B

2.1.1. Preparation of medium

Airway epithelial BEAS-2B cells were grown in DMEM media (SIGMA, at#D6546, UK) supplemented with 10% FBS (cat#F7524, SIGMA, UK) and L-Glutamine–Penicillin–Streptomycin solution (cat# G6784, SIGMA, UK).

2.1.2. Culture of BEAS-2B cells

BEAS-2B cells were used in experiments to model the activity of normal human epithelial cells. BEAS-2B cells are derived from human bronchial epithelium transformed by an adenovirus 12-SV40 hybrid virus. Firstly, all external surfaces of supplement vials and medium bottles were decontaminated with 70% ethanol. Cryovials tubes of BEAS-2B cells were removed from store in liquid nitrogen and immediately placed at 37°C in a water bath until around 80% thawed. Cells were pipetted into a sterile universal tube followed by addition of 5ml of warm complete DMEM medium to avoid osmotic shock. Afterwards, cells were centrifuged at 400g for 10 minutes, the supernatant discarded and pellet re-suspended in 15 ml volume DMEM. Cells were grown in T75 tissue-culture flasks containing complete DMEM medium and incubated at 37°C in an atmosphere including 5% CO_2 and 95% air. After 24h of culture, cells were examined under the light microscope to ensure that they were attached and the culture media was changed to remove dead cells and replenish nutrients.

2.1.3. Subculturing of BEAS-2B cells

Cells were subcultured when 70-80% confluent (Figure 2.1). Culture medium was removed and cells washed twice with 5mL sterile phosphate buffered saline PBS (SIGMA, cat#P3813) or complete DMEM medium. 2.5 ml of Trypsin/EDTA solution 1:10 (SIGMA, cat# T3924) was then added to T75 flask and the flask placed directly into incubator at 37C°, 5% CO_2 for 2 minutes. Microscopically, cells were examined to ensure that most of them had ‘rounded up’ and detached from the flask surface. Next, 6 ml of complete DMEM medium was added and cells aspirated by gently pipetting. Cells were centrifuged at 400g for 10 minutes, the supernatant

discarded and the pellet re-suspended in 5 ml complete DMEM medium. The total number of cells was counted using a haemocytometer. Depending on how many cells were needed, cells were diluted with complete DMEM medium and pipetted into 12-well plates (2.5 $\times 10^5$ cells /ml) or T75 flask (2.5 $\times 10^6$ cells /ml). Subsequently, cells were placed in incubator at 37C°, 5% CO_2 for 24h and media was changed. Cells were grown until confluent again.

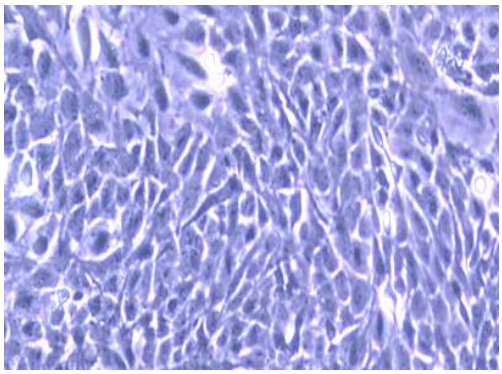

Figure 2.1. Light microscope image of BEAS-2B cells confluent 80%

BAES-2B cells were grown at 1× 10^6 cells/ml in T 25 flask contained complete DMEM for 3 days. Magnification (40x).

2.1.4. Freezing of BEAS-2B cells

Culture medium was removed and cells washed twice with sterile PBS. Cells were dissociated with trypsin, placed in 5-10 ml media and transferred into sterile centrifuge tube and centrifuged at 400g for 10 minutes, the supernatant discarded and the pellet re-suspended in 1 ml complete DMEM. Next, cells were counted and viability estimated by trypan blue (SIGMA, Cat# T6146**)** exclusion. Viability should be over 90% to ensure cells are healthy enough for freezing. Cells were then centrifuged again at 400g for 5 minutes and medium removed. Subsequently, they were re-suspend in cell freezing medium (SIGMA, cat# C6164) at a concentration of $1x10^6$ cells per ml, cells mixed and aliquots of 1 ml placed into storage cryovials. Cells were transferred immediately to -20°C for one hour, followed by -80°C overnight before long term storage in liquid nitrogen.

2.1.5. Stimulation of BEAS-2B cells with cytokines

1.5×10^4 BEAS-2B cells /ml were seeded with DMEM complete medium in 12-well plates. Cells at 70% confluence, were treated with cytokines (200ng/ml) including IFN-α (PEPROTECH, cat#300-02A), IFN-β (PEPROTECH, cat#300-02BC), IL- β (PEPROTECH, cat#200-01B) dsRNA (Invivogen,cat#tlrl-pic) and LPS (SIGMA, cat#L2630) for 0, 3, 6, 12, 24 and 48h. Supernatants and RNA were collected and analyzed for protein and mRNA expression respectively.

2.1.6. Concentration of supernatants

BEAS-2B cells were plated at $1x10^6$ cells per ml in T25 flask until about 80% confluent. DMEM media was removed and cells washed twice with media free from serum and antibiotics. 2.5ml supplement free media were added to flask. BEAS-2B cells were infected with RSV at a multiplicity of infection (MOI= 1 PFU/cell), and non-infected cells used as control. Cells were rocked gently for two hours at 37°C. 2.5 ml complete DMEM media were added and incubated at 37°C for 48h. The supernatant of BEAS-2B cells was concentrated using Centriplus YM-10 filter (Millipore).

2.1.7. Neutralization of IFN-β

In order to determine if BAFF expression was directly induced by RSV infection or if it was indirectly dependent on interferon β production by RSV infected cells, BAFF expression in BAES-2B cells was compared in the presence or absence of an anti-interferon β-neutralising antibody (eBioscience, UK, cat# 16-9978, concentration =1 mg/ml). 5 µl of anti-interferon β-neutralising antibody (20 µg/mL) was added into BEAS-2B cells cultured into 96-well plate at 2×10^4 cells/ml. Expression of mRNA BAFF was measured by RT-PCR after 12h of RSV infection.

2.1. 8. Inhibition of furin convertase

In order to determine if the mechanism of BAFF cleavage is furin like protease dependent BEAS-2B cells were infected with RSV at MOI =1 and incubated with (50 or 100 μM) furin convertase inhibitor (chloromethylketone) (Enzo, cat# Alx-260-022-M001) added at time 6h after RSV infection for 24h or 48h. To further understand the mechanism of BAFF cleavage, BEAS-2B cells infected with RSV or stimulated with IFN-β were incubated with Brefeldin A (1:100) (eBioscience, cat#00-4506-51) after RSV infection of 6hours for 24 and 48h.

2.2: Isolation of Human lymphocytes

Human lymphocyte cells were prepared from the peripheral blood of healthy laboratory donors after obtaining informed consent and with the approval of the Liverpool Research Ethics Committee (LREC 2K/175). Lymphocytes were isolated from the peripheral blood by firstly adding an equal volume of Ficoll-Paque PREMIUM (GE Healthcare Life Sciences, UK, cat# 17-5442-02) to 20 ml blood followed by centrifugation, 400g for 30min at room temperature. The centrifuge was run with the brake off in order to achieve better separation. This method relies on density gradient for separation. After centrifugation, two layers were formed, the interface layer (containing lymphocytes) was collected and cells washed twice with sterile PBS contain 0.02% BSA. Cells were re-suspended in 1ml of RPMI complete medium (RPMI-1640, SIGMA, cat# R8758) plus 0.02% BSA and purified cells counted (normally 2.5×10^7 cells /in 20 ml blood).

2.2.1. Purification of Human B cells

Human peripheral bloods were obtained from healthy donors. The PBMC were isolated using Ficoll separation method. From the lymphocyte layers, B cells were purified using human B cell enrichment kit (STEMCELL, cat#19054). Briefly, lymphocytes were suspended at a concentration of 5×10^7 cells/ml in 2ml of RPMI media and transferred into a polystyrene tube (BD Bioscinences, cat#352057). 2ml of the human B cells enrichment kit was added to the cells and incubated at room temperature for 10 minutes. After that, 2 ml of magnetic particles were added to cell suspension and incubated at room temperature for 5 minutes. Then, 3ml of RPMI media was added to the cell suspension and the cell suspension tube placed into magnet for 5 minutes. After that, desired cells were poured off into new tube, whereas unwanted cells remain bound in the original tube by the magnetic field. B cells were re-suspended in PBS containing 0.02% BSA to block non-specific antibody binding and stained with B cells marker anti-CD19 (Cat#560993, BD Pharmingen$^{TM)}$ for 30 min in the dark at 4°C. Then B cells were gated and analyzed with a BD FACS (BD Biosciences).The purity of the B cells was assessed by FACS to be >99% (Figure 2.2).

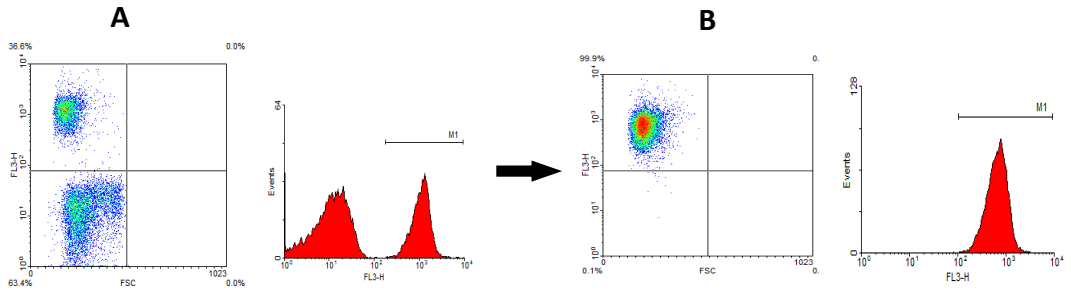

CD 19 before purification (36.6 %) CD19 after purification (99.9 %)

Figure 2.2. Isolation and purification of human B cells from the peripheral blood

B cells were isolated and stained with anti-CD19 and the purity assessed by FACS. In (A) dot blot and histogram represent CD19 from normal B cells before purification .In (B) dot blot and histogram represent expression of CD19 normal B cells after purification. In (A) the percentage of CD19 cells before purification was (36.6) and in (B) after purification was (99.9) .The purity was >99.9%.

2.2.2. Measurement of Cell Number by haemocytometer

10 µl of a re-suspended cell pellet was mixed with 10 µl trypan blue to count the viable cells that are not stained and dead cells which can be stained with it. A volume of 10 µl of mixed cells suspension was added into the haemocytometer slide. Then, cells were counted in each of the four large quarters multiplied by 2 and divided by 4 and multiplied by 10^5 and the total cell number calculated taking into account the volume.

2. 3: Animals

2.3.1. Experiment design

All experiments involving animals were carried out by Prof Jurgen Schwatze and Miss Amanda McFarlane working at Queens Medical Research Institute at the University of Edinburgh. All studies were conducted in accordance with Home office procedures for animal experimentation and Prof Schwarze holds ethical committee approval for the studies at the University of Edinburgh. BALB/c mice were maintained under specific-pathogen-free conditions. All mice were 8 weeks of age and anesthetized and then infected intranasally (i.n.) with RSV A2 (2×10^6 PFU in 0.1ml) or UV treated RSV or PBS.

Kindly, three groups of RSV mice were provided for the experiments. The first set of experiments includes day 0, 1, 2, 4 and 7 days. The second group consists of day 0, 1, 2, 4, 6 ,7 and 8 days and the third group includes day 0, 1, 2, 4, 7, 10, 14, 21days. At day 0 mice were given PBS and for each day on which samples were collected, three mice were infected with RSV, whereas three mouse where infected with RSV which had been inactivated by UV treatment as a further control.

After collection, lungs were divided into 3 parts, left upper lobe to study protein, left lower lobe for mRNA preparation and the whole right lungs to study the frozen sections.

2.3.2. Measurement of the total protein concentration (BCA)

2.3.2.1. Principle

Bicinchoninic acid assay is a colorometric assay used for determining the total concentration of protein in a sample (range from 0-2000 µg/mL). The total protein concentration is shown by a colour change of the sample solution from green to purple in proportion to protein concentration, which can then be measured using a plate reader. The principle of this method relies on two reactions. The protein present in the sample reduces from Cu+2 to Cu+1, and it then can react with bicinchoninic acid forming purple-coloured products and the optical density measured.

2.3.2.2. Preparation of protein standard

A seven point standard curve using 2-fold serial dilutions in sterile distilled water was prepared and a high standard of 2000 µg/mL and blank well applied as control (Thermo scientific, cat#23209).

2.3.2.3. Preparation of reagent solution

The working reagent was made up to 1:50 dilution, 1 parts B (blue/green) (Thermo scientific, cat#1859078) and 50 part A (colourless) (Thermo scientific, cat#23221).

2.3.2.4. Preparation of plate

25µL of each standard or unknown sample was pipetted in duplicate into a microplate well. Samples were diluted in sterile distilled water (23µl water+ 2µl sample = 1:12.5 dilution). Subsequently, 200µL of reagent solution was added to each well. The plate was mixed thoroughly on a plate shaker for 30 seconds then covered and incubated at 37°C for 30 minutes before cooling to room temperature. The absorbance was measured at 540 nm on a plate reader.

2.3.2.5. Calculation

$$\text{Normalised relative to total protein} = \frac{\text{Sample concentration Pg/ml}}{\text{Total protein concentaton mg /ml}}$$

2.4. RNA Extraction and Isolation

2.4.1. RNeasy Mini kit

Extraction of RNA should be done under clean and sterile conditions. Total RNA was extracted from BEAS-2B or mouse lung (Left Lower Lope) using RNeasy Mini kit according to the manufacturer's instructions (QIAGEN, cat#74104). This product combines the selective binding properties of a silica-based membrane with the speed of microspin technology. A specialized high-salt buffer system allows up to 100 µg of RNA longer than 200 bases to bind to the RNeasy silica membrane. To enhance RNA extraction, β-mercaptoethanol (SIGMA, cat# 60-24-2) was added to the lysing buffer RLT (100 µl+9990 µl) which contains the denaturant guanidine-thiocyanate. This inactivates RNases to ensure purification of intact RNA. Briefly, 500µl of lysis buffer RLT was added into each well of 12–well plate that had about 2.5×10^5 cells. Cells were mixed well and transferred into autoclaved eppendorf tubes. Next, 300µl of 70 % sterile ethanol was added to the homogenised lysate in each tube, mixed and placed into RNeasy Mini column. This aimed to provide appropriate binding conditions. Tubes were centrifuged at full speed for 15 sec. After that, collection tubes were discarded and 700 µl of wash buffer RWI was added and centrifuged at full speed for 15 sec. Subsequently, cells were washed twice with 500 µl of RPE for 15 sec and for two minutes. Next, the collection tubes were removed and replaced with new tubes. RNeasy Mini columns were centrifuged at full speed for two minutes. Finally, 50 µl of free DNAse /RNAse free water were added into each tube for one minute at room temperature. The total RNA was collected by centrifuging the Mini column into sterile eppendrof tubes. In order to determine the yield and concentration of RNA the concentration of total RNA was measured by NaNoDrop (Biotech International).

2. 4.2. Reverse Transcription

The cDNA single-strand was synthesized with SuperScript II reverse transcriptase and random primers (A&B applied biosystem, cat#4368814). The following components were added to each 10 µl of RNA for each sample to be reverse transcribed:

1.10X RT Buffer (2 µl)
2. 25X dNTP Mix (100mM) (2 µl)
3. 10X RT Random Primers (2 µl)
4. Free RNA/DNA water (3µl)
5. MultiscribeTM Reverse Transcriptase (1µl)

Samples were then left in a water bath at 37°C for one hour. Once synthesized the cDNA was stored at -20^{o}C until further required for PCR and then diluted with nuclease-free water, depending on how much cDNA was needed (typically 80µl of free DNA RNA water was added into each sample).

2.4. 3. Real-Time Polymerase Chain Reaction (RT-PCR)

TaqMan real-time RT-PCR was performed using an Applied Biosystems 7500 Sequence Detection System in 25µl reactions. The TaqMan® probes (Table 2.1) were added into TaqMan® gene expression master mix (Applied Biosystems, cat#4369016), which contains the DNA polymerase. 13.75µl of probes mixed with master mix were pipetted into each well of 96-well plate. Samples of cDNA (11.25µl) were added into each well to give a final volume of 25µl. Each sample was prepared in duplicate. The plate was sealed with a cover and gently centrifuged for 10 seconds. Finally, PCR plate was placed into the PCR machine for 2-3 hours according to the number of cycles entered.

2.4.4. Principle of PCR

The main aim of this technique is to amplify specific target of DNA. PCR involves three essential steps including:

1. Denaturing: At 95°C, dsDNA is separated to yield single stranded DNA.
2. Annealing: At 40°C- 65°C, primers bind the single target DNA
3. Extending: At 72°C , DNA polymerase extends the primers

The RT-PCR is standard PCR with the advantage of detecting the amount of DNA formed at the early phases of the reaction.

There are three phases (Figure 2.3) in total throughout the PCR amplification:

1. Exponential: The product at this phase has exactly doubling of products at every cycle and the efficiency of this reaction is 100%. During this phase the Real-Time PCR quantifies the amplicons.

2. Linear: reaction's components reduce due to being consumed during the reaction

3. Plateau: Reaction stops and no more products are being made.

The threshold cycle (Ct) is the point between an amplification curve and the threshold line, where fluorescent signal is detected. This line is set during the exponential phase. Once the sample reaches this level, the cycle number is quantified and measure of the concentration of target in the PCR reaction.

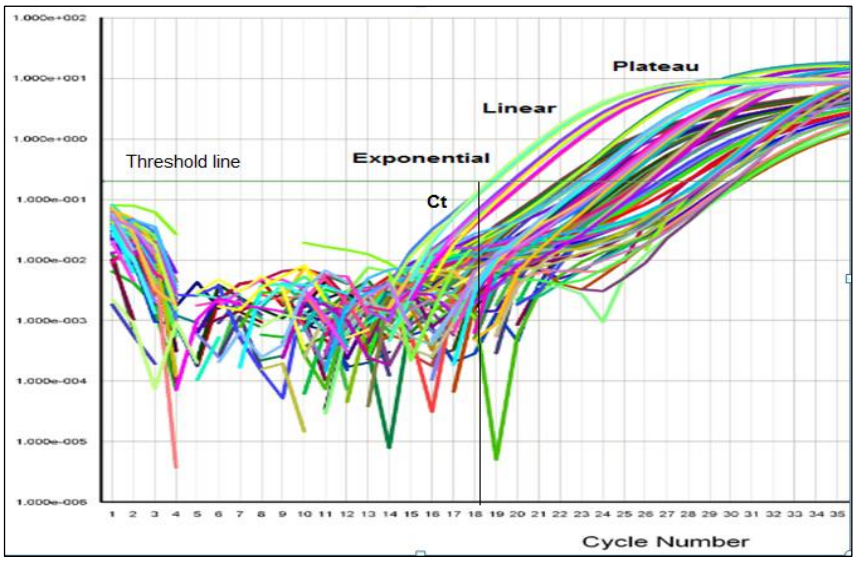

Figure 2.3. RT-PCR amplification curve of data analysed

TaqMan® probes	Human	Murine
MRPL32	Hs00388301_m1	Mm00503378_m1
APRIL	Hs00182565_m1	Mm03809849_s1
BAFF	Hs00198106_m1	Mm00446347_m1
CXCL13	Hs00757930_m1	Mm00444533_m1
CCL19	Hs00171149_m1	Mm00839967_g1
CCL21	Hs00989654_g1	Mm03646971_gh
CXCL12	Hs00930455_a1	
RSV N	30 µl RSVn+10 µl RSV R + 10 µl RSV F +50 µl clean water. Three primers, RSVAF (forward) 1µM, RSVAR (reverse) 1µM and RSVN-TAQ (10uM), were obtained individually and prepared. RSVAF and RSVAR primers were mixed together with Nuclease-free water in a 1 in 10 dilution. RSVN-TAQ was diluted 1 in 10 separately, with Nuclease-free water. (Dewhurst-Maridor *et al.* 2004)	

Table 2.1.TaqMan® Gene Expression Assay Product Number (Life technologies).

2.4.4.1 Analysing RT-PCR Data

The following steps were used to analyse the RT-PCR data:

1) All Ct values of the samples were averaged
2) The Ct value of samples for each probes were corrected to the house keeping gene L32

   For example: The L32 expression - BAFF. This produced a Ct value relative to L32 expression.

3) Corrected to relative control by taking the Ct value produced in step 2 minus the cycle value for the relative control (non-stimulated cells).
4) Fold expression in comparison to L32. This can be calculated by 2 to the power of n, where n = value determined in step 2. This calculation converts the value from a Ct number to the fold difference. This particular calculation is because every cycle is a 2 times increase during the exponential phase.

2.5. Enzyme-Linked ImmunoSorbant Assay (ELISA)

2.5.1. Principle

The main purpose of using an ELISA method is to determine if a particular protein is present or not in the sample of interest and if so, how much by its concentration. This method can be done in two ways termed direct and indirect Sandwich ELISA. This method has been used to find out protein concentration in BEAS-2B cells culture supernatant and homogenised mouse lung tissue.

2.5.2. Plate Preparation

The capture Antibody was diluted to the working concentration in PBS without carrier protein and 96- well plate coated with 100 µl per well of the diluted antibody. Plates were sealed and incubated overnight at room temperature. Then, the plate was washed with the wash buffer (0.05% Tween-20 in PBS (400 µl) by use the auto washer (ELx50 Microplate Strip Washer-Bio-Tek) for total of three times and ensured that removing any remaining wash buffer by aspirating or by inverting the plate and blotting it against clean paper towels. Plate was blocked with Reagent Diluent, 1% BSA (SIGMA, cat#A7030) in PBS, by adding 300 µl for one hour at room temperature and the plate washed three times with wash buffer.

2.5.3. Sample preparation

Human BAFF and chemokines including CXCL13, CCL19 and CCL21 were measured in the culture supernatants of BEAS-2B cells. In mouse lung the left upper lobe was homogenised in 2 ml of PBS+ protease inhibitors. BAFF, CXCL12, CXCL13, CCL19 and CCL21 were measured in the homogenised tissue supernatants (Table 2.2)

Human	Lower limit of detection (pg/ml)	Murine	Lower limit of detection (pg/ml)
BAFF (R&D Systems, cat#DBLYSOB)	5	BAFF (cat#MBLYS0, R&D Systems)	47
CXCL13 (R&D Systems#DY801)	16	CXCL13 (R&D Systems,cat#DY 470)	16
CCL19 (R&D Systems cat#DY361)	16	CCL19 (cat#DY440, R&D Systems)	16
CCL21 (R&D Systems ,cat#DY366)	31.25	CCL21 (cat#DY457, R&D Systems)	16
		CXCL12 (cat#) DY460	47

Table 2.2: Human and murine ELISA number of product.

2.5.4. Preparation of standard

A seven point standard curve using 2-fold serial dilutions in Reagent Diluent was prepared. A high standard of 1000 pg/ml is recommended for mouse CXCL13, CCL19 and CCL21, whereas 3000 pg/ml was recommended for CXCL12. For the human cytokine ELISA assays a high standard of 1000 pg/ml is recommended for CXCL 13 and CCL19, whereas 4000 pg/ml was recommended for CCL21. The standard curve was calculated using a computer programme (KC Junior) generating a four parameter logistic (4-PL) curve-fit.

2.5.5. Assay Procedure

A total volume of 100µl/sample or standards in Reagent Diluent per well was added to the plate, previously coated with capture antibody and blocked with BSA. Then, the plate was covered with an adhesive strip and incubated for 2 hours at room temperature. The plate was then washed three times with the wash buffer (0.05 % tween 20 in PBS). After that, 100µl of the detection antibody diluted in Reagent Diluent (1% BSA in PBS) were added per well and the plate incubated for two hours at room temperature. Then, the plate was washed three times with the wash buffer. Next, 100 µl of the working dilution of Streptavidin-HRP diluted in reagent diluent

(1:200) was added to each well and incubated for 20 minutes at room temperature without light.. Plates were then washed three times with the wash buffer. 100 µl of substrate solution (TMB Substrate solution, Thermo scientific, cat# N301 Solution) was added to each well and incubated for 20 minutes at room temperature in dark condition and monitored the development of the colour. 50 µl of Stop Solution (H_2SO_4) was added to each well (the colour changes from blue to yellow). The optical density (OD) of each well was determined using a microplate reader (BioTek ELx800 Absorbance Microplate Readers) set to 450 nm. KC Junior software was used to find out the concentration.

2. 6. RSV A2 preparation

The main aim of preparation of RSV is to ensure that we have enough stock to achieve infection. The following steps described the propagation of RSV A2 in the laboratory.

2. 6.1. RSV propagation

Hep2 cells were seeded in a T75 flask at 30,000 cells/cm2 in a total volume of 15ml of DMEM plus 10% FCS, and grown for 24h at 37°C in 5% until 50% confluent. Media removed and cells washed twice with sterile PBS. RSV A2 stock was placed in 4ml of FCS-free medium and added to Hep-2 monolayers cells. To ensure infection over the whole flask they were rocked gently for two hours at 37°C. Then, 11ml of media was added and the flask left overnight in the incubator. After 24hours, 11 ml of media was removed and replaced with DMEM plus (2% FCS total). Cells were assessed daily for cytopathic effect (e.g. dead cells floating, until the cytopathic effect reached approximately 50%, typically 48h. The monolayer was then harvested using a cell scraper, and centrifuged at 400g for 5 minutes in precooled centrifuge at 4°C and lysed on ice by use of 1-2ml syringe and needle (25 gauge). Aliquots were snap frozen and stored at −80°C.

2. 6.2. RSV Plaque assay

RSV titre was determined using a modified plaque-forming unit assay. Briefly, the virus was serially diluted and added to A549 cell monolayers containing about 2 x 10^4 cells/ml grown in 96-well plates (total volume 50 µl). The cells were incubated for 24h before being fixed in methanol and stained with an anti-RSV biotinylated antibody goat anti-RSV, AbD Serotec (Oxford, cat #7950-0104, UK) labelled using an extravidin peroxidise colour development substrate (Sigma Fast-Red, Sigma-Aldrich). Plaques were visualized using light microscopy and counted (Figure 2.4). Plaque forming units (PFU) were calculated as: number of plaques/ml × dilution factor × 20 (for 50 µl culture volume).

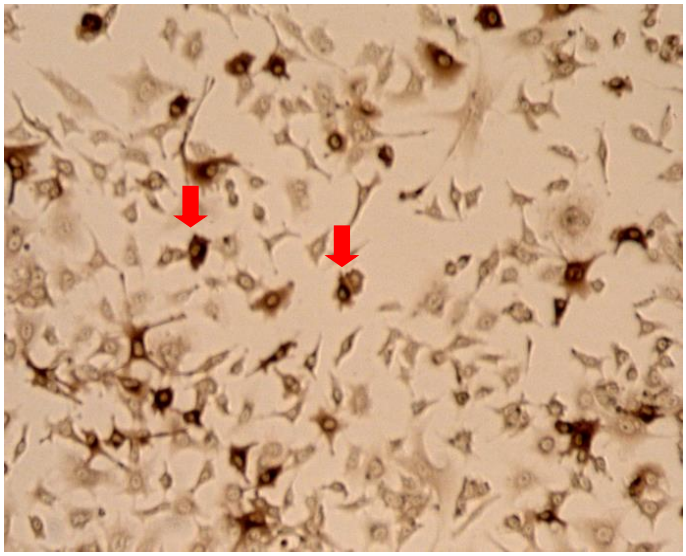

Figure 2.4. Light microscopy image of A549 cells after RSV infection

'Plaque' of RSV +ve cells (dark brown) as indicated by arrows were formed after staining with an anti-RSV biotinylated antibody goat anti-RSV, labelled using an extravidin peroxidise colour development substrate.

2. 7. RSV infection of BEAS-2B cells

BEAS-2B cells were grown in 12 wells plates until about 80% confluent. DMEM media was removed and cells washed twice with media free from serum and antibiotics. 250µl supplied free media were added to each well. Confluent monolayer cultures of BEAS-2B cells were infected with RSV at a multiplicity of infection (MOI= 0.025, 0.25, 1 and 2.5 PFU/cell), and non -infected cells used as control. Then cells rocked gently for two hours at 37ºC. 250 µl complete DMEM media was added and incubated at 37ºC at different time points, including 0, 3, 6, 12, 24, 48h.

2. 8. Immunofluorescence staining assay

2. 8. 1. Coated glass microscopy slides with ploy-l-lysine

Microscopy slides were coated with poly-L-lysine (Sigma, UK cat#P8920) diluted in distilled water (1:10) for 5 minutes. Slides were then air dried at room temperature overnight. This aids in the adhesion of tissue sections to slides.

2. 8.2. Preparation and cutting of tissue for frozen sections (Cryostat)

Mouse tissues, lungs and spleen, were embedded into frozen media immediately after extraction and stored at -80 C. This media was used to keep the tissue fresh and well structured. An area of around 1 square centimeter of each specimen was cut using a scalpel and placed onto a metal tissue disc which was then secured in a cryostat chuck. Frozen tissue support media (Bright, UK, and cat #53581-1) was rapidly added and samples cooled at –20 to –30°C for 20minutes. Subsequently, the frozen tissue block was attached to the cryostat. The tissue block allowed to equilibrate to the cryostat temperature (-20°C) before cutting sections. Sections were cut at 10 microns thick and picked up onto coated slides. During cutting sections the surface temperature of tissue might change, and can be cooled using cryospray (Bright, UK, cat#57713-1) to enhance the efficiency of cutting. Tissue sections were air dried at room temperature for 20 minutes until sections are firmly adhered to the slide. After that, tissues were fixed with pre-cooled acetone 100 % (4°C) for 10 minutes, before air dying for 20 min at room temperature. Slides were stored at -80°C for further use.

2. 8.3. Immunostaining of frozen tissue sections

Slides were rehydrated in PBS for 3 min. Non-specific binding of antibodies was blocked with blocking buffer (5 % Milk in PBS), and sections incubated in a humidified chamber at room temperature for 1h, then washed twice with PBS plus1% Tween 20 for 2 changes, 5 min each. Following that, tissue sections were incubated with appropriately diluted primary antibody in blocking buffer (Table 2.3), and incubated in a humidified chamber for 1h at room temperature. Subsequently, sections were washed twice with PBS plus1% Tween 20 for 2 changes, 5 min each. Tissue sections were incubated with appropriately diluted secondary antibody in blocking buffer (Table 2.3) and incubated in a humidified chamber for 1h at room temperature. Then, sections were washed twice with PBS plus1% Tween 20 for 2 changes, 5 min each. DAPI stain (1:10000 in PBS) (SIGMA, cat#D8417) was added for 3 minutes. Slides were rinsed with PBS plus Tween 20 for 5 min, followed by adding one drop of mounting media (R&D, UK, and cat #NL996); afterwards slides were covered with a coverslip and sealed with one drop of nail varnish. Eventually, tissue sections were examined under the confocal microscope (LEICA DM 2500).

Primary antibodies and their Isotypes	Secondary antibodies
Rat anti-BAFF -FITC(Abcam ,ca#16082) (1 mg /ml) used at 1:50 Isotype: Rat IgM, kappa monoclonal [RTK2118] (FITC) (Abcam, -cat#ab35774) (0.5 mg/ml) used at 1:25	Direct labelling
Rat monoclonal to CD20 [AISB12] (Abcam,cat#ab171203) (1 mg/ml) used at 1:100 Isotype:Rat IgG_{2A} (R&D cat#MAB006) (0.5 mg /ml) used at 1:50	Donkey anti-Rat 1 mg /ml used at (1:200) R&D (cat#NL013)
Rat anti-CD3 MAb (Clone 17A2), IgG2B (R&D ,cat # MAB4841) (0.5mg /ml) used at 1:50 Isotype: Rat IgG2B Isotype Control (Clone 141945), Rat IgG2B R&D (Cat # MAB0061)(0.5mg /ml) used at 1:50	Goat Anti-Rat IgG NL493 Affinity Purified PAb R&D (Cat # NL015) 1 mg /ml used at (1:200)
Anti–mouse CXCL13 (R&D ,cat#AF470) (0.2 mg/ml) used at 1:15 Isotype: Normal Goat IgG Control, Goat IgG (1 mg/ml) (R&D ,cat# AB-108-C)	Donkey anti- goat R&D (cat#NL001) 1 mg /ml used at (1:200)
Goat anti- RSV (Abcam ,cat#ab20745) (4 mg/ml) used at 1:100 Isotype: Normal Goat IgG Control, Goat IgG (R&D, cat# AB-108-C) (1 mg /ml) used at (1:30)	Donkey anti- goat R&D (cat#NL001) 1 mg /ml used at (1:200)

Table 2.3. List of primary and secondary antibodies with their isotype controls used in Immunofluorescence Staining.

2. 9. MTT assay

The MTT assay is a colorimetric assay used to assess cell viability. MTT is a yellow tetrazolium salt which is reduced to purple formazan by mitochondrial activity of living cells. The formazan crystals are then solubilized, and the concentration determined by optical density which reflects the cell viability. For the analysis of the biological activity of secreted BAFF by the epithelial cells, BEAS-2B cells were cultured in complete DMEM medium and then infected with RSV A2 at MOI 1 for 48h. The supernatant was concentrated using centriplus YM-10 (Millipore, cat#43040). Purified B cells were cultured at a density of 2×10^5 cells/100 µl/well of a 96-well flat-bottom microtitre plate in RPMI 1640 (SIGMA,cat#R5886) supplemented with 10% FBS, 100 U/ml penicillin, and 100 µg/ml streptomycin. Media alone, B cells, B cells plus 10 ng/ml rBAFF (R&D, cat# 2149-BF-010) and B cells plus 1: 20 of concentrated supernatant of epithelial cells infected with RSV for 48h and incubated for 5 days. To detect intracellular enzyme activity, 20 µl of MTT reagent (SIGMA, cat#Tox1) was added for the last 4 h of incubation. After 4h, 100 µl of detergent reagent (SIGMA, cat#Tox1) was added to all wells. Cells were mixed very well and the plate placed in microtitre plate reader. Absorbance at 540nm was measured. All the samples were done in triplicate by taking the average of three readings.

2. 10. Western blot analysis

Western blot was used to determine the molecular weight of the specific protein of interest such as BAFF, and to also to investigate the forms, including membrane bound and soluble that airway epithelial cells can express following RSV infection both *in vitro* and *in vivo*. Briefly, a mixture of proteins is separated based on their molecular weight. The proteins are separated through gel electrophoresis and then transferred into a membrane, where a band for each protein can be detected after incubated with specific antibodies to the protein of interest, which also can be visualized by developing the film.

2. 10.1. Sample preparation

BEAS-2B cells were plated into 24-well plate 2.5×10^{6} cells/ml. Media was removed and the cells were disrupted by cell scraper. Cells were washed with PBS, the pellet lysed with SDS buffer containing 10% DTT and protease inhibitors (1:100). Mouse lung tissues were homogenised and then lysed in 100 µl of SDS plus 10 µl of 10% DTT and 2 µl of protease inhibiters.

2. 10.2. Gel electrophoresis

BEAS-2B cells and mouse lungs tissue were denatured by boiling for 3min at 100°C. Thereafter, samples and ladder (Biorad, UK, cat#161-0373) (10µl) were loaded into the gel placed in the electrophoresis apparatus containing the running buffer. Proteins were always separated using 12% precast gel (Bio-Rad .UK, Cat#456-1046) at voltage 140 (Bio-Rad power supply, 1000/500) for 1h.

2. 10.3. Transfer blot

Proteins were transferred onto nitrocellulose membranes (Biorad, UK, cat#170-4156) by using a transfer system (trans-blot turbo, Biorad, UK) for 7 minutes. Following transfer, the membranes were blocked with 5% skim milk in Tris-buffered saline with Tween 20 (TBST) for half an hour and then washed with 1%TBST and incubated with the primary antibody rat anti BAFF (1:1000) (ab16081) for overnight at 4°C. Membranes were then washed for 30 minutes with 1% TBST and then incubated with HRP-conjugated secondary antibodies (1:20,000) (ab98373) for 1 hour at room temperature. After that, the membrane was washed for 30 minutes with1%TBST. Then, the membrane was placed into cling film and incubated with ECL (GE healthcare, cat#RPN2232) for 5 minutes and then placed in the hypercassette.

2. 10.4. Detection

A dark room was used when developing the film. Briefly, the film (GE healthcare, UK, cat# 28-9068-35) was exposed to the membrane inside the hypercassette (Amersham Biosciences). Then, the film was placed into the developer, water and fixer respectively.

2. 10.5. Adding β- actin

β- actin was used as control to see how much of protein was loaded into each lane. Membranes were blocked with 5% marvel for half hour and then incubated with appropriate diluted primary antibody in blocking buffer for one hour at room temperature. Next, membranes were washed with 1% TBST for 1 min, 3 min, 10 min, 5 min, and 5 min. After that, the membrane was incubated with appropriately diluted secondary antibody in blocking buffer for one hour at room temperature (Table 2.4). Next, membranes were washed with 1% TBST for 1 min, 3 min, 10 min, 5 min, and 5 min as the same method mentioned above.

	Primary Ab	Secondary Ab
Human	Anti-beta Actin (Abcam, cat#ab8226) used at (1:1000)	Goat Anti-Mouse IgG HRP Affinity Purified PAb, Goat IgG (HAF007,R&D) used at (1:1000)
Mouse	Anti-Actin ,ab produced in rabbit (1:1000) (SIGMA,cat#A2668)	Goat anti rabbit–HRP (1:20,000) (SIGMA,A0545)

Table 2.4. Human and mouse primary and secondary antibodies used for β-actin.

2. 11. Flow cytometery

This technology measure emission of fluorochrome molecules to generate specific multi-parameter data from particles and cells as they flow in a fluid stream through a beam of light (laser). Fresh lung tissue from mice either RSV infected or challenged with UV treated RSV was disrupted mechanically and cells washed in PBS. Cells were stained using anti-B220 (ebiosciences, cat#48-0452-82) and anti-CD19 antibodies (Biolegend, cat no 115522). B cells numbers were counted by BD FACS Calibur™. This work was kindly done by Dr A McFarlane in Edinburgh.

2.12. List of reagents and solutions

- TBS 10x (concentrated TBS)
  a. 20mM 24.228 g Tris

b. 150mM 87.66 g NaCl
c. Mix up to 1000 ml distilled water.
d. pH to 7.5 with conc HCl.

To prepare TBS-T x1 in 1 litre

100 ml of TBS 10x + 900 ml distilled water + 1ml Tween20

- Bromophenol blue lysis buffer (SDS)

a. 10% glycerol (10ml)
b. 125mM TRIS buffer (pH 6.8) (12.5ml)
c. 3% SDS (3ml of 10% SDS or 3g)
d. 0.2% bromophenol blue (a few grains)
e. Make up to 90ml with distilled water

- Phosphate buffered saline (PBS)

One pack of phosphate buffered saline PBS (SIGMA, cat#P3813) was dissolved in (1) litre distilled water. The PBS was autoclaved if required sterile.

- Running buffer

a. Tris Base 3.03 g
b. Glycine 14.4 g
c. SDS 1g
d. Make up to1 litre with distilled water

2.13. Statistical Analysis

In chapter three, data was expressed as mean ± SEM and one way ANOVA test followed with Bonferroni post-hoc test used to calculate the statistical significance. In chapter four and five, data was expressed as mean ± of standard deviation (SD) and the two way ANOVA followed with Bonferroni post-hoc test was used to calculate statistical significance. GraphPad Prism 5.0 software was used to find out the stats. P-values indicate significance. (* for $p<0.05$, ** for $p<0.001$ and *** for $p<0.0001$). The software (KC Junior) was used to find out the ELISA protein concentration.

CHAPTER 3. *IN VITRO,* INDUCTION OF BAFF AND APRIL EXPRESSION BY RSV INFECTION OR CYTOKINE STIMULATION IN CULTURED HUMAN AIRWAY EPITHELIAL BEAS-2B CELLS

3.1 Aims

BAFF expression both in BAL samples and by primary airway epithelial cells during acute human RSV infection has previously been demonstrated (McNamara *et al.* 2013). To begin to understand the potential role of the airway epithelium to support a B cell response by production of BAFF and APRIL (chapter 1, sections 1.2.1 and 1.2.2) airway epithelium cell line BEAS-2B was used. The works described in this chapter aimed to:

1- Characterize expression of BAFF and APRIL by cultured BEAS-2B airway epithelial cells, stimulated either by RSV infection or cytokine.
2- Examine what form or forms of BAFF epithelial cells express after RSV infection and the mechanisms regulating expression.
3- Determine if BAFF derived from BEAS-2B cells has functional activity on B cell survival.
4- Establish if epithelial cells have the potential to support adaptive immune responses by expression of homeostatic chemokines, including, CXCL13, CCL19, CCL21 and CXCL12 (chapter 1, section 1.4).

3.2. Results

3.2.1. RSV N gene RNA is detected after RSV infection of BEAS-2B cells

BEAS-2B cells were grown on 12-well plates until 80% confluent. Cultures of BEAS-2B cells were infected with RSV at a multiplicity of infection (MOI) of 0.025, 0.25 and 2.5 PFU/cell, with non-infected cells used as control for 12h. To confirm that BEAS-2B cells were infected with RSV, RNA was prepared and RSV N gene measured by RT-PCR (chapter 2, table 2.4). RSV N gene expression was measured by RT-PCR (table 3.1). There was no RSV N RNA in non-infected control cultures. However, after RSV infection (Figure 3.2.1), RSV N RNA was induced significantly at MOI=0.025 (fold expression relative to L32 = 0.05, P=0.02), MOI =0.25 (0.29, P=0.01) and MOI =2.5 (2.31, P=0.02) relative to L32 (Figure 3.1). RSV infection of BEAS-2B cells was increased by increase the viral load of MO1.

	1. Average of L32 Ct value	2. Average of RSV N Ct value	3. L32-RSV N (n)	4. Fold expression relative to L32(2 to the power of n)
Experiment 1				
Control	21.99	ND	ND	ND
RSV infection at 0.025	25.43	30.28	-4.85	0.03
0.25	24.50	26.08	-1.57	0.33
2.5	22.11	21.24	0.87	1.83
Experiment 2				
Control	22.18	ND	ND	ND
RSV infection at 0.025	25.12	29.15	-4.03	0.06
0.25	23.81	25.98	-2.17	0.22
2.5	23.57	22.48	1.08	2.12
Experiment 3				
Control	22.11	ND	ND	ND
RSV infection at 0.025	24.22	28.34	-4.11	0.05
0.25	25.42	27.22	-1.79	0.28
2.5	22.64	21.07	1.57	2.97

Table 3.1: Summary of steps used to calculate fold expression of RSV N from initial RT-PCR values

RNA relative to L32 in three separate experiments. 1) all L32 Ct values of the samples were averaged, 2) all RSV N probes Ct values were averaged, 3) the CT value of samples for RSV N probe were corrected to the house keeping gene L32. For example: The L32 expression – RSV N. This produced a Ct value relative to L32 expression, 4) Fold expression relative to L32 and this can be calculated by 2 to the power of n, where n = value determined in step 3 .This calculation converts the value from a Ct number to the fold difference. This particular calculation is because every cycle results in an increase in the amount of product two fold. Expression of RSV N RNA in BEAS-2B cells post RSV A2 (MOI=1) infection in three independent experiments (ND = not determined, Ct =cycle threshold, which is defined as the number of cycles required for the fluorescent signal to cross a threshold value).

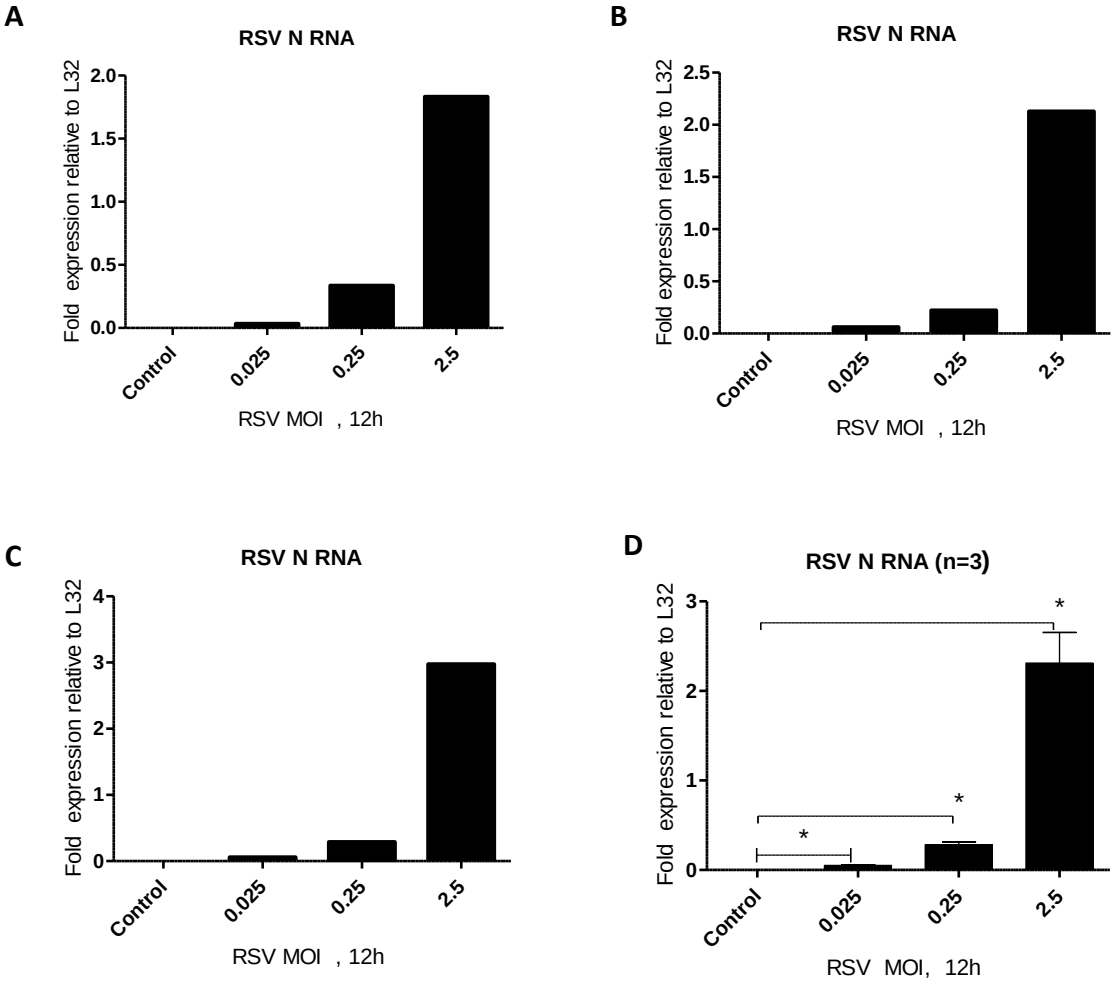

Figure 3.1. Detection of RSV RNA in BEAS-2B cells by RT-PCR

*BEAS-2B cells were infected with RSV at different MOI (0.025, 0.25 and 2.5) for 12h (A-C). RSV N RNA was induced in a dose dependent manner at each dose. The expression of RSV N RNA was increased significantly with increased MOI. Values are shown as fold expression in comparison to L32. The average of three independent experiments is shown in (D). (ND = not determined). Mean with SEM are shown (one way ANOVA followed with Bonferroni post-hoc test, *P <0.05, n=3).*

3.2.2. Following RSV infection BEAS-2B cells express BAFF mRNA in time-dependent manner

The influence of RSV infection on expression of BAFF mRNA by cultured airway epithelial cells was examined. 80% confluent of BEAS-2B cells were infected with RSV (A2 strain) at a multiplicity of infection of 1 (MOI= 1 PFU/cell) at time points, including time 0 (non-infected),3, 6, 12, 24, and 48h as described in (chapter 2, 2.7). At the time points indicated after RSV infection cell supernatants were removed and stored. Cells were isolated and RNA prepared using Qiagen (chapter 2, 2.4). Interestingly, BAFF mRNA was expressed consistently in non-infected BEAS-2B cells (less than -5 cycles relative to L32) (table 3.2). After RSV infection, BAFF mRNA expression was increased significantly at 6h (Fold increase relative to control = 9.35, P= 0.06) 12h, (91.05, P=0.04), 24h (48, P= 0.03) and 48h, (5.197, P=0.02) in comparison to non-infected control (Figure 3.2). BAFF mRNA expression was highest at 12h after RSV infection and declining significantly by 48hours.

	1. Average of L32 Ct value	2. Average of BAFF Ct value	3. L32-BAFF	4. Corrected to relative control (n)	5. Fold expression relative to control (2 to the power of n)
Experiment 1					
Control	24.35	29.85	-5.50	0	1
RSV infection at 3h	24.10	28.29	-4.19	1.30	2.47
6h	24.21	27.48	-3.27	2.23	4.69
12h	23.79	22.40	1.39	6.89	119.08
24h	23.95	23.46	0.49	5.99	63.82
48h	24.95	28.00	-3.05	2.45	5.47
Experiment 2					
Control	26.59	34.96	-8.37	0	1
RSV infection at 3h	25.08	34.91	-9.83	-1.46	0.36
6h	26.25	31.08	-4.83	3.54	11.65
12h	24.74	26.41	-1.67	6.69	103.86
24h	26.38	29.12	-2.73	5.63	49.71
48h	26.21	31.97	-5.76	2.61	6.11
Experiment 3					
Control	27.49	34.37	-6.88	0	1
RSV infection at 3h	26.26	34.77	-8.51	-1.62	0.32
6h	26.76	30.10	-3.33	3.54	11.69
12h	25.200	26.43	-1.23	5.64	50.20
24h	28.07	30.02	-1.94	4.93	30.66
48h	28.14	33.02	-4.88	2.00	4.003

Table 3.2. Summary of steps used to calculate fold expression of BAFF mRNA from initial RT-PCR values

BEAS-2B cells were infected with RSV A2 at (MOI=1) and BAFF mRNA expression was measured in three separate experiments. 1) All L32 Ct values of the samples were averaged, 2) all BAFF probes Ct values were averaged, 3) the CT value of samples for BAFF probe were corrected to the house keeping gene L32. For example: The L32 expression – BAFF. This produced a Ct value relative to L32 expression, 4) Corrected to relative control by taking the CT value produced in step 3 minus the cycle value for the relative control (unstimulated cells). 5) Fold expression relative to L32 and this can be calculated by 2 to the power of n, where n = value determined in step 4. This calculation converts the value from a ct number to the fold difference. This particular calculation is because every cycle is two fold. (ND = not determined, Ct =cycle threshold, which is defined as the number of cycles required for the fluorescent signal to cross the threshold).

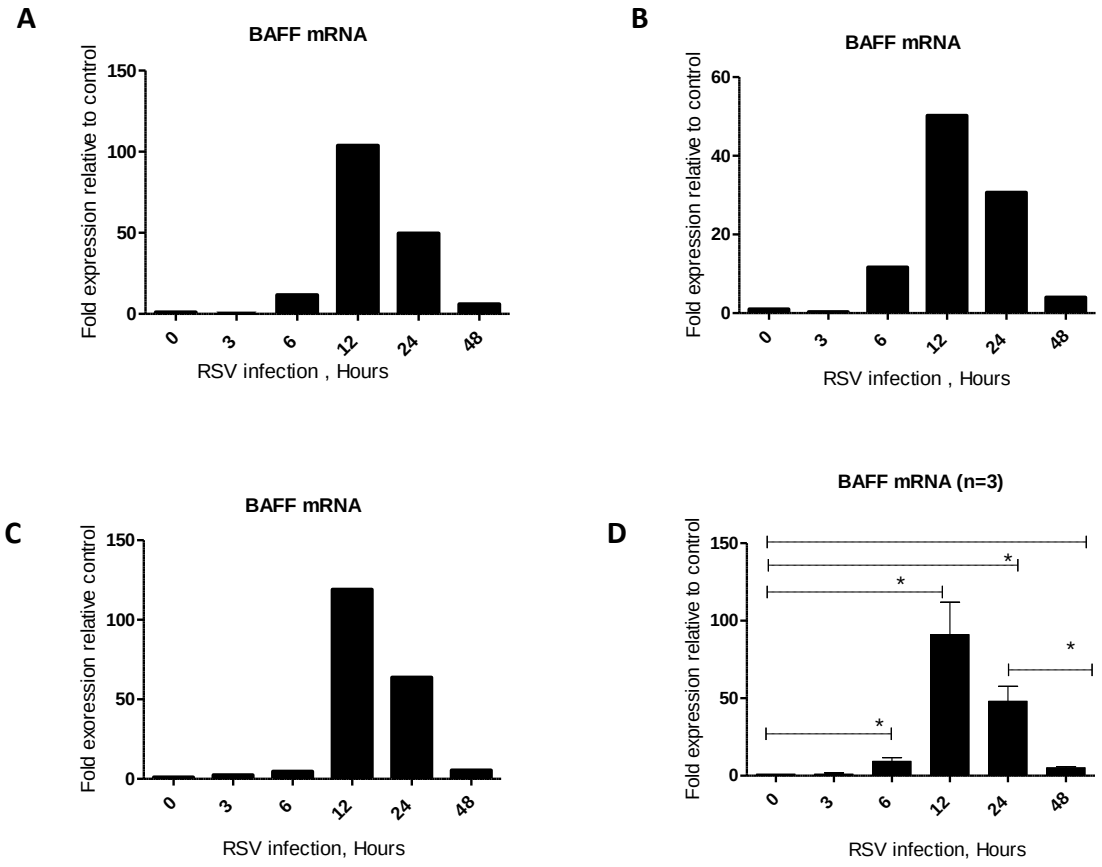

Figure 3.2. RSV infection of BEAS-2B cells induced BAFF mRNA expression in time- dependent manner

*BEAS-2B cells were infected with RSV A2 infection (MOI=1) for 0, 3, 6, 12, 24 and 48h. BAFF mRNA was measured by RT-PCR in three independent experiments (A-C). BAFF mRNA expression was induced significantly in a time –dependent manner, including 3, 6, 12, 24 and 48hours. Values are shown as fold expression in comparison to non-infected control. The average of three results is shown in (D). Mean with SEM are shown (one way ANOVA followed with Bonferroni post-hoc test, *P <0.05, n=3).*

3.2. 3. RSV infection of BEAS-2B cells results in increased BAFF mRNA expression in a dose –dependent manner

To determine the relationship between the level of RSV infection, or MOI of RSV infection and BAFF expression, BEAS-2B cells where infected with increasing amounts of RSV A2 (Figure 3.3) MOIs of (0.025, 0.25 and 2.5) for 12h. After infection the supernatants were removed, RNA prepared from the cells and BAFF mRNA expression analysed by RT-PCR. 12h was previously shown to be the optimum time point for BAFF mRNA expression (Figure 3.2.2). BAFF expression was elevated significantly at an MOI of 0.025 (fold increase 5, P=0.01), MOI of 0.25 (57, P=0, 01) and MOI of 2.5 (121, P=0.01) in comparison to non-infected control (1). BAFF mRNA expression was increased by increasing RSV load.

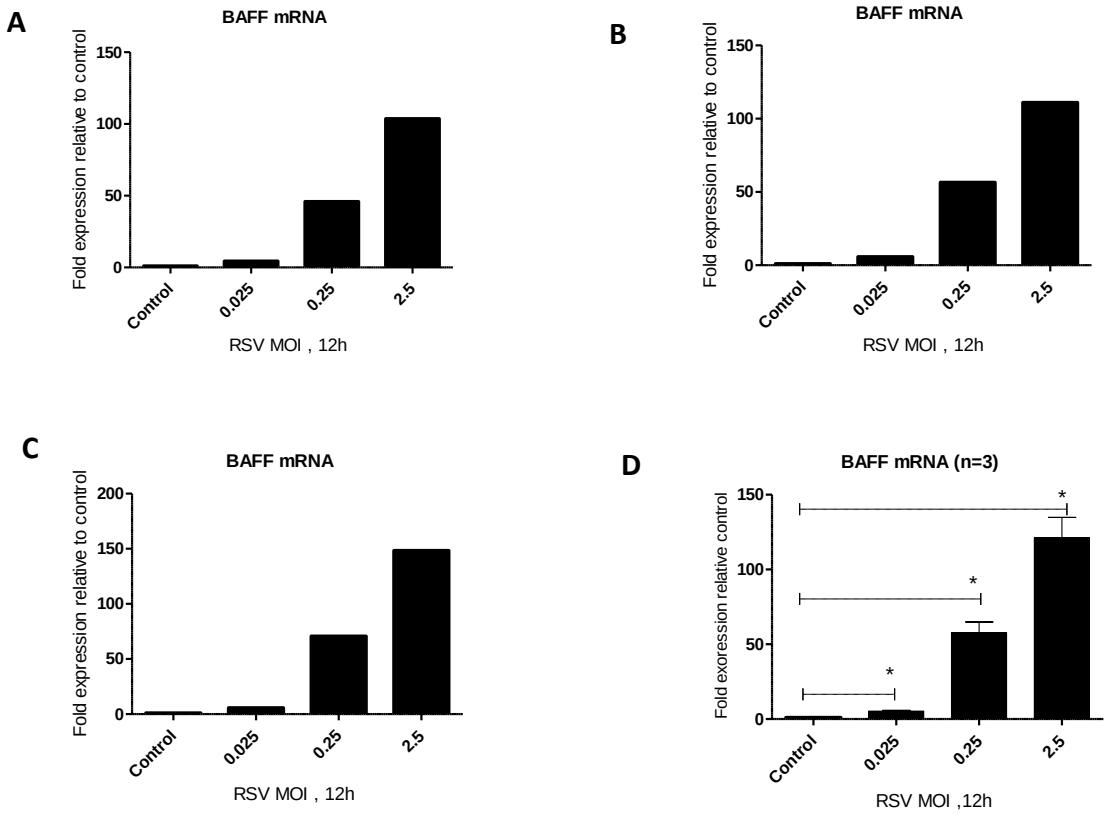

Figure 3 3. RSV infection of BEAS-2B cells induced BAFF mRNA expression in dose-dependent manner

*BEAS-2B cells were infected with various MOI of RSV A2 (0.025, 0.25 and 2.5) for 12h. BAFF mRNA expression was measured by RT-PCR. BAFF mRNA was significantly increased at each dose of MOI (A-C). Values are shown as fold expression in comparison to control. The average of three independent experiments is shown in (D). Mean with SEM are shown (one way ANOVA followed with Bonferroni post-hoc test, *P <0.05, n=3).*

3.2.4. RSV infection did not significantly up regulate APRIL mRNA expression

In order to determine if APRIL (Figure 3.4) can be also expressed after RSV infection, BEAS-2B cells were infected with different concentrations of RSV (A2) (MOI =0.025, 0.25 and 2.5) for 12h, supernatants removed and RNA prepared using Qiagen as described in (chapter 2, 2.4). APRIL mRNA expression was analysed by RT-PCR. There was no significant increase in expression of APRIL mRNA after RSV infection at MOI =0.025 (fold increase 1.07, P=0.4), MOI=0.25 (1.5, P=0.4) and MOI=2.5=0.1) in comparison to non-infected control.

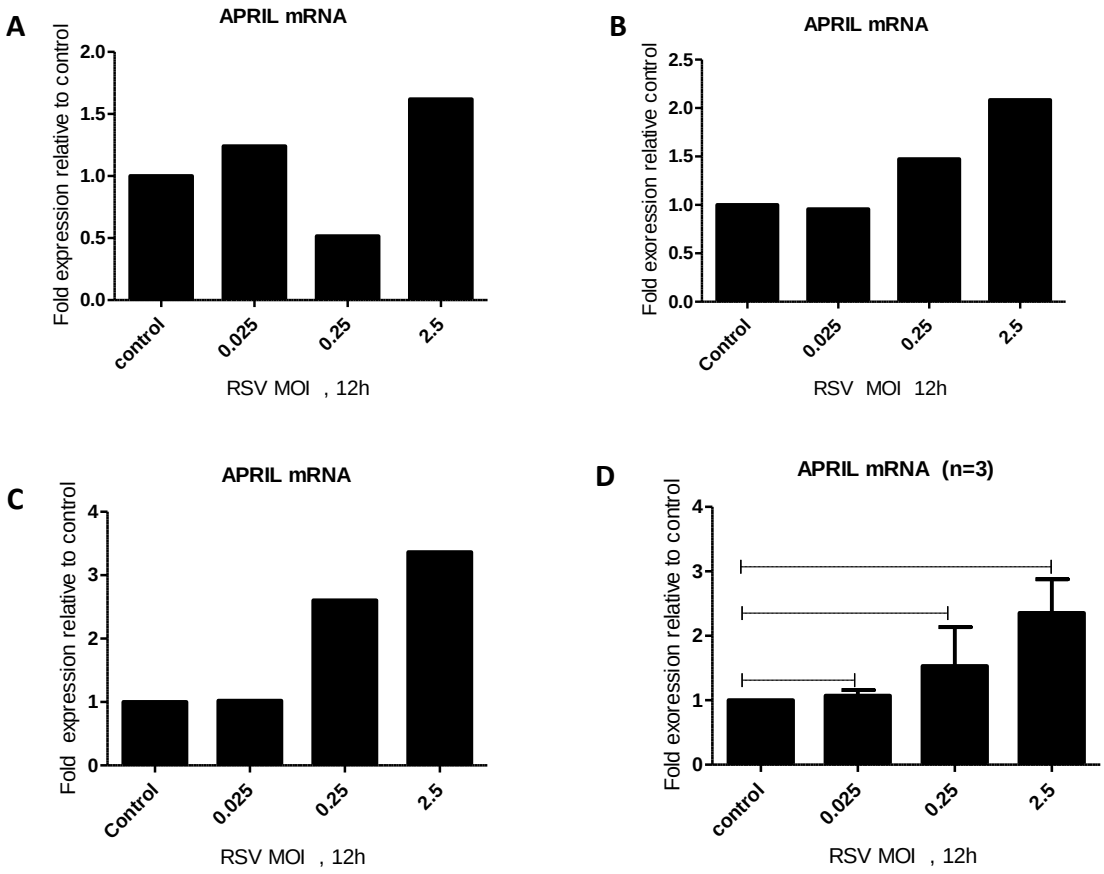

Figure 3.4. RSV infection of BEAS-2B cells did not significantly increase APRIL mRNA expression

*BEAS-2B cells were infected with RSV at MOI (0.025, 0.25 and 2.5) for 12h. APRIL mRNA was measured by RT-PCR. There was no significant increase of APRIL mRNA after RSV infection (A-C). Values are shown as fold expression in comparison to time 0 control. The average of three independent experiments is shown in (D). Mean with SEM are shown (one way ANOVA followed with Bonferroni post-hoc test, *P <0.05, n=3).*

3.2. 5. RSV infection of BEAS-2B results in increased BAFF protein expression in dose dependent manners

To confirm epithelial production of BAFF protein and not only mRNA after RSV infection, BAFF protein concentration (Figure 3.5) was measured in cell culture supernatants using a specific BAFF ELISA (chapter 2, 2.5). Significant levels of soluble BAFF were detected in the culture supernatant after RSV infection with different MOI in a dose dependent manner. Production of BAFF protein was increased significantly at MOI =0.025 (mean=11, P=0.01), MOI=0.25 (28, P=0.002) and MOI=2.5 (42, P=0.02) in comparison to non-infected control. BAFF protein levels were increased by increased RSV MOI.

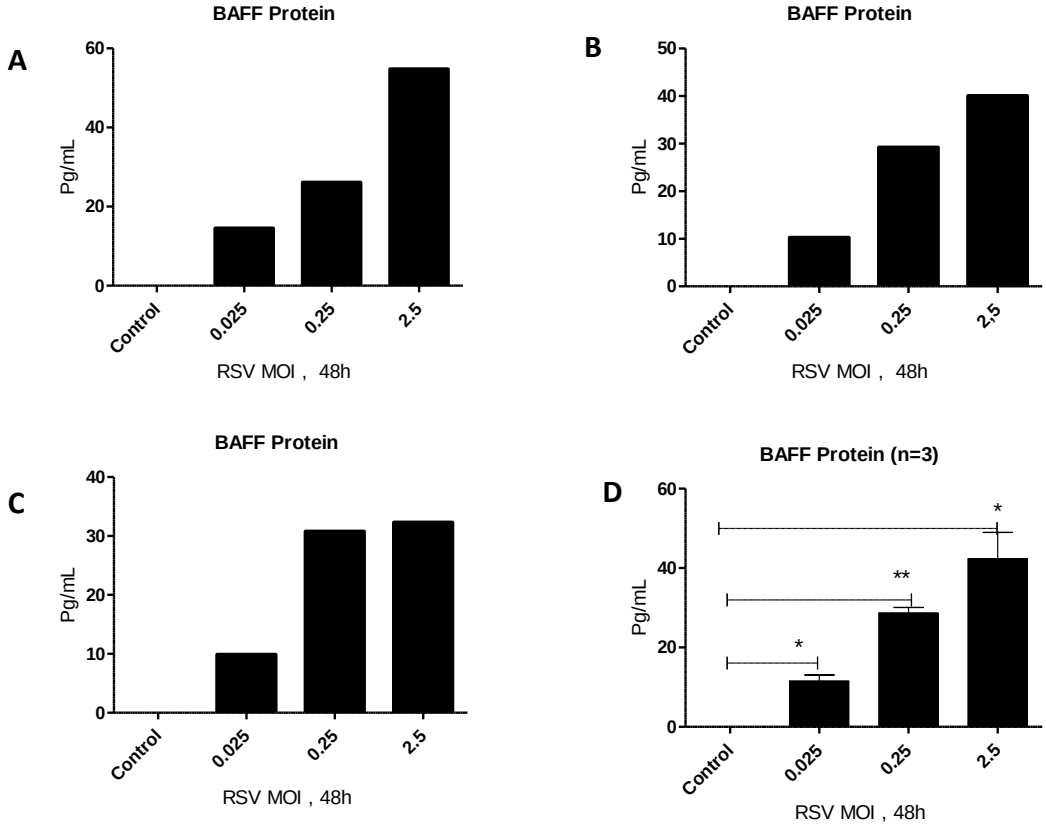

Figure 3.5. RSV infection of BEAS-2B results in increased BAFF protein expression in dose dependent manners

*BEAS-2B cells were infected with RSV A2 at MOI's of (0.025, 0.25 and 2.5) for 48h. BEAS-2B cells cultures supernatant were collected and BAFF protein measured using a specific Human BAFF ELISA. BAFF protein levels were increased significantly after RSV infection and increased at high MOI (A-C). The average values from these three independent experiments are shown in (D). The software (KC Junior software) was used to find out the BAFF protein concentration. Mean with SEM are shown (one way ANOVA followed with Bonferroni post-hoc test, *P <0.05, n=3).*

3.2.6. Effect of cytokines on the expression of BAFF in BEAS-2B cells

To determine if pro-inflammatory cytokines (Figure 3.6) can induce APRIL or BAFF expression BEAS-2B cells were stimulated with the pro-inflammatory cytokines IFN-α, IFN-β and IL-1β and also LPS and dsRNA (200 ng /ml) for 12h. Among these stimuli, IFN- β was found to significantly induce BAFF mRNA expression (fold increase relative to control=177, P=0.01) in comparison to unstimulated control (1). Furthermore, there was no significant increase in expression of BAFF mRNA after stimulation of BAES-2B cells with IFN-α (18.13, P=0.2), IL-1 β (1.3, P=0.7), LPS (2.60, P=0.4), and dsRNA (2.66, P=0.3).

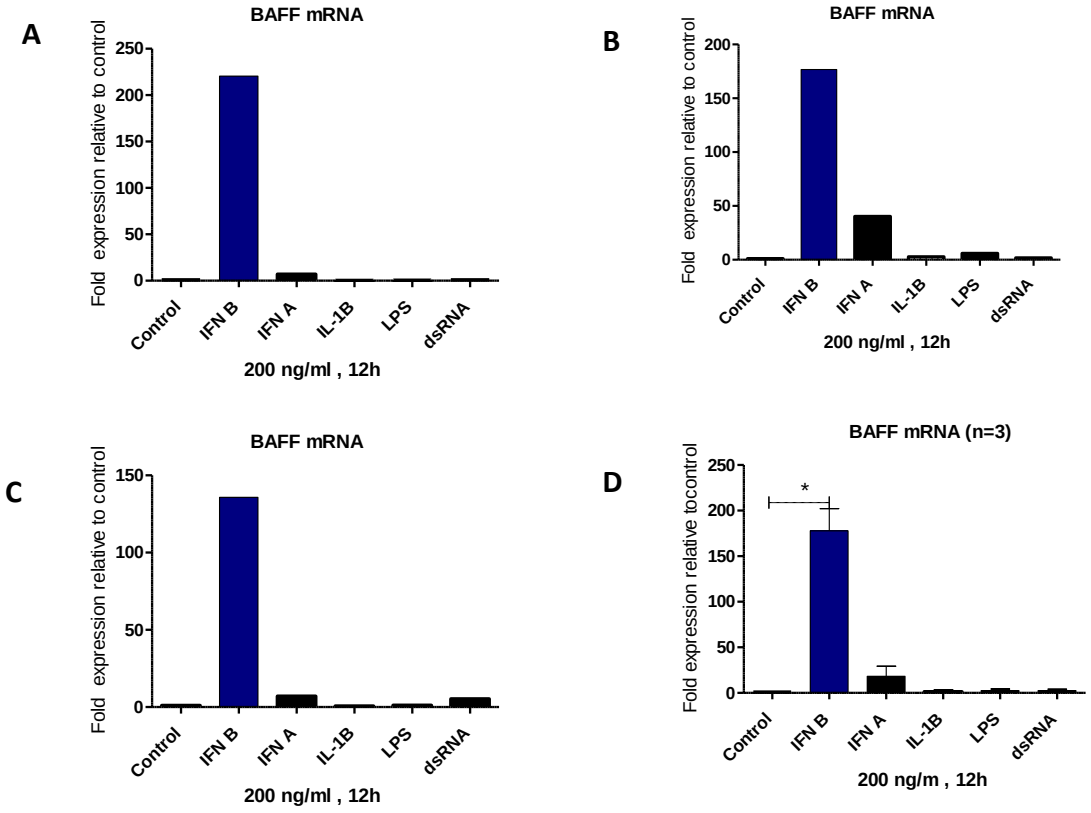

Figure 3.6. Effect of cytokines on the expression of BAFF mRNA in BEAS-2B cells

*BEAS-2B cells were stimulated with 200 ng/ml dsRNA, IL-1β, ng/ml, IFNα, LPS or IFN-β for 12h (A-C). BAFF mRNA was measured by RT-PCR. IFN-β was found to induce significant levels of BAFF mRNA. Values are shown as fold expression in comparison to control .In (D) results shown are average of three independent experiments. Mean with SEM are shown (one way ANOVA followed with Bonferroni post-hoc test, *P <0.05, n=3).*

3.2. 7. IFN-β stimulation of BEAS-2B cells induces BAFF mRNA expression in a dose dependent manner

To determine if BAFF expression is increased in a dose dependent manner by IFN-β treatment, BEAS-2B cells were incubated with increasing concentrations of IFN-β, (1 ng/ml, 5 ng/ml, 10 ng/ml, 100 ng/ml and 200 ng/ml) for 12h. Significant increases in levels of BAFF mRNA (Figure 3.7) expression were observed. This increase occurred in a dose-dependent manner after stimulation of IFN-β at 1 ng/ml (fold increase relative to control= 68, P=0.04), 5 ng/ml (120, P=0.03), 10 ng/ml (150, P=0.007), 100 ng/ml (169, P=0.0009) and 200 ng/ml (182, P=0.01) in comparison to non-infected control (1).

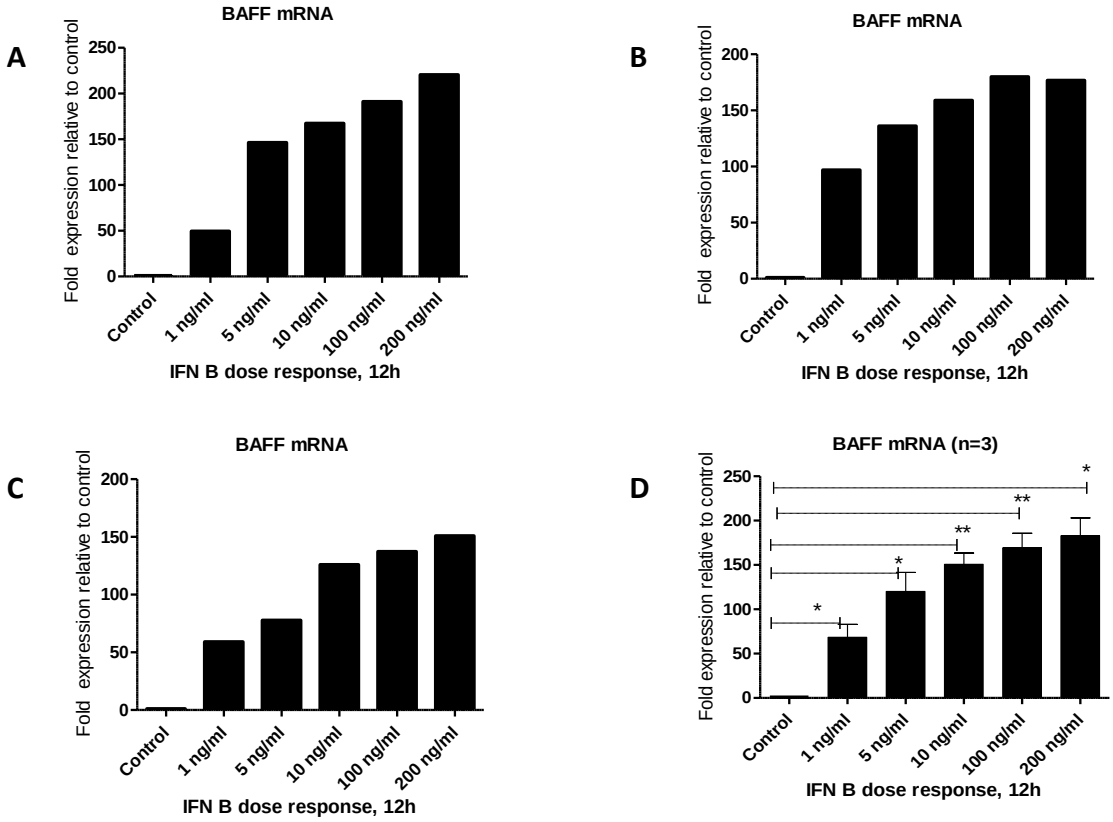

Figure 3.7. IFN-β stimulation of BEAS-2B cells induces BAFF mRNA expression in a dose dependant manner

*BEAS-2B cells were stimulated various concentrations of IFN-β (1 ng/ml, 5 ng/ml, 10 ng/ml, 100 ng/ml and 200 ng /ml) for 12h. BAFF mRNA was measured by RT-PCR. BAFF mRNA was induced significantly in a dose dependent manner (A-C). Values are shown as fold expression relative to control. The average of three independent experiments (D). Mean with SEM are shown (one way ANOVA followed with Bonferroni post-hoc test, *P <0.05, n=3).*

3.2. 8.IFN-β induced BAFF mRNA expression in time –dependent manner

To evaluate the influence of IFN-β stimulation on expression of BAFF mRNA by cultured airway epithelial cells BEAS-2B cells were incubated with 200 ng/ml of IFN-β, for varying times (Figure 3.8). This concentration was shown previously to induce the highest level of BAFF expression for different times (0, 3, 6, 12, 24, 48h). IFN β stimulation significantly induced BAFF mRNA expression in time dependent manner at 3h (fold increase relative to control=45, P=0.03), 6h (179, P=0.02) and 48h (6, P=0.04). The expression of BAFF mRNA reached high levels at 12h (245, P=0.01). Afterwards, BAFF mRNA was decreased significantly at 24h (30, P=0.007) and reached lower levels at 48h (6, P=0.01).

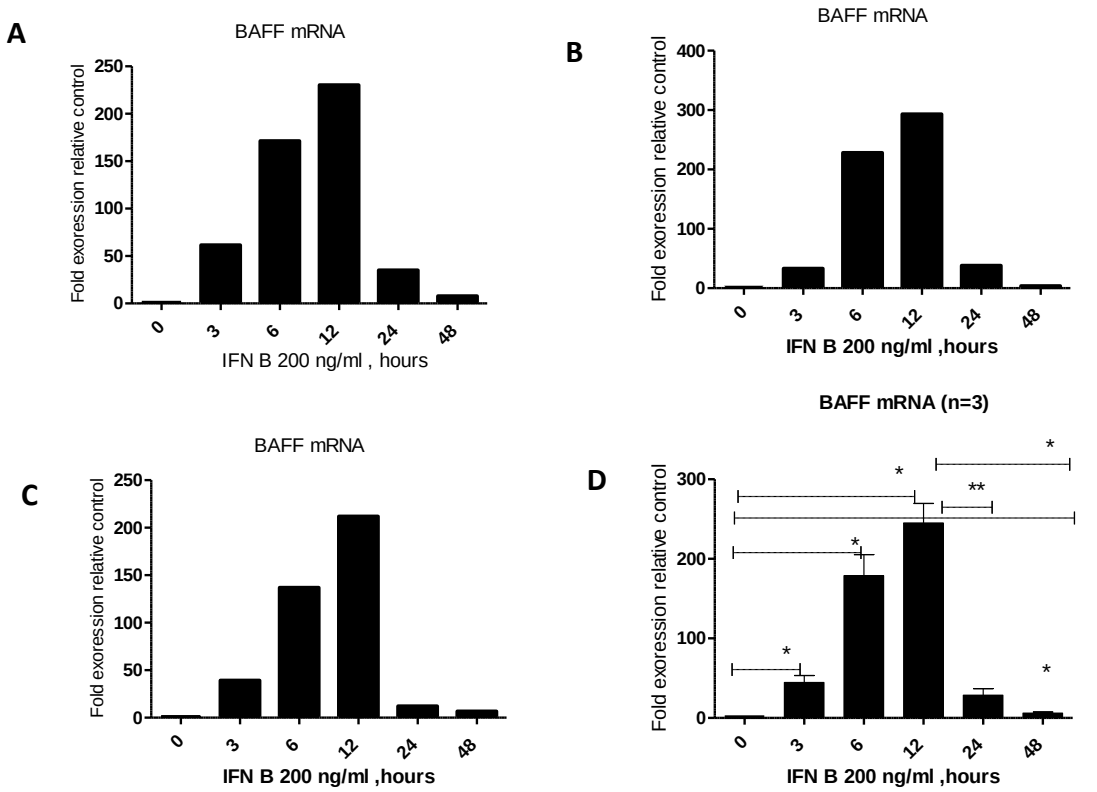

Figure 3.8. IFN-β induced BAFF mRNA expression in time–dependent manner

*BEAS-2B cells were stimulated with IFN-β 200 ng/ml for (0, 3, 6, 12, 24 and 48h). BAFF mRNA was measured by RT-PCR. BAFF mRNA was increased significantly in time dependent manner. BAFF mRNA reached high levels at 12h after IFN β stimulation (A- C). Values are shown as fold expression relative to control. The average of three independent experiments (D). Mean with SEM are shown (one way ANOVA followed with Bonferroni post-hoc test, *P <0.05, n=3).*

3.2.9. IFN-β induced BAFF protein expression in dose–dependent manner

To confirm epithelial production of BAFF protein and not only mRNA, BEAS-2B cells were stimulated with IFN-β at concentrations of 1 ng/ml, 5 ng/ml, 10 ng/ml, 100 ng/ml and 200 ng/ml for 48h. Significant levels of BAFF protein (Figure 3.9) were detected in the culture supernatant. Production of BAFF protein was increased significantly by stimulation with IFN-β at a concentration of 1 ng/ml (mean 127, P=0.0009), 5 ng/ml (172, P=0.003), 10 ng/ml (219, P=0.0009), 100 ng/ml (204, P=0.001) and 200 ng/ml (233, P=0.002) in comparison to non-stimulated control (0).

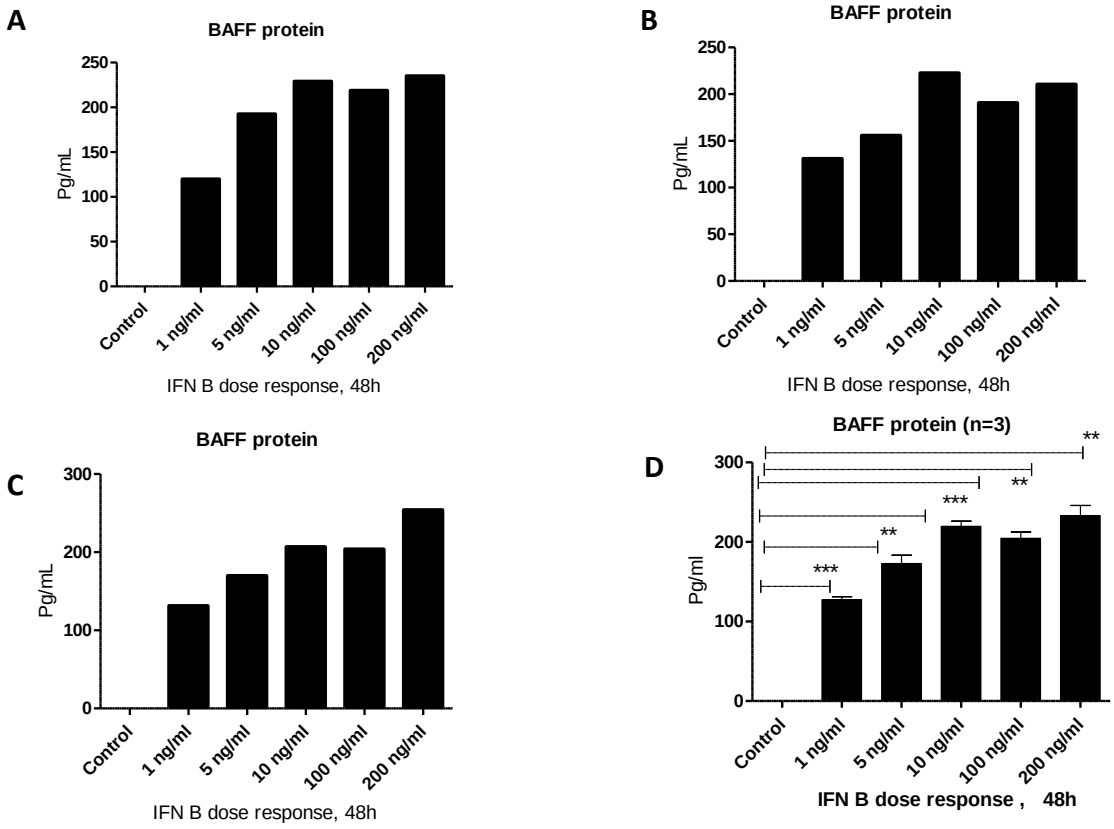

Figure 3.9. IFN-β induced BAFF protein expression in dose dependent manner

*BEAS-2B cells were stimulated with various concentrations of IFN-β (1 ng/ml, 5 ng/ml, 10 ng/ml, 100 ng/ml and 200 ng/ml) for 48h. BAFF protein was measured in the culture supernatants by specific human BAFF ELISA (A-C). BAFF protein concentrations were increased significantly in dose dependent manner. The average of three independent experiments (D). Mean with SEM are shown (one way ANOVA followed with Bonferroni post-hoc test, *P <0.05, n=3).*

3.2.10. RSV infection of cultured BEAS-2B cells induces BAFF expression by an IFN-β dependent mechanism

In order to determine if BAFF expression was directly induced by RSV infection or if it was indirectly dependent on interferon β production by RSV infected cells, BAFF expression in BEAS-2B cells was compared in the presence or absence of an anti-interferon β-neutralising antibody. 5 µl of anti-IFN-β (20 µg/mL, chapter 2, 2.1.7) was added into BEAS-2B cells cultured into 96-well plate at 2 x 10^4 cells/ml. BAFF mRNA expression (Figure 3.10.1) was induced significantly after RSV infection at 12h (fold increase relative to control= 21, P=0.04) relative to control. Moreover, BAFF protein (Figure 3.10.2) was induced significantly after RSV infection at 48h (mean 20, P= 0.003) in comparison to control (0). However, treatment with neutralising anti-interferon β antibody inhibited production of BAFF mRNA (8.80, P=0.04) and protein expression (mean 13, P=0.04). These results indicate that BAFF produced initially following RSV infection, at the very least, is dependent on interferon β production.

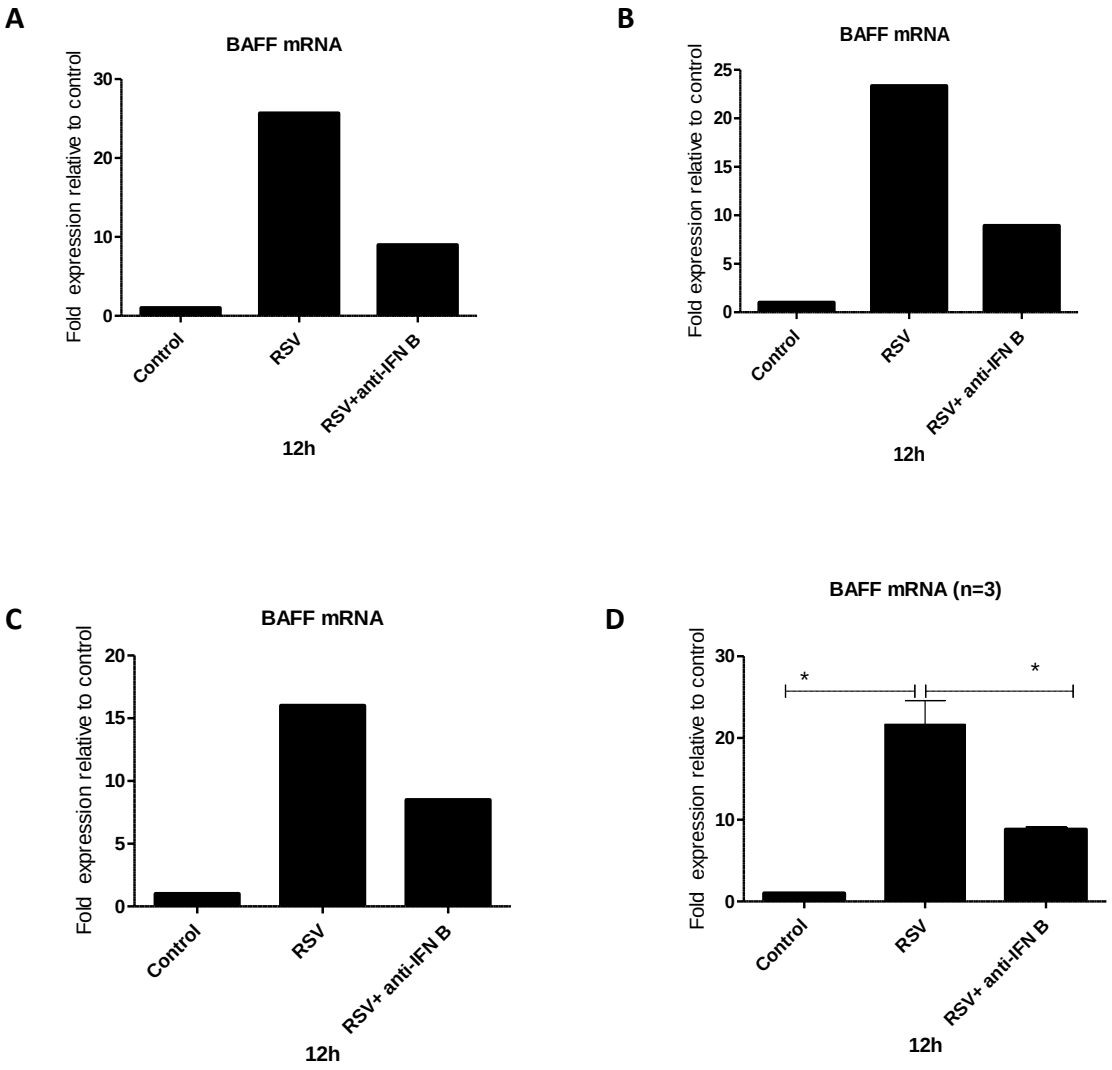

Figure 3. 10.1: BAFF mRNA expression following RSV infection is dependent on IFN β

*BEAS-2B cells were infected with RSV at (MOI =1) for 12h. Matched samples contained addition of a neutralizing anti-human IFN β antibody (A-C). RSV infection of BEAS-2B cells induced significant BAFF mRNA at 12h and after added anti-IFN β antibody, BAFF mRNA was decreased significantly. Values are shown as fold expression in comparison to control. In (D) results shown are average of three independent experiments. Mean with SEM are shown (one way ANOVA followed with Bonferroni post-hoc test, *P <0.05, n=3).*

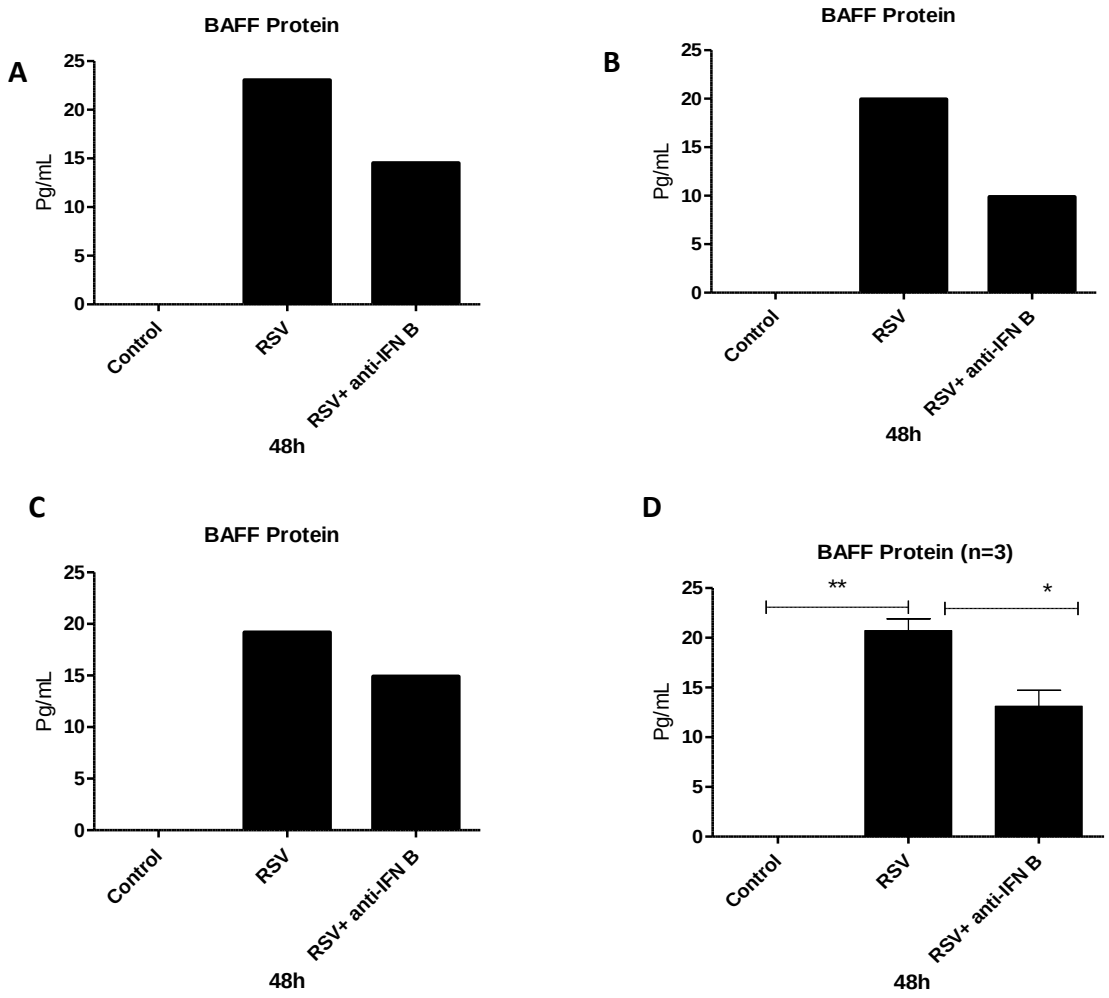

Figure 3. 10.2. BAFF protein expression following RSV infection is dependent on IFN-β

*BEAS-2B cells were infected with RSV at (MOI =1) for 48h. Matched samples also contained a neutralizing anti-human IFN-β antibody. RSV infection of BEAS-2B cells induced significant BAFF protein at 48h and after added anti-IFN β antibody, BAFF protein was decreased significantly. In (D) results shown are average of three independent experiments. Mean with SEM are shown (one way ANOVA followed with Bonferroni post-hoc test, *P <0.05, n=3).*

3.2.11. Cell surface expression of BAFF after RSV infection in BEAS-2B cells

To examine what form of BAFF (chapter 1, section 1.2.1.3) airway epithelial cells express after RSV infection, BEAS-2B cells were plated into a 24-well plate at 8×10^3 cells/well and infected with RSV at MOI=1 for 12, 24 and 48h. Then, cells were extracted by cell scraper, washed with PBS and centrifuged at 400 g/ for 10 minutes, the pellet was lysed with (SDS) buffer containing 10% DTT and protease inhibitors (1:100) and analysed by western blot (chapter 2, 2.10). Interestingly, non-infected epithelial cells expressed membrane BAFF (31kD) (Figure 3.11.A). However, after RSV infection membrane BAFF was expressed at 12hours and slightly less in 24hours. At 48hours after RSV infection supernatants were collected and BAFF protein measured by specific human BAFF ELISA. BAFF protein (17 kD) was expressed significantly (mean =29, P=0.002) in comparison to control after RSV infection (Figure 3.11.B).

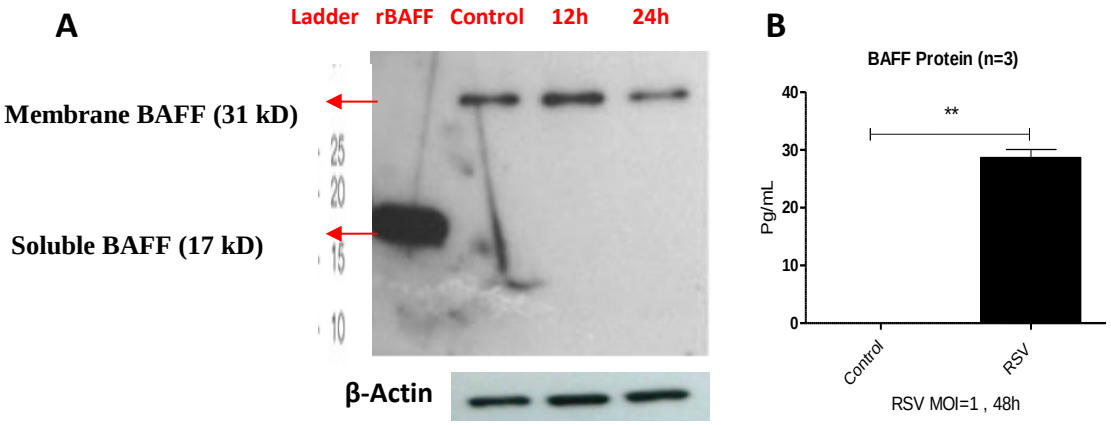

Figure 3.11. Western blot of analysis of BAFF expression by BEAS-2B cells after RSV infection

BEAS-2B cells were infected with RSV at MOI=1 for 12 and 24h (A). Western blot was run under reduced conditions. Non -treated BEAS-2B cells expressed membrane BAFF (31kD). The RSV infected BEAS-2B cells expressed membrane BAFF (31 kD). B-actin control was used to ensure all the samples were loaded equally. Human recombinant BAFF (rBAFF) was used as positive control for soluble BAFF (17 kD). Ladder was used to determine the molecular weight of BAFF. In (B) soluble BAFF (17 kD) was detected at 48h int the culture supernatant of BEAS-2B cells after RSV infection by using specific human BAFF ELISA (paired t test, n=3).

3. 2.12.Mechanism of BAFF cleavage

BAFF can be found into two forms, a membrane bound and a soluble molecule. It has been reported that soluble BAFF is derived from the membrane-bound BAFF by cleavage with a putative furin family protease or derived from intracellular processing of the longer form by the same enzyme (Nardelli *et al.* 2001; Scapini *et al.* 2003).

Thus, I hypothesized that if production of soluble BAFF during RSV infection was furin dependent, inhibition of furin convertase enzyme would result in increased expression of membrane bound BAFF.

To test this hypothesis and determine if soluble BAFF release relies on furin cleavage, BEAS-B cells were infected with RSV at MOI =1 and incubated with 50 or 100 μM of the furin convertase inhibitor chloromethylketone 6hours after RSV infection and samples collected at 24 and 48h (Figure 3.12).

Non-infected BEAS-2B cells expressed membrane BAFF at 24h and 48h. Moreover, RSV induced membrane BAFF expression at 24h and disappeared at 48h. Targeting furin convertase enzyme did not increase the expression of membrane BAFF at 24h and 48h. However, at high concentration of furin convertase inhibitor 100 Mm membrane BAFF expressions was reduced. This could be as a result of toxicity.

Furthermore, Brefeldin A is known to inhibit protein secretion by cells. Thus, adding Brefeldin A to the RSV infected BEAS-2B cells should not alter BAFF production if it is cleaved from the cell surface by a furin convertase. Expression of membrane BAFF was not affected by Brefeldin A at 24 and 48h (Figure 3.12).

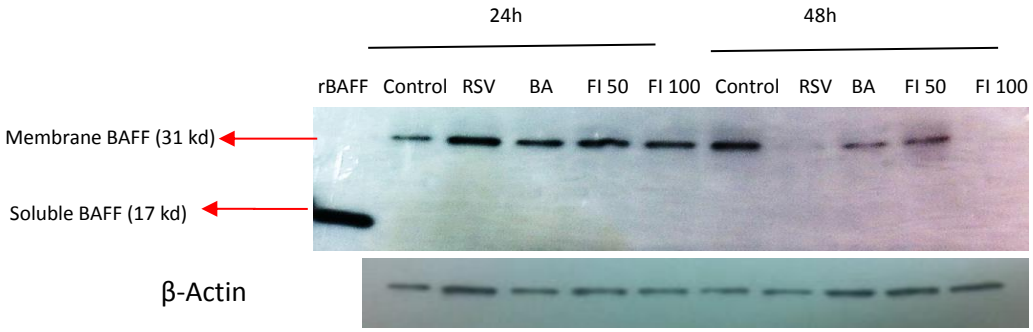

Figure 3.12. Effect of Brefeldin A (BA) and furin convertase inhibitor (FI) on the expression of BAFF following RSV infection

BEAS-2B cells were infected with RSV at MOI=1 for 24h and 48h. BEAS-2B cells were incubated with Brefeldin A (BA 1:100) and furin convertase inhibitor (FI) (50 μM*, 100* μM*). Non-infected cells expressed membrane BAFF. RSV induced expression of membrane BAFF after 24h and disappears at 48h. Targeting furin did not increase the expression of membrane BAFF at 24h and 48h. However, at high concentration of FI 100* μM *membrane BAFF expression was reduced. There was no clear effect of BA on the expression of membrane BAFF at 24h after RSV infection, which suggests that BAFF cleaved form the cell surface. β actin control was used to ensure all the samples were loaded equally. Human recombinant BAFF (rBAFF) was used as positive control for soluble BAFF (17 kD).*

3.2.13. Immunofluorescent localization of BAFF expression in cultured BEAS-2B cells

3.2.13.1. IFN-β induces BAFF expression in BEAS-2B cells

To further confirm BAFF expression, BEAS-2B cells were treated with different concentrations of IFN-β, including 1ng/ml, 10 ng/ml and 100 ng/ml for 24h and nonstimulated cells used as control. BAFF has been stained with specific monoclonal antibody anti-BAFF FITC (green). Of note, un-stimulated BEAS-2B cells expressed BAFF (Figure 3.13.1.A) and BAFF was localized around cells as indicated by arrow. This further confirmed that non stimulated cells express BAFF (Figures 3.11 and 3.12). However, after IFN-β stimulation there was strong positive staining of BAFF that could be soluble BAFF bound to the extra cellular matrix around cells and nearby (Figure 3.13.1.B-D), and no comparable staining was noticed with the isotype control.

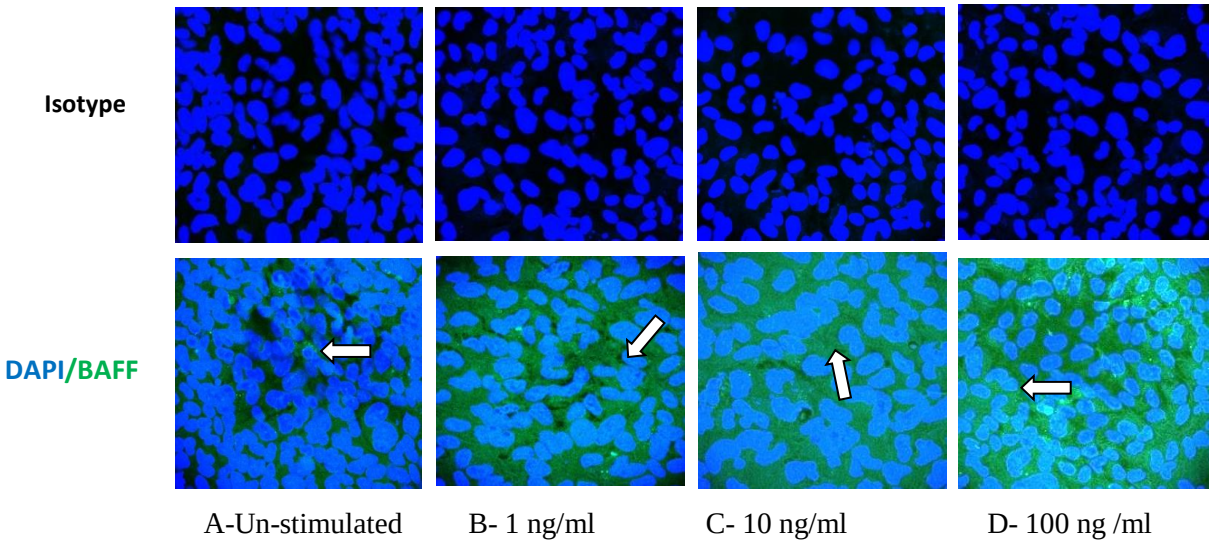

Figure 3.13.1. Localization of BAFF in BEAS-2B cells stimulated with IFN-β

BEAS-2B cells were stimulated with different concentrations of IFN-β (1ng/ml, 10 ng/ml and 100 ng/ml) for 24h. In (A) un-stimulated BEAS-2B cells expressed BAFF (green) as indicated by arrow. In (B-D) there was strong positive staining of BAFF (green) after IFN-β stimulation. Isotype control was applied in each test and no comparable staining was noticed with the isotype control. Cell nuclei shown in blue (DAPI). Images A–D were originally obtained using confocal microscopy at 40x magnification.

3.2.13. 2. RSV infection of BEAS-2B cells induced BAFF expression

To evaluate expression of BAFF in BEAS-2B cells after RSV infection both BAFF and RSV were visualized by immunofluorescence staining. BEAS-2B cells were infected with RSV at (MOI =1) for 24h. BAFF (green) was expressed in non-infected BEAS-2B cells (Figure 3.13.2. A). However, after RSV infection, there was strong positive staining of BAFF (Figure 3.2.13.2.B), and RSV (red) was detected in cytoplasm of infected cells (Figure 3.13.2.C), and no comparable staining was noticed with the isotype control.

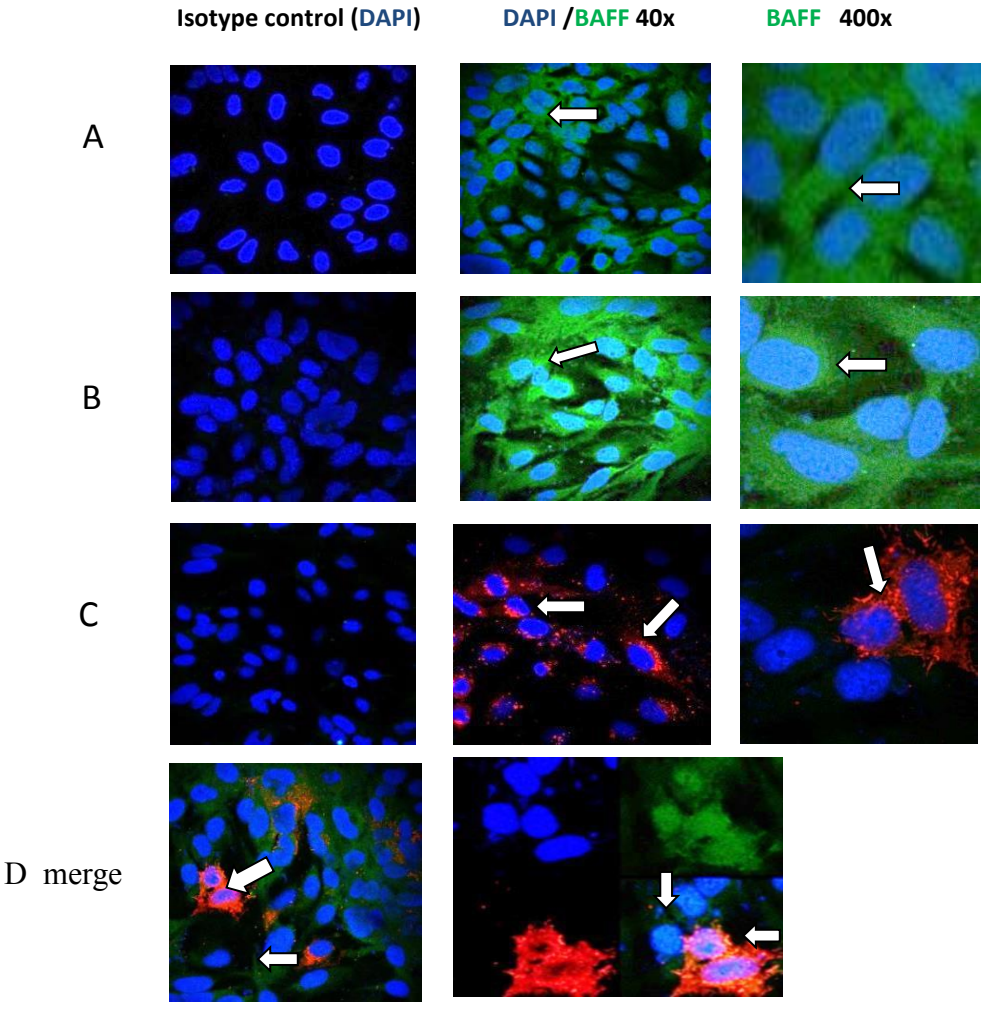

Figure 3.13.2. Localization of BAFF in BEAS-2B cells following RSV infection

BEAS-2B cells were infected with RSV at (MO1=1) for 24h. In (A) non infected BEAS-2B cells showed positive staining of BAFF (green). In (B) there was strong positive staining of BAFF (green) after RSV infection. In (C) RSV was detected in the cytoplasm of infected cells (red). In (D) RSV (red) and BAFF (green) were detected after RSV infections. All the isotype controls were applied in each test. Cell nuclei shown in blue (DAPI). Images (A–D) were originally obtained using confocal microscopy at 40x and 400x magnification.

3.2.14. The functional activity of BAFF secreted by RSV infected BEAS-2B on the survival of B cells

To determine if BAFF derived from RSV infected epithelial cells was able to support B cell survival, purified human B cells (chapter 2, section 2.2.1) were cultured with or without addition of concentrated supernatant from RSV infected or non-infected BEAS-2B cells for 5 days and B cell survival measured by MTT assay (Chapter 2.9). For stimulation, culture supernatants were collected from BEAS-2B cells infected for 48hours with RSV, and from cultures without RSV infection and concentrated (Chapter 2.1.6). Comparison was made between B cells incubated alone, with addition of recombinant BAFF as a positive control, or with concentrated supernatants from BEAS-2B cells, either non infected or infected with RSV. Human recombinant BAFF (10 ng/ml) significantly enhanced B cell survival compared with media alone (mean OD=0.18, P=0.006) (Figure 3.14). Furthermore, RSV concentrated supernatant significantly increased B cell survival in comparison to RSV non- infected control (mean 16, P=0.04), which significantly suppressed B cell survival (0.09, P=0.03).

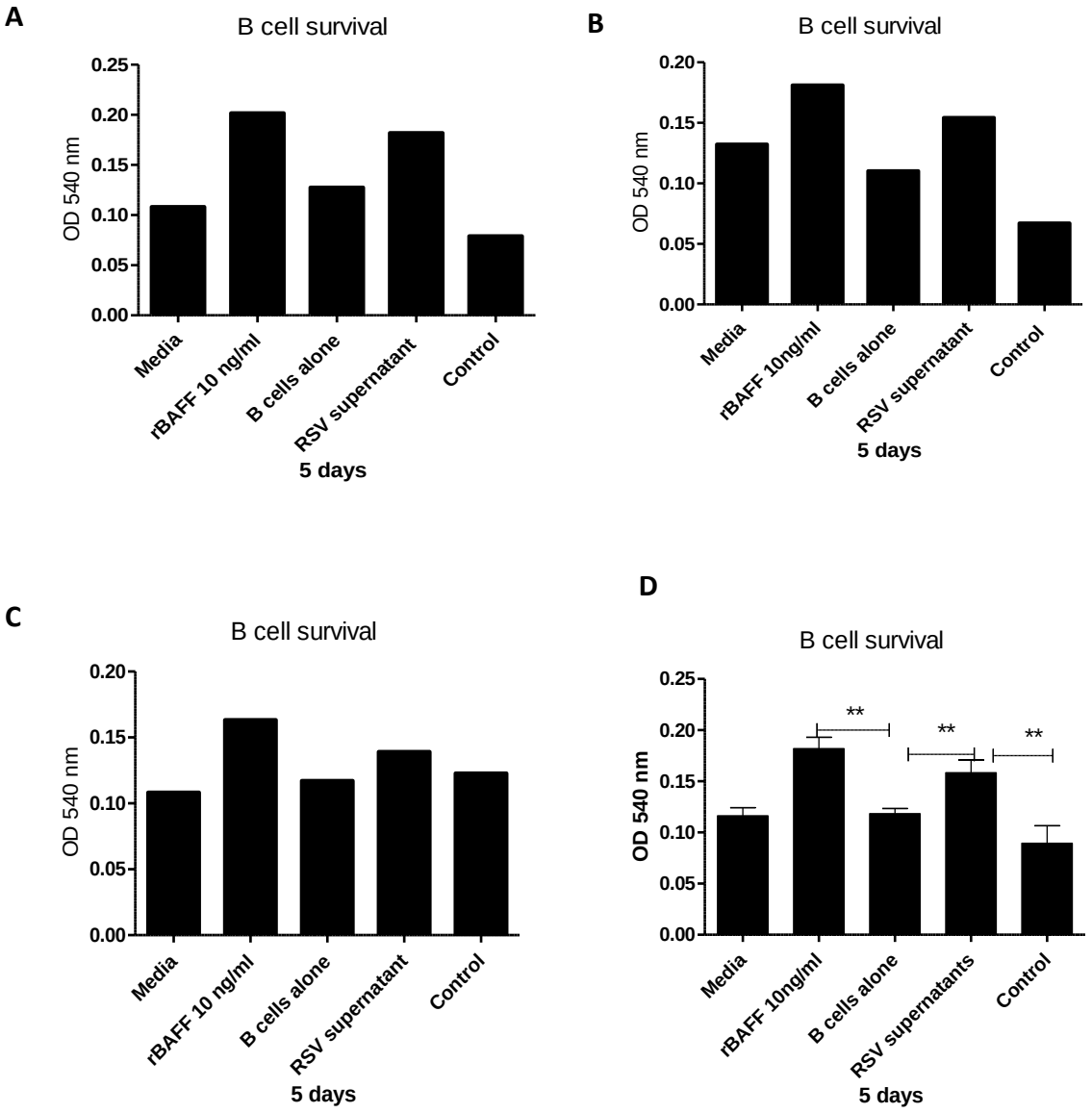

Figure 3.14. Effect of epithelial cells secreted BAFF on the cell survival of B cells

*Purified Human B cells were incubated alone with media, stimulated with 10 ng/ml rBAFF, or concentrated supernatants from RSV infected and non-infected of BEAS-2B collected at 48h, for 5 days. Each sample was triplicated with taken the average (A-C). The average of three independent experiments is shown in (D). The O.D. absorbance was 540 nm. B cell survival was measured by MTT assay. Mean with SEM are shown (one way ANOVA followed with Bonferroni post-hoc test, *P <0.05, n=3).*

3.2.15. RSV infection of BEAS-2B cells induce expression CCL21 mRNA, but not CXCL12, CXCL13 and CCL19

To further understand the ability of epithelial cells to support the adaptive immune response by recruitment of B cell responses, expression of chemokines, CXCL12, CXCL13, CCL19 and CCl21 (Chapter 1.4) by BEAS-2B cells following RSV infection was studiedFigure. BEAS-2B cells were infected at an MOI of 1 for 3, 6, 12, 24 and 48 and 72 h. After infection supernatant was collected and RNA prepared from the cells using Qiagen as described in the (chapter 2, 2.4). There was no mRNA or protein expression for CXCL12, CXCl13, CCL19 and CCL21 after RSV infection.

3.3. Discussion

3.3.1. Determination of RSV infection in BEAS-2B cells

The main targets of RSV infection are bronchial and bronchiolar epithelial cells, especially those that are ciliated (Johnson *et al.* 2007). To confirm that BEAS-2B cells were infected and determine the level of RSV infection for 12h, RSV N RNA was measured by RT-PCR. There was no expression of RSV N RNA in non-infected control cells. However, after RSV infection, RSV N RNA was induced significantly at MOI=0.025, 0. 25 and 2.5 (Figure 3.1). RSV A2 titre obtained in the PCR analysis of BEAS-2B cells was increased by increasing the virus dose and BEAS-2B cells showed permissive replication and response to RSV infection.

In vitro, the most common models for the study of airway epithelial cells responses to RSV infection are immortalized respiratory epithelial cell lines such as BEAS-2B cells. However, their response to RSV infection is different from primary airway epithelial cells and might not accurately reflect the actual immune response to RSV infection by primary cells. These variations include different kinetics of viral replication, decreased cytotoxic responses and reduced production of pro-inflammatory cytokines (Fonceca *et al.* 2012).

Measuring RSV infection by RT-PCR has several advantages over the plaque assay method (Chapter 2.6.2). RT-PCR is more sensitive, specific, rapid and allows quantification of RSV replication. However, RT-PCR only measures N gene RNA, whereas for plaque assay the whole infective plaque forming unit of virus is measured.

3.3.2. RSV infection of BEAS-2B cells significantly induced expression of BAFF mRNA and protein but not APRIL

Non-infected BEAS-2B cells consistently expressed low levels of BAFF mRNA (less than 5 cycles relative to L32 control, (Table 3.2). In contrast, after RSV infection, BAFF mRNA expression was increased significantly at 6h after RSV infection in comparison to non-infected control (FFigure 3.2). BAFF mRNA reached highest levels after 12h and declined significantly at 48h, which suggested that BAFF protein is released at this time point where it has been measured in the culture supernatant (FFigure 3.5).

Furthermore, BAFF mRNA (Figure 3.3) and protein (Figure 3.5) expression were elevated significantly at different MOIs of RSV in comparison to non-infected control. These results demonstrated that RSV infection of airway epithelial cells induces significant expression of both BAFF mRNA and BAFF protein and their expression are increased at higher RSV MOIs, this could be as a result of increased production of IFN-β following RSV infection.

APRIL mRNA expression but not protein was also measured by RT-PCR. By contrast to BAFF, there was no significant increase of APRIL mRNA after RSV infection or at different MOI in comparison to non-infected control (Figure 3.4). Due to the lack of any measurable increase in APRIL mRNA expression and the low sensitivity of commercially available APRIL ELISA assays which have minimal detection levels of around 400 pg/ml, APRIL protein expression was not studied further in these experiments.

Furthermore, BAL samples taken from infants with severe RSV infection in comparison to control infants did not show increased expression of APRIL protein, although APRIL mRNA was constitutively expressed at levels five times higher than BAFF in primary epithelial brushings from healthy control children (McNamara *et al.* 2013). However, APRIL protein (1518±635 pg/ml) has previously been detected in nasopharyngeal secretion samples from surviving infants with acute bronchiolitis and detected in the lower respiratory tract in an immunohistochemical analysis of lung tissue from infants who died of acute RSV (Reed *et al.* 2009). Thus, it could be possible that the source of APRIL *in vivo* is not epithelial cells or the time at which samples have been collected is not appropriate to allow detection of APRIL mRNA.

Moreover, expression of APRIL *in vivo* needs to be confirmed and it has been addressed further in chapter 4.

3.3.3. Do dsRNA and LPS induced BAFF mRNA expression?

To mimic viral and bacterial infection, BEAS-2B cells were treated with TLR ligands including, LPS (TLR4) and dsRNA (TLR3, and mimic of viral RNA) (200 ng/ml) for 12h. There was no significant increased expression of BAFF mRNA (Figure 3.6). However, BAFF production by BEAS-2B cells stimulated with dsRNA has been reported (Kato *et al.* 2006). Thus, it could be possible that BAFF was not induced in high levels due to the low concentration of dsRNA used (200 ng/ml), as it was used at up to 25 μg/ml (Kato *et al.* 2006). Moreover, epithelial cells express TLR4 and more response to LPS had been expected (Schulz *et al.* 2002). However, there was no significant increase of BAFF mRNA by BEAS-2B cells stimulated with LPS (200 ng/ml). Thus it could be possible that BAFF expression also requires a high LPS concentration but this data suggests that LPS is not a strong inducer of BAFF expression.

3.3.4. What other cytokines can induce expression of BAFF and APRIL in BEAS-2B cells?

To determine if other pro-inflammatory cytokines can induce APRIL or BAFF expression, BEAS-2B cells were stimulated with the cytokines IFN-α, IL-1β and IFN-β (200 ng/ml) for 12h (Figure 3.6). Among these stimuli, only IFN-β (200 ng/ml) was found to significantly induce the highest level of BAFF mRNA expression (fold increase relative to control= 177, P=0.01) in comparison to non-stimulated control after 12h of stimulation.

This finding correlates with another study that found IFN-β strongly induced BAFF expression by BEAS-2B cells 6h after stimulation (Kato *et al.* 2006). Furthermore, IFN-β stimulation of BEAS-2B cells also significantly induced BAFF mRNA expression in a time dependent manner (Figure 3.8). The expression of mRNA BAFF reached high levels at 12h (245, P=0.01). Afterwards, BAFF mRNA was decreased significantly at 24h (30, P=0.007) and reached low levels at 48h (6, P=0.01) (Figure 3.2.8). BAFF mRNA expression was increased by increasing the concentration of IFN-β (Figure 3.7).

To confirm epithelial production of BAFF protein and not only mRNA, BEAS-2B cells were stimulated with various concentration of IFN-β for 48h. Significant levels of BAFF protein were detected in the culture supernatant (Figure 3. 9).

Furthermore, concentrations of IFN-β as low as 1 ng/ml induced BAFF expression. The response of BAFF mRNA to IFN-β was more rapid than the response to other stimulus, which indicates that IFN-β is a potent and rapid stimulator of BAFF mRNA and protein expression in airway epithelial cells. In addition, BAFF mRNA and protein expression increased by increasing the concentration of IFN-β, which suggests that the level of interferon is a key regulator of BAFF expression following RSV infection.

3.3. 5. RSV infection of cultured BEAS-2B cells induces BAFF expression by an Interferon β dependent mechanism

To examine the mechanism of BAFF production after RSV infection and investigate if BAFF expression was directly induced by RSV infection, or if it was indirectly dependent on interferon β production by RSV infected cells, BEAS-2B cells were incubated with or without neutralizing anti-interferon β antibody and infected with RSV for 12h. BAFF mRNA was induced significantly after RSV infection (fold increase relative to control= 21, P=0.04). However, treatment with neutralising anti-interferon β antibody inhibited BAFF mRNA expression (fold decrease relative to not treated= 8.8, P=0.04) (Figure 3.10.1).

Moreover, to confirm that not only mRNA was inhibited but also BAFF protein (3.10.2), it was measured after treatment with neutralising anti-interferon β antibody and significantly inhibited BAFF protein expression (mean 13 pg/ml, P=0.04). These results indicate that early BAFF produced following RSV infection, at the very least, is dependent on interferon β production. Furthermore, these finding are supported by those of others using similar studies (Kato *et al.* 2006; McNamara *et al.* 2013). However, it has been reported that RSV protein, including NS1 and NS2 can inhibit Type 1interferon production during infection (Spann *et al.* 2004; Spann, Tran & Collins 2005). RSV can inhibit Type 1interferon which then affect the interferon expression and likely RSV can inhibit BAFF expression.

3.3.6. What form of BAFF do BEAS-2B cells express after RSV infection and BAFF cleavage?

BAFF can be found in two main forms (Chapter 1.2.1.3), membrane bound or soluble. It has been reported that soluble BAFF is derived from the membrane-bound BAFF by cleavage with a putative furin family protease or derived from intracellular processing of the longer form by the same enzyme (Nardelli *et al.* 2001; Scapini *et al.* 2003). Therefore, to investigate what molecular weight or form of BAFF is expressed in BEAS-2B cells after RSV infection, BEAS-2B cells were infected with RSV for 12h and 24h and analyzed by Western blot. Interestingly, resting epithelial cells expressed membrane bound BAFF (31kD). In this regard, low levels of BAFF mRNA were also observed in non-infected epithelial cells (table 3.2), which suggested that resting epithelial cells express BAFF under normal conditions. However, after RSV infection membrane BAFF was expressed at 12h and slightly less at 24h (Figure 3.11 and Figure 3.12). After 48h of RSV infection soluble BAFF protein was measured by specific human BAFF ELISA. BAFF protein was induced significantly (mean =28 pg/ml, P=0.002) compared to non-infected control BEAS-2B cells. Thus, it could be possible that at later time point (48h) soluble BAFF (17 kD) was cleaved from the membrane and released in the culture supernatant (Figure 3. 1; 3.9 and 3.11.B).

Soluble BAFF has been reported to form homotrimers or a capsid-like assembly of 20 trimers a 60-mer (Chapter 1.2.1.3). It is not possible from western blots such as these to determine which type of soluble BAFF has been detected in the culture supernatant of BEAS-2B cells after 48h. Expression of membrane BAFF was further confirmed by the immunofluorescence staining (Figures 3.13.1 and Figure3.13.2), BAFF was expressed in non-infected BEAS-2B cells and after RSV infection there was strong positive staining of BAFF.

Thus, to understand the mechanism of BAFF cleavage after RSV infection in airway epithelial cells, I hypothesised that resting epithelial cells expressed membrane BAFF (Figure 3.15.A) and upon RSV infection and IFN-β stimulation, soluble BAFF is cleaved from the membrane and released. Thus, inhibition of furin or furin like convertases may lead to increased membrane BAFF expression and reduce or block soluble BAFF formation (Figure 3.15.B). In addition, to ensure that soluble

BAFF was cleaved from the cell surface and not intracellularly, Brefeldin A was used as an inhibitor of classical protein secretion by cells (Figure 3,15.C).

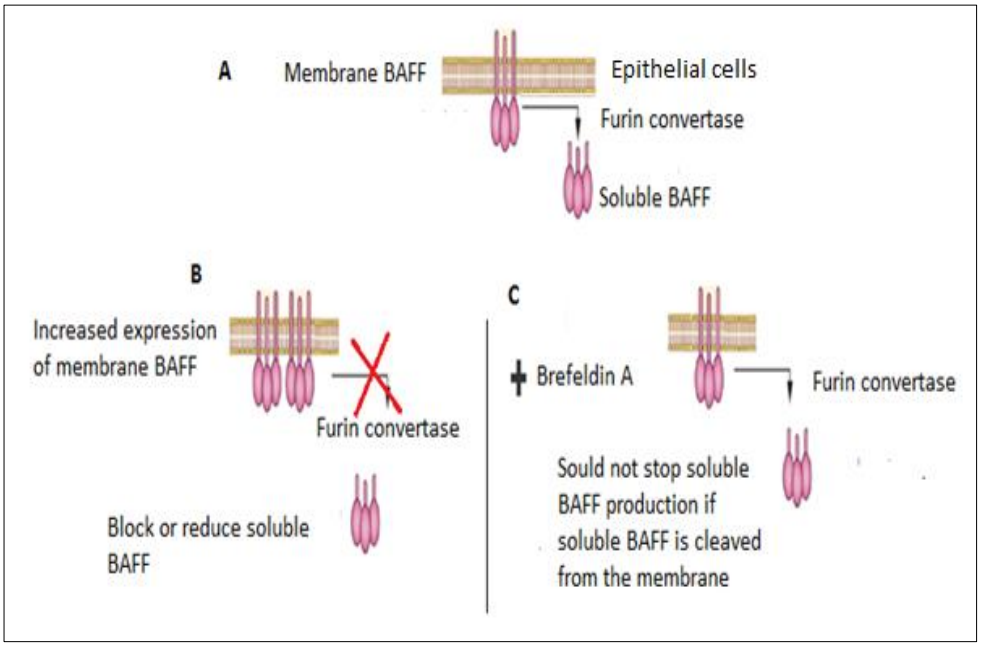

Figure 3.15. Proposed mechanism of BAFF cleavage during RSV infection

Resting epithelial cells express membrane bound BAFF. Release is dependent on furin cleavage (A). Inhibition of furin convertase should reduce or block soluble BAFF production (B). To ensure that soluble BAFF produced as results of cleaved from the membrane bound upon RSV infection Brefeldin A was used as an inhibitor of classical protein secretion (C).

RSV infected BEAS-2B cells were analysed with Western blot (Figure 3.12) and there was no increased expression of membrane BAFF as expected after targeting of furin convertase by chloromethylketone. However, at high concentration of this Furin inhibitor (100 μm) membrane BAFF was inhibited. This could be explained as a result of toxicity. It has been shown that induction of soluble BAFF by dsRNA was completely suppressed by targeting the furin convertase like enzyme using a specific furin convertase inhibitor which suggests that the mechanism of production of soluble BAFF in airway epithelial cells may be similar to that found in myeloid cells (Kato *et al.* 2006; Scapini *et al.* 2003). Taken together, this suggests that there is another pathway of cleavage of BAFF in addition to the known one or it could be possible that the experiment did not work because the furin inhibitor was not sufficiently active.

In addition, there was no effect of Brefeldin A at the level of expression of membrane BAFF which confirmed that soluble BAFF is only cleaved form the cell surface and not intracellularly as APRIL has been reported to be (Lopez-Fraga *et al.* 2001).

3.3.7. Does BAFF produced by RSV infected BEAS-2B cells support B cell survival?

It has been reported that BAFF directly promotes proliferation, cell survival, CSR, and Ig production in B cells through a CD40-independent and T cell-independent pathway (Castigli *et al.* 2005; Litinskiy *et al.* 2002; Mackay *et al.* 2003; Moore *et al.* 1999) (Chapter 1.2.4.2). To determine if BAFF derived from RSV infected epithelial cells was able to induce B cell survival, purified human B cells (Chapter 2.2.1) were cultured with or without concentrated supernatant from RSV infected or non-infected cells and with recombinant human BAFF (10 ng/ml). Recombinant Human BAFF significantly enhanced B cell survival compared with media alone (mean=0.18, P=0.006). Furthermore, RSV concentrated supernatant significantly increased B cell survival in comparison to RSV control (mean 16, P=0.04).

These results suggest that after RSV infection epithelial cell-derived BAFF is active and could promote B cell survival (Figure 3.14). These findings correlate with those of a study that looked at the biological activity of BAFF derived from epithelia cells stimulated with IFN-β and has showed this could support B cell survival (Kato *et al.* 2006). These experiments indicate that supernatants from RSV infected BEAS-2B cells can support B cell survival and they contain BAFF, a cytokine known to promote B cell survival. However to further confirm if BAFF alone and/or other factors present in these preparations actually mediated B cell survival then the BAFF should be neutralized or its receptors blocked and B cell survival examined.

3.3.8. Expression of CXCL12, CXCL13, CCl19 and CCL21 in BEAS-2B cells following RSV infection

To determine if BEAS-2B cells have a potential role in support of adaptive immune responses through production of lymphoid chemokines, including CXCL12, CXCL13, CCL19 and CCl21 (chapter 1, 1.4), that could influence lymphocytes B and T cells trafficking during RSV infection, BEAS-2B cells were infected with RSV at MOI of 1 for 3, 6, 12, 24, 48 and 72h. No mRNA or protein expression for CXCL12, CXCL13, CCL19 and CCL21 were detected after RSV infectionFigure, which suggests that the signals could come from other sources and not airway epithelial cells.

3.4. Summary

RSV infection and IFN-β stimulation of BEAS-2B cells induced expression both of BAFF mRNA and protein. BAFF mRNA expression reached the highest levels at 12h and declined at 48h, where BAFF protein was released and measured in the culture supernatant. BAFF mRNA expression following RSV infection is via IFN-β dependent pathway. IFN-β is a potent and rapid stimulator of BAFF expression in airway epithelial cells. Western blot analysis demonstrated that non-infected BEAS-2B cells expressed membrane BAFF (31kD).Thus, it could be possible that after RSV infection soluble BAFF (17kD) was cleaved from the membrane and released into the culture supernatant. Inhibition of Furin convertase did not alter BAFF expression, which could suggest another way of cleavage rather than the known way. In addition, adding Brefeldin A did not change the pattern of BAFF, and this showed that soluble BAFF is cleaved form the cell surface. Overall, these results demonstrated the importance of the epithelium to maintain B cells response and survival in the airway through production of the key B cell survival factor BAFF.

CHAPTER 4: EXPRESSION OF BAFF AND APRIL CYTOKINES IN A MURINE MODEL OF HUMAN RESPIRATORY SYNCYTIAL VIRUS INFECTION

4.1. Aims

BAFF expression both in BAL samples and by primary airway epithelial cells during acute human RSV infection has previously been demonstrated (McNamara *et al.* 2013). The experiments described in chapter 3 additionally demonstrate BAFF mRNA and protein were expressed by BEAS-2B cultured airway epithelial cells following RSV infection. Murine models of human RSV infection have been used extensively to study RSV infection (Openshaw 2013). The work described in this chapter aimed to further understand the production of BAFF and APRIL during RSV infection by using an animal model of RSV infection. Specific aims were:

1- To demonstrate RSV infection in BALB/c mice after infection by RT-PCR.
2- To define the Kinetics of both BAFF and APRIL expression following RSV infection by RT-PCR and ELISA.
3- Investigate what form of BAFF is expressed in murine lungs after RSV infection by western blot analysis.
4- Examine RSV localization in murine lung sections by Immunofluorescence staining.
5- Examine BAFF localization in lung sections following RSV infection by Immunofluorescence staining.

4.2. Experimental design

Samples from three groups of mice were kindly provided by Prof Jurgen Schwarze and Miss Amanda McFarlane working at Queens Medical Research Institute at the University of Edinburgh. All animal work associated with these experiments were conducted in Edinburgh. Three independent experiments were carried out and in each case comparison made between animals challenged with RSV or UV inactivated RSV as a control. Control RSV was inactivated by the UV in order to see if the observed response was due to live RSV infection and not due to the cell lysate which is a part of the inoculate. Three animals were used at each time point for each

treatment. At the start of each experiment, samples were collected from a group challenged with PBS only as control. This group is referred to as day 0. In experiment 1, samples were collected at day 0, 1, 2, 4 and 7 days after challenge. The second experiment included additional groups collected at day 8 consisting of (day 0, 1, 2, 4, 6, 7 and 8 days) and the third experiment included day 0, 1, 2, 4, 7, 10, 14, 21days to extend the time series. After collection, lungs were divided into 3 parts, left upper lobe for analysis of protein expression, left lower lobe for mRNA preparation and quantitative PCR and the whole right lung frozen for immunofluorescence (Figure 4.1).

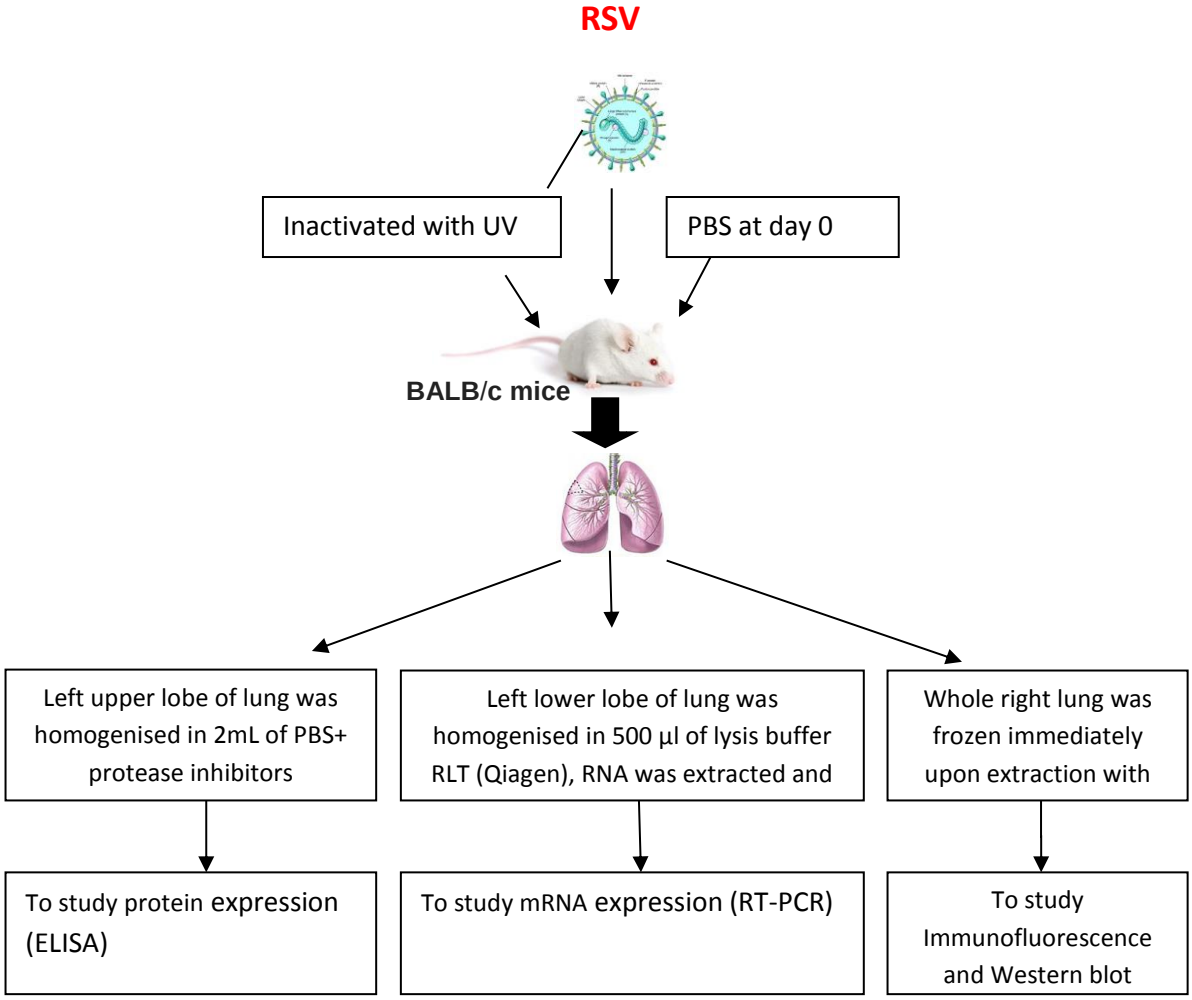

Figure 4.1. Diagram shows the structure of three independent experiments used to study RSV infection in BALB/c mice

The first experiment included (day 0, 1, 2, 4, and 7), the second experiment included (day 0, 1, 2, 4, 7 and 8 and the third experiment included (day 0, 1, 2, 4, 7, 10, 14 and 21). At day 0 mice were given PBS as control and at each day 3 mice were infected with RSV and 3 mice were infected with UV-RSV control as further control. Mice lungs were extracted and divided into three parts, left upper lob for study protein expression , left lower lobe for study mRNA expression and the whole right lung for study tissue sections staining and western blot analysis.

The results are presented from each of three individual experiments starting from measurement of RSV N RNA by RT-PCR as well as BAFF, APRIL, CXCL12, CXCL13, CCL19 and CCL21. In addition, measurements of protein for BAFF, CXCL12, CXCL13, CCL19 and CCL21 by ELISA and immunofluorescence staining of RSV, BAFF and CXCL13 are presented.

4.3. Results

4.3.1. Experiment- I

To ensure RSV infection of mouse lungs after challenge with RSV (strain A2), mouse lungs were homogenised and RNA prepared using Qiagen as described in (chapter 2.4). RSV N RNA was measured by RT-PCR. The PCR values obtained for experiment 1 and how the data was calculated are shown below (Table 4.1). There was no expression of RSV N RNA in non-infected mice at day 0 (Figure 4.2). However, after RSV infections RSV N RNA was observed at day 1 (fold expression relative to L32 = 0.64, P=0.1), day 2 (0.74, P=0.2), day 4 (0.91) and less in day 7 (0.08) after RSV infection in comparison to control UV RSV control on day 1 (0), day 2 (0), day 4 (0) and day 7 (0). The maximal expression of RSV N RNA was at day 4 and at day 7 was substantially reduced, approaching control levels.

Days after RSV infection	1. Average of L32 Ct value	2. Average of RSV N Ct value	3. L32-RSV N (n)	4. Fold expression relative to L32 (2 to the power of n)
PBS1 Day0	25.77	ND		
PBS2 Day0	24.20	ND		
PBS3 Day0	30.57	ND		
UV1 Day1	25.43	38.96	-13.53	8.43
UV2 Day1	28.49	38.07	-9.57	0.0013
UV3 Day1	29.46	39.03	-9.57	0.0013
RSV1 Day1	27.007	29.13	-2.12	0.2295
RSV2 Day1	28.83	28.36	0.47	1.38
RSV3 Day1	31.49	33.26	-1.76	0.29
UV1 Day2	26.20	ND		
UV2 Day2	24.91	ND	-22.57	1.59
UV3 Day2	25.85	41.51	-15.66	1.92
RSV1 Day2	31.46	30.67	0.79	1.73
RSV2 Day2	24.74	26.576	-1.83	0.28
RSV3 Day2	30.60	32.918	-2.31	0.20
UV1 Day4	26.27	ND		
UV2 Day4	27.13	ND		
UV3 Day4	28.47	ND		
RSV1 Day4	25.47	24.85	0.61	1.52
RSV2 Day4	26.34	26.35	-0.012	0.99
RSV3 Day4	27.19	29.36	-2.16	0.22
UV1 Day7	26.08	ND		
UV2 Day7	24.59	ND		
UV3 day7	26.30	ND		
RSV1 Day7	24.69	29.24	-4.55	0.042
RSV2 Day7	23.67	31.49	-7.82	0.004
RSV3 Day7	24.89	27.41	-2.52	0.174

Table 4.1. Summary of steps used to analyze RT-PCR data and calculate fold expression of RSV N RNA relative to housekeeping gene control L32

1) All L32 Ct values of the samples were averaged, 2) all RSV N probe Ct values were averaged, 3) the CT value of samples for RSV N probe were corrected to L32. For example: The L32 expression – RSV N. This produced a Ct value relative to L32 expression, 4) Fold expression relative to L32 and this can be calculated by 2 to the power of n, where n = value determined in step 3. This calculation converts the value from a ct number to the fold difference. This particular calculation is because every cycle result in an increases the amount of product two fold. (ND= not determined, Ct= cycle threshold the number of cycles required for the fluorescent signal to cross the threshold).

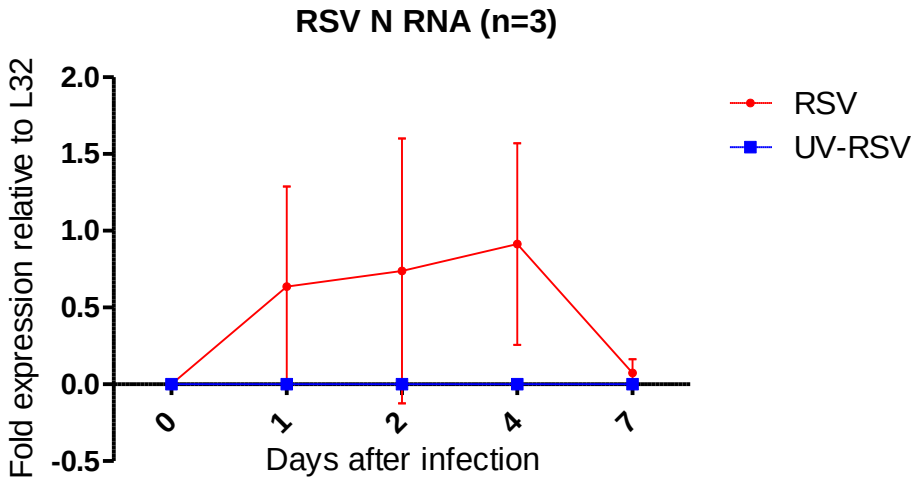

Figure 4.2. Expression of RSV N RNA after RSV infection or challenge with UV-RSV control

RSV N RNA was measured by RT-PCR. RSV N RNA was detected in day 1, 2, 4 and less in day 7 after RSV infection in comparison to RSV UV control at the same time points and non-infected at day 0. Values are shown as fold expression relative to L32. Result shown is the average of three animals in the first experiment. Mean and SD are shown (two way ANOVA with Bonferroni post-hoc test, n=3).

4.3.1.1. Expression of BAFF mRNA after RSV infection in mice

BAFF mRNA was firstly measured by RT-PCR (Figure 4.3). Non-infected mice at day 0 expressed BAFF mRNA (fold increase relative to control = 0.83). After RSV infection BAFF mRNA expression was increased significantly at day 1 (fold increase = 1.18, P=0.03) and day 7 (1.7, P=0.02) in comparison to UV RSV control at day 1 (0.7) and day 7 (0.9). BAFF mRNA was expressed consistently in non-infected mice at day 0 and UV RSV control. BAFF mRNA reached high levels at day 1 and 7 and declined at day 4 after RSV infection relative to UV RSV control.

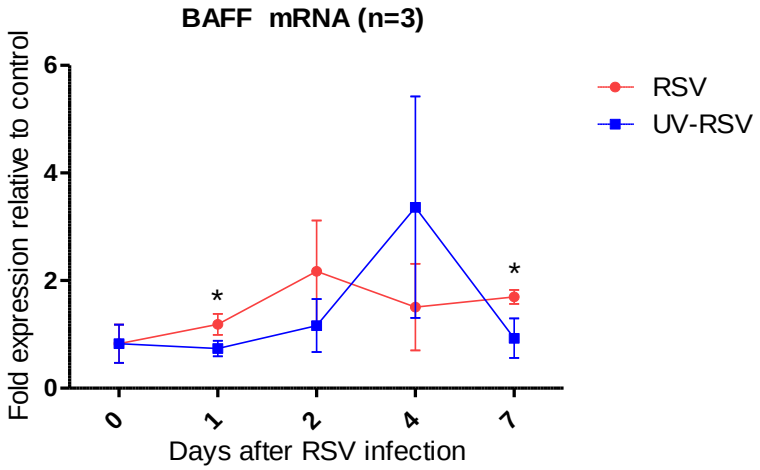

Figure 4.3. Expression of BAFF mRNA after RSV infection or challenge with UV-RSV control

*BAFF mRNA expression was measured by RT-PCR. BAFF mRNA expression was increased significantly after RSV infection on day 1 and 7 in comparison to UV RSV control at the same time points. Values are shown as fold expression relative to control. Result shown is the average of three animals in the first experiment. Mean and SD are shown (two way ANOVA with Bonferroni post-hoc test, *P <0.05, n=3).*

4.3.1.2. Expression of BAFF protein RSV infection in mice

To confirm production of BAFF protein and not only mRNA after RSV infection, BAFF protein concentration was measured in homogenised lung using a murine BAFF ELISA (Chapter 2.5). BAFF protein was present in lung homogenate prepared from non-infected mice at day 0, mean= 402 pg/ml (Figure 4.4). However, after RSV infection significantly increased levels of soluble BAFF were detected. BAFF protein was elevated significantly on day 2 (1157 pg/ml, P=0.01) and day 7 (2941 pg/ml, P=0.0001) in comparison to UV RSV control at day 2 (370 pg/ml) and day 7 (393pg/ml). BAFF protein reached high levels at day 2 and 7 and declined at day 4 after RSV infection relative to UV RSV control.

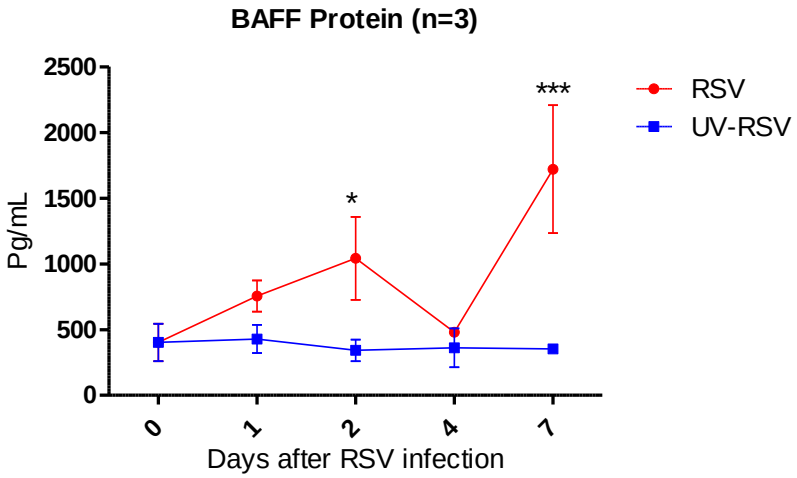

Figure 4.4. Expression of BAFF protein after RSV infection or challenge with UV-RSV control

*BAFF protein was measured by use specific murine BAFF ELISA. BAFF protein was increased significantly after RSV infection at day 2 and 7 in comparison to UV RSV control at the same time points. Result shown is the average of three animals in the first experiment. Mean and SD are shown (two way ANOVA with Bonferroni post-hoc test, *P <0.05, n=3).*

4.3.1.3. BAFF protein expression in comparison to total protein concentration after RSV infection

Although standardised procedures were used to prepare lung homogenates, changes in protein concentration or yield could result in apparent changes in BAFF concentration, BAFF protein concentrations (pg/ml) were Normalization of to total protein (pg/ng) as measured by total protein assay BCA (Chapter 2.3.2; Figure 4.5). BAFF protein was elevated significantly after RSV infection at day 1 (mean 755 pg/ng, P=0.02), day 2 (1042 pg/ng, P=0.02) and day 7 (1720 pg/ng, P=0.008) in comparison to UV RSV control at day 1 (428 pg/ng), day 2 (342 pg/ng) and day 7 (353 pg/ng). BAFF protein reached high levels at day 2, 7 and declined at day 4.

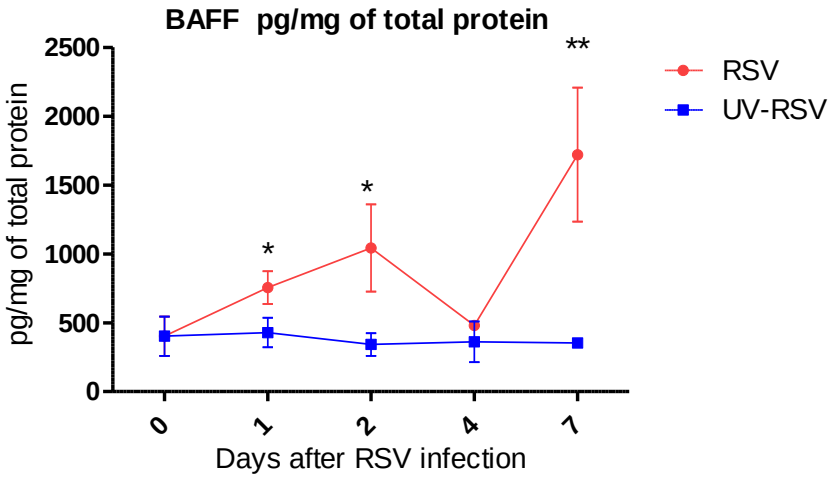

Figure 4.5. Normalized BAFF protein to total protein after RSV infection or challenge with UV-RSV control

*BAFF protein levels were normalized to total protein (pg/ng) by BCA assay. BAFF protein was increased significantly after RSV infection on day 1, 2 and 7 in comparison to UV RSV control at the same time points. Result shown is the average of three animals in the first experiment. Mean and SD are shown (two way ANOVA with Bonferroni post-hoc test, *P <0.05, n=3).*

4.3.1. 4. RSV infection did not significantly up regulate APRIL mRNA expression

To determine if RSV infection of mice resulted in increased APRIL mRNA expression, mouse lungs were homogenised and RNA prepared using Qiagen, as described in the (chapter 2, section 2.4). APRIL mRNA was expressed in non-infected mice at day 0 (fold expression relative to control =1.47) (Figure 4.6). However, after RSV infection there was no significant increase of APRIL mRNA observed at day 1 (2.06, P=0.8), day 2 (5.02, P=0.5), day 4 (3.15, P=0.4) and day 7 (1.3, P=0.7) in comparison to the RSV UV control on day 1 (2.45), day 2 (3.14), day 4 (6.5) and day 7 (1.7). There was no significant increased expression of APRIL mRNA after RSV infection relative to UV RSV controls.

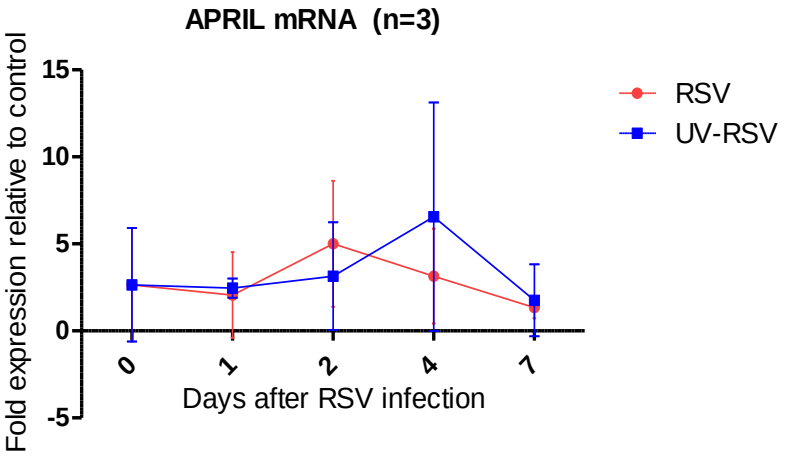

Figure 4.6. Expression of APRIL mRNA after RSV infection or challenge with UV-RSV control

*APRIL mRNA was measured by RT-PCR. RSV infection of mice did not significantly up regulated APRIL mRNA expression at day 1, 2, 4 and 7 in comparison to UV RSV control at the same time points. Values are shown as fold expression relative to control. Result shown is the average of three animals in the first experiment. Mean and SD are shown (two way ANOVA with Bonferroni post-hoc test, *P <0.05, n=3).*

4.3.2. Experiment- II

4.3.2.1. RSV N RNA is expressed after RSV infection in mice

To determine if RSV infection of mouse lungs expressed RSV N RNA after challenge with RSV (A2), mouse lungs were homogenised and RNA prepared using Qiagen as described in the (chapter 2, 2.4) and RSV N RNA measured and analysed by RT-PCR. There was no expression of RSV N RNA in non-infected mice at day 0 (Figure 4.7). However, RSV N RNA was observed at day 1 (fold expression relative to L32= 2.5, P=0.1), day 2 (0.66, P=0.1) and day 4 (2.83, P=0.1) after RSV infection in comparison to the UV RSV control on day 1 (0), day 2 (0) and day 4 (0).

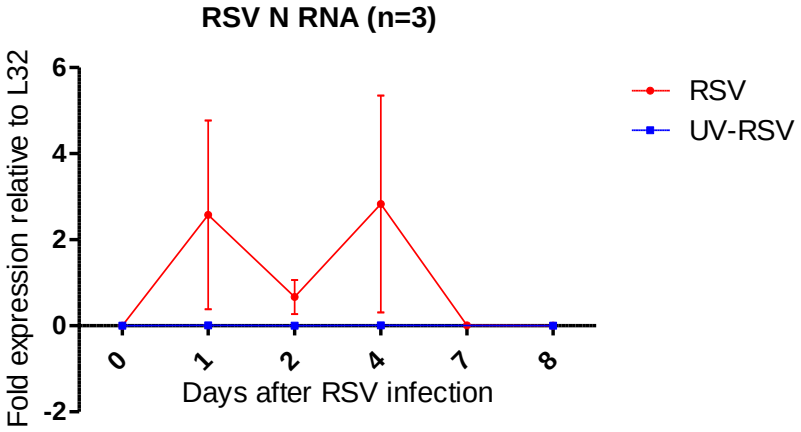

Figure 4.7. Expression of RSV N RNA after RSV infection or challenge with UV-RSV control

*RSV N RNA was measured by RT-PCR. RSV N RNA was detected in day 1, 2 and 4 after RSV infection in comparison to RSV UV control at the same time points and non-infected control at day 0. Values are shown as fold expression relative to L32. Result shown is the average of three animals in the second experiment. Mean and SD are shown (two way ANOVA with Bonferroni post-hoc test, *P <0.05, n=3).*

4.3.2.2. Expression of BAFF mRNA after RSV infection in mice

To determine the influence of RSV on expression of BAFF mRNA *in vivo*, murine were infected with RSV (A2 strain) at different time points, including day 0 (non-infected), 1, 2, 4 7 and 8. At the time points indicated after RSV infection mouse lung tissue were homogenized and RNA was isolated and prepared using Qiagen as described (chapter 2, 2.4). After RSV infection BAFF mRNA was measured and analyzed by RT-PCR. Non-infected mice at day 0 expressed BAFF mRNA (fold increase=0.67) (Figure 4.8). However, BAFF mRNA expression was increased significantly after RSV infection on day 7 (fold increase relative to control = 1.2, P=0.04) and day 8 (1.09, P=0.01) in comparison to UV RSV control on day 7 (0.8), day 8 (0.5). BAFF mRNA reached highest levels at day 7 and 8 after RSV infection relative to UV RSV control.

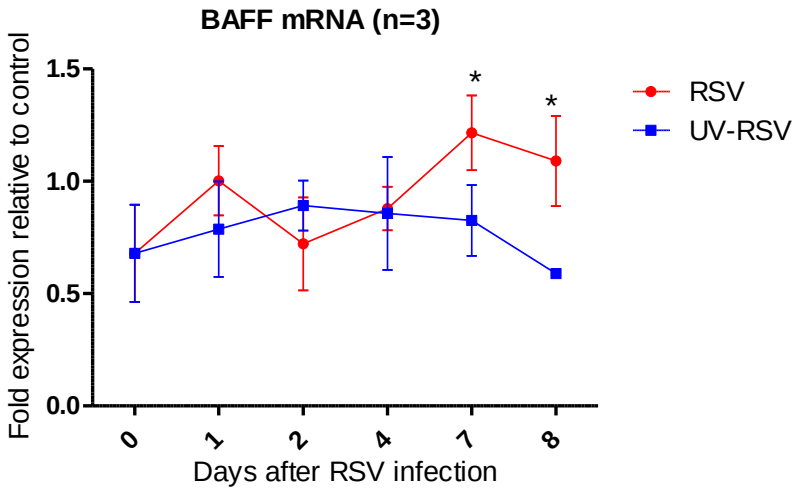

Figure 4.8. Expression of BAFF mRNA after RSV infection or challenge with UV-RSV control

*BAFF mRNA expression was measured by RTPCR. BAFF mRNA expression was increased significantly after RSV infection on day 7 and 8 in comparison to UV RSV control at the same time points. Values are shown as fold expression relative to control. Result shown is the average of three animals in the second experiment. Mean and SD are shown (two way ANOVA with Bonferroni post-hoc test, *P <0.05, n=3).*

4.3.3.3. Expression of BAFF protein after RSV infection in mice

To confirm production of BAFF protein and not only mRNA after RSV infection, BAFF protein concentrations were measured in homogenized lung tissues using murine BAFF ELISA (chapter 2, 2.5). BAFF protein was expressed in non-infected mice at day 0 (mean = 484 pg/ml) (FFigure 4.9). However, BAFF protein levels were elevated significantly after RSV infection at day 1 (1832 pg/ml, P= 0.0007), day 2 (1737 pg/ml, P= 0.0001), day 4 (925 pg /ml, P= 0.003), day 7 (3203 pg /ml, P= 0.0007) and day 8 (2355 pg /ml, P=0.004) in comparison to UV treated RSV control on day 1 (497 pg/ml), day 2 (498 pg/ml), day 4 (481 pg/ml), day 7 (401 pg/ml) and day 8 (473 pg/ml). BAFF protein reached high levels at day 2 and 7 and declined at day 4 after RSV infection relative to UV RSV controls.

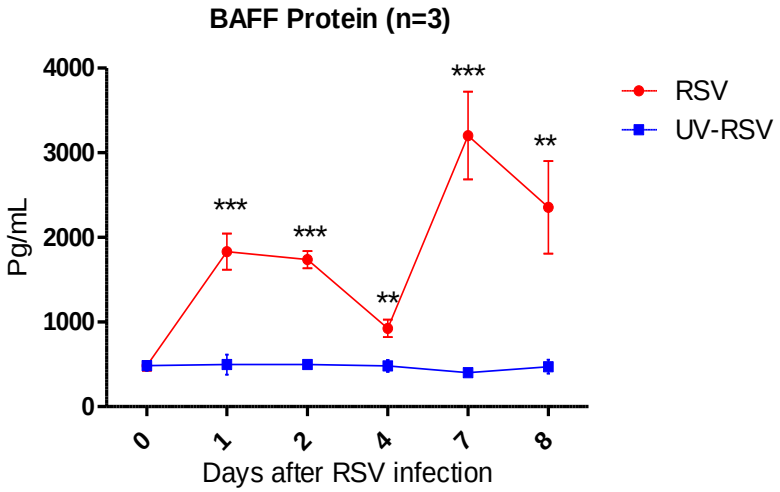

Figure 4.9. Expression of BAFF protein after RSV infection or challenge with UV-RSV control

*BAFF protein was measured by specific murine BAFF ELISA. BAFF protein was increased significantly after RSV infection at day 1, 2, 4, 7 and 8 in comparison to UV RSV control at the same time points. Result shown is the average of three animals in the second experiment. Mean and SD are shown (two way ANOVA with Bonferroni post-hoc test, *P <0.05, n=3).*

4.3.3.4. BAFF protein expression in compression to total protein concentration after RSV infection in mice

BAFF protein concentrations (pg/ml) were normalized to total protein (pg/ng) (Figure 4.10). BAFF protein was elevated significantly after RSV infection at day 1 (mean=269 pg/ng, P=0.0004), day 2 (197 pg/ng, P=0.04), day 4 (129 pg/ng, P=0.003), day 7 (455 pg/ng, P=0.0008) and day 8 (344 pg/ng, P=0.001) in comparison to UV RSV control on day 1 (74 pg/ng), day 2 (71 pg/ng), day 4 (67 pg/ng), day 7 (59 pg/ng) and day 8 (67 pg/ng). BAFF protein reached high levels at day 1, 7 and 8 and declined at day 4.

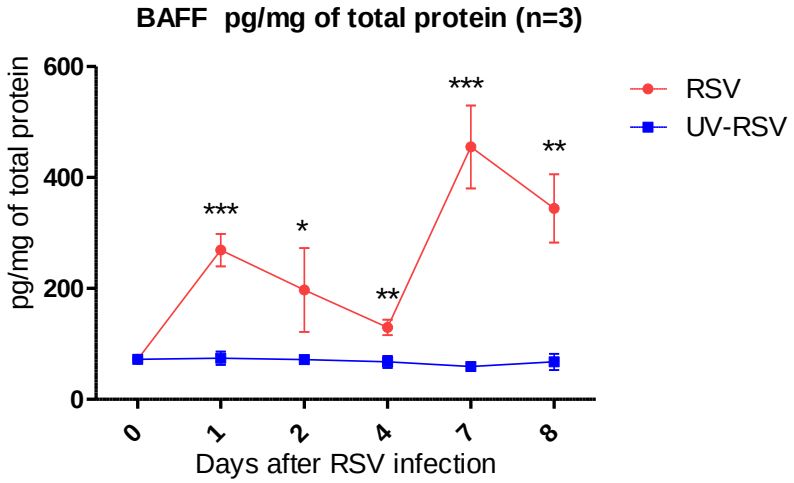

Figure 4.10. Normalization of BAFF protein to total protein after RSV infection or challenge with UV-RSV control

*BAFF protein levels were normalized to total protein (pg/ng) by BCA assay. BAFF protein was increased significantly after RSV infection on day 1, 2, 4, 7 and 8 in comparison to UV treated RSV control at the same time points. Result shown is the average of three animals in the second experiment. Mean and SD are shown (two way ANOVA with Bonferroni post-hoc test, *P <0.05, n=3).*

4.3.3.5. RSV infection did not significantly up regulate APRIL mRNA expression

To determine whether RSV infection induced APRIL mRNA expression, mouse lungs were homogenised and RNA prepared using Qiagen as described in the (chapter 2, 2.4). APRIL mRNA was expressed in non-infected mice at day 0 (fold expression relative to control=1.47) (Figure 4.11). However, after RSV infection there was no significant increase of APRIL mRNA at day 1 (4.02, P=0.6) day 2 (2.57 , P=0.5) , day 4 (2.82, P=0.2) , day 7 (0.918, P=0.1) and day 8 (2.963, P=0.6) in comparison to the RSV UV treated on day 1 (5.99), day 2 (3.96), day 4 (5.27),day 7 (4.25) and day 8 (4.007).

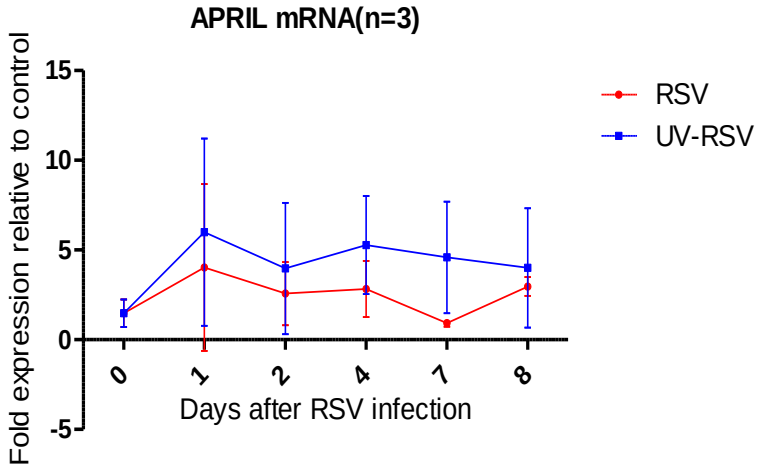

Figure 4.11. Expression of APRIL mRNA after RSV infection or challenge with UV-RSV control

*APRIL mRNA expression was measured by RT-PCR. RSV infection of mouse lungs did not significantly increase APRIL mRNA expression at day 1, 2, 4,7 and 8 in comparison to RSV UV control at the same time points. Values are shown as fold expression relative to control. Result shown is the average of three animals in the second experiment. Mean and SD are shown (two way ANOVA with Bonferroni post-hoc test, *P <0.05, n=3).*

4.3.3. Experiment- III

4.3.3.1. RSV N RNA is expressed after RSV infection in mice

In order to achieve better understanding of the kinetics of BAFF and APRIL expression following RSV infection, RSV N RNA has been examined at various time points, including day 10, 14 and 21. RSV N RNA (Figure 4.12.) was detected at day 1 (fold expression relative to L32= 0.58, P= ns), day 2 (0.06, P= ns), day 4 (8.35, P= ns) and day 7 (0.0263, P= ns) after RSV infection in comparison to the UV RSV control on day 1 (0), day 2 (0) day 4 and day 7 (0). RSV N RNA was detected at day 1 and day 2 but not at day 4. These results suggested that mice did not have appropriate infection as the first and second experiment.

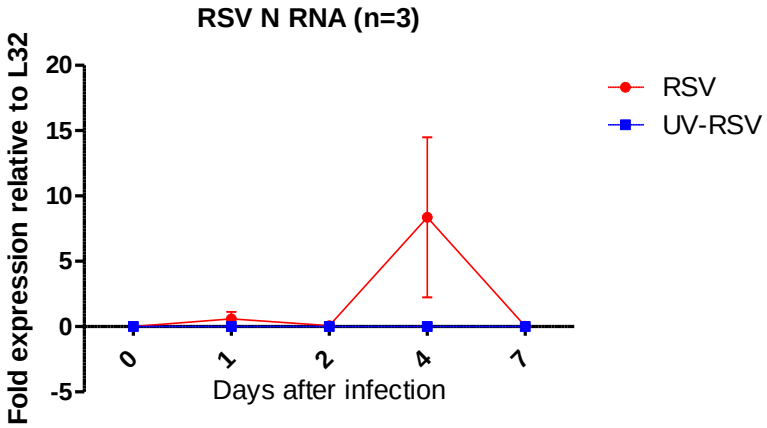

Figure 4.12. Expression of RSV N RNA after RSV infection or challenge with UV-RSV control

*RSV N RNA was measured by RT-PCR. RSV N RNA. There was weak expression of RSV N RNA on day1, 2, and 4 after RSV infections in comparison to RSV UV control. Values are shown as fold expression relative to L32. Result shown is the average of three animals in the third experiment. Mean and SD are shown (two way ANOVA with Bonferroni post-hoc test, *P <0.05, n=3).*

4.3.3.2. Expression of BAFF protein after RSV infection

BAFF protein was expressed in non-infected mice PBS at day 0 (mean= 42 pg/ml) (Figure 4.13). However, after RSV infection BAFF protein was increased significantly at day 21 (69 pg/ml, P=0.001) in comparison to RSV UV control at day 21 (48 pg/ml). BAFF protein concentrations were lower than first and second experiments (Figures 4.4 and Figure4.9) as a result of the weak RSV infection (Figure 4.12).

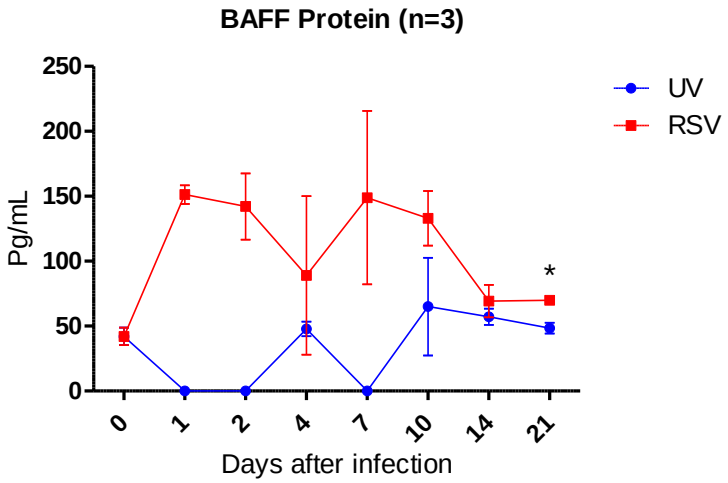

Figure 4.13. Expression of BAFF protein after RSV infection or challenge with UV-RSV control

*BAFF protein was measured by specific murine BAFF ELISA. BAFF protein was increased significantly after RSV infection at day 21 in comparison to UV RSV control at day 21. Result shown is the average of three animals in the third experiment. Mean and SD are shown (two way ANOVA with Bonferroni post-hoc test, *P <0.05, n=3).*

4.3.3.3. BAFF protein expression in comparison to total protein after RSV infection in mice

BAFF protein concentrations (pg/ml) were Normalization of to total protein (pg/ng) (Figure 4.14). BAFF protein was increased significantly after RSV infection at day 14 (53 pg/ng, P=0.001) and day 21 (55 pg/ng, P=0.002) in comparison to UV RSV control at day 14 (40 pg/ng) and day 21 (34 pg/ng). BAFF protein concentrations were lower compared with previous experiments.

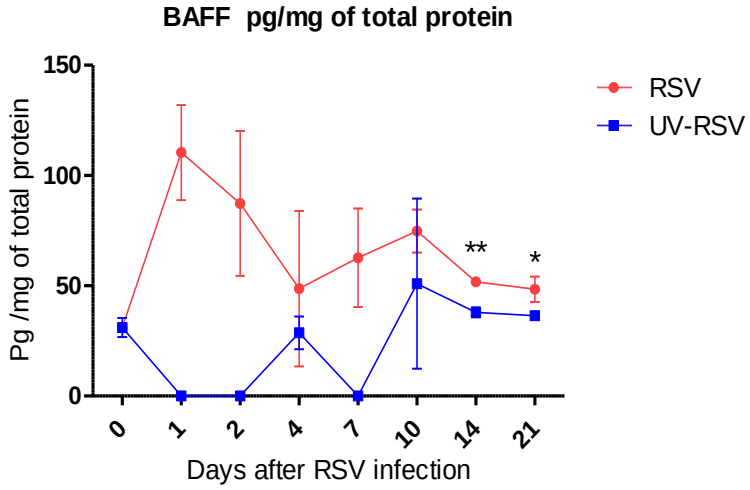

Figure 4.14. Normalized levels of BAFF protein to total protein after RSV infection or challenge with UV-RSV control

*BAFF protein levels were Normalization of to total protein (pg/ng) by BCA assay. BAFF protein was increased significantly after RSV infection at day 14 and 21 in comparison to UV RSV control at the same time point. Result shown is the average of three animals in the third experiment. Mean and SD are shown (two way ANOVA with Bonferroni post-hoc test, *P <0.05, n=3).*

4.3.4. An average of experiment-I and experiment- II

4.3.4.1. Average of RSV N RNA after RSV infection in mice

There was no expression of RSV N RNA in non -infected mice at day 0 (Figure 4.15). However, after RSV infection RSV N RNA was elevated significantly at day 1 (fold expression relative to L32= 1.60, P=0.05), day 2 (0.70, P=0.02) and day 4 (1.87, P=0.12) in comparison to the UV RSV control at day 1 (0), day 2 (0) and day 4 (0). This is the overall average of experiments one and two, experiment three is not included in this analysis. Moreover, two peaks of RSV N RNA were detected. The maximal expression of RSV N RNA was at day 1 and 4 and substantially reduced at day 7 and undetectable at day 8.

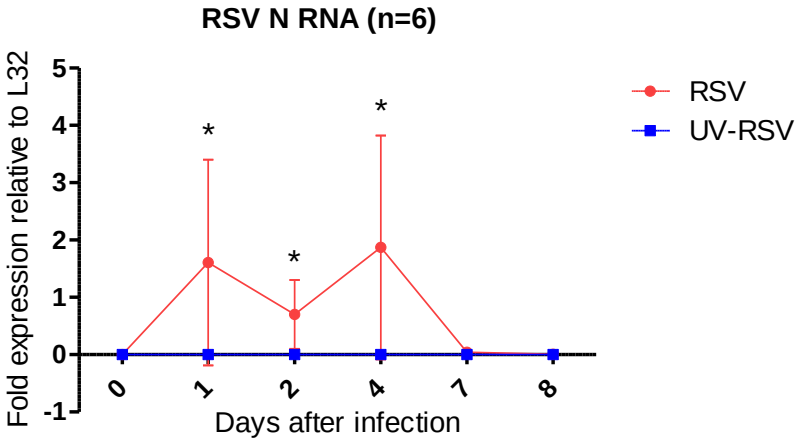

Figure 4.15. Average of RSV N RNA expression after RSV infection or challenge with UV-RSV control

*RSV N RNA was measured by RT-PCR. RSV N RNA was expressed significantly after RSV infection at day 1, 2 and 4 in comparison to UV RSV control at the same time points. Result shown is the average of six animals from the first and second experiments .Values are shown as fold expression relative to L32. Mean and SD are shown (two way ANOVA with Bonferroni post-hoc test, *P <0.05, n=3).*

4.3.4.2. Average of BAFF mRNA after RSV infection in mice

BAFF mRNA was expressed in non-infected mice PBS at day 0 (fold increase relative to control= 0.75; Figure 4.16). However, after RSV infection BAFF mRNA expression was increased significantly on day 1 (fold increase relative to control= 1.09, P=0.008), day 7 (1.5, P=0.004) and day 8 (1.09, P=0.01) in comparison to UV treated RSV control on day 1 (0.7), day 7 (0.8) and day 8 (0.5). This is the overall average of experiments one and two and three is not included in this analysis. BAFF mRNA reached high levels at day 7 declined at day 8 after RSV infection relative to UV RSV control.

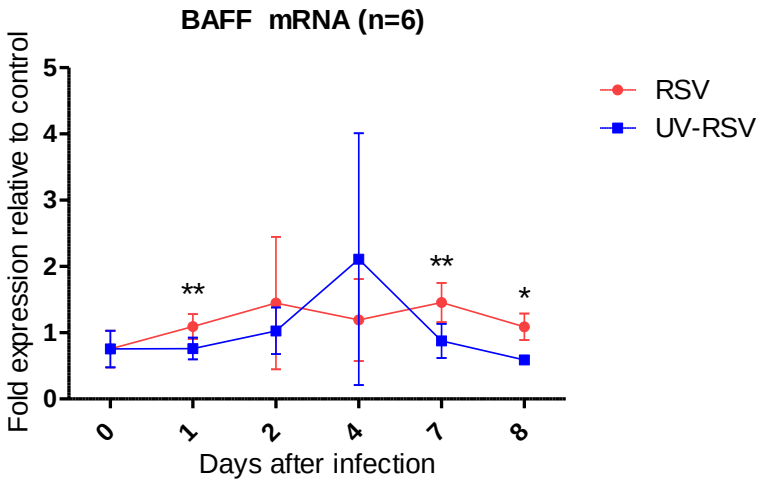

Figure 4.16. Average of BAFF mRNA expression after RSV infection or challenge with UV-RSV control

*BAFF mRNA was measured by RT-PCR. BAFF mRNA expression was increased significantly after RSV infection on days 1, 7 and 8 in comparison to UV RSV control on days 1, 7 and 8. Result shown is the average of six animals from the first and second experiments. Values are shown as fold expression in comparison to control. Mean and SD are shown (two way ANOVA with Bonferroni post-hoc test, *P <0.05, n=6).*

4.3.4.3. Average of BAFF protein after RSV infection in mice

BAFF protein was expressed in non-infected mice at day 0 (mean = 478 pg/ml) (Figure 4.17). However, after RSV infection BAFF protein was elevated significantly at day 1 (1379 pg/ml, P=0.002), day 2 (1447 pg/ml, P=0.0001), day 7 (3272 pg/ml, P=0.0001) and day 8 (2355 pg /ml, P=0.004) in comparison to UV RSV control at day 1 (460 pg/ml), day 2 (434 pg/ml), day 7 (398 pg/ml) and day 8 (473 pg/ml). This is the overall average of experiments one and two. Experiment three is not included in this analysis. Two kinetics of BAFF were noticed at day 2 and 7, and BAFF declined at day 4.

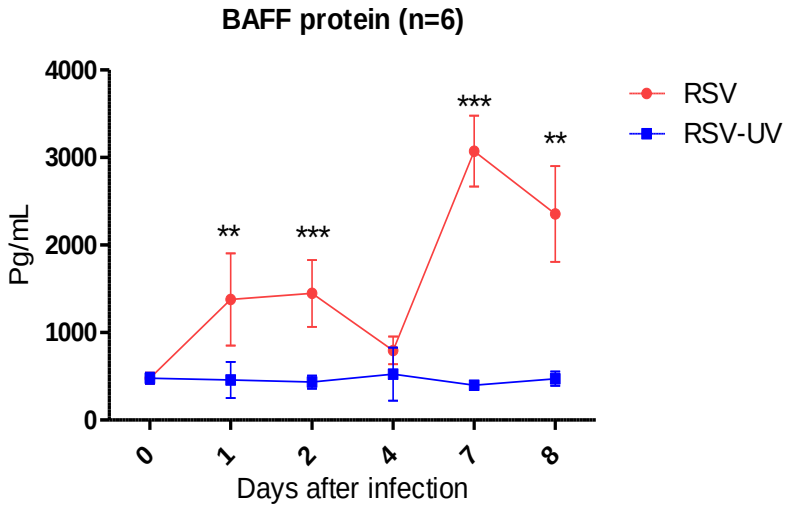

Figure 4.17: Average of BAFF protein expression after RSV infection or challenge with UV-RSV control

*BAFF protein was measured by specific murine BAFF ELISA. BAFF protein was increased significantly after RSV infection at days 1, 2, 7 and 8 in comparison to UV RSV control at the same time points. Result shown is the average of six animals from the first and second experiments. Mean and SD are shown (two way ANOVA with Bonferroni post-hoc test, *P <0.05, n=6).*

4.3.4.4. Average of APRIL mRNA after RSV infection in mice

APRIL mRNA was expressed in non-infected mice at day 0 (fold expression relative to control=2.06) (Figure 4.18). However, after RSV infection, there was no significant increase of APRIL mRNA at day 1 (3.04, P=0.5) day 2 (3.79 ,P=0.8), day 4 (2.98, P=0.1), day 7 (1.13 , P=0.1) or day 8 (2.96, P=0.6) in comparison to the RSV UV control on day 1 (4.22), day 2 (3.55), day 4 (5.9), day 7 (3.17) and day 8 (4.007). RSV infection of mice did not significantly increase APRIL expression relative to UV RSV control at the same time points.

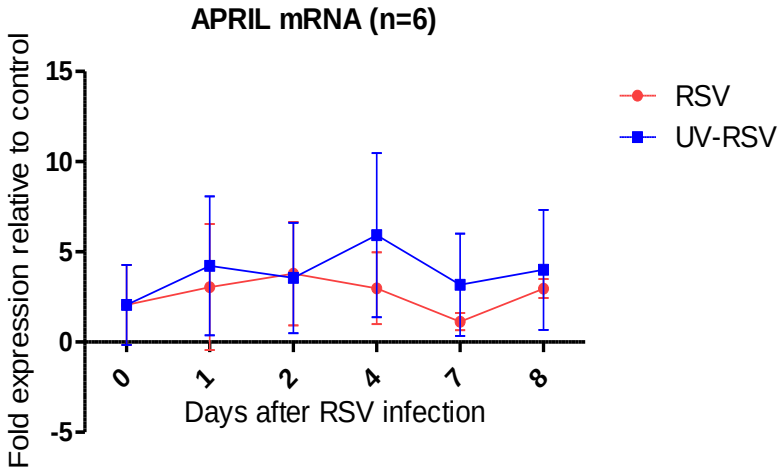

Figure 4.18. Average of APRIL mRNA expression after RSV infection or challenge with UV-RSV control

*APRIL mRNA was measured by RT-PCR. There was no significantly increase of APRIL mRNA after RSV infection at days 1, 2, 4, 7 and 8 in comparison to UV RSV control at the same time points.Values are shown as fold expression relative to control. Result shown is the average of six animals from the first and second experiment. Mean and SD are shown (two way ANOVA with Bonferroni post-hoc test, *P <0.05, n=6).*

4.3.5. Examination of the form of BAFF in murine lung after RSV infection

To determine what form of BAFF is expressed after RSV infection, mice lung tissues were homogenized and analysed by western blot (Figure 4.19). The non-infected BEAS-2B cells used as the positive control expressed a 31kD molecular weight form consistent with membrane BAFF (31kD). Membrane BAFF was expressed slightly on non-infected mice PBS at day 0, day 2 and day 4. However, after RSV infection a lower molecular weight form at around 20kD consistent with soluble BAFF (20kD) was detected on day 1, 2, 4 and 7.

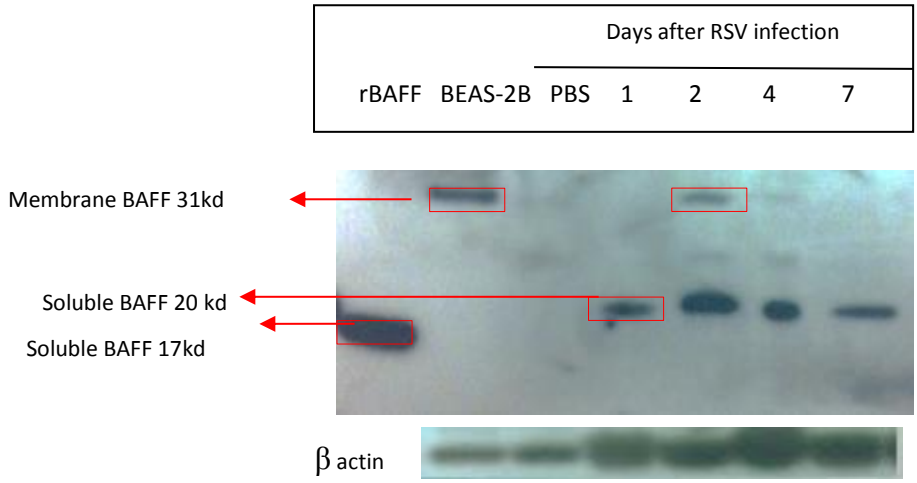

Figure 4.19. Western blot of analysis of BAFF expression by murine lungs after RSV infection

The non-infected BEAS-2B cells expressed membrane BAFF (31kD). Murine membrane BAFF was expressed slightly on non-infected mice PBS at day 0 (34 kD). After RSV infection soluble BAFF (20 kD) was expressed at day 1, 2, 4 and 7. β-Actin was used as a control to show any differences in amount of sample loaded on the gel. Human recombinant BAFF (17kD) was used as positive control for soluble BAFF.

4.3.6. Immunofluorescence staining

Immunofluorescence staining was used to confirm RSV infection and to examine the location of virus within the lung and to identify RSV-infected cells and study the histological structure after RSV infection comparing control non-infected mice at day 0 and UV RSV control. Mouse lung section was prepared and stained with anti-RSV (red) and anti-BAFF (green) as described in (chapter 2, section 2.8).

4.3.6. 1. Detection of RSV in mice lung tissue after RSV infection

4.3.6.2. Detection of RSV in mice lung tissue at day 0

Murine at day 0 were given PBS as negative control of RSV infection. No positive staining for RSV was detected at day 0 and there was no comparable staining observed with the isotype control. No clear damage of airways and no obvious epithelial damage was seen (Figure 4.20).

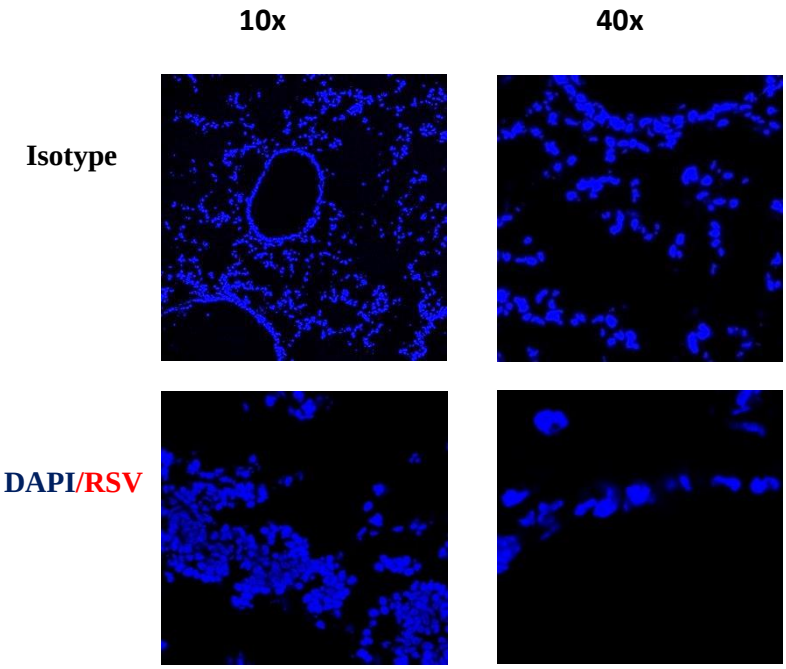

Figure: 4.20. RSV staining of lung sections taken from mice treated with PBS at day 0

No RSV (red) was detected. DAPI (Blue) staining was used to stain cell nucleus. Isotype control was applied. Images were originally obtained at 10 x and 40x magnifications.

4.3.6. 3. Detection of RSV in mice lung tissue after RSV infection at day 1

Immunofluorescent staining of mouse lung tissue showed strong positive staining of RSV (red) at day 1 after RSV infection (Figure 4.21) indicated as white arrow and there was no comparable staining observed with the isotype control. RSV was localized in the cytoplasm of infected cells and appeared near to the airway epithelium. However, it has been shown that the predominant infected cell is the Type I alveolar pneumocyte (Openshaw 2013). Furthermore, it is likely that other cells may be infected with RSV such as alveolar macrophages and DCs. In addition, the structure of some RSV infected cells appeared to be affected possibly due to the cytopathic effect of RSV. In addition, some inflammatory cells were noticed in the lung sections as indicated (green arrow).

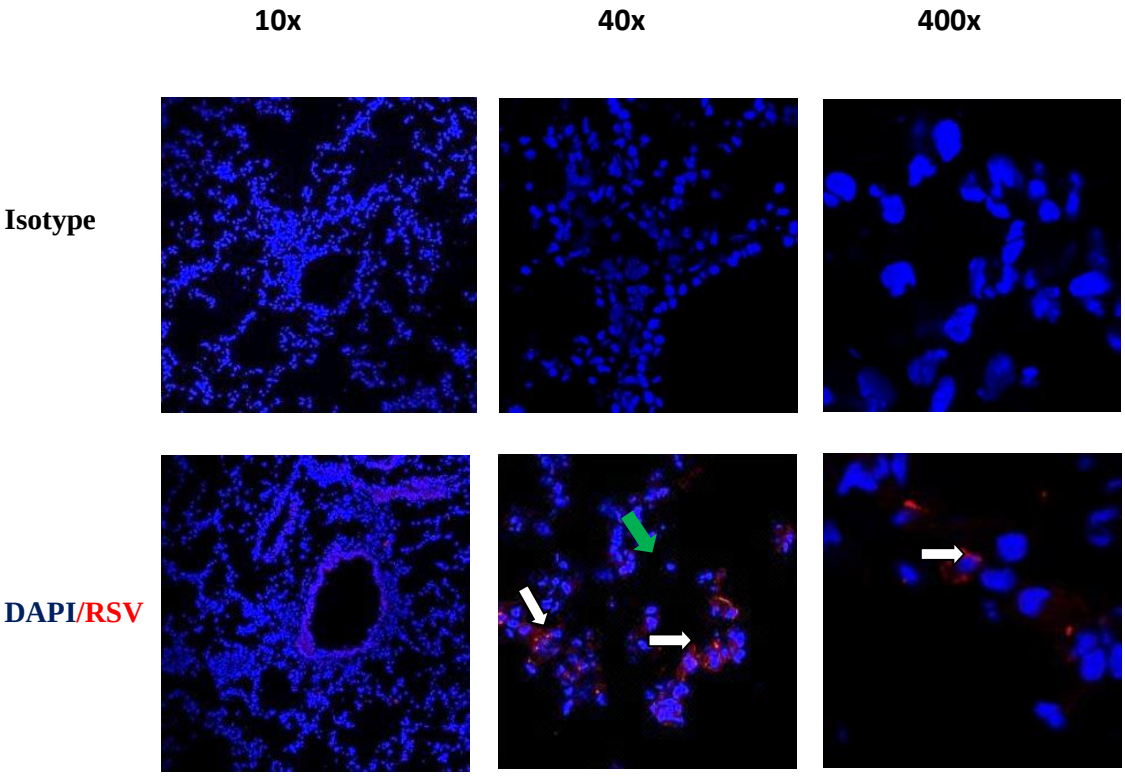

Figure: 4.21. Immunohistochemical localization of RSV A2 proteins in lung sections prepared from mice at day 1 after RSV infection

RSV (red) was detected around alveolar and airways as well as some inflammatory cells (green arrow). Cell nuclei shown in blue (DAPI). Isotype control was applied. Images were originally obtained using confocal microscopy at 10 x, 40x and 400x magnifications.

4.3.6. 4. UV treated RSV in mouse lung after challenge at day 1

As expected to observe, no RSV was detected from mouse lung tissue at day 1 after challenge with RSV UV treated (Figure 4.22) and no comparable staining was observed with the isotype control. In addition, no visible histological changes were seen after challenge, airways were clear with no obvious epithelial damage and the tissue structures appeared similar to non-infected mice at day 0 (Figure 4.20). However, some inflammatory cells were observed (green arrow).

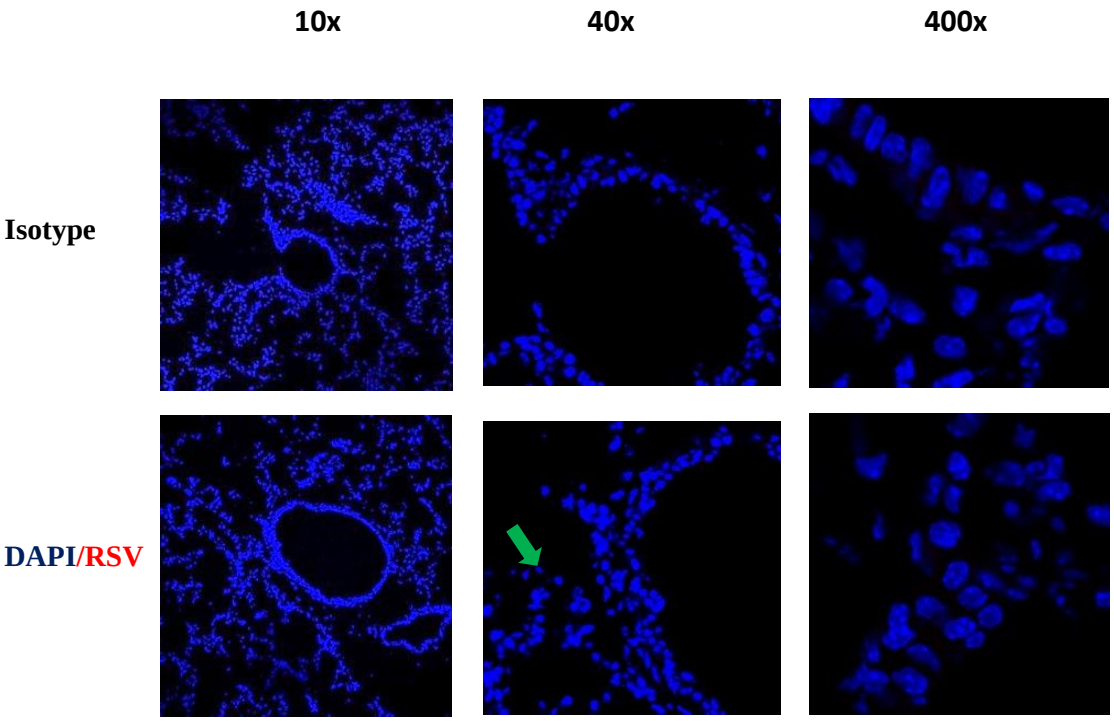

Figure: 4.22. RSV is absent from mice challenged with RSV UV treated at day 1

RSV (red) was not detected in the airways. Cell nuclei shown in blue (DAPI). Isotype control was applied. Images were originally obtained using confocal microscopy at 10x, 40x and 400x magnifications.

4.3.6.5. Detection of RSV in mice lung tissue after RSV infection at day 2

Strong positive staining of RSV (red) was observed at day 2 after RSV infection (Figure 4.23) as indicated (white arrow), and no comparable staining was noticed with the isotype control. RSV was detected in the cytoplasm of infected cells. RSV was localized close to airways. In addition, infiltrated inflammatory cells as indicated (green arrow) were also observed between epithelium and alveolar spaces. RSV induced morphological changes including, epithelial damage that resulted in shrinkage and presence of debris, in comparison to non-infected PBS (Figure 4.20).

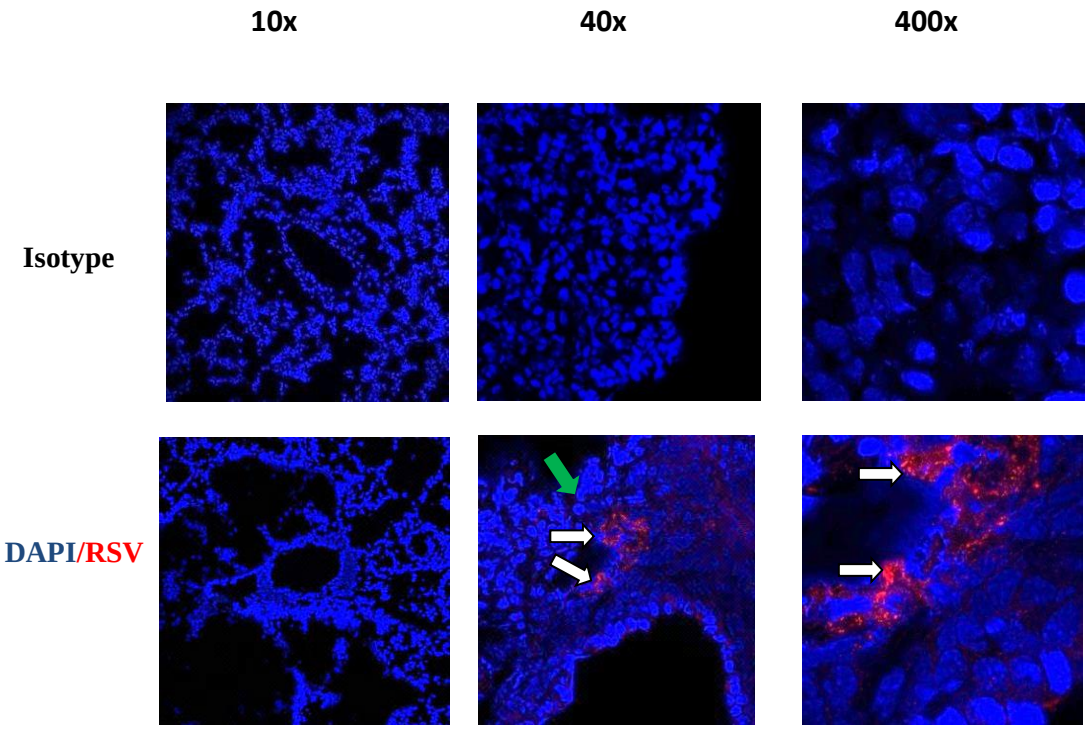

Figure: 4.23. Immunohistochemical localization of RSV A2 proteins in lung sections prepared from mice day 2

RSV (red) was detected around alveolar and airways as indicated by arrow. Cell nuclei shown in blue (DAPI). Isotype control was applied. Images were originally obtained using confocal microscopy at 10x, 40x and 400x magnifications.

4.1.3.6. UV treated RSV in mice lung after challenge at day 2

No RSV (red) was detected in mouse lung tissue at day 2 after challenge with UV treated RSV (Figure 4.24), and no comparable staining was noticed with the isotype control. Furthermore, no histological damage caused after challenge and the tissue structures were comparable to non-infected mice at day 0 (Figure 4.20) although there was some inflammatory cell infiltration (green arrow).

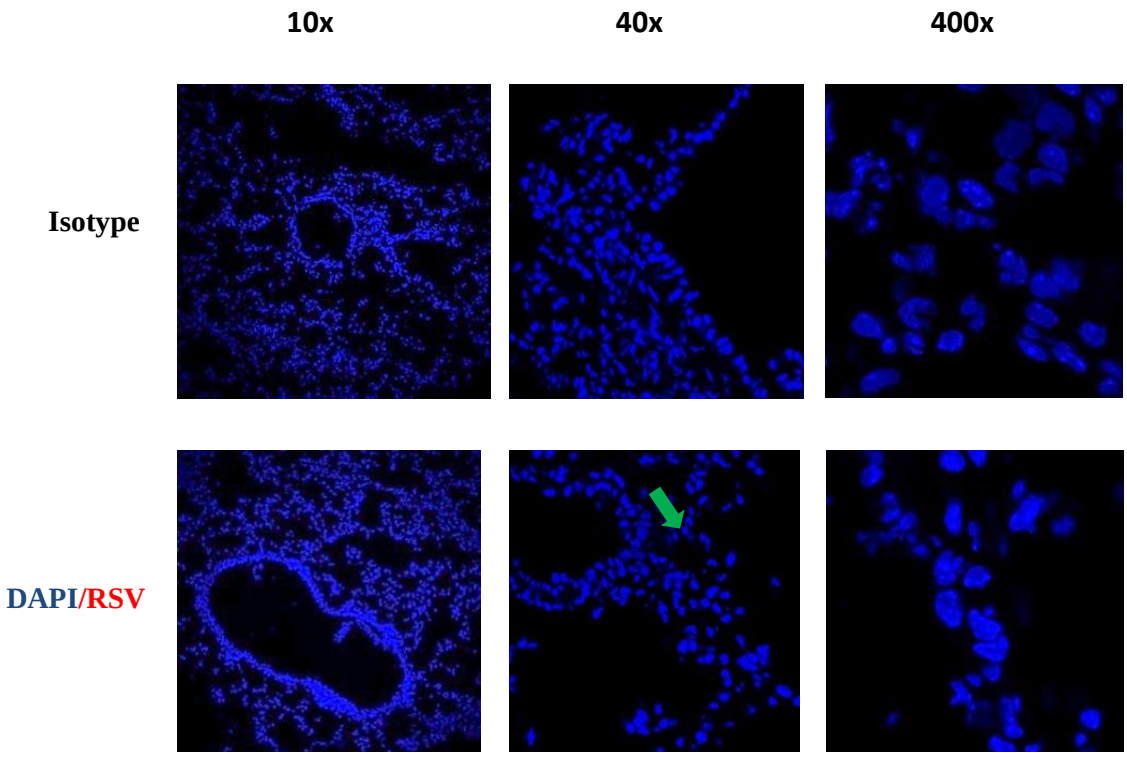

Figure 4.24. RSV is absent from mice challenged with RSV UV treated on day 2

RSV (red) was not in the airways. Cell nuclei shown in blue (DAPI). Isotype control was applied. Images were originally obtained using confocal microscopy at 10x, 40x and 400x magnifications.

4.3.6.7. Detection of RSV in mice lung tissue after RSV infection at day 4

Strong positive staining of RSV (red) was observed at day 4 after RSV infection (Figure 4.25) as indicated by arrow, and no comparable staining was noticed with the isotype control. In addition, RSV was detected into the cytoplasm of infected cells. RSV was localized near to airways epithelium and alveolar. RSV induced morphological changes including, epithelial damage that resulted in shrinkage of infected cells and infiltration of inflammatory cells (green arrow).

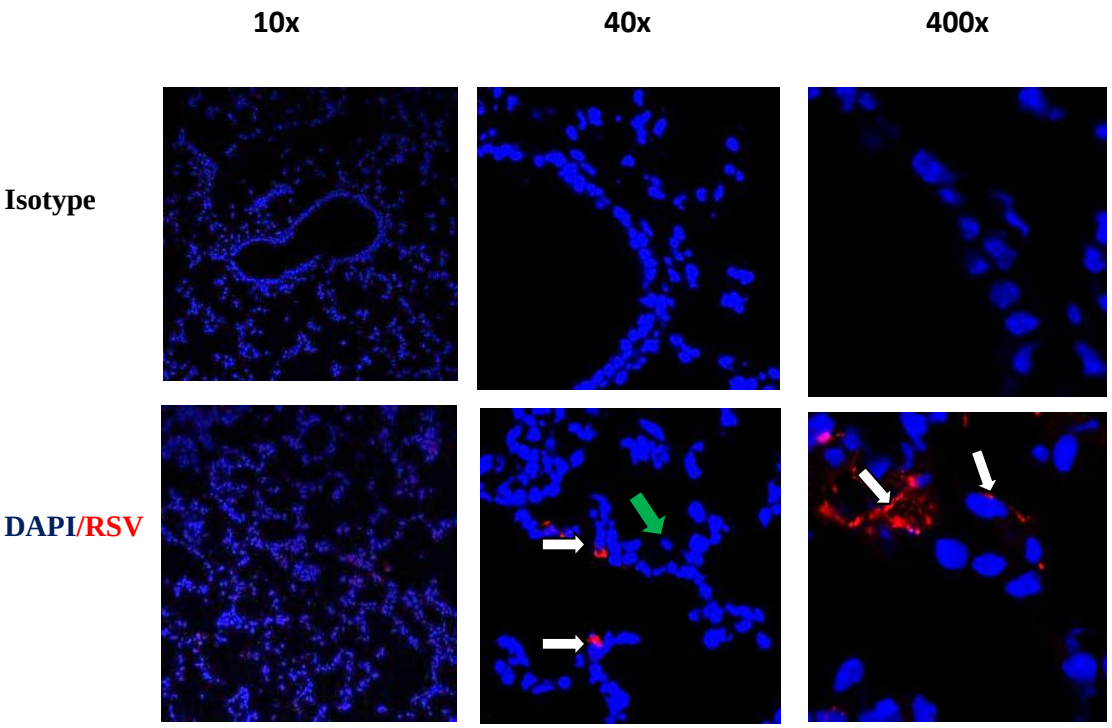

Figure: 4.25 Immunohistochemical localization of RSV proteins in lung sections prepared from mice day 4 after infection with RSV

RSV (red) was detected around alveolar and airways as indicated by arrow. Cell nuclei shown in blue (DAPI). Isotype control was applied. Images were originally obtained using confocal microscopy at 10x, 40x and 400x magnifications.

4.3.6.8. UV treated RSV in mice lung tissue after challenge at day 4

No RSV staining was observed after challenge with RSV UV treated (Figure 4.26) at day 4, and no comparable staining was noticed with the isotype control. In addition, no histological damage was observed and the tissue structures were quite similar to non-infected mice PBS (Figure 4.20) and there were some inflammatory cells noticed (green arrow).

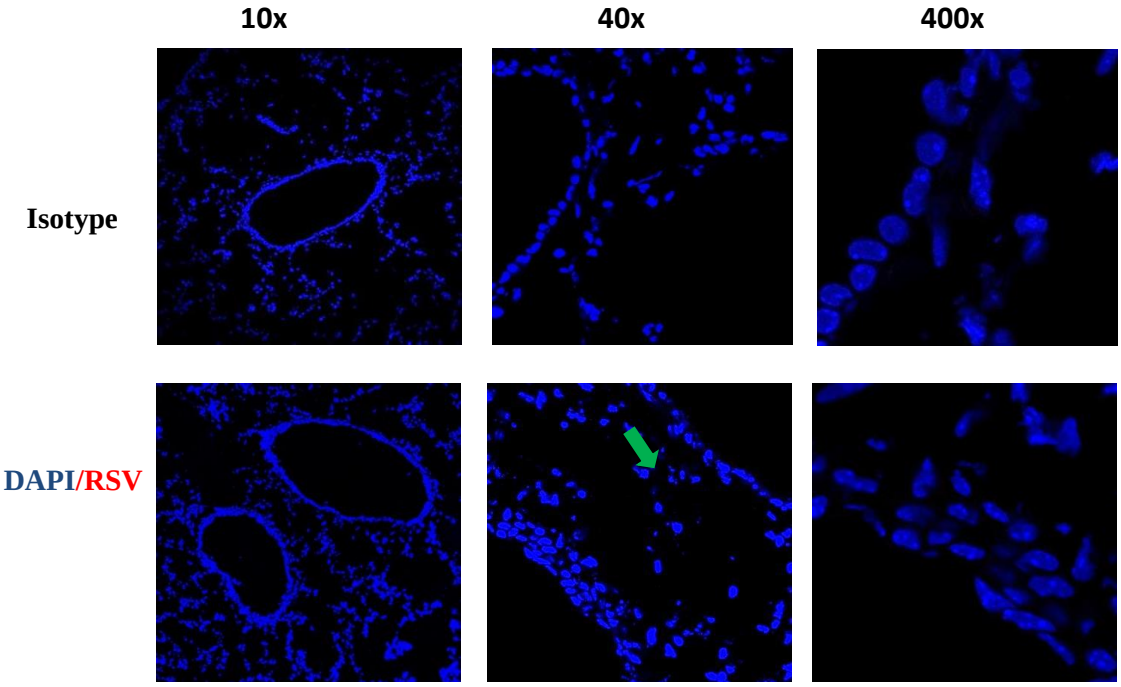

Figure 4.26. RSV is absent from mice infected with RSV UV treated on day 4

No RSV (red) was detected in the airways. Cell nuclei shown in blue (DAPI). Isotype control was applied. Images were originally obtained using confocal microscopy at 10x, 40x and 400x magnifications.

4.3.6.9. Detection of RSV in mice lung tissue after RSV infection at day 7

RSV (red) was detected at day 7 after RSV infection (FFigure 4.27) as indicated by arrow, and no comparable staining was noticed with the isotype control. RSV was detected in the cytoplasm of infected cells. RSV induced morphological changes including, shrinkage of infected cells, and spread of debris and obstruction of airways as well as infiltration of inflammatory cells (green arrow) in comparison to non-infected at day 0 (Figure 4.20).

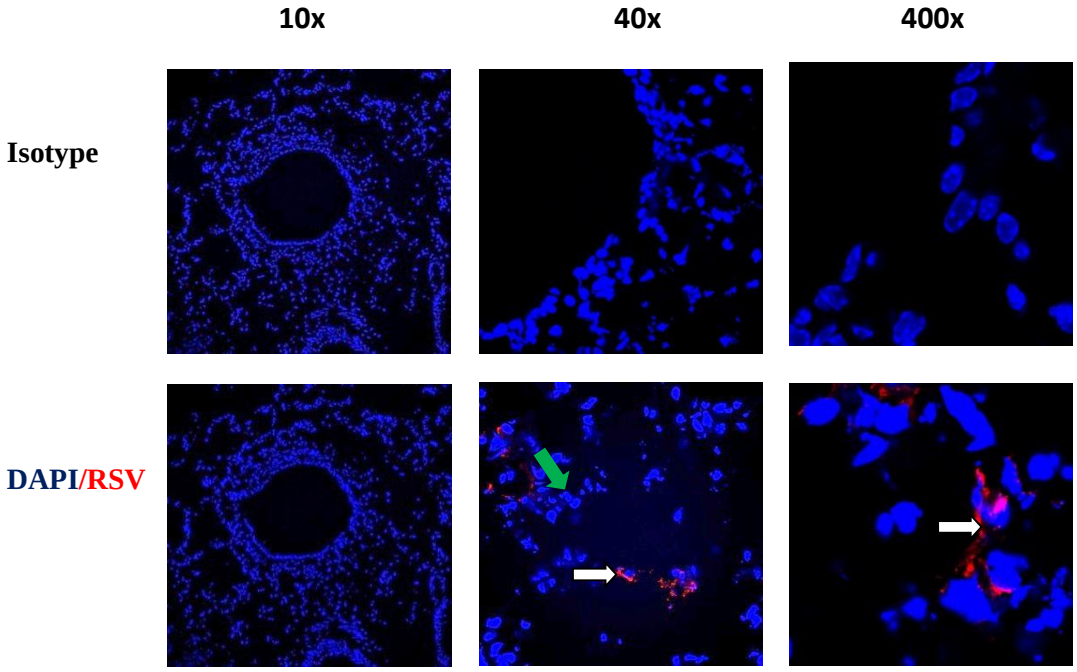

Figure 4.27. Immunohistochemical localization of RSV proteins in lung sections prepared from mice day 7 after infection with RSV

There was positive staining of RSV (red) detected around alveolar and airways as indicated by arrow. Cell nuclei shown in blue (DAPI). Isotype control was applied. Images were originally obtained using confocal microscopy at 10x, 40x and 400x magnifications.

4.3.6.10. UV treated RSV in mice lung tissue after challenge at day 7

No RSV staining was observed after challenge with RSV UV treated (FFigure 4.28) at day 7, and no comparable staining was noticed with the isotype control. In addition, limited histological damage observed and the tissue structures were quite similar to non-infected mice PBS (Figure 4.20) and there some inflammatory cells were noticed (green arrow).

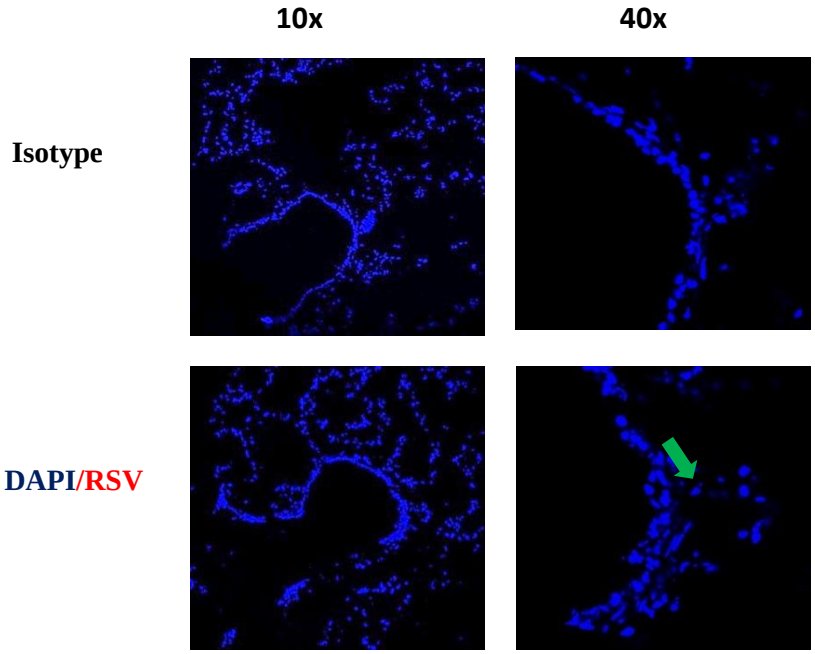

Figure 4.28. RSV was not detected in mice challenged with RSV UV treated at day 7

RSV (red) was not in the airways. Cell nuclei shown in blue (DAPI). Isotype control was applied. Images were originally obtained using confocal microscopy at 10x and 40x magnifications.

4.3.6.11. Detection of RSV in mice lung tissue after RSV infection at day 8

No RSV was detected from mouse lung tissue at day 8 after RSV infection (Figure 4.29), and no comparable staining was noticed with the isotype control. In addition, there was limited histological damage and some infiltration of inflammatory cells was observed (green arrow).

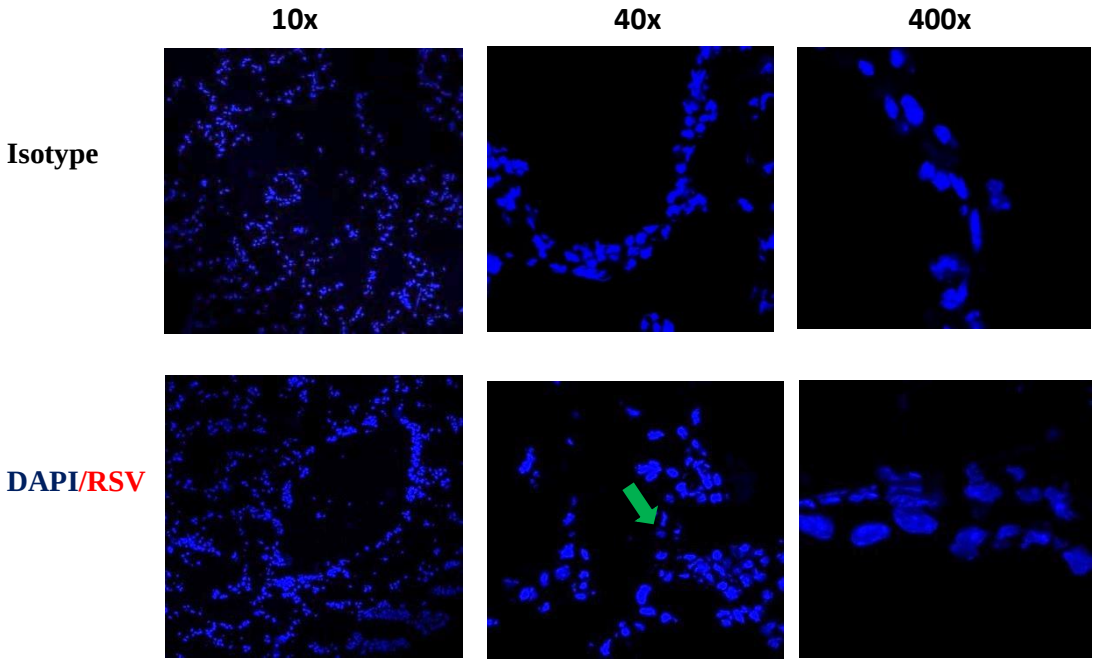

Figure 4.29. RSV is absent from mice infected with RSV at day 8

No RSV (red) was detected in the airways. Cell nuclei shown in blue (DAPI). Isotype control was applied. Images were originally obtained using confocal microscopy at 10x, 40x and 400x magnifications.

4.3.6.12. UV treated RSV in mice lung tissue after challenge at day 8

No RSV was detected from mouse lung tissue at day 8 after RSV UV treated challenge (Figure 4.30), and no comparable staining was noticed with the isotype control. There was limited histological damage and some inflammatory cells were observed (green arrow).

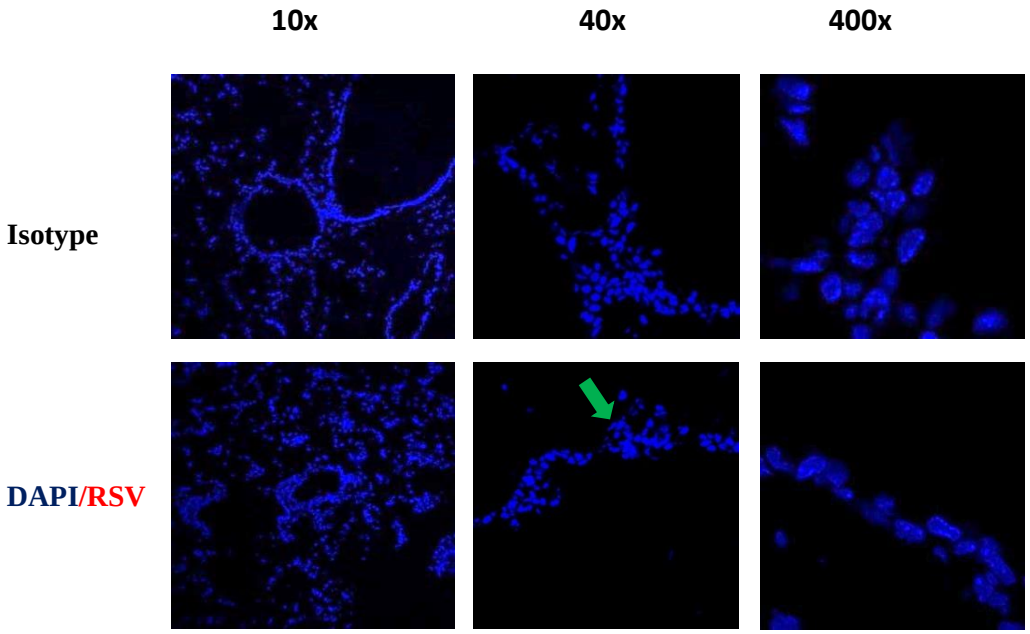

Figure 4.30. RSV is absent from mice challenged with RSV UV treated at day 8

RSV (red) was not in the airways. Cell nuclei shown in blue (DAPI). Isotype control was applied. Images were originally obtained using confocal microscopy at 10x, 40x and 400x magnifications.

4.3.6.2. Detection of BAFF in lung tissue after RSV infection

4.3.6.2.1. Mouse spleen positive control sections

BAFF is normally expressed in secondary lymphoid tissue such as spleen (Mackay & Browning 2002). Thus, BAFF (green) has been stained in mouse spleen sections as positive control (Figure 4.31).

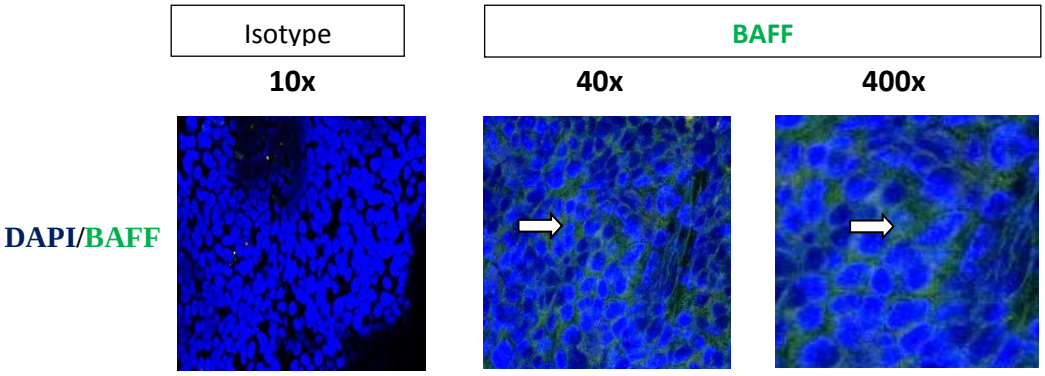

Figure 4.31. BAFF is normally expressed in mouse spleen section

BAFF (green) was detected around cells as indicated by arrow. Cell nuclei shown in blue (DAPI). Isotype control was applied. Images were originally obtained using confocal microscopy at 10x, 40x and 400x magnifications.

4.3.6.2. 2. BAFF is expressed in non-infected mice at day 0

Mouse lung sections at day 0 showed positive staining of BAFF (green) in the lungs (Figure 4.32), and no comparable staining was noticed with the isotype control. BAFF was expressed around the epithelium.

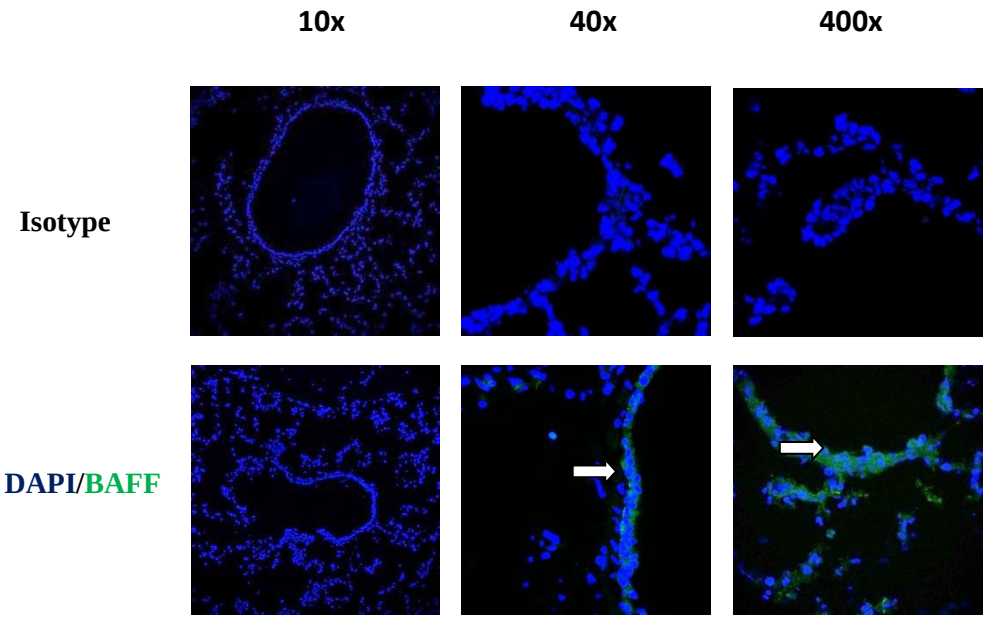

Figure 4.32. Expression of BAFF in non-infected mice at day 0

BAFF (green) was detected around epithelium and airways as indicated by arrow. Cell nuclei shown in blue (DAPI). Isotype control was applied. Images were originally obtained using confocal microscopy at 10x, 40x and 400x magnifications.

4.3.6.2.3. RSV infection of mice lungs induced BAFF expression at day 1

Immunofluorescent staining of a lung section from mouse infected with RSV at day 1 showed strong positive staining BAFF (green), and no comparable staining was noticed with the isotype control. Moreover, BAFF was localized around epithelium and alveoli (Figure 4.33), as indicated by arrow. In addition, there were morphological changes of lungs' structure, including epithelial damage, and obstruction of airways with fragmented and mixed inflammatory cells (brown arrow), that may also express BAFF.

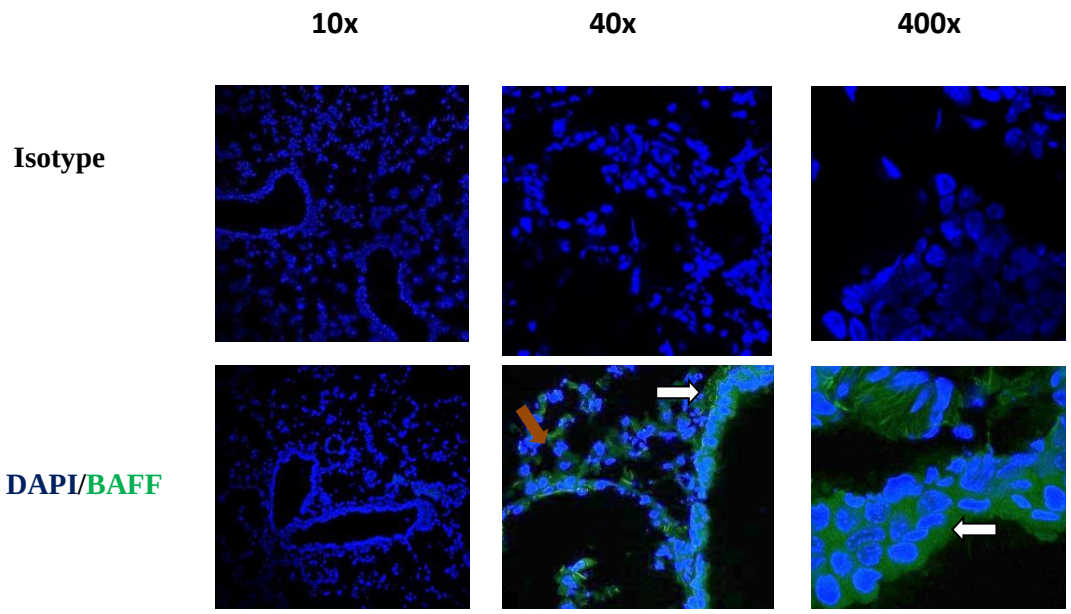

Figure 4.33. Expression of BAFF in mouse lung section after RSV infection at day 1

There was strong positive staining of BAFF (green) detected around epithelium, alveoli and some inflammatory cells as indicated by arrow. Cell nuclei shown in blue (DAPI). Isotype control was applied. Images were originally obtained using confocal microscopy at 10x, 40x and 400x magnifications.

4.3.6.2.4. UV treated RSV challenge of mouse lungs expressed BAFF at day 1

Lung sections from mice challenge with UV treated RSV at day 1 showed positive staining of BAFF (green) (Figure 4.34), and no comparable staining was noticed with the isotype control. BAFF was localized around airway and some infiltrated inflammatory cells (brown arrow) also expressed BAFF.

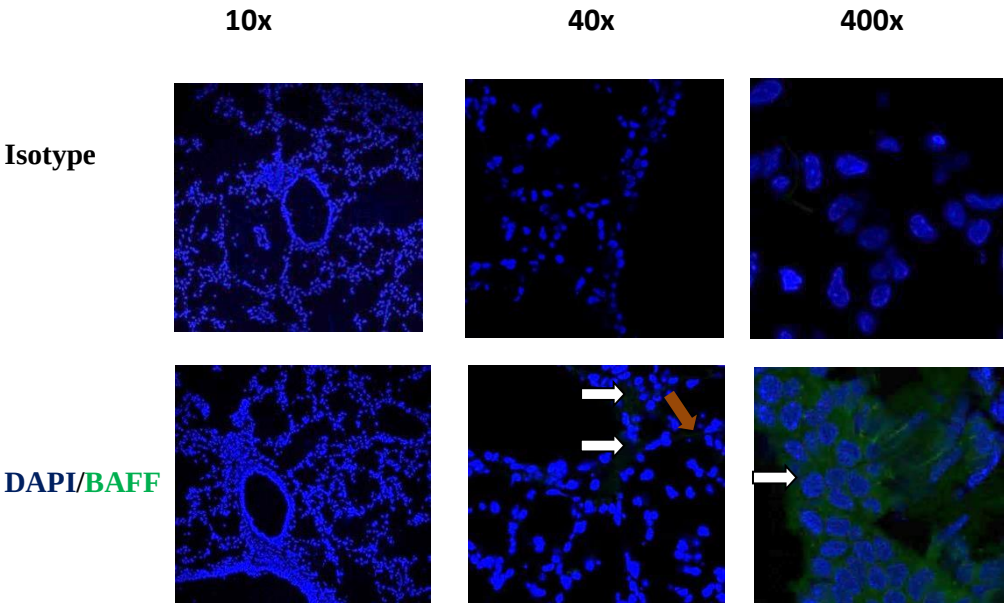

Figure 4.34. Expression of BAFF in RSV UV treated mouse at day 1

There was positive staining of BAFF (green) detected around epithelium and airways as indicated by arrow. Cell nuclei shown in blue (DAPI). Isotype control was applied. Images were originally obtained using confocal microscopy at 10x, 40x and 400x magnifications.

4.3.6.2.5. RSV infection of mice lungs induced BAFF expression at day 2

Lung sections from mice infected with RSV at day 2 showed strong positive staining of BAFF (green), and no comparable staining was noticed with the isotype control. BAFF is expressed around epithelium (Figure 4.35) and some infiltrating inflammatory cells (brown arrow) also expressed BAFF.

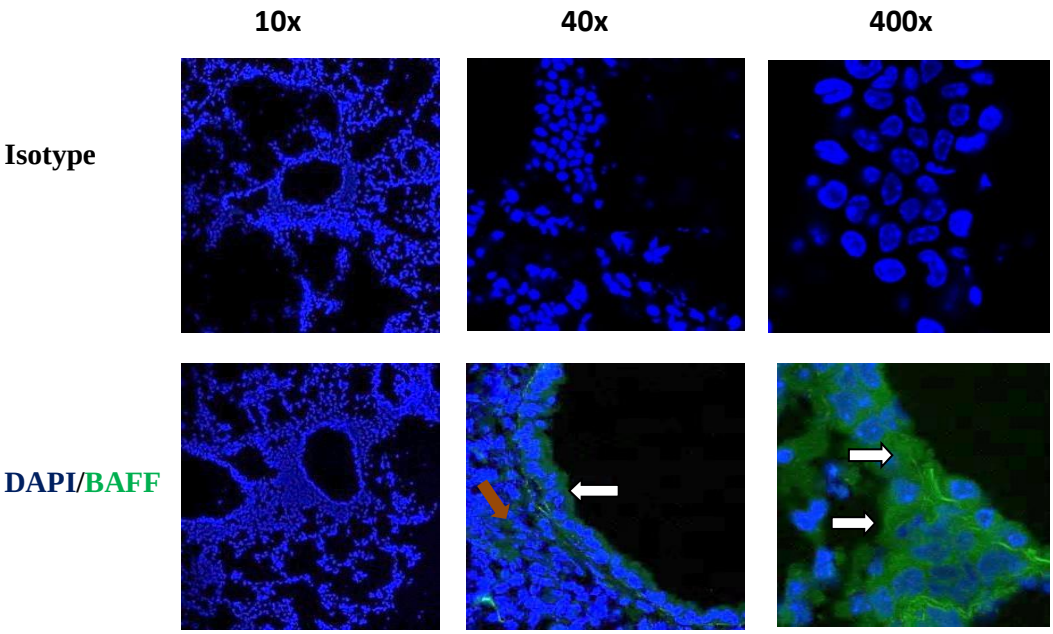

Figure 4.35. Expression of BAFF in mouse lung section after RSV infection at day 2

There was strong positive staining of BAFF (green) detected around epithelium, airways and some inflammatory cells as indicated by arrow. Cell nuclei shown in blue (DAPI). Isotype control was applied. Images were originally obtained using confocal microscopy at 10x, 40x and 400x magnifications.

4.3.6.2.6. UV treated RSV of mice lungs challenge expressed BAFF at day 2

Lung sections from mice challenge with UV treated RSV at day 2 showed positive staining of BAFF (green) (Figure 4.36), and no comparable staining was noticed with the isotype control. BAFF was localized around airway and some infiltrating inflammatory cells also expressed BAFF (brown arrow).

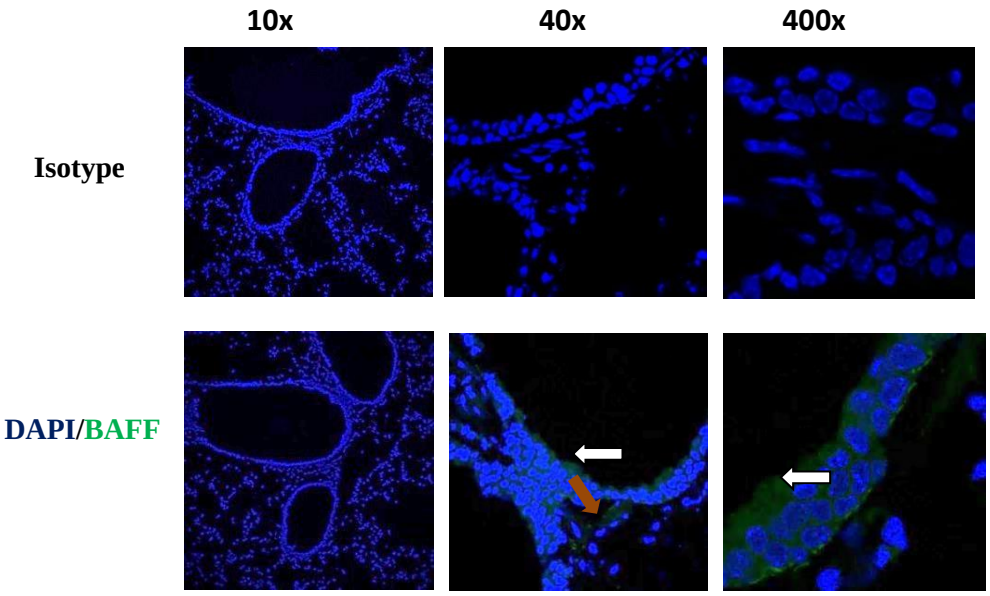

Figure 4.36. Expression of BAFF after RSV UV treated challenged at day 2

There was positive staining of BAFF (green) detected around epithelium, airways and inflammatory cells as indicated by arrow. Cell nuclei shown in blue (DAPI). Isotype control was applied. Images were originally obtained using confocal microscopy at 10x, 40x and 400x magnifications.

4.3.6.2.7. RSV infection of mice lungs induced BAFF expression at day 4

Lung sections from mice infected with RSV at day 4 showed positive staining of BAFF (green) (Figure 4.37), and no comparable staining was noticed with the isotype control. BAFF is expressed around epithelium and some infiltrating inflammatory cells.

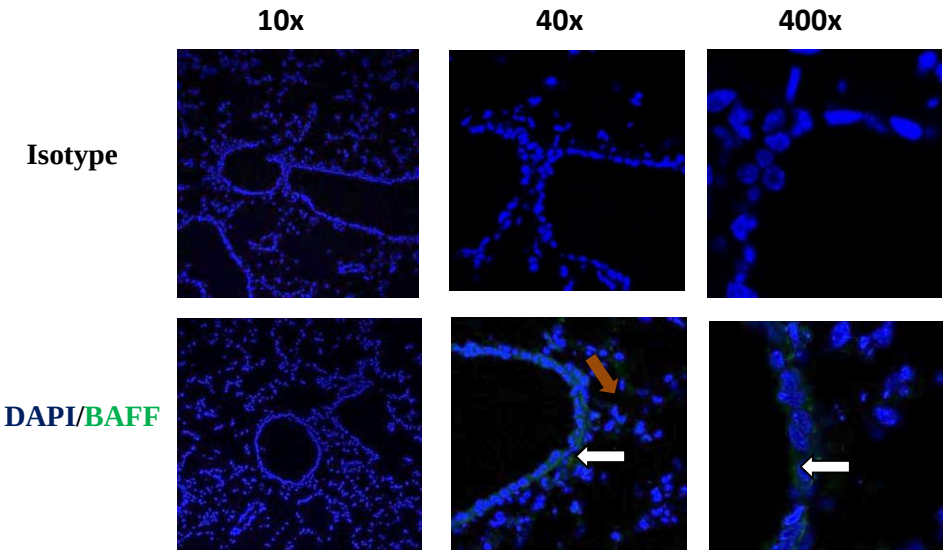

Figure 4.37. Expression of BAFF after RSV infection at day 4

There was positive staining of BAFF (green) detected around epithelium, airways and inflammatory cells as indicated by arrow. Cell nuclei shown in blue (DAPI). Isotype control was applied. Images were originally obtained using confocal microscopy at 10x, 40x and 400x magnifications.

4.3.6.2.8. UV treated RSV mice lungs challenge expressed BAFF at day 4

Lung sections from mice challenge with UV treated RSV at day 4 showed positive staining of BAFF (Figure 4.38), and no comparable staining was noticed with the isotype control. BAFF (green) was localized around epithelium and some infiltrating inflammatory cells (brown arrow).

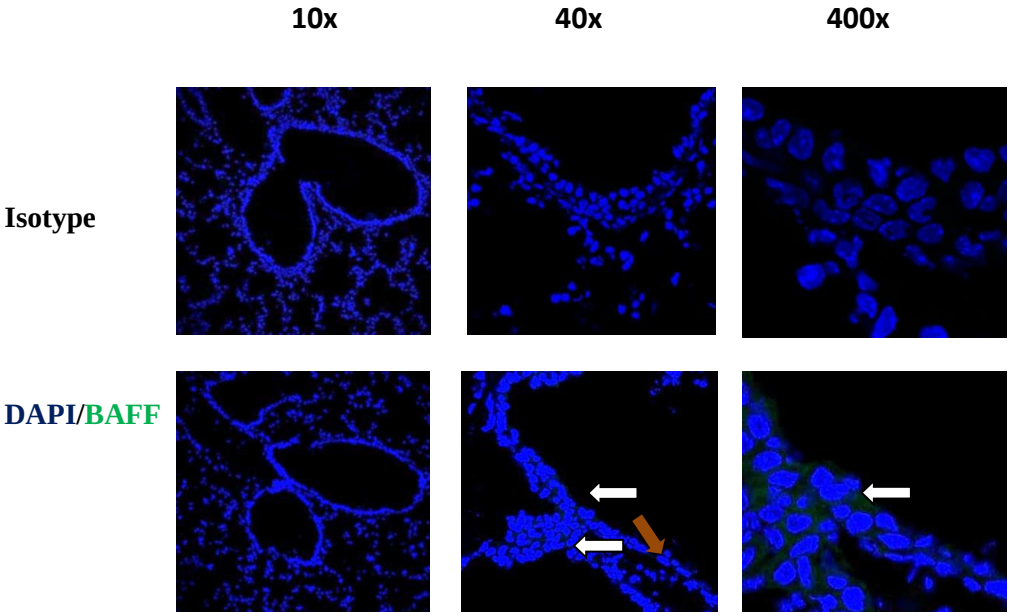

Figure 4.38. Expression of BAFF after RSV UV treated challenged at day 4

There was positive staining of BAFF (green) detected around epithelium, airways and inflammatory cells as indicated by arrow. Cell nuclei shown in blue (DAPI). Isotype control was applied. Images were originally obtained using confocal microscopy at 10x, 40x and 400x magnifications.

4.3.6.2.9. RSV infection of mice lungs induced BAFF expression at day 7

Lung sections from mice infected with RSV at day 7 showed strong positive staining of BAFF (green) ,and no comparable staining was noticed with the isotype control (Figure 4.39). BAFF was localized around epithelium and some inflammatory cells (brown arrow) have also expressed BAFF.

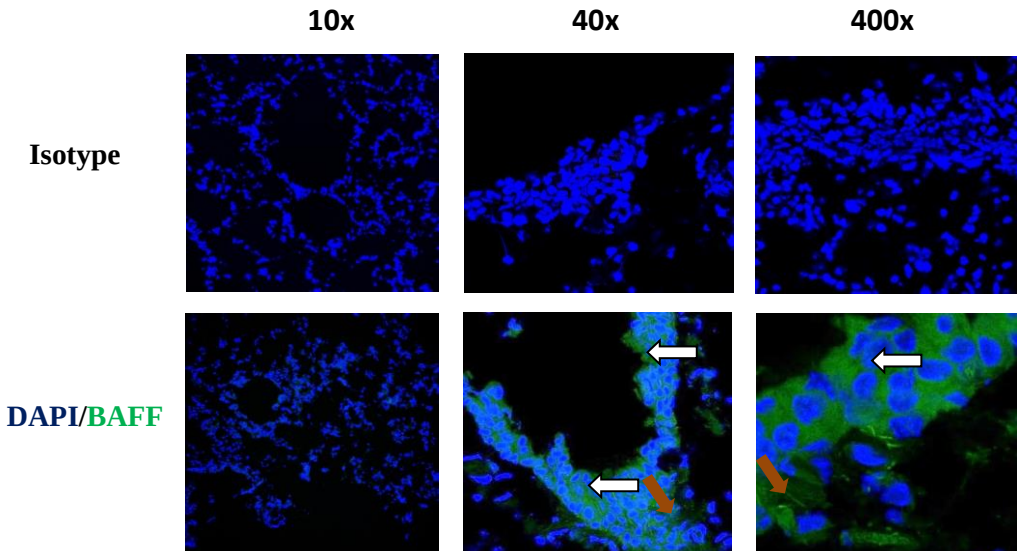

Figure 4.39. Expression of BAFF after RSV infection at day 7

There was strong positive staining of BAFF (green) detected around epithelium, airways and some inflammatory cells as indicated by arrow. Cell nuclei shown in blue (DAPI). Isotype control was applied. Images were originally obtained using confocal microscopy at 10x, 40x and 400x magnifications.

4.3.6.2.10 .UV treated RSV mice lungs challenge expressed BAFF at day 7

Lung sections from mice challenge with UV treated RSV at day 7 showed positive staining of BAFF (green), and no comparable staining was noticed with the isotype control (Figure 4.40). BAFF was localized around epithelium and some infiltrated inflammatory cells (brown arrow).

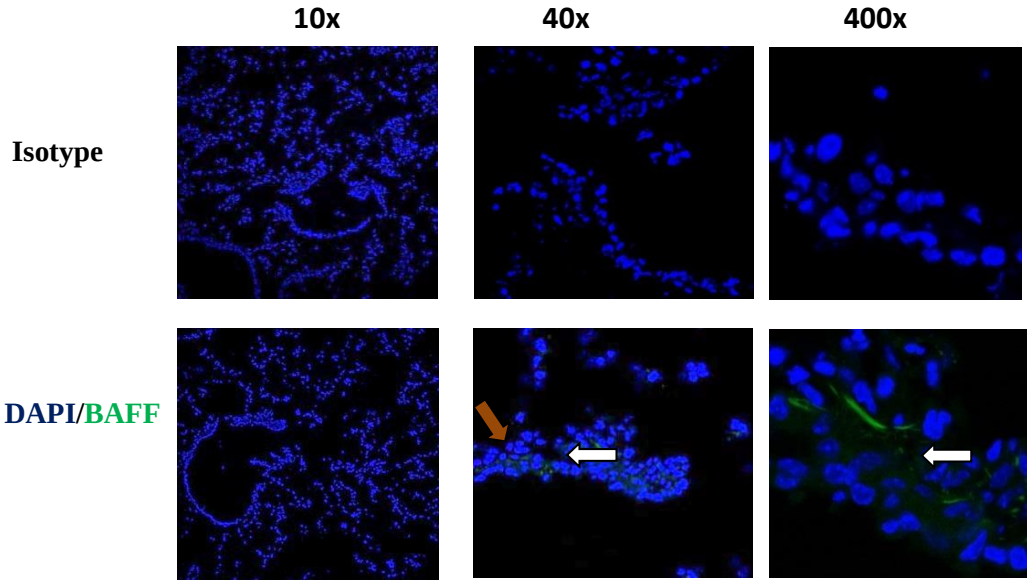

Figure 4.40. Expression of BAFF after RSV UV challenged at day 7

There was positive staining of BAFF (green) detected around epithelium, airways and inflammatory cells as indicated by arrow. Cell nuclei shown in blue (DAPI). Isotype control was applied. Images were originally obtained using confocal microscopy at 10x, 40x and 400x magnifications

4.3.6.2.11. RSV infection of mice lungs induced BAFF expression at day 8

Lung sections from mice infected with RSV at day 8 showed strong positive staining of BAFF (green), and no comparable staining was noticed with the isotype control (Figure 4.41). BAFF was localized around epithelium and some inflammatory cells (brown arrow) that also expressed BAFF.

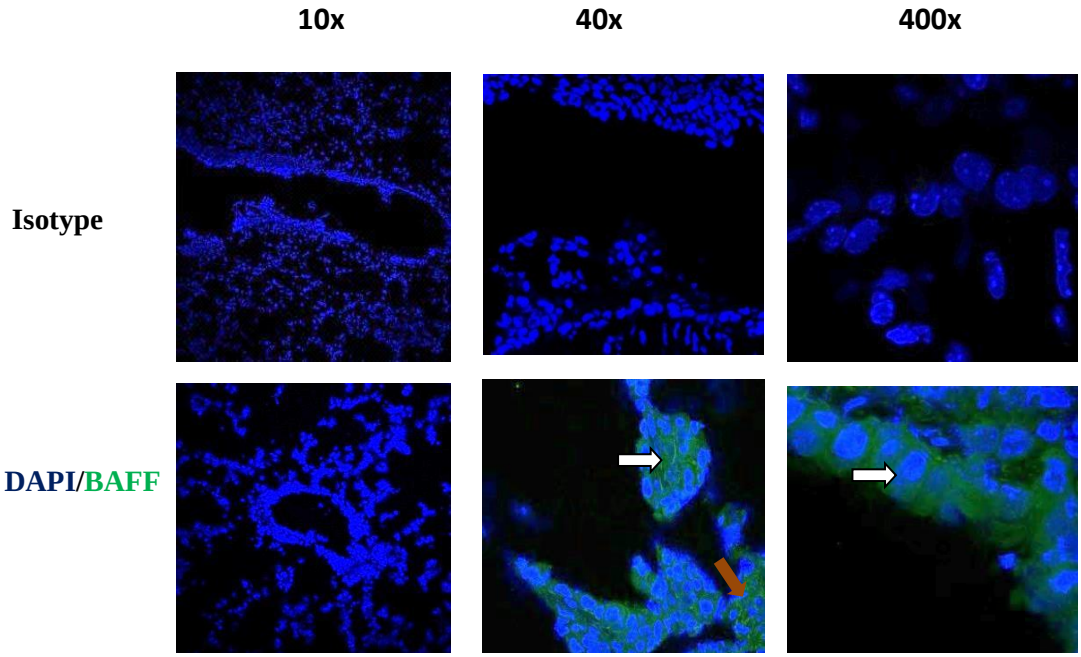

Figure 4.41. Expression of BAFF after RSV infection at day 8

There was strong positive staining of BAFF (green) detected around epithelium, airways and some inflammatory cells as indicated by arrow. Cell nuclei shown in blue (DAPI). Isotype control was applied. Images were originally obtained using confocal microscopy at 10x, 40x and 400x magnifications.

4.3.6.2.12. UV treated RSV mice lungs challenge expressed BAFF at day 8

Lung sections from mice challenge with UV treated RSV at day 8 showed positive staining of BAFF (green), and no comparable staining was noticed with the isotype control (Figure 4.42). BAFF was localized around epithelium and some infiltrated inflammatory cells (brown arrow).

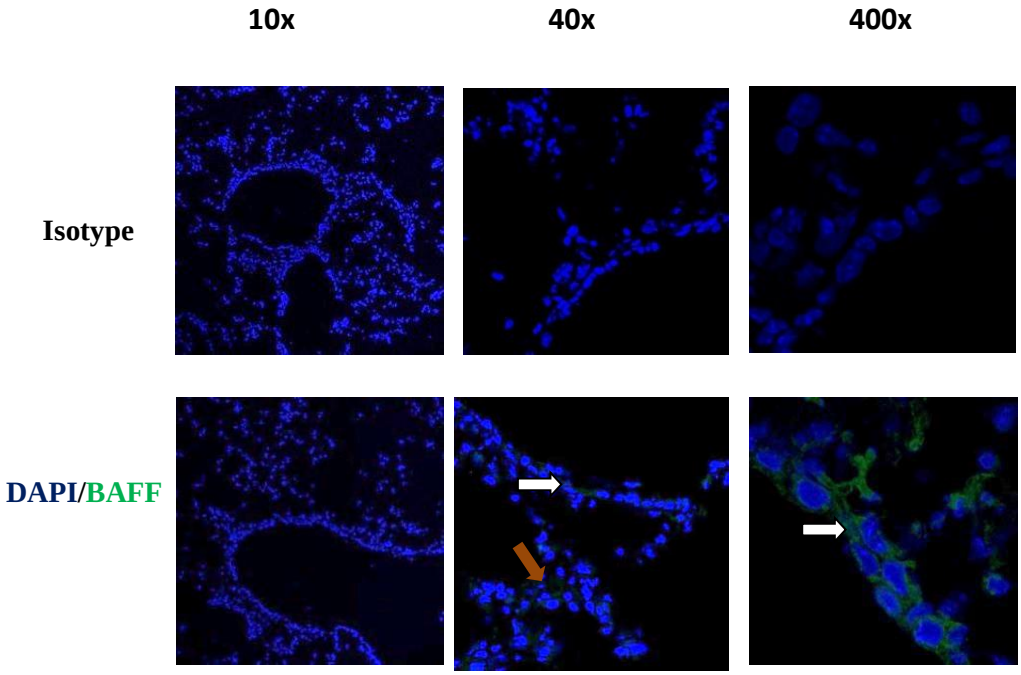

Figure 4.42. BAFF Expression after UV RSV challenged at day 8

There was positive staining of BAFF (green) detected around epithelium, airways and inflammatory cells as indicated by arrow. Cell nuclei shown in blue (DAPI). Isotype control was applied. Images were originally obtained using confocal microscopy at 10x, 40x and 400x magnifications.

4.3.7. Discussion

4.3.7.1. Detection of RSV infection in BALB/c mice after infection

To demonstrate that intranasal RSV A2 challenge of mice resulted in RSV infection within the lower airway, RSV N RNA expression was measured by RT-PCR. These experiments were carried out using homogenized lung tissue from RSV infected and UV treated RSV control and non-infected mice challenge with PBS at day 0. Increasing levels of RSV were significantly detected at day 1, 2 and day 4 (1.87, P=0.12) after RSV infection in comparison to the UV RSV controls at the same time points. RSV N RNA was significantly higher 4 days after infection and began to decline by 7 days after infection (F). RSV infection was undetectable 8 days after infection. Overall, there were two peaks of RSV, at day1 and 4. This is the overall average of experiments one and two, experiment three is not included in this analysis as result of weak infection (Figure 4.12). Overall, these findings are in agreement with other study that found at day 4 after infection viral load peaks at days 4–5 and after which the viral load declined (Openshaw 2013; Taylor *et al.* 1984) .

Moreover, RSV infection was further confirmed by immunofluorescence staining. As expected, RSV (red) was detected at day 1 (Figure 4.21), day 2 (Figure 4.23), and day 4 (Figure 4.25). There was strong positive staining of RSV at day 4, weak at day 7 (Figure 4.27) and undetectable on day 8 (Figure 4.29) in comparison to non-infected PBS and RSV-UV treated at the same time points. The results obtained using immunofluorescence staining of lung sections are correlated with the RT-PCR results measuring RSV N RNA (Figure 4.15).

Furthermore, immunofluorescence staining of RSV infected mice on day 1 (Figure 4.21), day 2 (Figure 4.23), day 4 (Figure 4.25) and day 7 (Figure 4.27) showed that RSV infection induced pathological changes including bronchiolar epithelial damage, and obstruction of some bronchioles with fragmented epithelium mixed with infiltrated inflammatory cells. However, these changes were less evident in non-infected at day 0 (Figure 4.20) and UV treated RSV animals at day 1 (Figure 4.22), day 2 (Figure 4.24), day 4 (Figure 4.26) and day 7 (Figure 4.28).

Furthermore, immunofluorescence staining indicated that the RSV was both localized around airway epithelium and in other alveolar cells, possibly macrophages

(Figures 4-21, 4-23, 4-25 and 4-27). However, it has been shown that the predominant infected cell is the Type I alveolar pneumocyte that line the alveolar surfaces of the lungs (Openshaw 2013). To ensure these cells were epithelium and that RSV infects murine epithelium, the epithelium could be labeled with a specific marker such as cytokeratin-19, and dual stained for RSV.

4.3.7.2. BAFF mRNA and protein, but not APRIL mRNA, were increased significantly during RSV infection, compared to UV treated RSV and non-infected animals

BAFF mRNA was expressed in non-infected mice at day 0 (fold increase 0.75). However, after RSV infection BAFF mRNA expression was increased significantly on day 1 (fold increase relative to control= 1.09, P=0.008), day 7 (1.5, P=0.004) and day 8 (1.09, P=0.01) in comparison to UV treated RSV control on day 1 (0.7), day 7 (0.8) and day 8 (0.5) (Figure 4.16).

BAFF protein was expressed in non-infected mice at day 0 (mean = 478 pg/ml). This could be released during preparation of samples or also it is possible that lung normally contains BAFF protein. However, after RSV infection BAFF protein was elevated significantly at day 1, 2, 4, 7 and day 8 in comparison to UV treated RSV control at the same time points (Figure 4.17).

Overall, there appear to be two peaks of both BAFF mRNA (Figure 4.16) and protein (Figure 4.17) expressions after RSV infection. BAFF was increased on day 1 and 2 and then declined on day 4. This increase could be as results of production of BAFF by the infected lung epithelial cells. On day 7 BAFF protein reached the peak level of expression. This could be due to further secretion by the infiltrated leukocytes and DC where B cells respond and differentiate (chapter 5).

Although BAFF expression after RSV infection has been reported to depend on production of IFN-β by the infected cells (McNamara *et al.* 2013), it is difficult to confirm whether this is the case in this model. Thus, to determine whether BAFF expression in this model was depending on IFN-β or not, we could inhibit IFN-β in mice prior to RSV infection and observe if production of BAFF depends on IFN-β at day 7 and 8 after RSV challenge. Furthermore, measuring IFN-β after infection

would also be useful to determine an increase production of IFN-β following RSV infection. Taken together, the kinetics of BAFF expressions were associated with RSV kinetics expression at day 1 and 2, although RSV reached highest levels at day 4, BAFF protein was significantly declined. Furthermore, the kinetics of BAFF protein expression initially parallel RSV kinetics suggesting that RSV is directy or indirectly inducing BAFF expression. At day 7 and 8 there was no evidence by PCR of the presence of RSV, which suggested that BAFF can be further released by inflammatory cells.

Expression of BAFF was further confirmed by immunofluorescence staining of mouse lung sections. It has been reported that BAFF is expressed normally in secondary lymphoid tissue such as spleen (Bossen & Schneider 2006), thus, mouse spleen was stained for BAFF as apositive control for lung sections (Figure 4.31).

Immunofluorescence staining of mouse lung on day 0 (Figure 4.32) and non-infected BEAS-2B cells (chapter 3, Figure 3.13.2.A) showed that BAFF was normally expressed.
Furthermore, western blot analysis of homogenized lung tissue showed membrane BAFF (34kD) was expressed by non-infected mice and resting BEAS-2B cells (31kD) (Figure 4.19). However, soluble BAFF was (20 kD) expressed at day 1, 2, 4 and 7 after RSV infection. This suggests that at later time points soluble BAFF (20 kD) was cleaved from the membrane bound form (34 kD) and soluble BAFF released by RSV infected epithelial cells may enhance the adaptive immune response by inducing infiltration of cells. In addition, the absence of a clear band of membrane BAFF expected in non-infected mice at day 0 could be as result of low protein loading as shown by beta actin.

Furthermore, there was strong positive staining of BAFF (green) detected at day 1 (Figure 4.33), 2 (Figure 35), 7 (Figure 4.39) and 8 (Figure 4.41) in comparison to UV treated RSV control where BAFF was expressed weaker than RSV infected at day 1 (Figure 4.34), day 2 (Figure 4.36), day 7 (Figure 4.40) and day 8 (Figure 4.42). BAFF was expressed around epithelium and some infiltrated inflammatory cells that could also induce BAFF expression such as neutrophils, monocytes and macrophages.

Expression of APRIL was studied by RT-PCR. Non-infected mice at day 0 expressed APRIL mRNA but there was no significant increase expression of APRIL mRNA after RSV infection relative UV RSV control at day 1, 2, 4, 7 and 8 (Figure 4.18).

In the absence of evidence from these PCR experiments that the level of APRIL mRNA expression increased as a result of RSV infection and the low sensitivity of commercial APRIL ELISA's assays, APRIL protein expression was not measured.

APRIL is known to be expressed at the cell surface or complexed to proteoglycans, which would also make detection difficult (Reijmers *et al.* 2011). It could also be possible that APRIL is expressed as a protein at later time points or it requires further signals to be released. In addition, this result correlates with our recent finding where there was no significant up regulation of APRIL observed during natural RSV infection in humans (McNamara *et al.* 2013), at least not in epithelial cells. Although here the study is limited to showing that there was no significant increased expression of APRIL mRNA, absence of APRIL protein could lead to decreased B cell maturation and memory cell responses (Xiao *et al.* 2011).

Human respiratory syncytial virus can re-infect symptomatically throughout life without significant antigenic change, suggestive of incomplete or short-lived immunity. In contrast, re-infection by influenza A virus largely depends on antigenic change, suggestive of more complete immunity (Le Nouen *et al.* 2011).

It has been suggested that BAFF has an important role at the early stages of B cell development, while APRIL is more essential at later stages of B cell responses when plasma cells are produced (Treml *et al.* 2009). Thus, it could be possible that influenza infection induces APRIL expression and therefore increases survival of long lived plasma cells, whereas RSV does not induce APRIL and for this reason no strong adaptive immune response is induced against RSV, allowing later re-infection.

In vivo, it has been shown that mice infected with influenza virus for 35 days and later treated for 2 weeks with TACI-Fc that neutralizes both BAFF and APRIL have a reduced percentage and total number of Ab-secreting cells, including virus-specific Ab-secreting cells, in lungs and BM. This was associated with a significant reduction

in antiviral serum IgG, as well as virus-specific IgG and IgA in the BAL (Wolf *et al.* 2011). However, mice treated with anti-BAFF after 36 days of influenza infection had no effect on antiviral antibody protection measured by virus specific IgG and IgA titre in serum and BAL although $CD19^+$ B cells were significantly reduced in spleen, lung-draining medLN, and lungs. These observations suggested that blockade of BAFF and APRIL, but not BAFF alone, regulates ASC survival in response to influenza virus infection (Wolf *et al.* 2011). To further understand this process behind this mechanism of local antibody production in RSV infection, APRIL alone could be blocked to see if the survival of B cells will be affected since the study above targeted BAFF and APRIL or BAFF alone.

4.3.8. Summary

A mouse model of human RSV infection was successfully established and used to examine BAFF expression in response to RSV infection. Immunofluorescence staining indicated that the RSV was localized to the airway epithelium. However, it has been shown that the predominant infected cell is the Type I alveolar pneumocyte. RSV infection of mice induced significantly expression of BAFF mRNA and protein, but not APRIL relative to non-infected and UV-RSV challenge control. Two peaks of BAFF expression were observed. Immunofluorescence staining of mouse lung sections further confirmed expression of BAFF around epithelium and some inflammatory cells after RSV infection. Western blot analysis of homogenized lung tissue showed that non infected mice expressed membrane BAFF (34 kD) and after RSV infection soluble BAFF (20 kD) was noticed. These results suggest the importance of epithelium in supporting the adaptive immune response by production of BAFF in the lungs during RSV infection, and do not exclude production of BAFF by other inflammatory cells.

CHAPTER 5. EXPRESSION OF CXCL12, CXCL13, CCL19 AND CCL21 IN A MURINE MODEL OF HUMAN RESPIRATORY SYNCYTIAL VIRUS INFECTION

5.1. Aims

Experiments described in chapter 4 demonstrate increased expression of BAFF, a B cell growth and differentiation factor in the airway in response to RSV infection, raising the possibility that BAFF may act locally to enhance the adaptive immune response within the airway. For this to occur, lymphocytes would also need to be recruited to the lungs. The work described in this chapter aimed to use the murine model of human RSV infection described in chapter 4 to further understand how recruitment of B and T cells in response to RSV infection may be regulated. To better understand this process, the local expression of the lymphoid chemokines, including CXCL12, CXCL13, CCL19, and CCL21 (chapter 1, 1.4) were measured in homogenised mouse lung tissue after RSV infection. Specific aims were:

1 -To determine if the homeostatic chemokines CXCL12, CXCL13, CCL19 and CCL21 (chapter 1, 1.4) are expressed following RSV infection by RT-PCR and ELISA.

2- To examine localization of CXCL13 expression in lung murine sections following RSV infection.

3 -To determine if B (anti-CD20) and T cells (anti-CD3) were recruited into the lungs after RSV infection and examine their localization in lung sections following RSV infection.

5.2. Experimental design

The same samples as used in the previous chapter (chapter 4) were further used to analyse local expression of CXCL12, CXCL13, CCL19 and CCL21 by RT-PCR and ELISA. In addition, mouse lung sections were examined by immunofluorescence staining to study localization of CXCL13, B cells and T cells (Chapter 4, Figure 4.1).

5.3. Results

5. 3.1. Experiment 1

5. 3.1.1. Expression of CXCL13 mRNA and protein after RSV infection

To study CXCL13 mRNA expression *in vivo*, mice were infected with RSV (A2 strain) and samples collected at different time points, time day 0 (non-infected), 1, 2, 4 and 7 days. RNA was isolated and prepared using Qiagen as described (chapter 2, 2.4). CXCL13 mRNA was measured and analyzed by RT-PCR. Non-infected mice day 0 expressed CXCL13 mRNA (fold expression relative to control=0.07). However, after RSV infection CXCL13 mRNA expression was increased significantly at day 1 (1.36, P=0.04), day 2 (1.08, P=0.04) and day 7 (0.97, P=0.02) 7 in comparison to UV RSV control on day 1 (0.29), day 2 (0.08) and day 7 (0.08) (Figure 5.1.A). Furthermore, CXCL13 protein (Figure 5.1.B) was measured in homogenised lung tissue. CXCL13 protein was expressed in non-infected mice at day 0 (mean=296 pg/ml). However, after RSV infection CXCL13 protein was increased significantly at day 1 (762 pg/ml, P=0.01), day 2 (612 pg/ml, P=0.02), and day 7 (388 pg/ml, P=0.007) in comparison to UV RSV control at day 1 (374 pg/ml), day 2 (278 pg/ml) and day 7 (249 pg/ml). Overall, there were two peaks formed of both CXCL13 mRNA and protein at day 1 and 7 and declined at day 4.

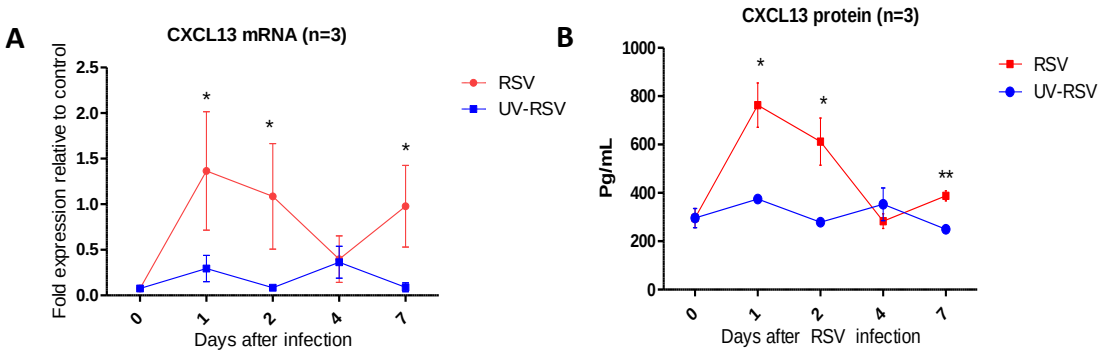

Figure 5. 1. Expression of CXCL13 mRNA (A) and protein (B) after RSV infection or challenge with UV-RSV control

*CXCL13 mRNA was measured by RT-PCR. CXCL13 mRNA expression was increased significantly after RSV infection on day 1, 2 and 7 in comparison to UV RSV control at the same time points. Values are shown as fold expression relative to control. CXCL13 protein was measured by use of specific murine CXCL13 ELISA. CXCL13 protein was increased significantly after RSV infection at day 1, 2, and 7 in comparison to UV RSV control at the same time points. Result shown is the average of three animals in the first experiment. Mean and SD are shown (two way ANOVA with Bonferroni post-hoc test, *P <0.05, n=3).*

5.3.1.2. CXCL13 protein expression in comparision to total ptotein concentration after RSV infection

CXCL13 protein (pg/ml) levels were normalised to total protein (pg/ng) (chapter 2, 2.3.2). CXCL13 protein was expressed in non-infected mice at day 0 (mean=256 pg/ng). After RSV infection there was no significant increase of CXCL13 protein (Figure 5.2) at day 1 (617 pg/ng, P=0.1), day 2 (567 pg/ng, P=0.1), day 4 (205 pg/ng, P=0.1) and day7 (222 pg/ng, P=0.9) in comparison to UV RSV control on day 1 (460 pg/ng), day 2 (258 pg/ng), day 4 (253 pg/ng) and day 7 (223 pg/ng).

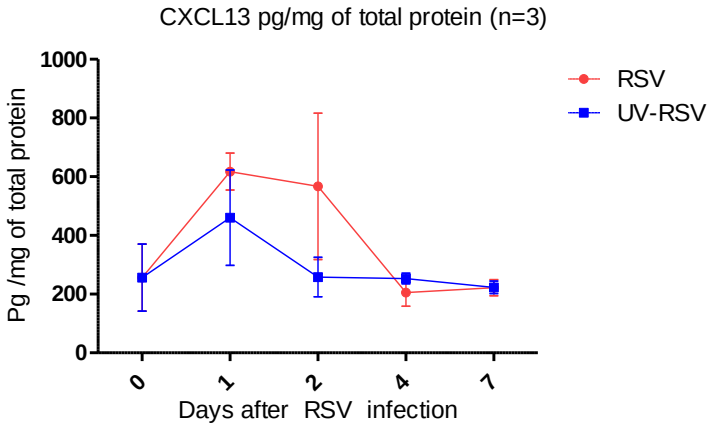

Figure 5.2. Normalized CXCL13 protein to total protein after RSV infection or challenge with UV-RSV control

*CXCL13 protein was expressed in non- infected mice at day 0 and after RSV infection there was no significant increase in comparison to UV RSV control on day 1, 2, 4 and 7. Result shown is the average of three animals in the first experiment. Mean and SD are shown (two way ANOVA with Bonferroni post-hoc test, *P <0.05, n=3).*

5. 3.1.3. RSV infection did not significantly up regulate CCL19 mRNA and protein expression

To determine if CCL19 mRNA is expressed after RSV infection, mice were infected with RSV (A2 strain) at time points, including time day 0 (non-infected), 1, 2, 4 and 7. At the time points indicated after RSV infection mouse lung tissues were homogenized and RNA was isolated and prepared using Qiagen as described (Chapter 2.4). There was significant increase of CCL19 mRNA (Figure 5.3.A) after RSV infection on day 4 (0.01, P=0.0005) in comparison to UV RSV control on day 4 (0.005). CCL19 protein (Figure 5.3.B) was measured in homogenized mouse lung tissue. Non - infected mice at day 0 expressed CCL19 protein (mean = 298 pg/ml). However, after RSV infection there was significant decrease of CCL119 protein at day 7 (200 pg/ml, P=0.03) in comparison to UV RSV control on day 7 (290 pg/ml).

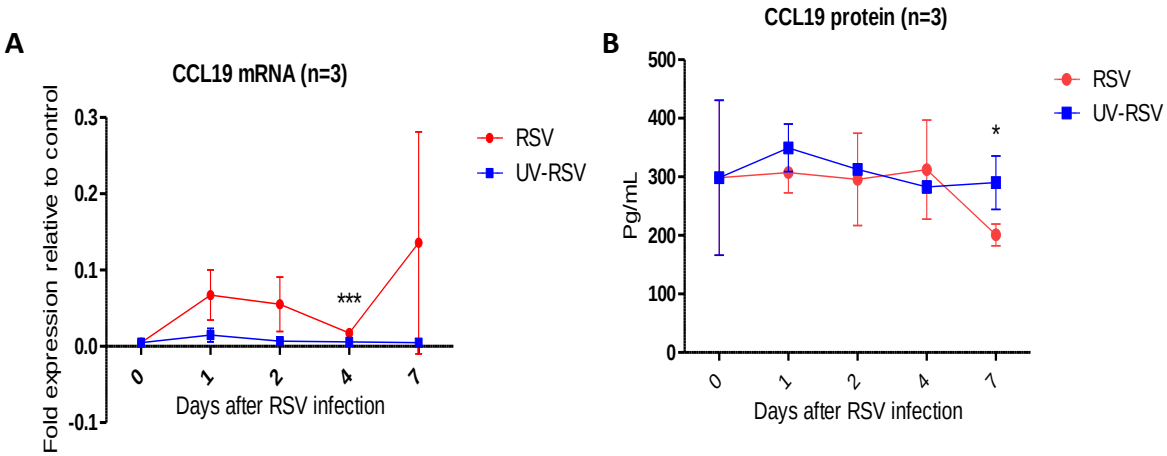

Figure 5.3. Expression of CCL19 mRNA (A) and protein (B) after RSV infection or challenge with UV-RSV control

*CCL19 mRNA was measured by RT-PCR. CCl19 was expressed at day 1, 2 and 7. However, on day 4 CCL19 mRNA was decreased significantly in comparison to UV treated RSV control at the same time point. Values are shown as fold expression relative to control. CCL19 protein was measured by using specific murine CCL19 ELISA. CCL19 protein was expressed in non-infected mice at day 0 and there was significant decrease after RSV infection at day 7 in comparison to UV RSV control at the same time point. Result shown is the average of three animals in the first experiment. Mean and SD are shown (two way ANOVA with Bonferroni post-hoc test, *P <0.05, n=3).*

5. 3.1.4. CCL19 protein expression in comparison to total protein concentration after RSV infection

CCL19 protein (pg/ml) levels were normalised to total protein (pg/ng) (chapter 2, 2.3.2). CCL19 protein (Figure 5.4) was expressed in samples collected at day 0 (mean =266 pg/ng). However, after RSV infection, CCL19 protein was decreased significantly at day 7 (115 pg/ng, P=0.003) in comparison to UV RSV control on day 7 (260 pg/ng).

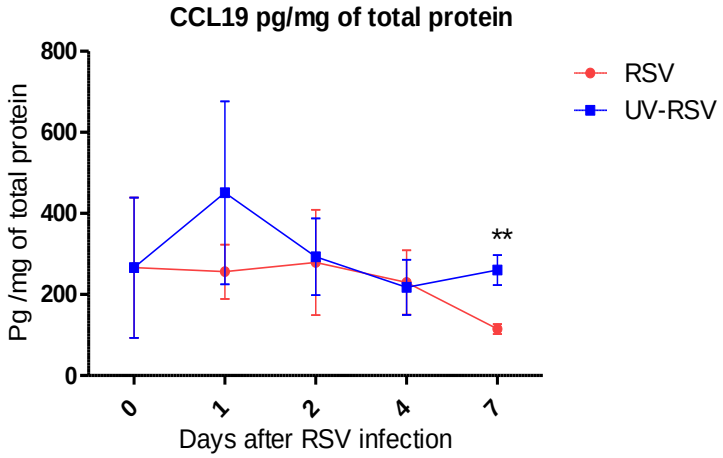

Figure 5.4. Normalized CCL19 protein to total protein after RSV infection or challenge with UV-RSV control

*CCL19 protein was expressed in non-infected mice at day 0 and there was significant decrease of CCL19 protein at day 7 after RSV infection in comparison to UV RSV control at day 7. Result shown is the average of three animals in the first experiment. Mean and SD are shown (two way ANOVA with Bonferroni post-hoc test, *P <0.05, n=3).*

5. 3.1.5. RSV infection did not significantly up regulate CCL21 mRNA and protein

To determine if CCL21 mRNA is expressed after RSV infection, mice were infected with RSV (A2 strain) at various time points, including time day 0 (non-infected), 1, 2, 4 and day 7. At the time points indicated after RSV infection mouse lungs tissue were homogenized and RNA was isolated and prepared using Qiagen as described (chapter 2, 2.4). CCL21 mRNA was expressed in non-infected mice at day 0 (fold expression relative to control= 3.64). After RSV infection, there was no significant increase of CCL21 mRNA expression at day 1 (2.9, P=0.9), day 2 (5, P=0.6), day 4 (4.31, P=0.1) and day 7 (2.62, P=0.8) in comparison to UV RSV control on day 1 (2.86), day 2 (3.81), day 4 (9.07) and day 7 (2.95) (Figure 5.5.A).

Furthermore, CCL21 protein (Figure 5.5.B) was measured in homogenised lung tissue. CCL21 protein was expressed in non-infected mice at day 0 (mean =571pg/ml). After RSV infection, CCL21 protein was decreased significantly at day 1 (408 pg/ml, P=0.04) in comparison to UV RSV control at day 1 (499 pg/ml).

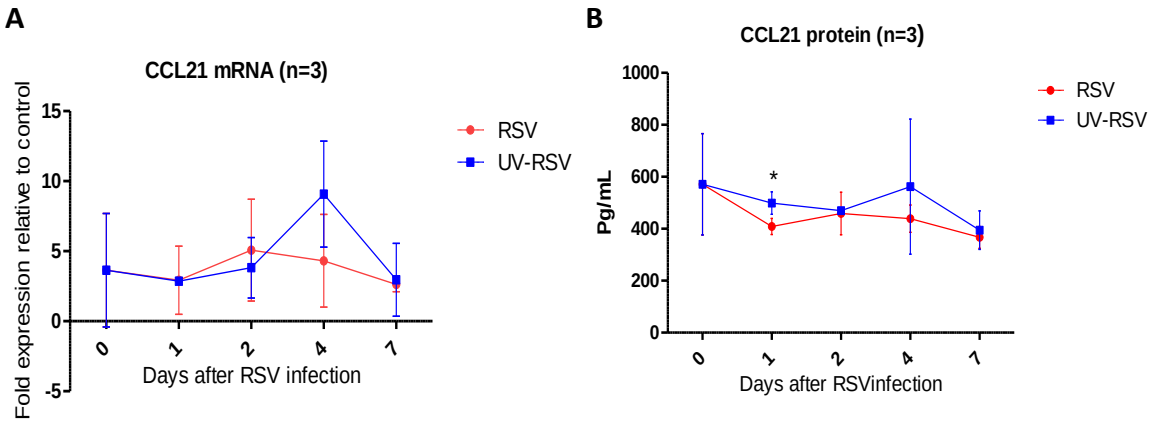

Figure 5.5. Expression of CCL21 mRNA (A) and protein (B) after RSV infection or challenge with UV-RSV control

*CCL21 mRNA was measured by RT-PCR. CCL21 mRNA was expressed in non-infected mice at day 0 and there was no significant increase after RSV infection on day 1, 2, 4 and 7 in comparison to UV RSV control at the same time points. Values are shown as fold expression relative to control. CCL21 protein was measured by use a specific murine CCL21 ELISA. CCL21 protein was expressed in non-infected mice at day 0 and after RSV infection CCL21 protein decreased significantly at day 1 relative to UV RSV control on day 1. Result shown is the average of three animals in the first experiment. Mean and SD are shown (two way ANOVA with Bonferroni post-hoc test, *P <0.05, n=3).*

5. 3.1.6. Normalised CCL21 protein to total protein after RSV infection

CCL21 protein levels (pg/ml) were normalised to total protein (pg/ng) (chapter 2, 2.3.2). Non-infected mice expressed CCL21 protein at day 0 (mean= 500 pg/ng) (Figure 5.6). RSV infection did not significantly increase expression of CCL21 protein at day 1 (343 pg/ng, P=0.1), day 2 (427 pg/ng, P=0.9), day 4 (319 pg/ng, P=0.1) and day 7 (215 pg/ng, P=0.059) in comparison to UV RSV control on day 1 (633 pg/ng), day 2 (437 pg/ng), day 4 (391 pg/ng) and day 7 (354 pg/ng).

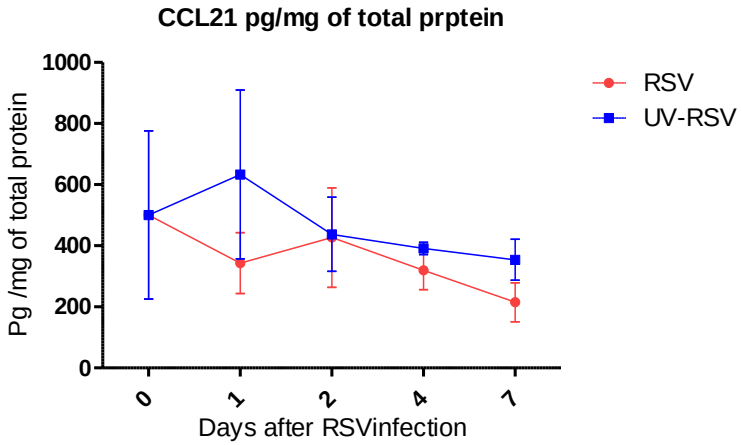

Figure 5.6. Normalized CCL21 protein to total protein content after RSV infection or challenge with UV-RSV control

*CCL21 protein was expressed in non-infected mice at day 0 and there was no significant increase of CCl21 protein after RSV infection in comparison to UV RSV control on day 1, 2, 4 and 7. Result shown is the average of three animals in the first experiment. Mean and SD are shown (two way ANOVA with Bonferroni post-hoc test, *P <0.05, n=3).*

5. 3.1.7. RSV infection did not significantly up regulate CXCL12 protein

To determine if CXCL12 protein is expressed after RSV infection, mice were infected with RSV (A2 strain) at different time points, including time day 0 (non-infected), 1, 2, 4 and 7. At the time points indicated after RSV infection mouse lung tissues were homogenized and CXCL12 protein was measured. Non-infected mice expressed CXCL12 protein (Figure 5.7) at day 0 (mean= 879 pg/ml). However, after RSV infection there was no significant increased expression of CXCL12 protein at day 1 (781, P=0.2), day 2 (790, P=0.5), day 4 (918, P= 0.9) and day 7 (669 pg/ml, P=0.2) in comparison to UV RSV control on day 1 (967 pg/ml), day 2 (847 pg/ml), day 4 (925 pg/ml) and day 7 (932 pg/ml).

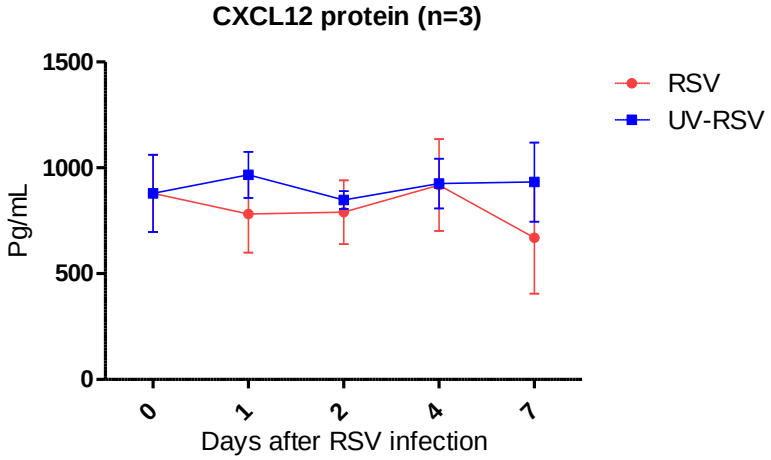

Figure 5.7. Expression of CXCL12 protein after RSV infection or challenge with UV-RSV control

*CXCL12 protein was measured by use of specific murine CXCL12 ELISA. CXCL12 protein was expressed in non-infected mice at day 0 and there was no significant increased after RSV infection at day 1, 2, 4 and 7 in comparison to UV RSV control at the same time points. Result shown is the average of three animals in the first experiment. Mean and SD are shown (two way ANOVA with Bonferroni post-hoc test, *P <0.05, n=3).*

5. 3.1.8. Normalised CXCL12 protein to total protein

CXCL12 protein (pg/ml) was normalised to total protein (pg/ng) (chapter 2, 2.3.2). Non-infected mice expressed CXCL12 protein (Figure 5.8) at day 0 (mean=764 pg/ng). RSV infection did not significantly increase expression of CXCL12 protein at day 1 (634 pg/ng, P=0.1), day 2 (739 pg/ng, P=0.8) and day 4 (675 pg/ng, P=0.8) and day 7 in comparison to UV RSV control on day 1 (1246 pg/ng), day 2 (793 pg/ng) and day 4 (701 pg/ng). In addition, at day 7, CXCL12 protein was decreased significantly after RSV infection (368 pg/ng, P=0.007) relative to UV RSV control at day 7 (833 pg/ng).

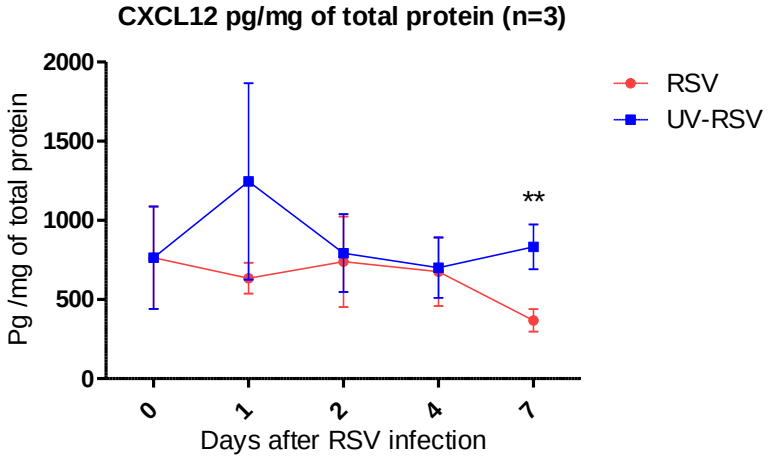

Figure 5.8. Normalised CXCL12 protein to total protein content after RSV infection or challenge with UV-RSV control

*CXCL12 protein was expressed in non-infected mice at day 0 and there was no significant increase after RSV infection in comparison to UV RSV control on day 1, 2and 4. In addition, at day 7, there was sifniccant decrease of CXCL12 protein relative to UV RSV control at day 7. Result shown is the average of three animals in the first experiment. Mean and SD are shown (two way ANOVA with Bonferroni post-hoc test, *P <0.05, n=3).*

5. 3.2. Experiment II

5. 3.2.1. Expression of CXCL13 mRNA and protein after RSV infection

Mice were infected with RSV (A2 strain) at various time points, including day 0 (non-infected), 1, 2, 4, 7 and 8. At the time points indicated after RSV infection mouse lungs tissue was homogenized and RNA was isolated and prepared using Qiagen as described (chapter 2, 2.4). CXCL13 mRNA was measured and analysed by RT-PCR. Non-infected mice (Figure 5.9.A) at day 0 expressed CXCL13 mRNA (fold expression relative to control=0.09). However, after RSV infection, CXCL13 mRNA expression was increased significantly at day 1 (1.76, P=0.03) in comparison to UV RSV control on day 1 (0.12).

CXCL13 protein was measured in homogenised tissue (Figure 5.9.B). CXCL13 protein was expressed in non-infected mice at day 0 (mean=246 pg/ml). However, after RSV infection CXCL13 protein was increased significantly at day 1 (787 pg/ml, P=0.006), day 2 (421 pg/ml, P=0.04), day 7 (331 pg/ml, P=0.009) in comparison to control day 1 (293.4 pg/ml), day 2 (302 pg/ml) and day 7 (235 pg/ml). CXCL13 mRNA and protein peaked at day 1, 7 and declined at day 4.

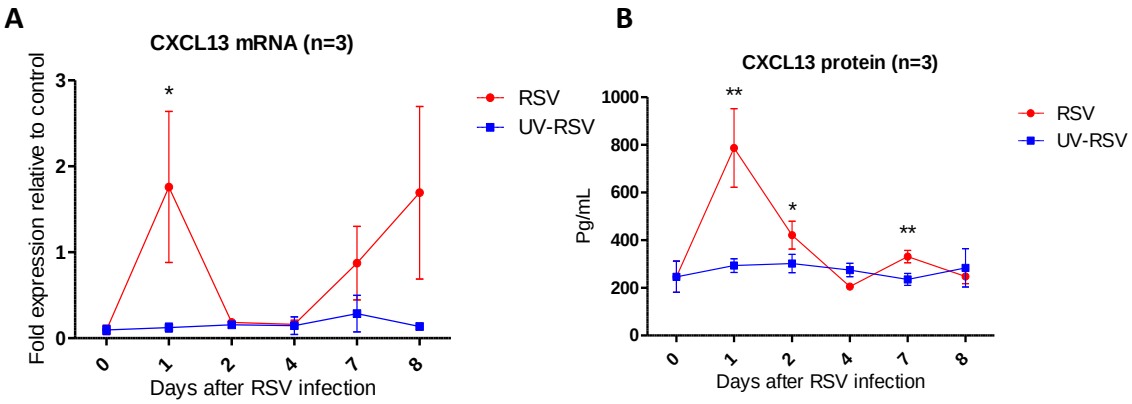

Figure 5.9. Expression of CXCL13 mRNA (A) and protein (B) after RSV infection or challenge with UV-RSV control

*CXCL13 mRNA was measured by RT-PCR. CXCL13 mRNA expression was increased significantly after RSV infection at day 1 in comparison to UV RSV control at the same time point. Values are shown as fold expression relative to control. CXCL13 protein was measured by use specific CXCL13 ELISA.CXCL13 protein was increased significantly after RSV infection at day 1, 2, and 7 in comparison to UV RSV control at the same time points. Result shown is the average of three animals in the second experiment. Mean and SD are shown (two way ANOVA with Bonferroni post-hoc test, *P <0.05, n=3).*

5. 3.2.2. CXCL13 protein expression in comparison to total protein concentration after RSV infection

CXCL13 protein (pg/ml) levels were normalised to total protein (pg/ng) (chapter 2, 2.3.2). CXCL13 protein was expressed in non-infected mice at day 0 (mean= 36 pg/ng). CXCL13 protein (Figure 5.10) was elevated significantly after RSV infection at day 1 (116 pg/ng, P=0.0008), and day 7 (47 pg/ng, P=0.01) in comparison to UV RSV control at day 1 (45 pg/ng) and day 7 (35 pg/ng).

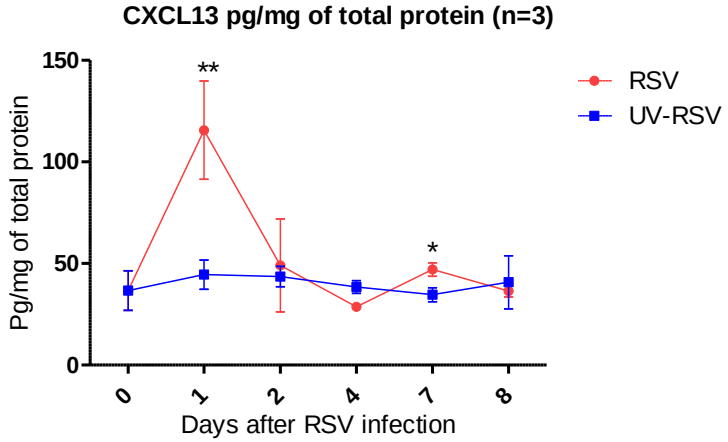

Figure 5.10. Normalized CXCL13 protein to total protein after RSV infection or challenge with UV-RSV control

*CXCL13 protein was expressed significantly after RSV infection on day 1 and 7 in comparison to RSV UV control at the same time points. Result shown is the average of three animals in the second experiment. Mean and SD are shown (two way ANOVA with Bonferroni post-hoc test, *P <0.05, n=3).*

5. 3.2.4. RSV infection did not significantly up regulate CCL19 protein expression

Mouse lung tissue was homogenised and CCL19 protein was measured using specific mouse CCL19 ELISA. CCL19 protein (Figure 5.11) was expressed in non-infected mice at day 0 (mean= 605 pg/ml). RSV infection of mice did not significantly increase expression of CCL19 protein at day 1 (589 pg/ml, P=0.4), day 2 (574 pg/ml, P=0.8), day 4 (325 pg/ml, P=0.1), day 7 (384 pg/ml ,P=0.9) and day 8 (323 pg/ml, P=0.1) in comparison to UV RSV control on day 1 (504 pg /ml), day 2 (583 pg/ml), day 4 (446 pg/ml), day 7 (388 pg/ml) and day 8 (488 pg/ml).

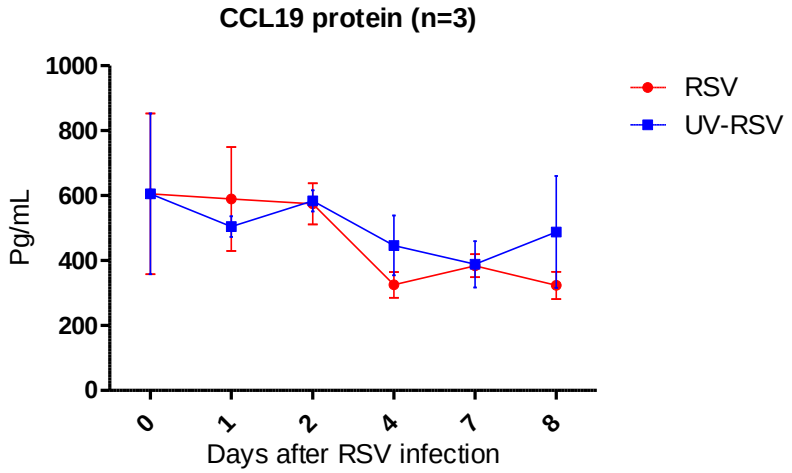

Figure 5.11. Expression of CCL19 protein after RSV infection or challenge with UV treated RSV control

*CCL19 protein was measured by ELISA. CCL19 protein was expressed in non-infected mice at day 0 and there was no significant up regulation after RSV infection at day 1, 2, 4, 7and 8 in comparison to UV RSV control at the same time points. Result shown is the average of three animals in the second experiment. Mean and SD are shown (two way ANOVA with Bonferroni post-hoc test, *P <0.05, n=3).*

5. 3.2.5. CCL19 protein expression in comparison to total protein concentration after RSV infection

CCL19 protein (pg/ml) levels were normalised to total protein (pg/ng) (chapter 2, 2.3.2). CCL19 protein (Figure 5.12) was expressed in non-infected mice (mean=90 pg/ng). However, after RSV infection there was no significant up regulation of CCL19 protein at day 1 (87 pg/ng, P=0.4), day 2 (68 pg/ng, P=0.4), day 4 (46 pg/ng, P=0.4), day 7 (55 pg/ng, P= 0.9) and day 8 (48 pg/ng, P= 0.9) in comparison to UV RSV control on day 1 (77 pg /ng), day 2 (85 pg/ng), day 4 (63 pg/ng), day 7 (58 pg/ng) and day 8 (70 pg/ng).

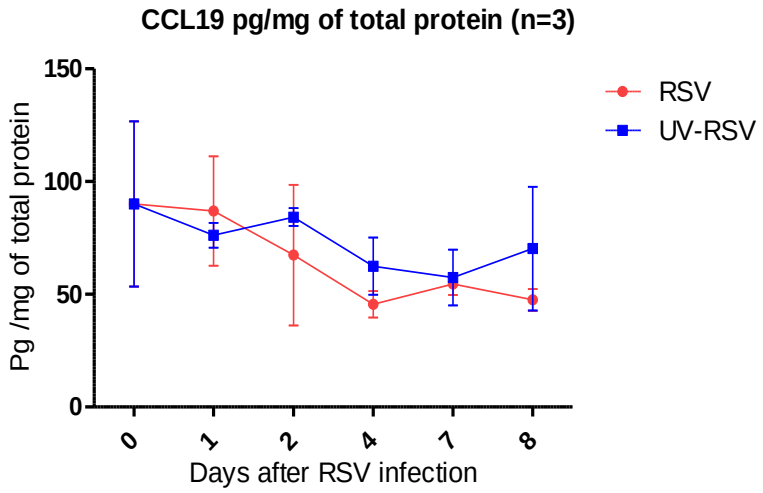

Figure 5.12. Normalized CCL19 protein to total protein after RSV infection or challenge with UV treated RSV control

*CCL19 protein was expressed in non-infected mice at day 0 and RSV infection did not significantly increase CCL19 protein expression in comparison to UV RSV control on day 1, 2, 4 and 7. Result shown is the average of three animals in the second experiment. Mean and SD are shown (two way ANOVA with Bonferroni post-hoc test, *P <0.05, n=3).*

5. 3.2.6. RSV infection did not significantly up regulate CCL21 protein expression

Mouse lung tissues were homogenised and CCL21 protein was measured. CCL21 protein (Figure 5.13) was expressed in non-infected mice at day 0 (mean= 800 pg/ml). However, after RSV infection there was no significant expression on day 1 (703 pg/ml, P=0.1), day 2 (764 pg/ml, P=0.2), day 4 (496 pg/ml, P=0.2) , day 7 (560 pg/ml ,P=0.3) and day 8 (537 pg/ml, P=0.1) in comparison to UV RSV control on day 1 (860 pg /ml), day 2 (870 pg/ml), day 4 (555 pg/ml), day 7 (609 pg/ml) and day 8 (629 pg/ml).

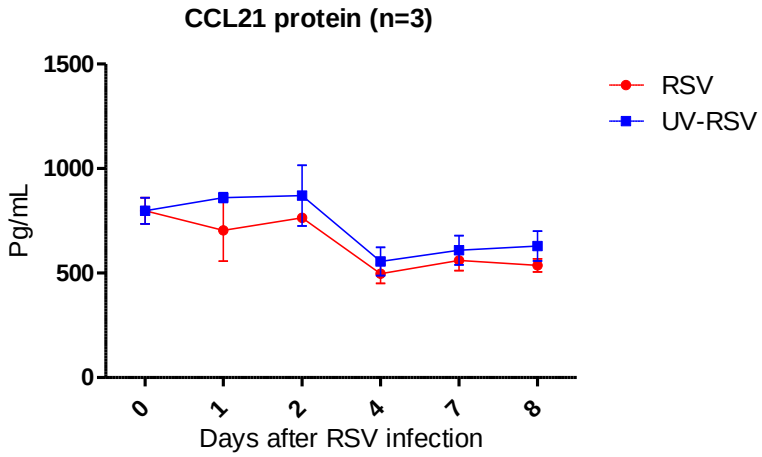

Figure 5.13. Expression of CCL21 protein after RSV infection or challenge with UV treated RSV control

*CCL21 protein was measured by use of specific murine CCL21 ELISA. CCL21 protein was expressed in non-infected mice at day 0 and there was no significant increased expression after RSV infection at day 1, 2, 4, 7 and 8 in comparison to UV RSV control at the same time points. Result shown is the average of three animals in the second experiment. Mean and SD are shown (two way ANOVA with Bonferroni post-hoc test, *P <0.05, n=3).*

5. 3.2.7. CCL21 protein expression in comparison to total protein concentration after RSV infection

CCL21 protein (pg/ml) levels were normalised to total protein (pg/ng) (chapter 2, 2.3.2). CCL21 protein (Figure 5.14) was expressed in non-infected mice (mean= 119 pg/ng). However, after RSV infection there was no significant increase of CCL21 protein at day 1 (103 pg/ng, P=0.1), day 2 (87 pg/ng, P=0.1), day 4 (69 pg/ng, P=0.1), day 7 (79 pg/ng ,P= 0.1) and day 8 (79 pg/ng, P= 0.2) in comparison to UV RSV control on day 1 (130 pg /ng), day 2 (125 pg/ng), day 4 (77 pg/ng), day 7 (89 pg/ng) and day 8 (89 pg/ng) .

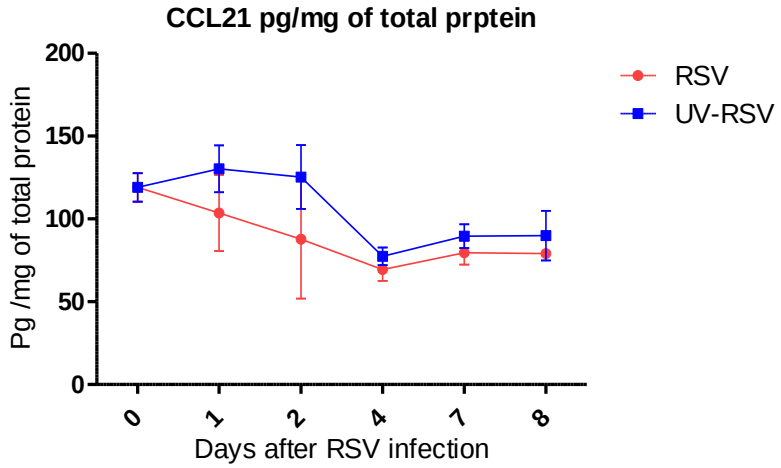

Figure 5.14. Normalized CCL21 protein to total protein after RSV infection or challenge with UV treated RSV control

*CCL21 protein was expressed in non-infected mice at day 0 and there was no significant increased expression after RSV infection in comparison to UV RSV control on day 1, 2, 4 and 7. Result shown is the average of three animals in the second experiment. Mean and SD are shown (two way ANOVA with Bonferroni post-hoc test, *P <0.05, n=3).*

5. 3.2.8. RSV infection did not significantly up regulate CXCL12 protein expression

Mouse lung tissue was homogenised and CXCL12 protein measured. CCL21 protein (Figure 5.15) was expressed in non-infected mice at day 0 (mean= 1895 pg/ml). However, after RSV infection there was no significant increase of CXCL12 at day 1 (pg/ml, P=0.3), day 2 (2033 pg/ml, P=0.5), day 4 (1333 pg/ml, P=0.1), day 7 (1626 pg/ml ,P=0.2) and day 8 (1477 pg/ml, P=0.5) in comparison to UV RSV control at day 1 (1780 pg /ml), day 2 (2114 Pg/ml), day 4 (1692 pg/ml), day 7 (1416 pg/ml) and day 8 (1692 pg /ml).

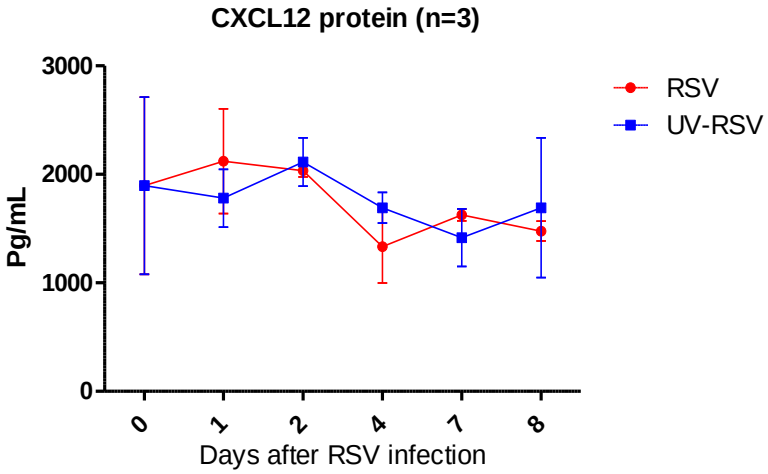

Figure 5.15. Expression of CXCL12 protein after RSV infection or challenge with UV treated RSV control

*CXCL12 protein was measured by use of specific murine CXCL12 ELISA. CXCL12 protein was expressed in non-infected mice at day 0 and there was no significant increase expression after RSV infection at day 1, 2, 4, 7 and 8 in comparison to UV RSV control at the same time points. Result shown is the average of three animals in the second experiment. Mean and SD are shown (two way ANOVA with Bonferroni post-hoc test, *P <0.05, n=3).*

5. 3.2.9. CXCL12 protein expression in comparison to total protein concentration after RSV infection

CXCL12 protein (pg/ml) levels were normalised to total protein (pg/ng) (chapter 2, 2.3.2). CXCL12 protein (Figure 5.16) was expressed in non-infected mice (mean=281 pg/ng). However, after RSV infection there was no significant up regulation of CXCL12 protein at day 1 (312 pg/ng, P=0.4), day 2 (233 pg/ng, P=0.2), day 4 (186 pg/ng, P=0.1) , day 7 (231 pg/ng ,P= 0.4) and day 8 (217pg/ng, P= 0.6) in comparison to UV RSV control on day 1 (268 pg /ng), day 2 (305 pg/ng), day 4 (237 pg/ng), day 7 (210 pg/ng) and day 8 (243 pg/ng).

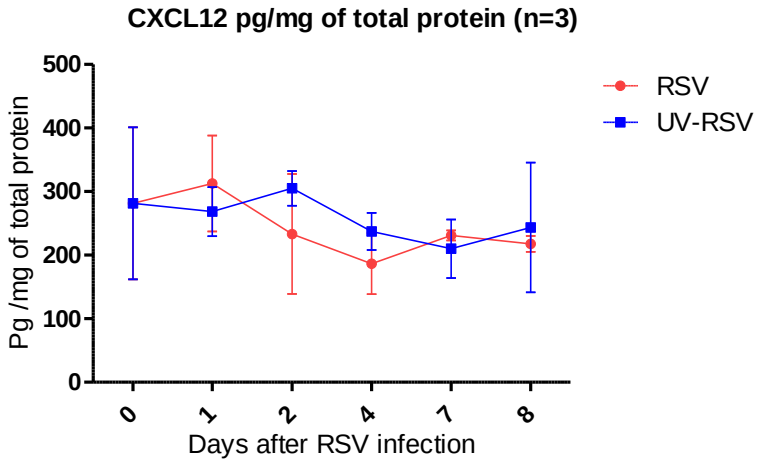

Figure 5.16. Normalized CXCL12 protein to total protein after RSV infection or challenge with UV treated RSV control

*CXCL12 protein was expressed in non-infected mice at day 0 and there was no significant increased expression of CXCL12 protein after RSV infection in comparison to UV RSV control on day 1, 2, 4 and 7. Result shown is the average of three animals in the second experiment. Mean and SD are shown (two way ANOVA with Bonferroni post-hoc test, *P <0.05, n=3).*

5. 3.3. Experiment -III

5. 3.3.1. Expression of CXCL13 protein after RSV infection

Mouse lungs tissues were homogenised and CXCL13 protein was measured (Figure 5.17). CXCL13 was expressed in non-infected mice PBS at day 0 (mean= 372 pg/ml). However, after RSV infection there was no significant increased expression of CXCL13 protein at day 1 (504 pg/ml, P=0.7), day 2 (389 pg/ml, P=0.3), day 4 (302 pg/ml, P=0.07), day 7 (306 pg/ml ,P=0.06) and day 10 (339 pg/ml, P=0.08) in comparison to UV RSV control at day 1 (467 pg/ml), day 2 (316 pg/ml), day 4 (380 pg/ml), day 7 (363 pg/ml) and day 10 (452 pg/ml). In addition, CXCL13 protein was significantly decreased after RSV infection at day 14 (375 pg/ml, P=0.002) and day 21 (315pg/ml, P=0.002) relative to UV RSV control at day 14 (590 pg/ml) and day 21(518 pg/ml).

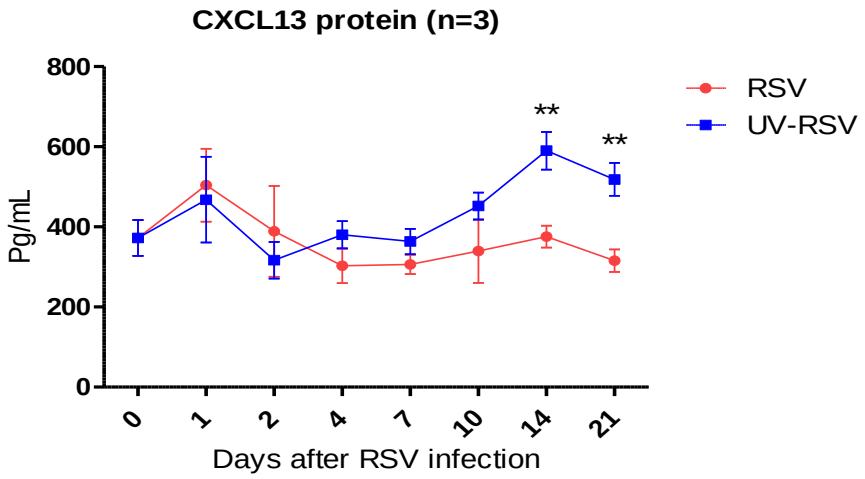

Figure 5.17. Expression of CXCL13 protein after RSV infection or challenge with UV treated RSV control

*CXCL13 protein was measured by use of specific murine CXCL13 ELISA.CXCL13 protein was expressed in non-infected mice at day 0 and there was no significant increased expression of CXCL13 protein at day 1,2,4,7 and 10 after RSV infection. However, CXCL13 protein was decreased at day 14 and 21 after RSV infection in comparison to UV RSV control at the same time points. Result shown is the average of three animals in the third experiment. Mean and SD are shown (two way ANOVA with Bonferroni post-hoc test, *P <0.05, n=3).*

5.3.3.2. CXCL13 protein expression in comparison to total protein concentration after RSV infection

CXCL13 protein (pg/ml) was normalised to total protein (pg/ng) (chapter 2, 2.3.2). CXCL13 protein (Figure 5.18) was expressed in non-infected mice (mean = 287 pg/ng). However, after RSV infection CXCL13 protein was decreased significantly at day 4 (161pg/ng, P=0.04), day 7 (133 pg/ng, P=0.004), day 10 (189 pg/ng, P=0.004), day 14 (286 pg/ng ,P= 0.02) and day 21 (219 pg/ng ,P= 0.01) in comparison to UV RSV control at day 4 (223 pg /ng), day 7 (233pg/ng), day 10 (334 pg/ng), day 14 (392 pg/ng) and day 21 (393 pg/ng).

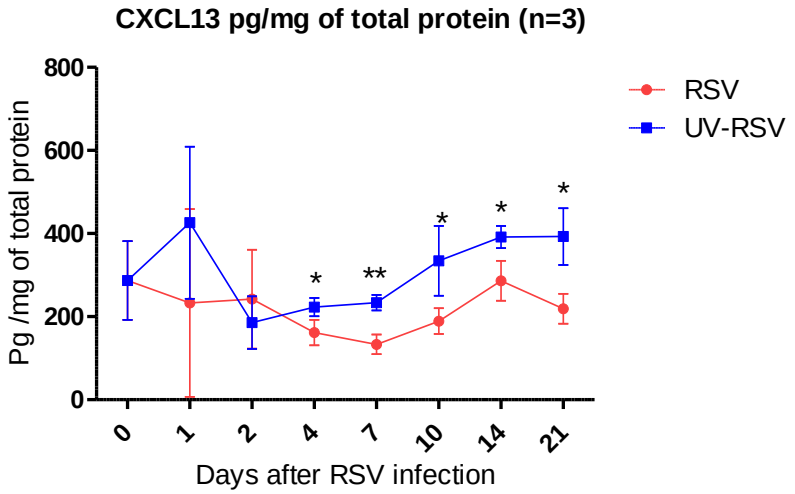

Figure 5.18. Normalized CXCL13 protein to total protein after RSV infection or challenge with UV treated RSV control

*CXCL13 protein was expressed in non-infected mice at day 0 and there was significant decreased expression after RSV infection at day 4, 7, 10, 14 and 21 in comparison to UV RSV control at the same time points. Result shown is the average of three animals in the third experiment. Mean and SD are shown (two way ANOVA with Bonferroni post-hoc test, *P <0.05, n=3).*

5. 3.3.3. Expression of CCL19 protein after RSV infection

Mouse lungs were homogenised and CCL19 protein was measured. CCL19 protein (Figure 5.19) was expressed in non-infected mice at day 0 (mean=705 pg/ml). However, after RSV infection CCL19 protein decreased significantly at day 4 (456 pg/ml, P=0.03), day 7 (460 pg/ml, P=0.04) and day 10 (569 pg/ml, P=0.02) in comparison to UV RSV control day 4 (674 pg/ml), day 7 (595 pg/ml) and day 10 (817 pg/ml).

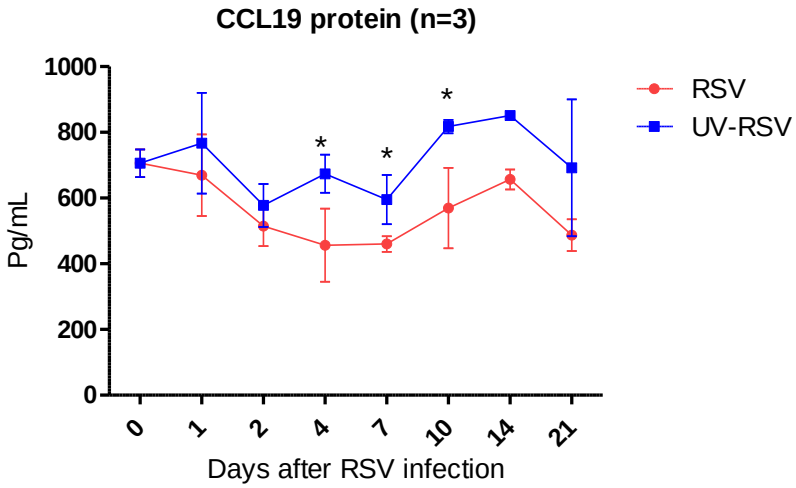

Figure 5.19. Expression of CCL19 protein after RSV infection or challenge with UV treated RSV control

*CCL19 protein was measured by use of specific murine CCL19 ELISA. CCL19 protein was expressed in non-infected mice at day 0 and after RSV infection. CCL19 protein expression was significantly decreased at day 4, 7 and 10 in comparison to UV RSV control at the same time points. Result shown is the average of three animals in the third experiment. Mean and SD are shown (two way ANOVA with Bonferroni post-hoc test, *P <0.05, n=3).*

5. 3.3.4. CCL19 protein expression in comparison to total protein concentration after RSV infection

CCL19 protein (pg/ml) was normalised to total protein (pg/ng) (chapter 2, 2.3.2). CCL19 protein (Figure 5.20) was expressed in non-infected mice at day 0 (mean= 543 pg/ng). However, after RSV infection CCL19 protein decreased significantly at day 4 (241 pg/mg, P=0.009), day 7 (198 pg/ng, P=0.0002) and day 10 (318 pg/ng, P=0.02) in comparison to UV RSV control at day 4 (396 pg/ng), day 7 (381 pg/mg) and day 10 (601 pg/ng).

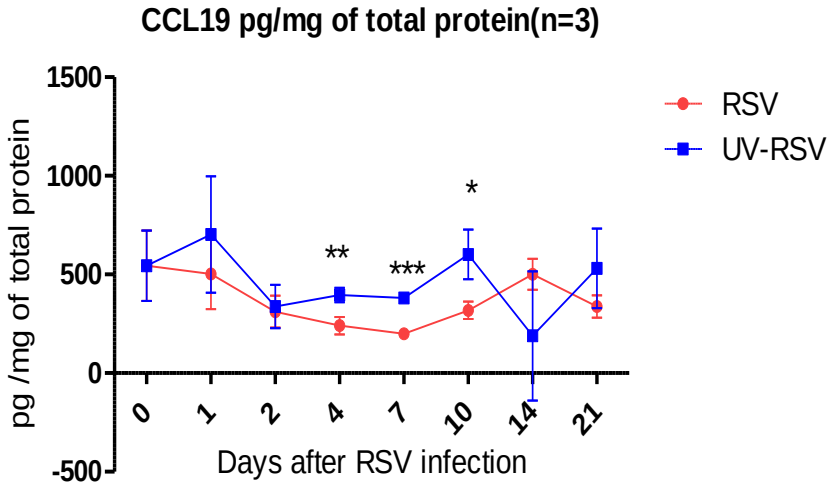

Figure 5.20. Normalized CCL19 protein to total protein after RSV infection or challenge with UV treated RSV control

*CCL19 protein was expressed in non-infected mice at day 0. CCL19 protein was significantly decreased after RSV infection at day 4, 7, 10 in comparison to UV RSV control at the same time points. Result shown is the average of three animals in the third experiment. Mean and SD are shown (two way ANOVA with Bonferroni post-hoc test, *P <0.05, n=3).*

5. 3.3.5. Expression of CCL21 protein after RSV infection

Mouse lung tissues were homogenised and CCL21 protein was measured. CCL21 protein (Figure 5.21) was expressed in non-infected mice at day 0 (mean= 5103 pg/ml). However, after RSV infection CCL21 protein was decreased significantly at day 4 (3647 pg/ml), day 10 (4885 pg/ml), day 14 (3256 pg/ml), day 21 (2948 pg/ml) in comparison to UV RSV control at day 4 (4868 pg/ml), day 10 (6840 pg/ml), day 14 (4685 pg/ml) and day 21 (4123 pg/ml).

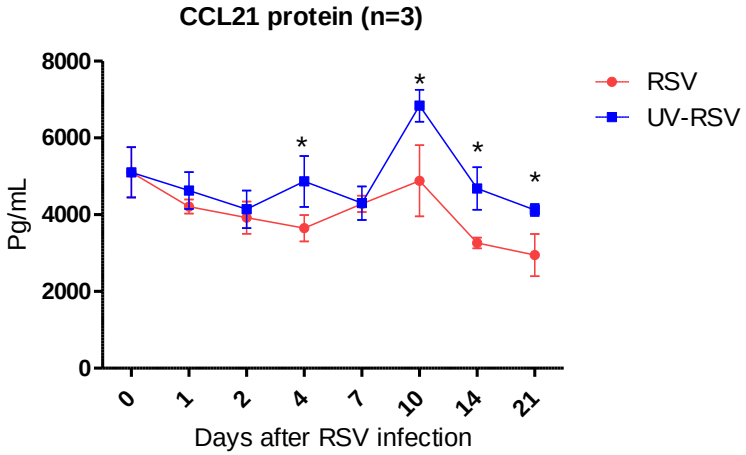

Figure 5.21. Expression of CCL21 protein after RSV infection or challenge with UV treated RSV control

*CCL21 protein was measured by use of specific murine CCL21 ELISA. CCL21 protein was expressed in non-infected mice at day 0 and after RSV infection. CCL21 protein expression was significantly decreased at day 4, 10, 14 and 21 in comparison to UV RSV control at the same time points. Result shown is the average of three animals in the third experiment. Mean and SD are shown (two way ANOVA with Bonferroni post-hoc test, *P <0.05, n=3).*

5. 3.3.6. CCL21 protein expression in comparison to total protein concentration after RSV infection

CCL21 protein (pg/ml) was normalised to total protein (pg/ng) (chapter 2, 2.3.2). CCL21 protein (Figure 5.22) was expressed in non-infected mice (mean=3913 pg/ng). However, after RSV infection CCL19 protein was decreased significantly at day 4 (1937 pg/ng, P=0.009), day 10 (2732 pg/ng, P=0.02) and day 21 (2026 pg/ml, P=0.02) in comparison to UV RSV control on day 4 (2872 pg/ng), day 10 (5018 pg/mg) and day 21 (3114 pg/ng).

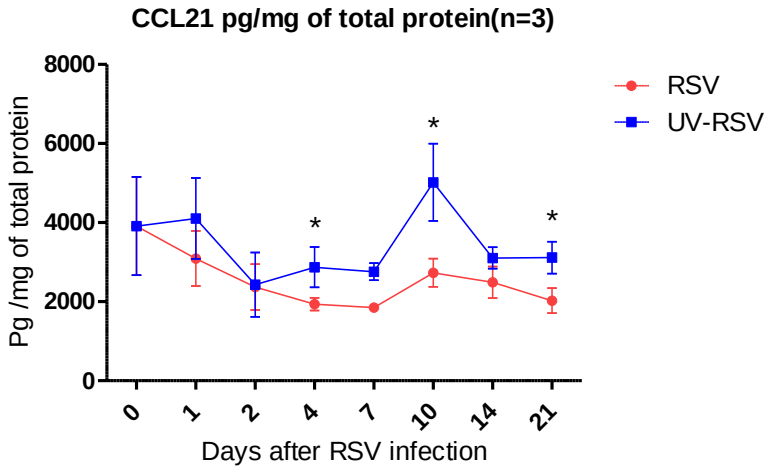

Figure 5.22. Normalized CCL21 protein to total protein after RSV infection or challenge with UV treated RSV control

*CCL21 protein was expressed in non-infected mice at day 0 and there was significantly decreased expression after RSV infection at day 4, 10 and 21 in comparison to UV RSV control at the same time points. Result shown is the average of three animals in the third experiment. Mean and SD are shown (two way ANOVA with Bonferroni post-hoc test, *P <0.05, n=3).*

5. 3.3.7. Expression of CXCL12 protein after RSV infection

CXCL12 protein was measured from lungs homogenised tissue. CXCL12 protein (Figure 5.23) was expressed in non-infected mice at day 0 (mean= 4280 pg/ml). However, after RSV infection CXCL12 protein was decreased significantly at day 4 (2798 pg/ml, P=0.01), day 10 (3838 pg/ml, P=0.03) and day 21 (1562 pg/ml, P=0.02) in comparison to UV RSV control at day 4 (4276 pg/ml), day 10 (4810 pg/ml) and day 21 (2534 pg/ml).

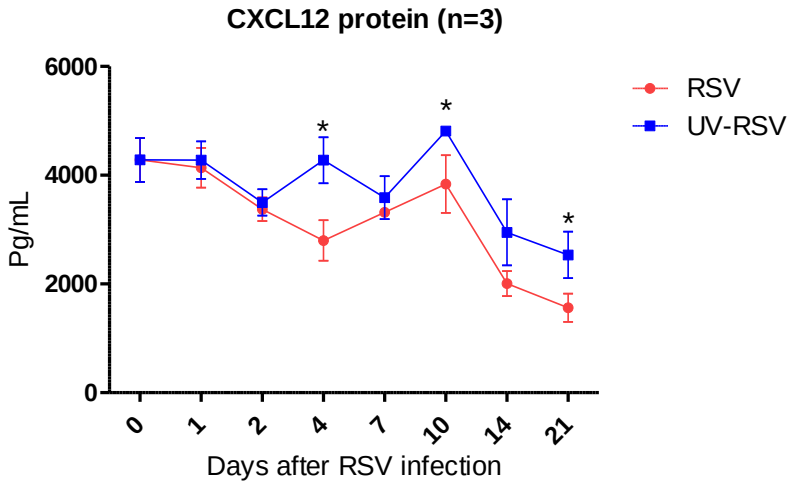

Figure 5.23. Expression of CXCL12 protein after RSV infection or challenge with UV treated RSV control

*CXCL12 protein was measured by use of specific murine CXCL12 ELISA. CXCL12 protein was expressed in non-infected mice at day 0 and after RSV infection. CXCL12 protein expression was significantly decreased at day 4, 10 and 21 in comparison to UV RSV control at the same time points. Result shown is the average of three animals in the third experiment. Mean and SD are shown (two way ANOVA with Bonferroni post-hoc test, *P <0.05, n=3).*

5.3.3.8. CXCL12 protein expression in comparison to total protein concentration after RSV infection

CXCL12 protein (pg/ml) was normalised to total protein (pg/ng) (chapter 2, 2.3.2). CXCL12 protein (Figure 5.24) was expressed in non-infected mice at day 0 (mean = 3283 pg/ng). However, after RSV infection CXCL12 protein was significantly decreased at day 4 (1486 pg/mg, P=0.003), day 7 (1439 pg/ng, P=0.004), day 10 (2154 pg/ng, P=0.02) and day 21 (1089 pg/ng, P=0.02) in comparison to UV RSV control on day 4 (2510 pg /mg), day 7 (3000 pg/ml), day 10 (3527 pg/ng) and day 21 (1896 pg/ng).

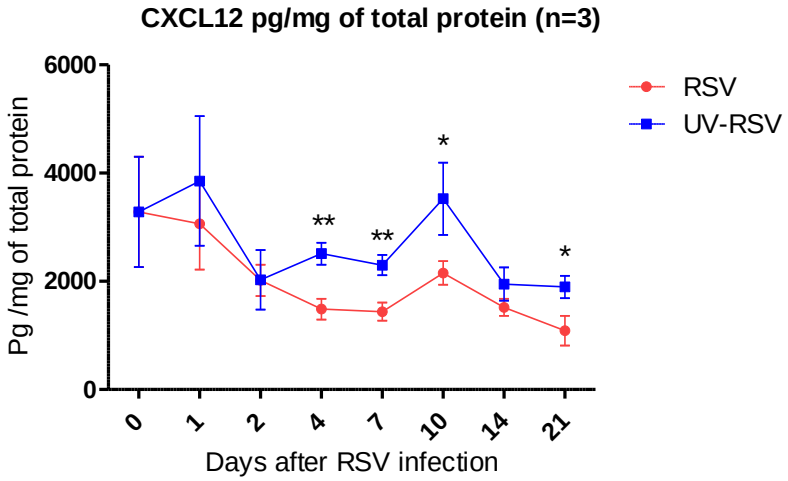

Figure 5.24. Normalized CXCL12 protein to total protein after RSV infection or challenge with UV treated RSV control

*CXCL12 protein was expressed in non-infected mice at day 0 and there was significantly decreased expression after RSV infection at day 4, 7, 10 and 21 in comparison to UV RSV control at the same time points. Result shown is the average of three animals in the third experiment. Mean and SD are shown (two way ANOVA with Bonferroni post-hoc test, *P <0.05, n=3).*

5. 3.4. An average of first and second experiments

5. 3.4.1. Average of CXCL13 mRNA and protein after RSV infection

Mice were infected with RSV (A2 strain) at various time points, day 0 (non-infected), 1, 2, 4, 7 and 8. At the time points indicated after RSV infection mouse lungs tissues were homogenized and RNA was isolated and prepared using Qiagen as described (chapter 2, 2.4). CXCL13 mRNA was measured and analysed by RT-PCR. Non-infected mice at day 0 expressed CXCL13 mRNA (fold expression relative to control= 0.08). However, after RSV infection CXCL13 mRNA expression (Figure 5.25.A) was increased significantly on day 1 (1.56, P=0.001) and day 7 (0.92, P=0.001) in comparison to UV RSV control on day 1 (0.20) and day 7 (0.18). Furthermore, CXCL13 protein (Figure 5.25.B) was expressed in non-infected mice at day 0 (mean =271 pg/ml). However, after RSV infection CXCL13 protein was significantly increased at day 1 (775 pg/ml, P=0.0001), day 2 (517 pg/ml, P=0.005), and day 7 (360 pg/ml, P=0.0002) in comparison to UV RSV control at day 1 (334 pg/ml), day 2 (290pg/ml) and day 7 (243 pg/ml). Overall, there were two peaks formed of CXCL13 mRNA and protein at day 1, 7 and declined at day 4.

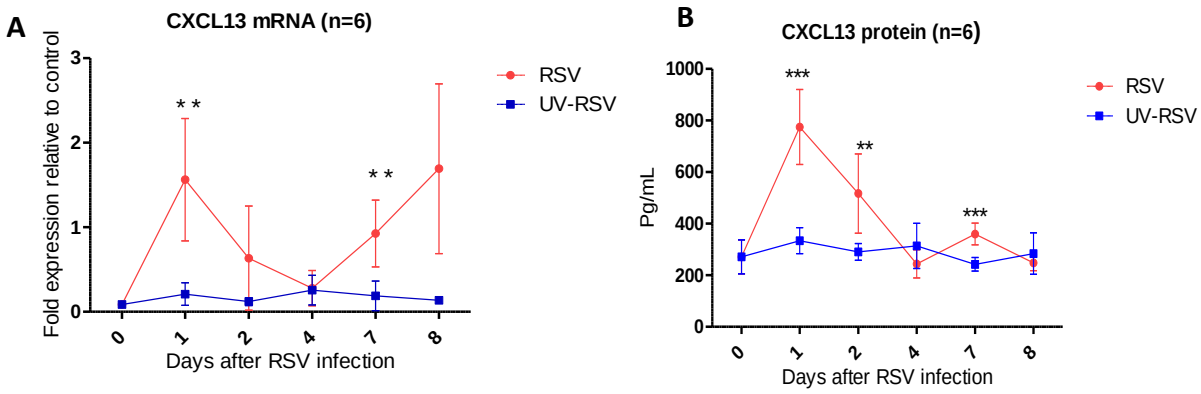

Figure 5.25. Expression of CXCL13 mRNA (A) and protein (B) after RSV infection or challenge with UV treated RSV control

*CXCL13 mRNA was measured by RT-PCR. CXCL13 mRNA was increased significantly after RSV infection on day 1 and 7 in comparison to UV RSV control at the same time points. Values are shown as fold expression relative to control. In (B) CXCL13 was measured by use of specific murine CXCL13 ELISA. CXCL13 protein was increased significantly after RSV infection at day 1, 2, and 7 in comparison to UV RSV control at the same time points. Result shown is the average of six animals from the first and second experiments. Mean and SD are shown (two way ANOVA with Bonferroni post-hoc test, *P <0.05, n= 6).*

5. 3.4.2. Average of CXCL12 protein after RSV infection

CXCL12 protein was expressed in non-infected mice at day 0 (mean= 1387 pg/ml). However, after RSV infection there was no significant increase of CXCL12 protein (Figure 5.26) at day 1 (1452 pg/ml, P=0.8), day 2 (1411 pg/ml, P=0.8), day 4 (1126 pg/ml, P=0.4), day 7 (1148 pg/ml ,P=0.9) and day 8 (1477 pg/ml, P=0.5) in comparison to UV RSV control on day 1 (1374 pg /ml), day 2 (1481 Pg/ml), day 4 (1309 pg/ml), day 7 (1174 pg/ml) and day 8 (1692 pg /ml).

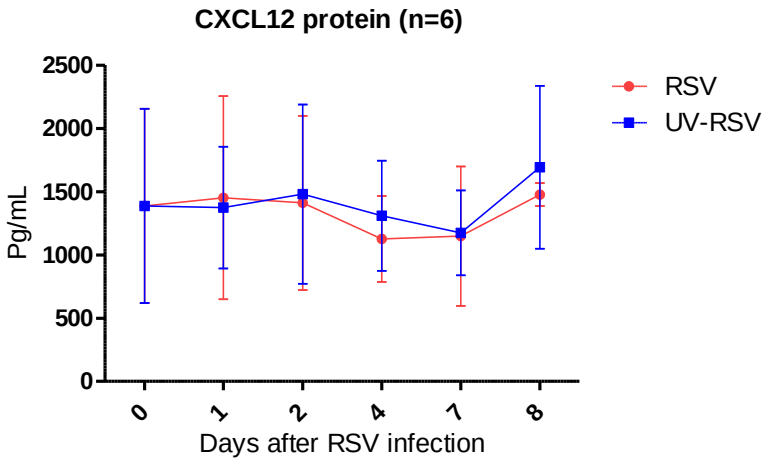

Figure 5.26. Expression of CXCL12 protein after RSV infection or challenge with UV treated RSV control

*CXCL12 protein was measured by use of specific murine CXCL12 ELISA. CXCL12 was expressed in non-infected mice PBS at day 0 and after RSV infection there was no significant increase expression of CXCL12 protein at day 1, 2, 4, 7 and 8 in comparison to UV RSV control at the same time points. Result shown is the average of six animals from the first and second experiments. Mean and SD are shown (two way ANOVA with Bonferroni post-hoc test, *P <0.05, n= 6).*

5. 3.4.3. Average of CCL19 protein after RSV infection

CCL19 protein (Figure 5.27) was expressed in non-infected mice at day 0 (mean= 452 pg/ml). However, after RSV infection there was no significant increase of CCL19 protein at day 1 (448 pg/ml, P=0.8), day 2 (435 pg/ml, P=0.8), day 4 (318 pg/ml, P=0.3), day 7 (292 pg/ml, P=0.3) and day 8 (323 pg/ml, P=0.1) in comparison to UV RSV control at day 1 (427 pg /ml) , day 2 (448 Pg/ml), day 4 (364.7 pg/ml) , day 7 (339.2 pg/ml) and day 8 (488 pg /ml).

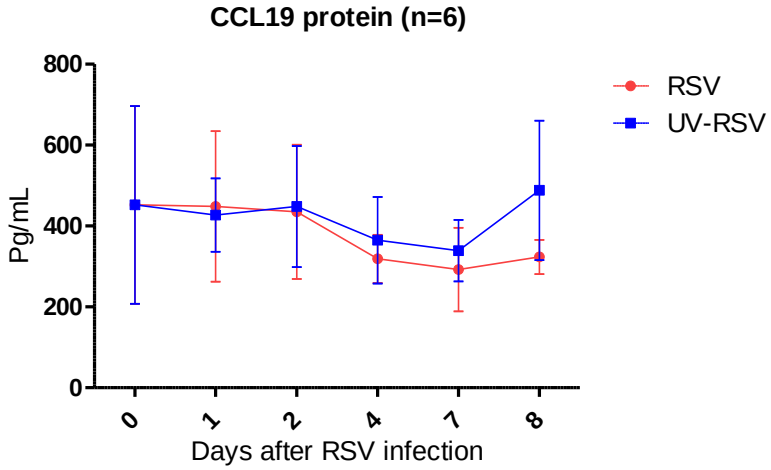

Figure 5.27. Expression of CCL19 protein after RSV infection or challenge with UV treated RSV control

*CCL19 protein was measured by use of specific murine CCL19 ELISA. CCL19 was expressed in non-infected mice PBS at day 0 and after RSV infection there was no significant up regulation of CCL19 in comparison to UV RSV control at the same time points. Result shown is the average of six animals from the first and second experiments. Mean and SD are shown (two way ANOVA with Bonferroni post-hoc test, *P <0.05, n= 6).*

5. 3.4.4. Average of CCL21 protein after RSV infection

CCL21 protein (Figure 5.28) was expressed in non-infected mice PBA at day 0 (mean= 684 pg/ml). However, after RSV infection there was no significant increase of CCL21 protein at day 1 (556 pg/ml, P=0.2), day 2 (611 pg/ml, P=0.6), day 4 (467 pg/ml, P=0.2), day 7 (463 pg/ml ,P=0.6) and day 8 (537 pg/ml, P=0.1) in comparison to UV RSV control on day 1 (680 pg /ml), day 2 (670 Pg/ml), day 4 (558pg/ml) , day 7 (502 pg/ml) and day 8 (537 pg /ml).

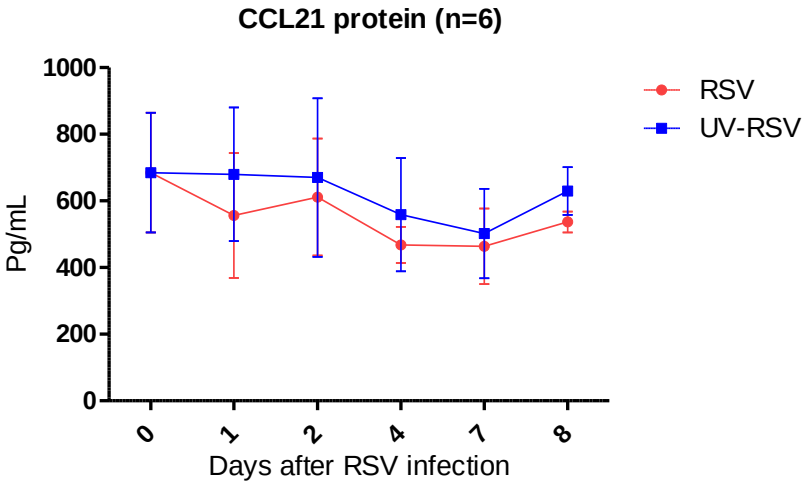

Figure 5.28. Expression of CCL21 protein after RSV infection or challenge with UV treated RSV control

*CCL21 protein was measured by use of specific murine CCL21 ELISA. CCL21 was expressed in non-infected mice PBS at day 0 and after RSV infection there was no significant increase of CCL21 in comparison to UV RSV control at the same time points. Result shown is the average of six animals from the first and second experiments. Mean and SD are shown (two way ANOVA with Bonferroni post-hoc test, *P <0.05, n= 6).*

5. 3.5. Immunofluorescence staining

To further prove expression of CXCL13 and to understand how recruitment of B and T cells occurs and to determine where they are expressed in the lung in response to RSV infection, mouse lung sections were prepared stained with anti-CXCL13, anti-CD20 (B cells) and anti-CD3 (T cells) antibodies (chapter 2, section 2.8).

5. 3.5.1.1. Expression of CXCL13 in mouse spleen sections

CXCL13 (chapter 1, 1.4) is normally expressed in secondary lymphoid tissue such as spleen (Rangel-Moreno *et al.* 2007). Therefore, mouse spleen sections were used as positive control to optimize the staining (Figure 5.29), and no comparable staining was noticed with the isotype control. CXCL13 (red) was secreted around some cells that could be B cells-rich follicles as indicated below (arrow).

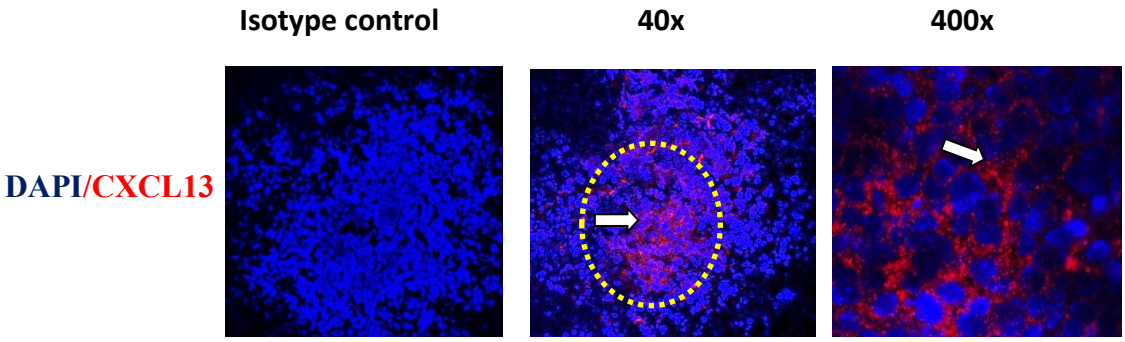

Figure 5.29. CXCL13 is normally expressed in mouse spleen section

CXCL13 (red) was detected around some cells that could be B cells-rich follicles and some other cells as indicated below (arrow). Isotype control was applied in each test. Cell nuclei shown in blue (DAPI). Images were originally obtained at 40x and 400x magnifications using confocal microscopy.

5.3.5.1.2. Expression of CXCL13 in non–infected mouse lung sections at day 0

Non-infected mice were given PBS as negative control. Positive staining of CXCL13 protein (red) was observed in non–infected mice at day 0 (Figure 5.30) as indicated (white arrow), and no comparable staining was noticed with the isotype control. CXCL13 was distributed around epithelium and other cells that might induce its expression such as DCs indicated below (brown arrow).

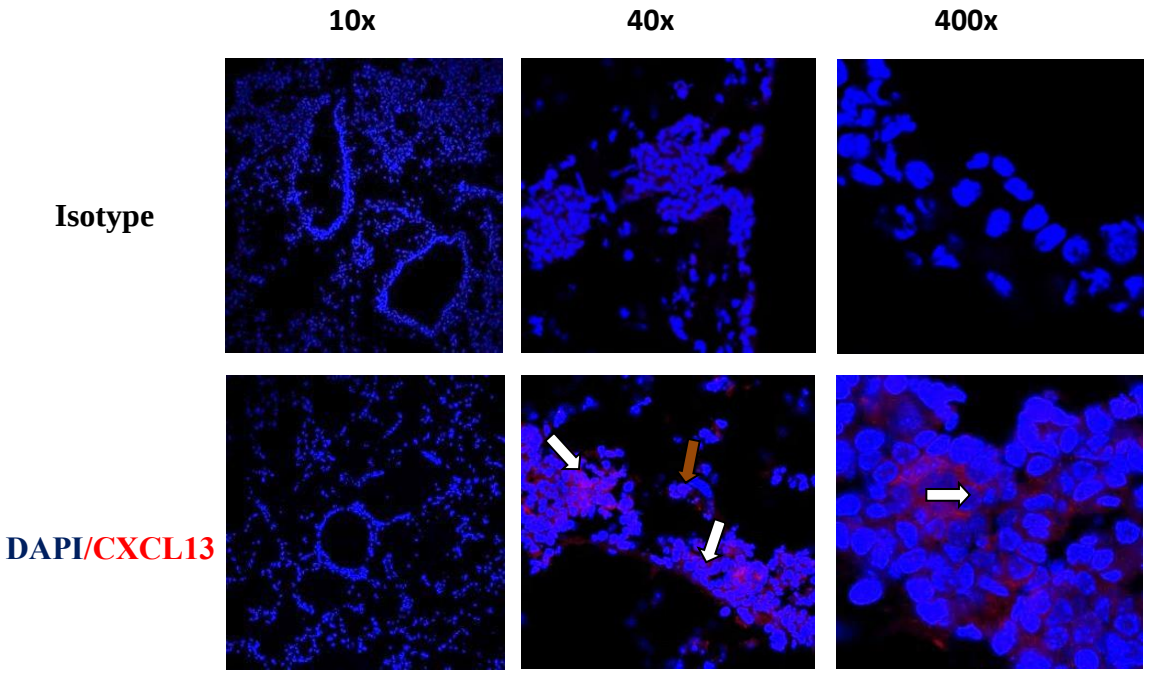

Figure 5.30. CXCL13 is normally expressed in non-infected mice at day 0

CXCL13 (red) was expressed around epithelium and some other cells as indicated by arrow. Isotype control was applied. Cell nuclei shown in blue (DAPI). Images were originally obtained at 10x, 40x and 400x magnifications using confocal microscopy.

5.3.5.1.3. Expression of CXCL13 in mouse lung sections after RSV infection at day 1

Strong positive staining of CXCL13 (red) was observed after RSV infection at day 1 (Figure 5.31) as indicated (white arrow), and no comparable staining was noticed with the isotype control. CXCL13 was accumulated in some areas and distributed between the cells as indicated below (arrow).

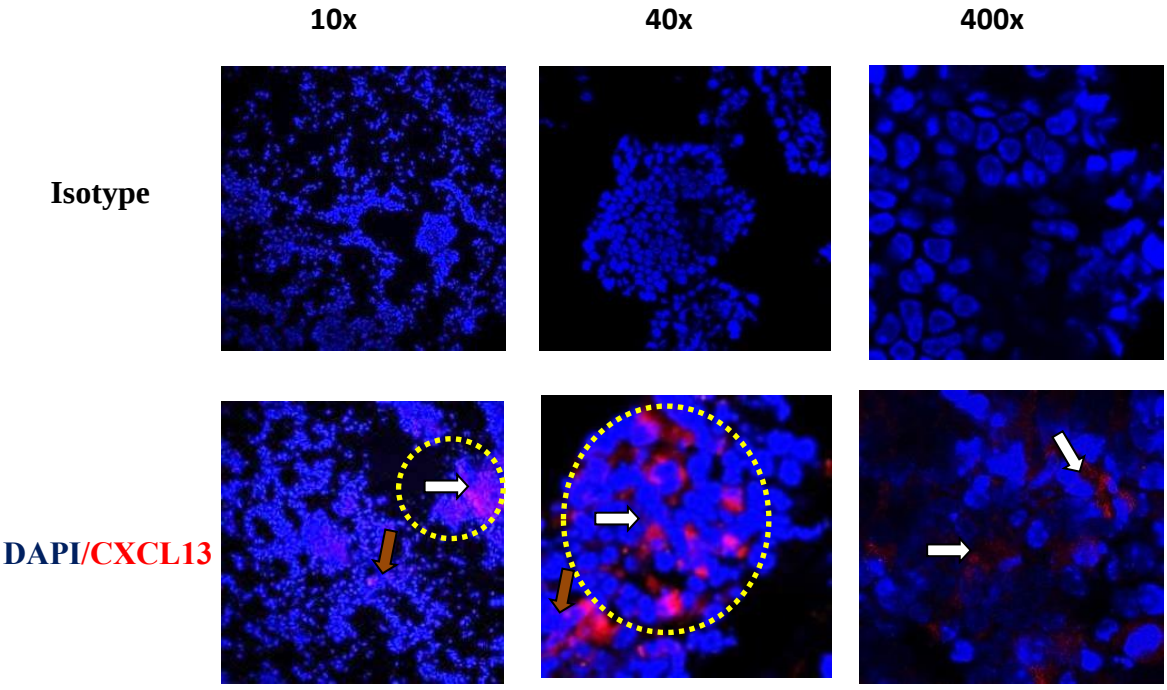

Figure 5.31. Expression of CXCL13 in mouse lung section after RSV infection at day1

There was strong positive staining of CXCL13 (red) that accumulated in some aggregates as indicated above (arrow). Isotype control was applied. Cell nuclei shown in blue (DAPI). Images were originally obtained at 10x, 40x and 400x magnifications using confocal microscopy.

5. 3.5.1.4. Expression of CXCL13 in mouse lung sections after UV RSV challenge at day 1

Positive staining of CXCL13 (red) was detected after mice challenge with UV RSV at day 1 (Figure 5.32), and no comparable staining was noticed with the isotype control. In addition, CXCL13 was distributed around epithelium and other cells that might also induce its expression as indicated below (arrow).

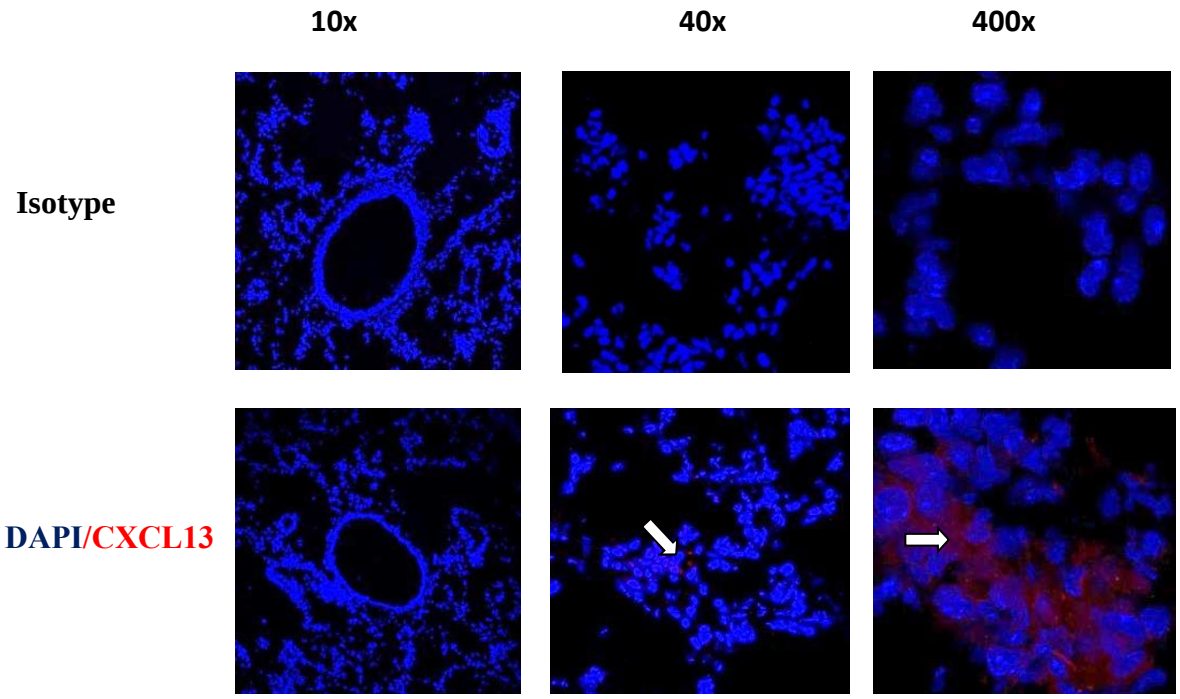

Figure 5.32. Expression of CXCL13 in mouse lung section after UV RSV challenged at day 1

There was positive staining for CXCL13 around epithelium and some cells. Isotype control was applied. Cell nuclei shown in blue (DAPI). Images were originally obtained at 10x, 40x and 400x magnifications using confocal microscopy.

5. 3.5.1.5. Expression of CXCL13 in mouse lung sections after RSV infection at day 2

Strong positive staining of CXCL13 (red) was observed after RSV infection at day 2 (Figure 5.33), and no comparable staining was noticed with the isotype control. In addition, CXCL13 was accumulated in aggregates nearby airways as indicated below (white arrow).

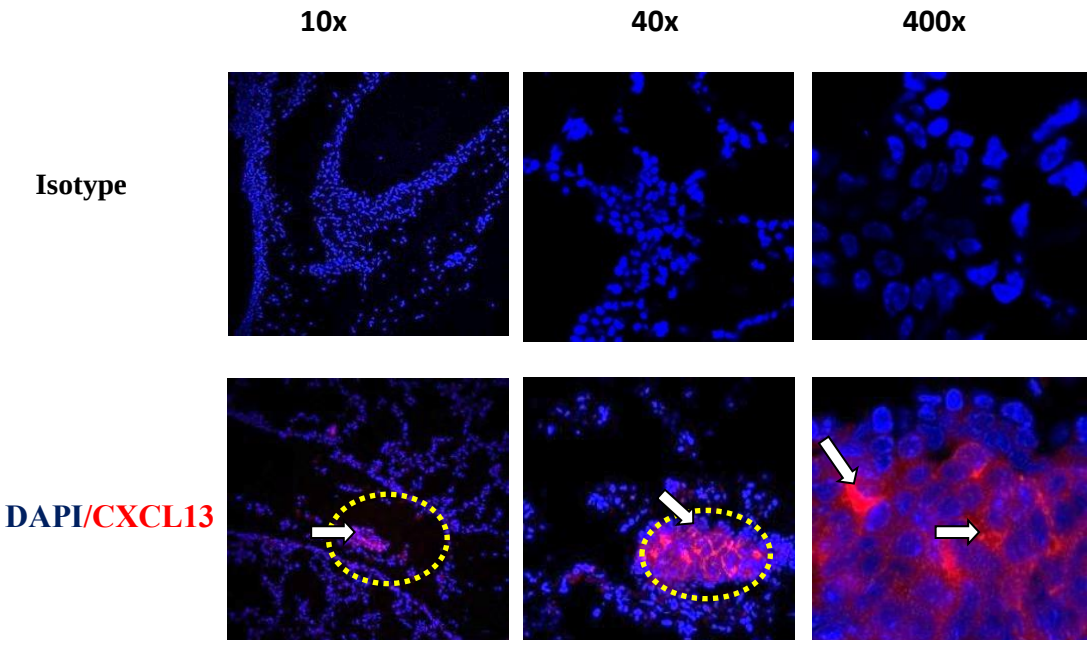

Figure 5.33. Expression of CXCL13 in mouse lung section after RSV infection at day 2

There was strong positive staining of CXCL13 (red) that accumulated in some aggregates that close to airways, as indicated above (arrow). Isotype control was applied. Cell nuclei shown in blue (DAPI). Images were originally obtained at 10x, 40x and 400x magnifications using confocal microscopy.

5.3.5.1.6. Expression of CXCL13 in mouse lung sections after UV RSV challenge at day 2

Positive staining of CXCL13 (red) was detected after challenge with UV RSV at day 2 (Figure 5.34), and no comparable staining was noticed with the isotype control. CXCL13 was distributed around epithelium and other cells that might also induce its expression, as indicated below (arrow).

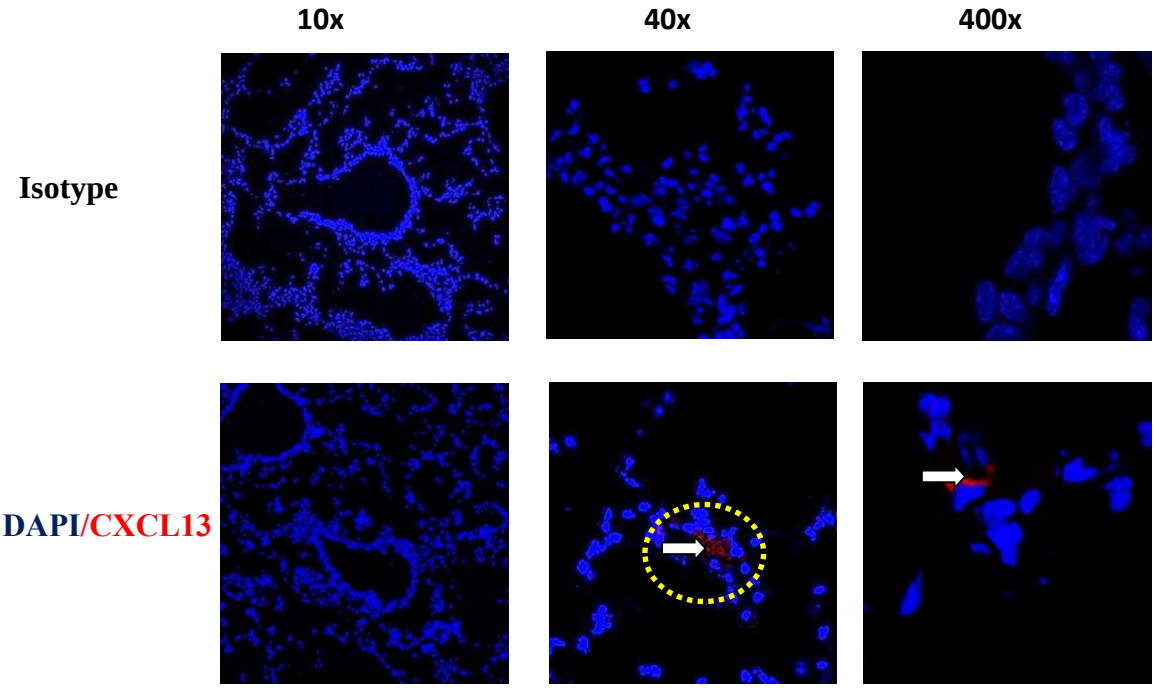

Figure 5.34. Expression of CXCL13 in mouse lung section after UV RSV challenged at day2

There was positive staining for CXCL13 around epithelium as indicated by arrow. Isotype control was applied. Cell nuclei shown in blue (DAPI). Images were originally obtained at 10x, 40x and 400x magnifications using confocal microscopy.

5. 3.5.1.7. Expression of CXCL13 in mouse lung sections after RSV infection at day 4

Positive staining of CXCL13 (red) was detected after RSV infection at day 4 (Figure 5.35), as indicated (white arrow), but not as strong as at day 1 and 2 and no comparable staining was noticed with the isotype control. CXCL 13 was distributed around epithelium and some infiltrated cells as indicated below (brown arrow).

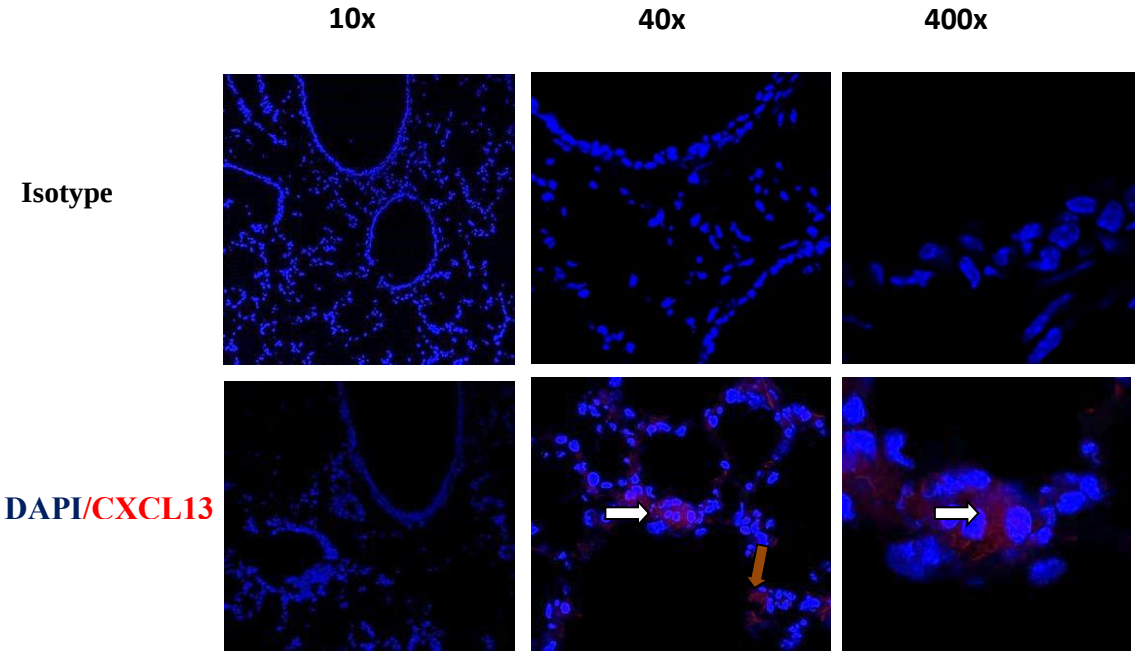

Figure 5.35. Expression of CXCL13 in mouse lung section after RSV infection at day 4

There was positive staining for CXCL13 (red) distributed around epithelium and some infiltrated cells as indicated (arrow). Isotype control was applied. Cell nuclei shown in blue (DAPI). Images were originally obtained at 10x, 40x and 400x magnifications using confocal microscopy.

5.3.5.1.8. Expression of CXCL13 in mouse lung sections after UV RSV challenge at day 4

Positive staining of CXCL13 (red) was detected in mouse lung sections after challenge with UV RSV at day 4 (Figure 5.36), and no comparable staining was noticed with the isotype control. CXCL13 was distributed around epithelium and other cells that might also induce its expression as indicated below (brown arrow).

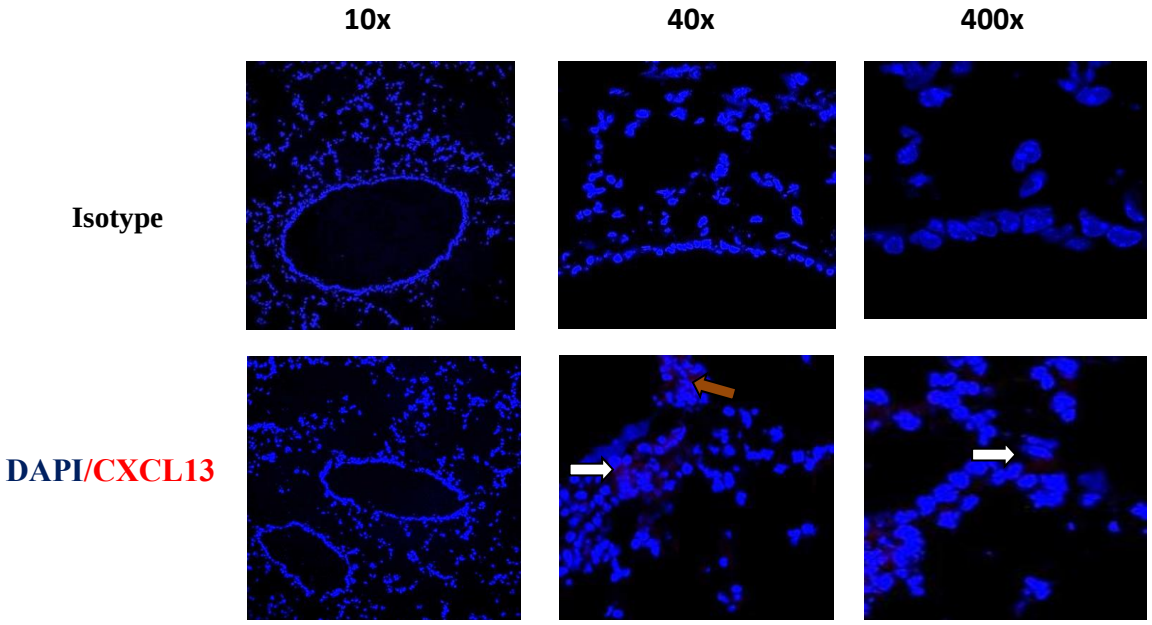

Figure 5.36. Expression of CXCL13 in mouse lung section after UV RSV challenged at day 4

There was positive staining for CXCL13 around epithelium as indicated (arrow). Isotype control was applied. Cell nuclei shown in blue (DAPI). Images were originally obtained at 10x, 40x and 400x magnifications using confocal microscopy.

5. 3.5.1.9. Expression of CXCL13 in mouse lung sections after RSV infection at day 7

Strong positive staining of CXCL13 (red) was detected after RSV infection at day 7 (Figure 5.37), and no comparable staining was noticed with the isotype control. In addition, CXCL 13 accumulated nearby airways and was distributed around some cells as indicated below (white arrow).

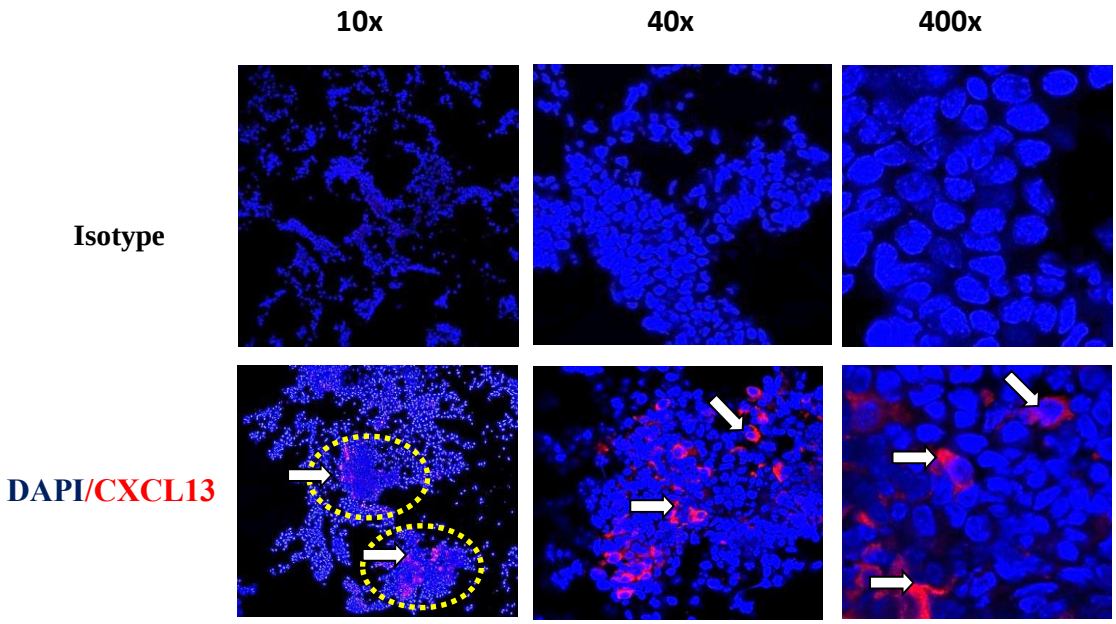

Figure 5.37. Expression of CXCL13 in mouse lung section after RSV infection at day 7

There was strong positive staining of CXCL13 (red) that accumulated in some aggregates that close to airway as indicated by (arrow). Isotype control was applied. Cell nuclei shown in blue (DAPI). Images were originally obtained at 10x, 40x and 400x magnifications using confocal microscopy.

5.3.5.1.10. Expression of CXCL13 in mouse lung sections after UV RSV challenge at day 7

Positive staining of CXCL13 (red) was detected in mice lung challenge with UV RSV at day 7 (Figure 5.38), and no comparable staining was noticed with the isotype control. CXCL13 was distributed around epithelium and other cells that might also induce its expression as indicated below (arrow).

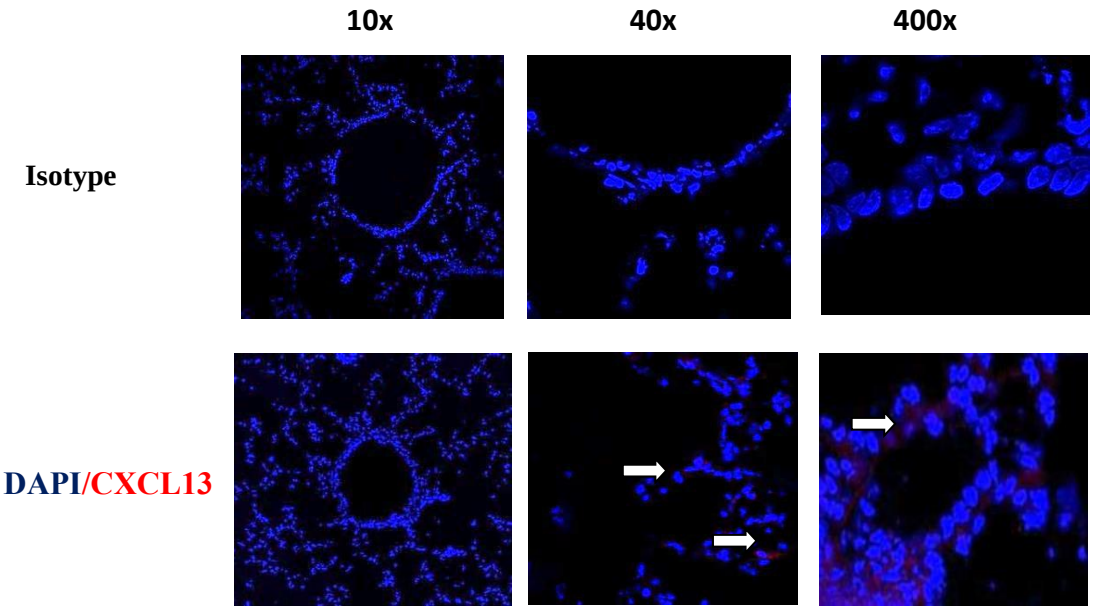

Figure 5.38. Expression of CXCL13 in mouse lung section after UV RSV challenged at day7

There was positive staining for CXCL13 (red) distributed around epithelium and some infiltrated cells as indicated (arrow). Isotype control was applied. Cell nuclei shown in blue (DAPI). Images were originally obtained at 10x, 40x and 400x magnifications using confocal microscopy.

5. 3.5.1.11. Expression of CXCL13 in mouse lung sections after RSV infection at day 8

Positive staining of CXCL13 (red) was detected after RSV infection at day 8 (Figure 5.39), and no comparable staining was noticed with the isotype control. CXCL 13 was distributed nearby airways and some areas of infiltrating cells as indicated below (white arrow).

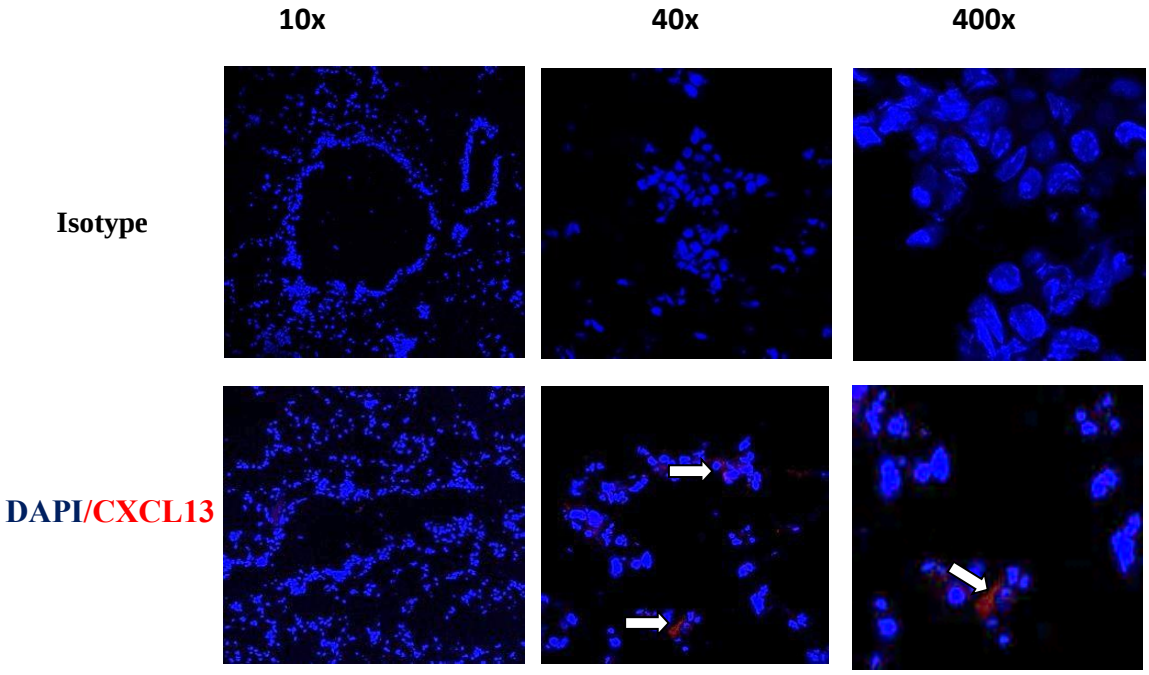

Figure 5.39. Expression of CXCL13 in mouse lung section after RSV infection at day 8

There was positive staining for CXCL13 (red) around epithelium as indicated (arrow). Isotype control was applied. Cell nuclei shown in blue (DAPI). Images were originally obtained at 10x, 40x and 400x magnifications using confocal microscopy.

5.3.5.1.12. Expression of CXCL13 in mouse lung sections after UV RSV challenge at day 8

Positive staining of CXCL13 (red) was detected after challenge with UV RSV at day 8 (Figure 5.40), and no comparable staining was noticed with the isotype control. CXCL13 was distributed around epithelium and other cells that might also induce its expression as indicated below (white arrow).

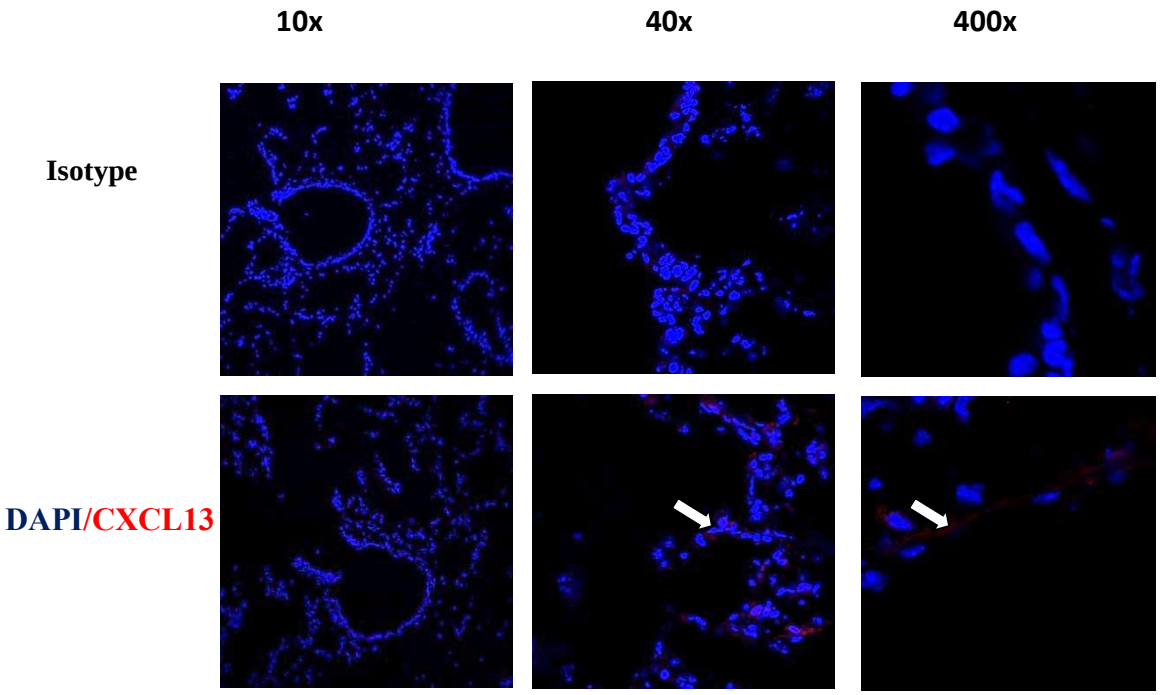

Figure 5.40. Expression of CXCL13 in mouse lung section after UV RSV challenged at day 8

There was positive staining for CXCL13 (red) distributed around epithelium and some infiltrated cells as indicated (arrow). Isotype control was applied. Cell nuclei shown in blue (DAPI). Images were originally obtained at 10x, 40x and 400x magnifications using confocal microscopy.

5. 3.5.2. Expression of B cells in mouse spleen section

B cells are normally found in secondary lymphoid tissue such as spleen (Klein & Dalla-Favera 2008). Therefore, mouse spleen sections were used as positive control to optimize the staining (Figure 5.41). Mouse spleen sections showed strong staining of B cells as indicated below (arrow) and no comparable staining was noticed with the isotype control.

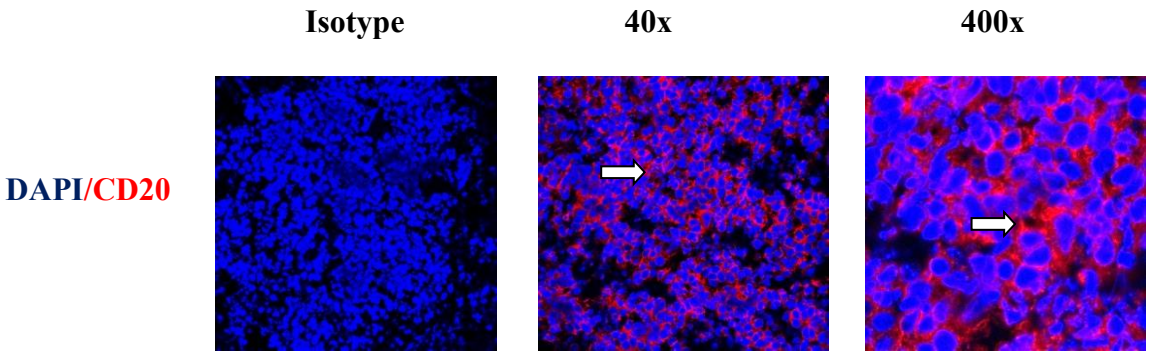

Figure 5.41. B cells are normally expressed in mouse spleen section

B cells (anti-CD20, red) were accumulated in some areas, could be B cells - rich follicles and distributed in spleen. Isotype control was applied. Cell nuclei shown in blue (DAPI). Images were originally obtained at 40x and 400x magnifications using confocal microscopy.

5. 3.5.2.1. Expression of B cells in non-infected mice at day 0

There was positive staining for B cells (red) in non-infected mice at day 0 (Figure 5.42), and no comparable staining was noticed with the isotype control. B cells were accumulated in aggregates and some are distributed around epithelium as indicated below (arrow).

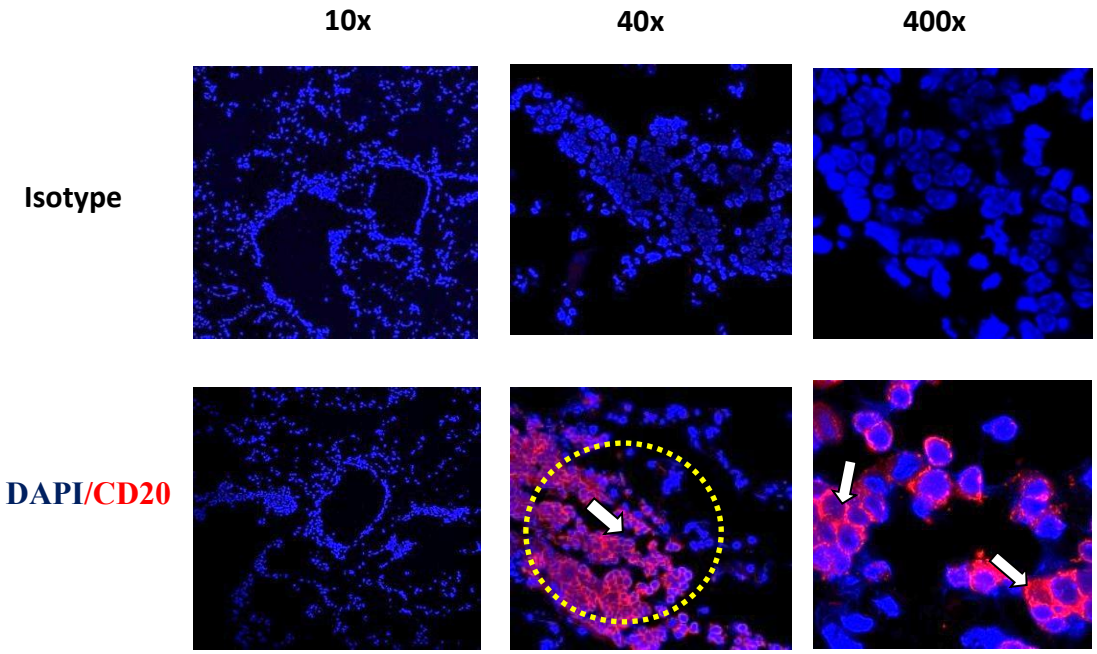

Figure 5.42. B cells are normally expressed in non-infected mice at day 0

B cells (anti-CD20, red) were accumulated in aggregates, distributed around epithelium and airway as indicated below (arrow). Isotype control was applied. Cell nuclei shown in blue (DAPI). Images were originally obtained at 10x, 40x and 400x magnifications using confocal microscopy.

5.3.5.2.2. Detection of B cells in mouse lung after RSV infection at day 1

Strong positive staining of B cells (red) was detected after RSV infection at day 1 (Figure 5.43), and no comparable staining was noticed with the isotype control. B cells were accumulated in aggregates and distributed around airway and epithelium as indicated below (arrow).

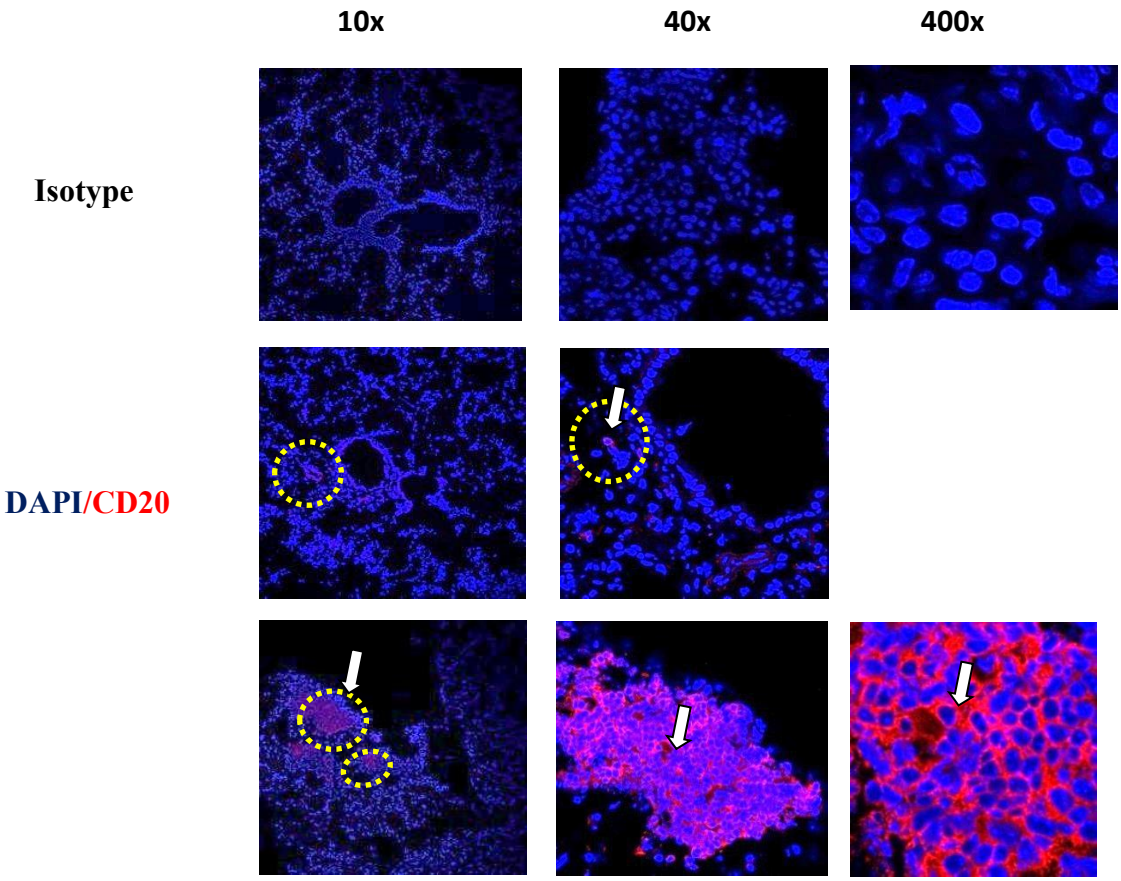

Figure 5.43. Expression of B cells in mouse lung section after RSV infection at day1

B cells (anti-CD20, red) were accumulated in aggregates and distributed around airway and epithelium as indicated (arrow). Isotype control was applied. Cell nuclei shown in blue (DAPI). Images were originally obtained at 10x, 40x and 400x magnifications using confocal microscopy.

5.3.5.2.3. Detection of B cells in mouse lung after UV RSV challenge at day 1

Positive staining of B cells (red) was detected after UV RSV challenge at day 1 (Figure 5.44), but not as strong as at day 1 after RSV infection (Figure 5.43). In addition, no comparable staining was noticed with the isotype control. B cells were located near the airway as indicated (arrow).

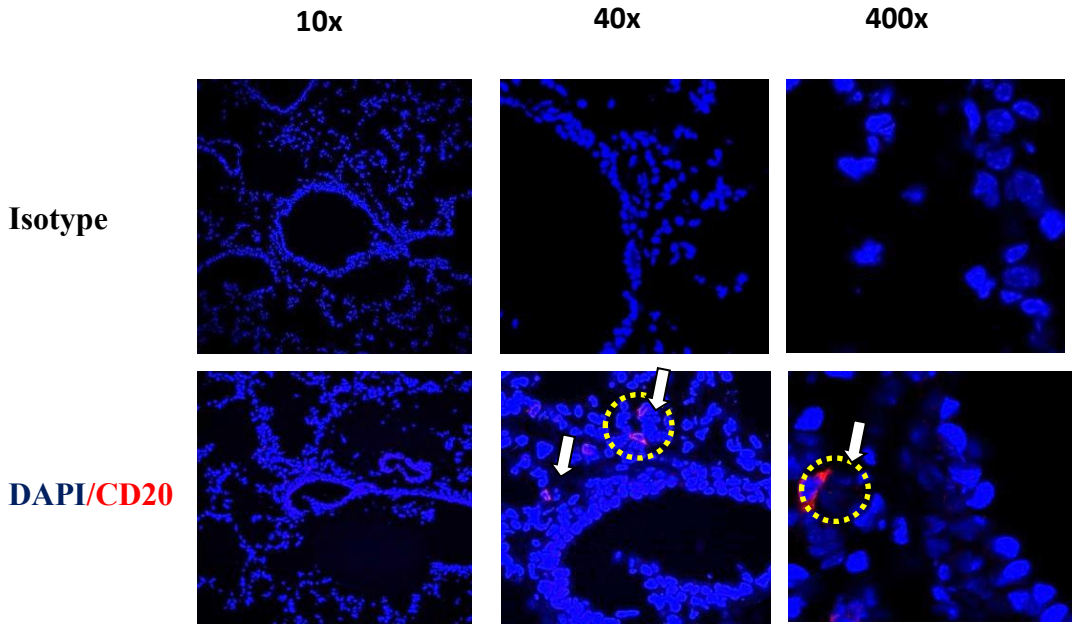

Figure 5.44. Expression of B cells in mouse lung section after UV RSV challenged at day 1

There was positive staining of B cells (anti-CD20, red) that were expressed nearby airway as indicated (arrow). Isotype control was applied. Cell nuclei shown in blue (DAPI). Images were originally obtained at 10x, 40x and 400x magnifications using confocal microscopy.

5.3.5.2.4. Detection of B cells in mouse lung after RSV infection at day 2

Strong positive staining of B cells were detected after RSV infection at day 2 (Figure 5.45), and no comparable staining was noticed with the isotype control. B cells were accumulated in aggregates close to airway and distributed around epithelium as indicated (arrow).

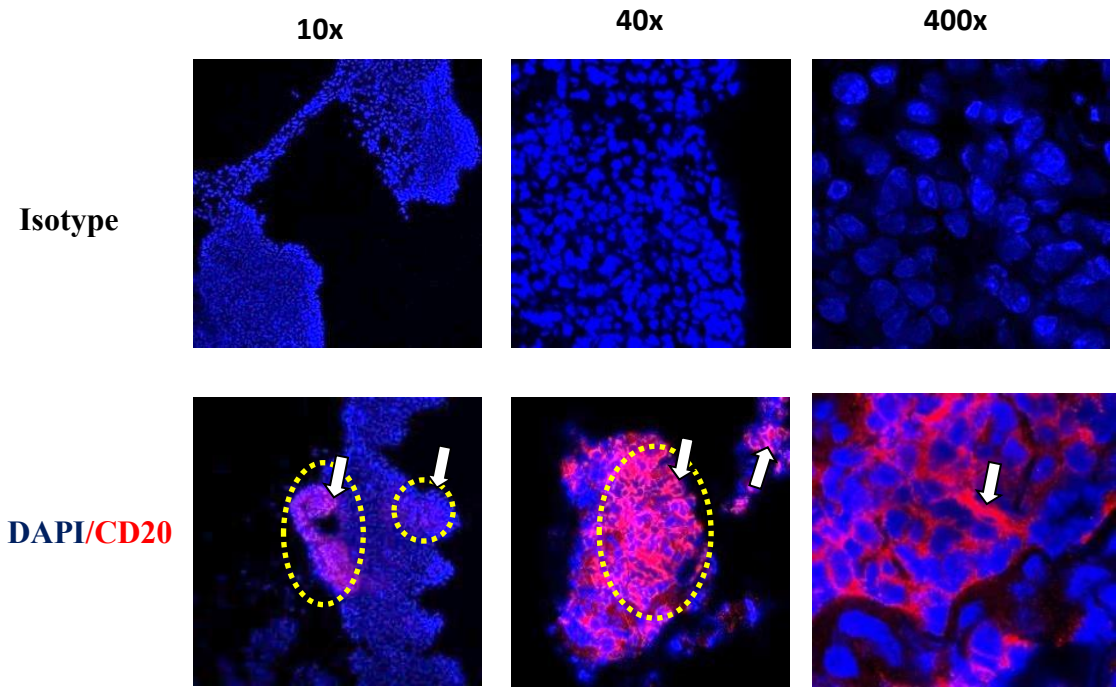

Figure 5.45. Expression of B cells in mouse lung section after RSV infection at day 2

B cells (anti-CD20, red) were accumulated in aggregates close to airway and distributed around epithelium as indicated (arrow). Isotype control was applied. Cell nuclei shown in blue (DAPI). Images were originally obtained at 10x, 40x and 400x magnifications using confocal microscopy.

5.3.5.2.5. Detection of B cells in mouse lung after UV RSV challenge at day 2

Positive staining of B cells (red) was detected after UV RSV challenge at day 2 (Figure 5.46), but not as strong as at day 2 after RSV infection (Figure 5.45). B cells were expressed nearby airway and distributed around cells as indicated (arrow).

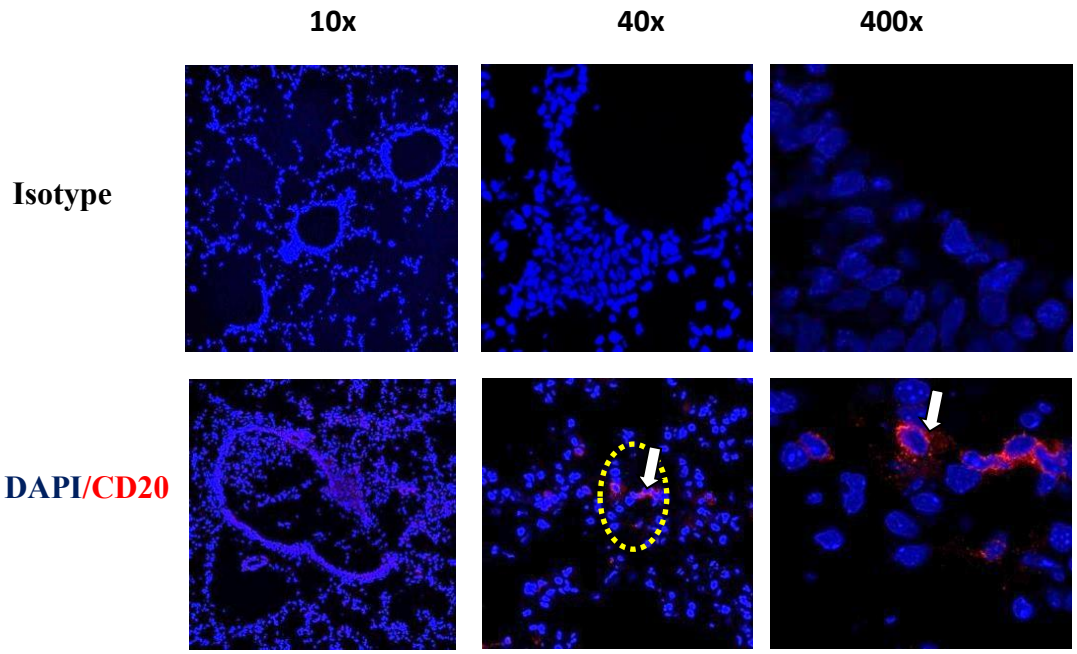

Figure 5.46. Expression of B cells in mouse lung section after UV RSV challenged at day 2

B cells (anti-CD20, red) were detected around airway as indicated (arrow). Isotype control was applied. Cell nuclei shown in blue (DAPI). Images were originally obtained at 10x, 40x and 400x magnifications using confocal microscopy.

5.3.5.2.6. Detection of B cells in mouse lung after RSV infection at day 4

Strong positive staining of B cells (red) were detected after RSV infection at day 4 (Figure 5.47), and no comparable staining was noticed with the isotype control. B cells were accumulated in aggregates close to the airway and distributed around epithelium as indicated (arrow).

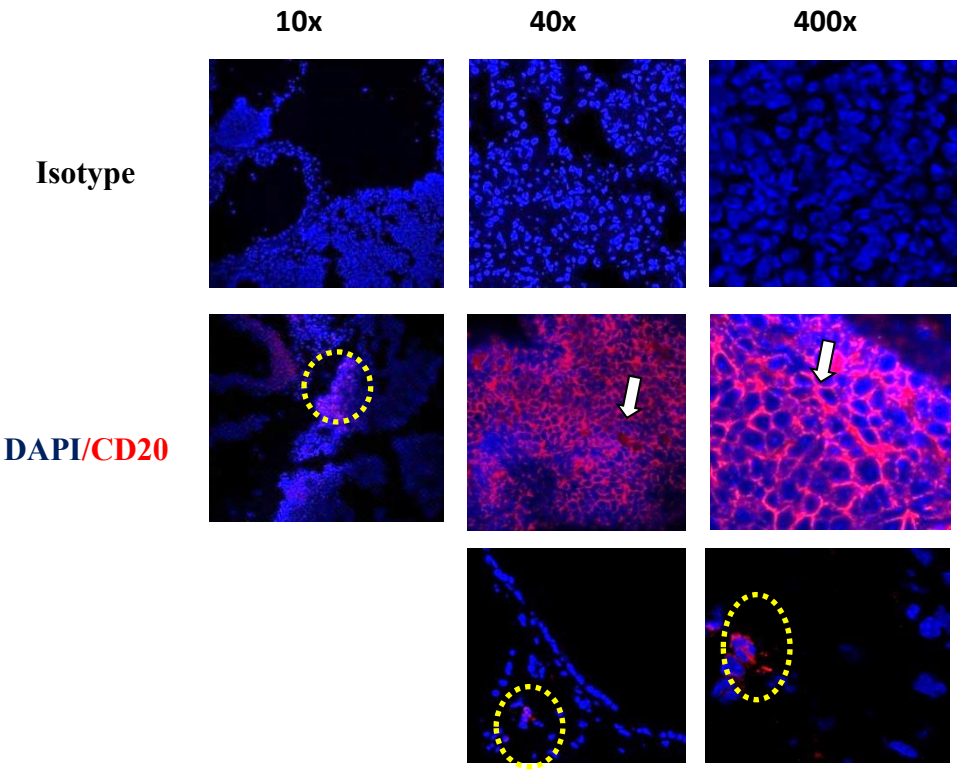

Figure 5.47. Expression of B cells in mouse lung section after RSV infection at day 4

There was strong staining of B cells (anti-CD20, red) accumulated in aggregates close to airway and distributed around epithelium as indicated (arrow). Isotype control was applied. Cell nuclei shown in blue (DAPI). Images were originally obtained at 10x, 40x and 400x magnifications using confocal microscopy.

5.3.5.2.7. Detection of B cells in mouse lung after UV RSV challenge at day 4

Positive staining of B cells (red) were detected after UV RSV challenge at day 4 (Figure 5.48), but not as strong as day 4 after RSV infection (Figure 5.47). In addition, no comparable staining was noticed with the isotype control. B cells were expressed near the airways and alveolar as indicated (arrow).

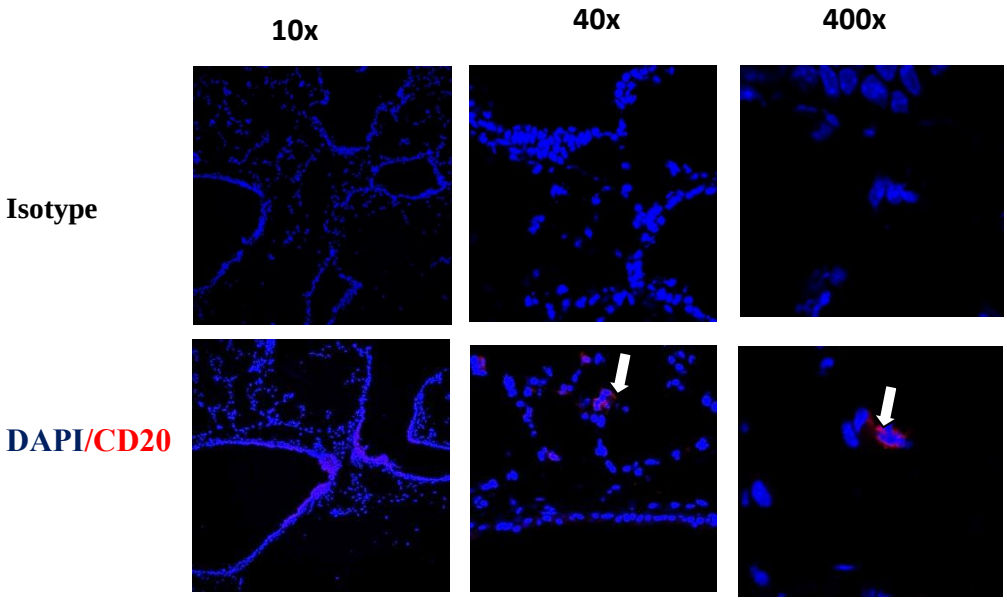

Figure 5.48. Expression of B cells in mouse lung section after UV-treated RSV challenge at day 4

There was positive staining of B cells (anti-CD20, red) that expressed nearby airway and alveolar as indicated (arrow). Isotype control was applied. Cell nuclei shown in blue (DAPI). Images were originally obtained at 10x, 40x and 400x magnifications using confocal microscopy.

5.3.5.2.8. Detection of B cells in mouse lung after RSV infection at day7

Strong positive staining of B cells (red) was detected after RSV infection at day 7 (Figure 5.49) and no comparable staining was noticed with the isotype control. B cells were accumulated in aggregates close to airway and distributed around epithelium as indicates (arrow).

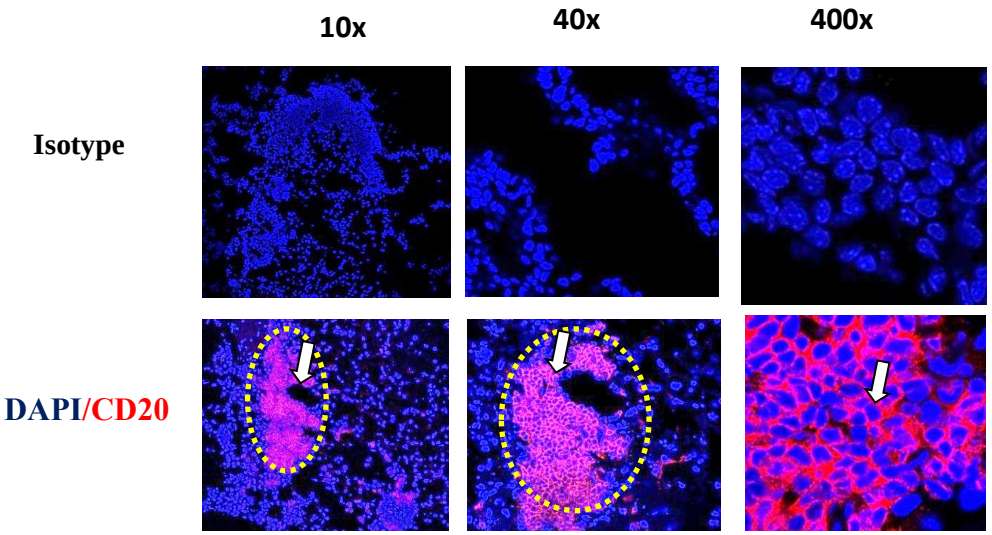

Figure 5.49. Expression of B cells in mouse lung section after RSV infection at day 7

There was strong positive staining of B cells that accumulated in aggregates close to airway and distributed around epithelium as indicates (arrow). Isotype control was applied. Cell nuclei shown in blue (DAPI). Images were originally obtained at 10x, 40x and 400x magnifications using confocal microscopy.

5.3.5.2.9. Detection of B cells in mouse lung after UV RSV challenge at day 7

Positive staining of B cells (red) was detected after UV RSV challenge at day 7 (Figure 5.50) and no comparable staining was noticed with the isotype control. Moreover, staining of B cells was not as strong as day 7 after RSV infection (Figure 5.49). B cells were expressed nearby airway and alveolar as indicated (arrow).

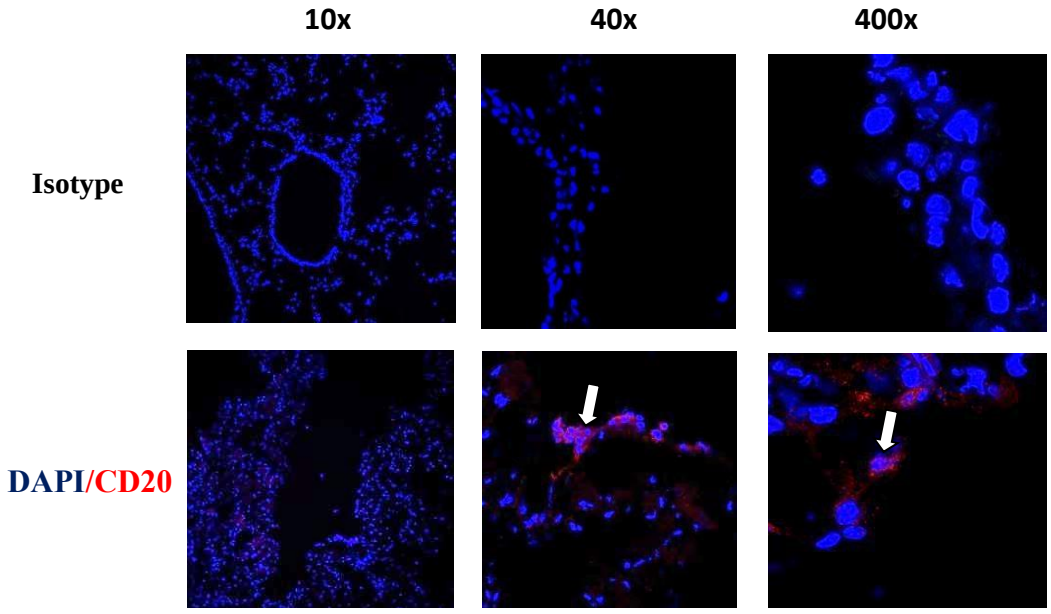

Figure 5.50. Expression of B cells in mouse lung section after UV-treated RSV challenge at day 7

B cells (red) were expressed around airway as indicated (arrow). Isotype control was applied. Cell nuclei shown in blue (DAPI). Images were originally obtained at 10x, 40x and 400x magnifications using confocal microscopy.

5.3.5.2.10. Detection of B cells in mouse lung after RSV infection at day 8

Strong positive staining of B cells (red) was detected after RSV infection at day 8 (Figure 5.51) and no comparable staining was noticed with the isotype control. B cells were accumulated in aggregates close to the airway and distributed around epithelium as indicated (arrow).

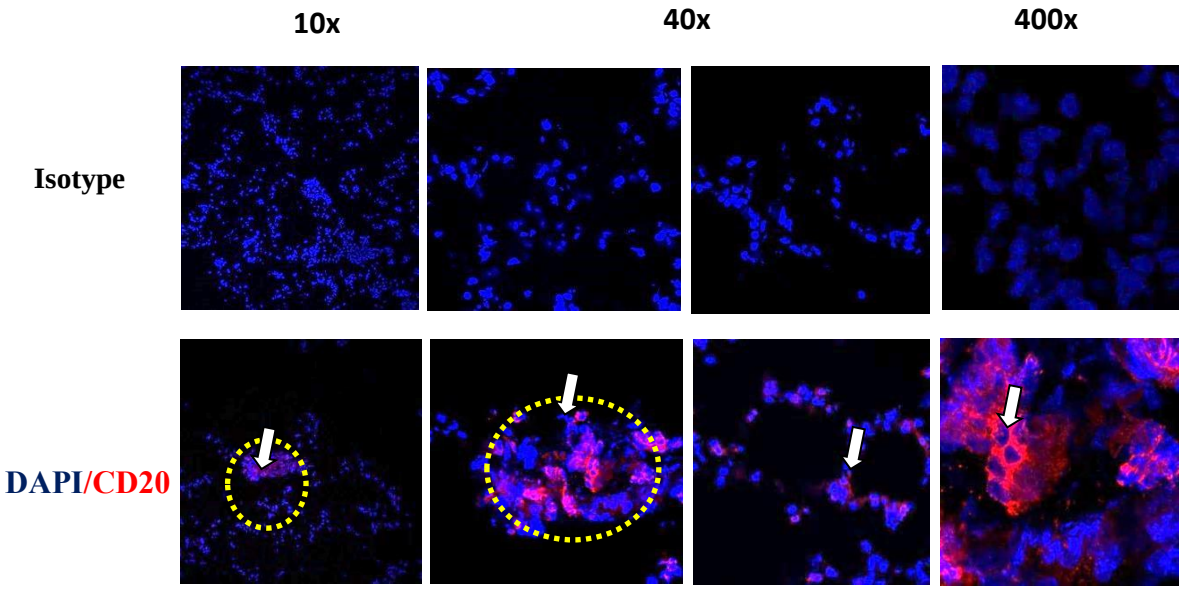

Figure 5.51. Expression of B cells in mouse lung section after RSV infection at day 8

B cells (red) were accumulated in aggregates close to airway and distributed around epithelium as indicated (arrow). Isotype control was applied. Cell nuclei shown in blue (DAPI). Images were originally obtained at 10x, 40x and 400x magnifications using confocal microscopy.

5.3.5.2.11. Detection of B cells in mouse lung after UV RSV challenge at day 8

There was positive staining of B cells after UV RSV challenge at day 8 (Figure 5.52) but not strong as day 8 after RSV infection (Figure 5.1.6.2.10). Moreover, no comparable staining was noticed with the isotype control. B cells were noticed nearby airway and distributed around cells as indicated (arrow).

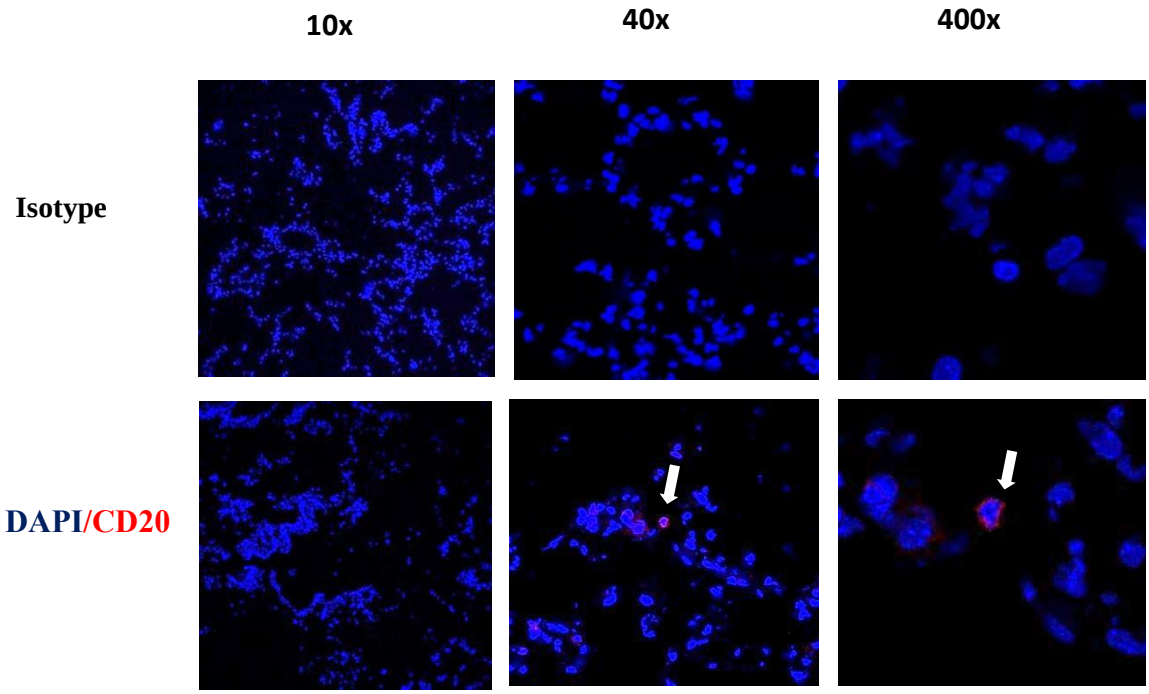

Figure 5.52. Expression of B cells in mouse lung section after UV-treated RSV challenge at day 8

B cells (red) were expressed around airway as indicated (arrow). Isotype control was applied. Cell nuclei shown in blue (DAPI). Images were originally obtained at 10x, 40x and 400x magnifications using confocal microscopy.

5. 3.5.2.12. B cells numbers increased significantly after RSV infection

From the immunofluorescence staining results of mouse lung sections, there was strong positive staining of B cells after RSV infection at days 1, 2, 4, 7 and 8 relative to UV RSV challenge at the same time points. To further confirm these results, B cells numbers (Figure 5.53) were measured by Amanda McFarlane at Queens Medical Research Institute at the University of Edinburgh by using FACS analysis. B cells numbers were increased significantly after RSV infection at day 6 and 8 (10×10^5) and (8.5×10^5) respectively in comparison to UV RSV control at day 6 (4.3×10^5) and day 8 (4.8×10^5).

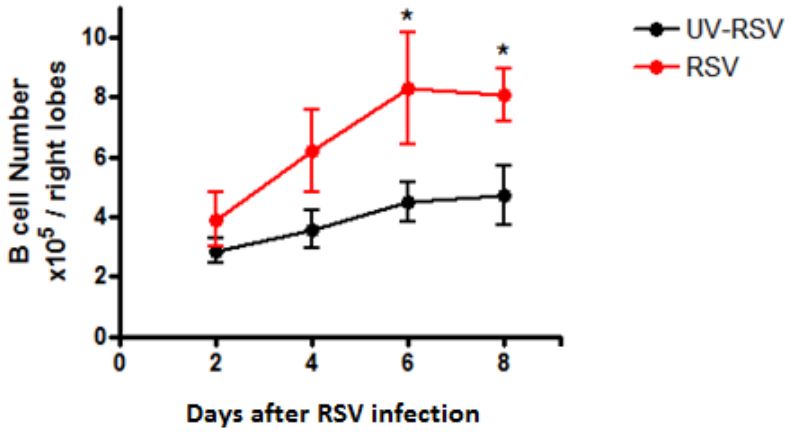

Figure 5.53. FACS analysis of B cells numbers from after RSV infection and UV RSV challenged

*Mice were infected with RSV or challenged with UV RSV for 2, 4, 6, 8 and 10 days. Mouse lungs (right lobes) were homogenised and B cells numbers were counted. B cells numbers increased significantly on day 6 and 8 relative to UV-RSV control at the same time points. Mean and SD are shown (two way ANOVA with Bonferroni post-hoc test, *P <0.05, n=3).*

5.3.5.3. Expression of CD3 in mouse spleen section

T cells are normally expressed in secondary lymphoid tissues, such as spleen (Klein & Dalla-Favera 2008). Thus, mouse spleen sections were used as positive control to optimize the staining (Figure 5.54). Mouse spleen sections showed strong staining for T cells, as indicated below (arrow).

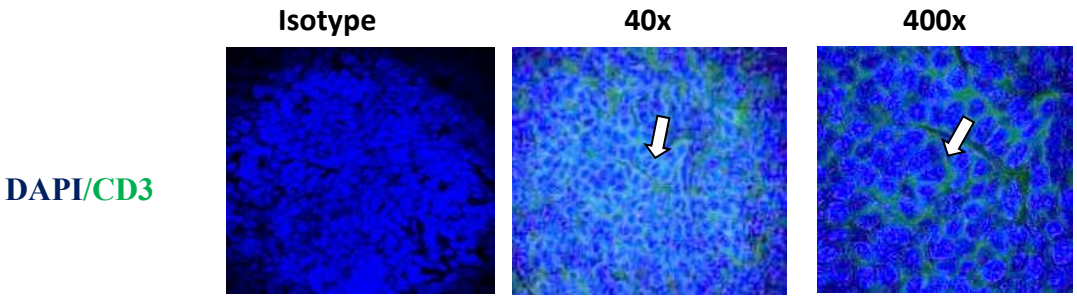

Figure 5.54. T cells are normally expressed in mouse spleen section

There was positive staining of T cells (anti-CD3, green) detected in spleen that are placed around spleen. Isotype control was applied. Cell nuclei shown in blue (DAPI). Images were originally obtained at 40x and 400x magnifications using confocal microscopy.

5.3.5.3.1. T cells are absent from mouse lung after RSV infection at day 2

No positive staining for T cells (CD 3, green) was observed after RSV infection at day 2 (Figure 5.55).

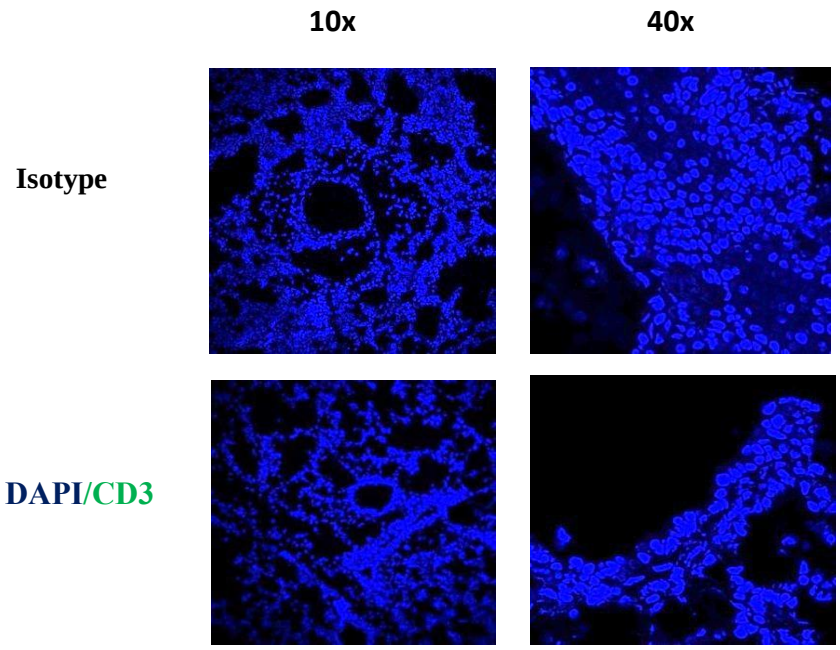

Figure 5.55. Absence of T cells in mouse lung section after RSV infection at day 2

There was negative staining of T cells (anti-CD3, green) in mouse lung section after RSV infection at day 2. Isotype control was applied. Cell nuclei shown in blue (DAPI). Images were originally obtained at 10x and 40x magnifications using confocal microscopy.

5.3.5.3.2. T cells are absent from mouse lung after UV RSV challenge at day 2

No positive staining for T cells (CD 3, green) was observed after UV RSV challenge at day 2 (Figure 5.56).

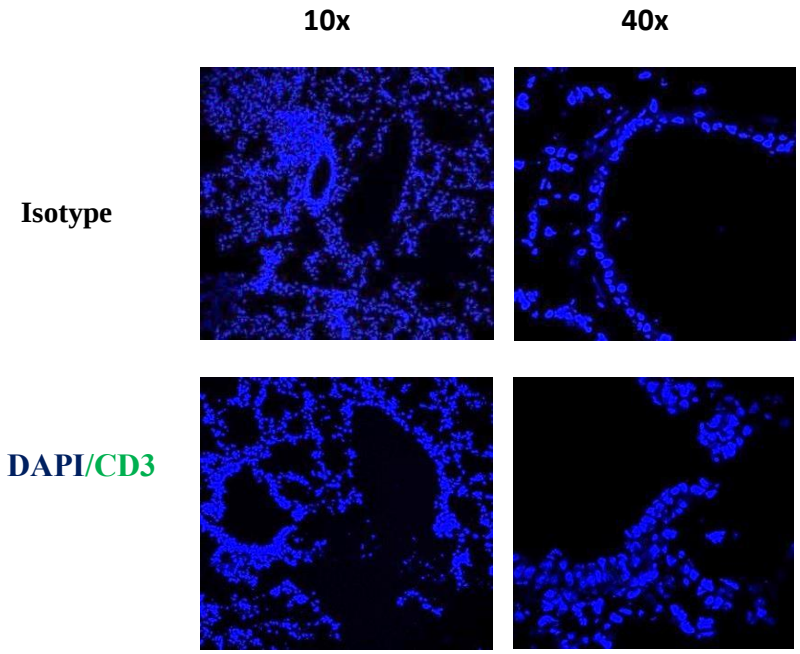

Figure 5.56. Absence of T cells in mouse lung section after UV-RSV challenged at day 2

There was negative staining of T cells (anti-CD3, green) in mouse lung section after RSV infection at day 2. Isotype control was applied. Cell nuclei shown in blue (DAPI). Images were originally obtained at 10x and 40x magnifications using confocal microscopy.

5.3.6. Summary of expression CXCL13 protein at various time points following RSV infection and recruitment of B cells into mice lung

CXCL13 protein (Figure 5.57 A) was expressed in non-infected mice at day 0 (mean 271 pg/ml). However, after RSV infection CXCL13 protein was significantly increased at day 1 (mean 775 pg/ml, P=0.0001), day2 (517 pg/ml, P=0.005), and day 7 (360 pg/ml, P=0.0002) in comparison to UV RSV control at day 1 (334 pg/ml), day 2 (290pg/ml) and day 7 (243 pg/ml). In addition, CXCL13 protein was further confirmed by immunofluorescence staining of mouse lung sections that also showed association of CXCL13 expression after RSV infection relative to UV RSV challenge at the same time points (Figure 5.57 B).

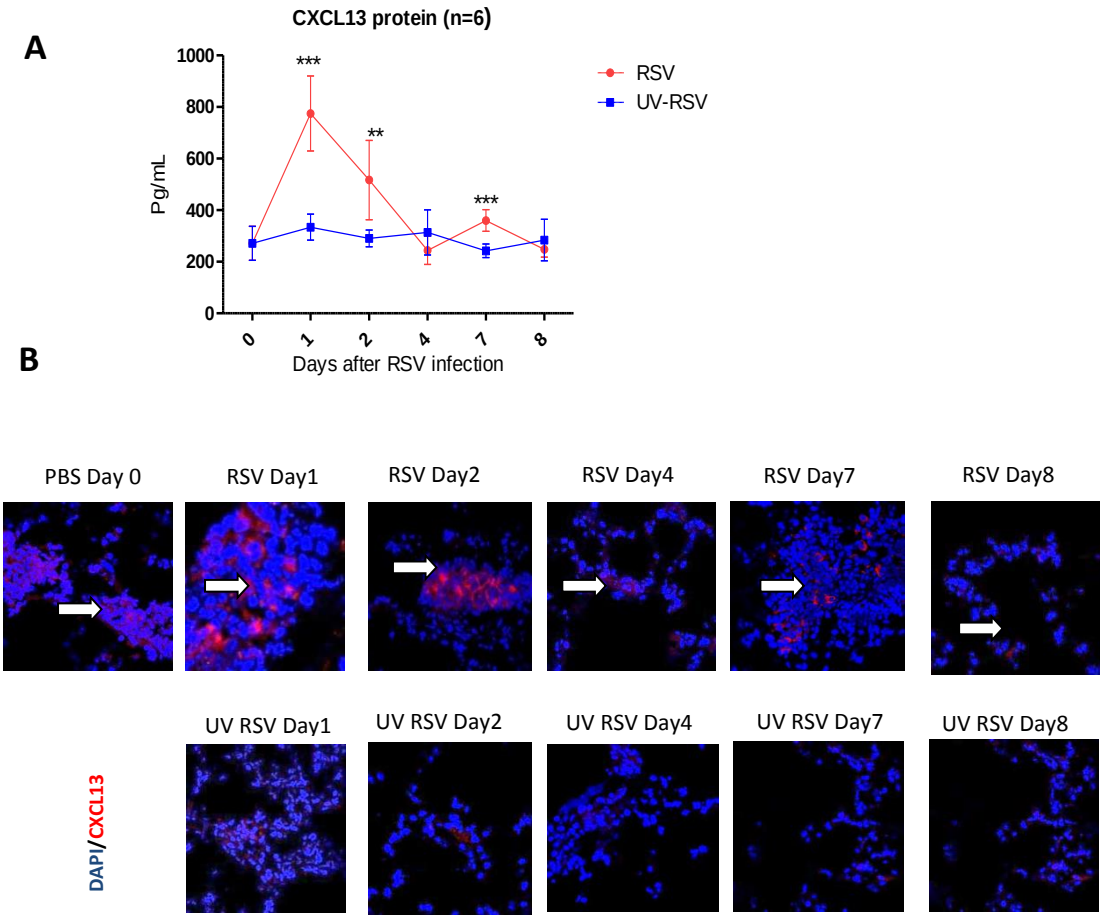

Figure 5.57. Expression of CXCL13 protein after RSV infection and UV RSV control

CXCL13 protein was measured by using specific murine CXCL13 ELISA (A). CXCL13 protein was increased significantly after RSV infection at day 1, 2 and 7 in comparison to UV RSV control at the same time points. Immunofluorescence staining of mouse lung sections (B) showed association expression of CXCL13 (red) as indicated (arrow) after RSV infection and UV RSV challenge at the same time points.

The immunofluorescent results shown below (Figure 5.58.C) that there was strong positive staining of B cells after RSV infection at day 1, 2, 4, 7 and 8 relative to UV RSV challenge at the same time points. Equally, B cells numbers (Figure 5.58 D) measured with FACS increased significantly after RSV infection at day 6 and 8 (10×10^5) and (8.5×10^5) respectively in comparison to UV RSV control at day 6 (4.3×10^5) and day 8 (4.8×10^5). Both suggest that RSV infection in mice leads to significantly increased B cells number in the lungs.

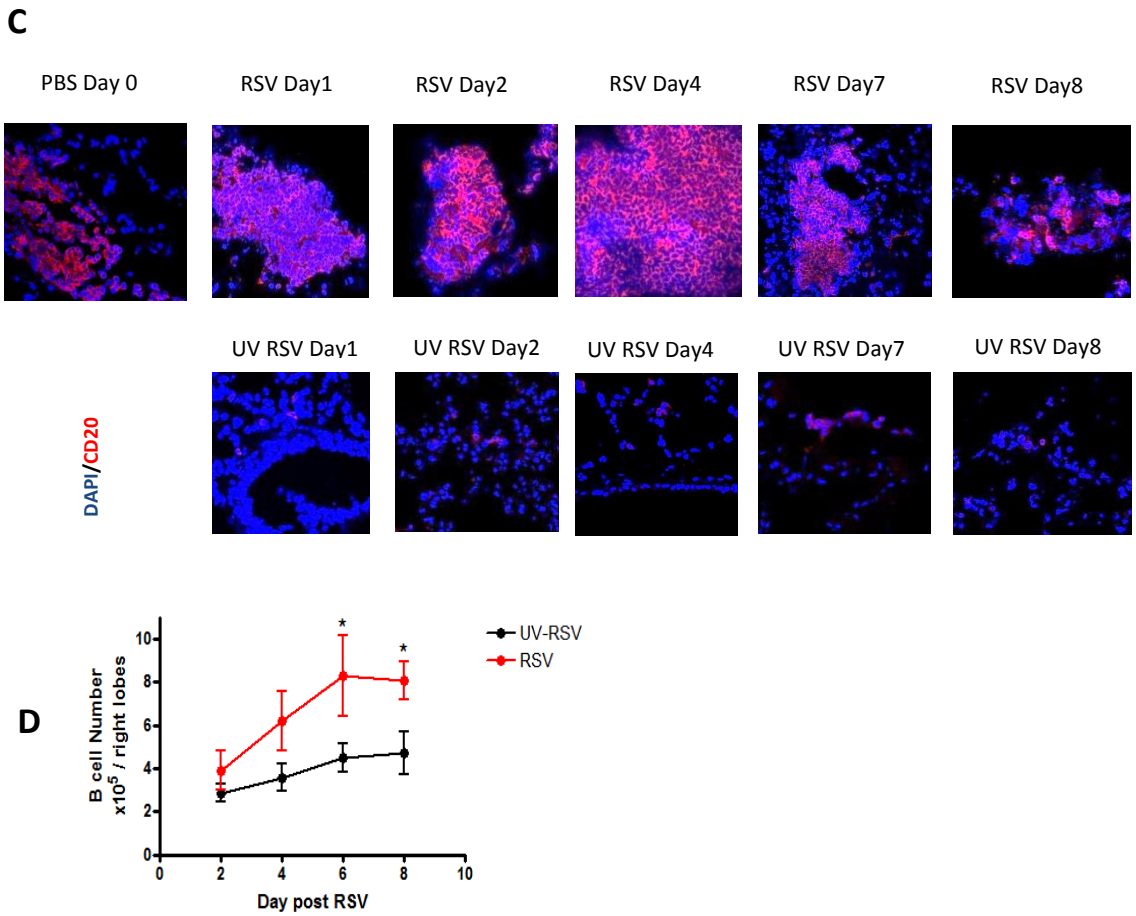

Figure 5.58. Expression of B cells after RSV infection and UV RSV control in mouse lung sections

*There was strong positive staining of B cells (anti-CD20, red) at day 1, 2, 4, 7 and 8 after RSV infection relative to UV RSV control at the same time points (C). B cells numbers of mouse right lobes were measure by FACS (D); B cells numbers were increased significantly at day 6 and 8 relative to UVRSV challenge at the same time points. Mean and SD are shown (two way ANOVA with Bonferroni post-hoc test, *P <0.05, n=3).*

5.3.7. Discussion

5.3.7.1. RSV infection of BALB/c mice significantly induced CXCL13 mRNA and protein expression

To further understand the B and T cell responses to RSV infection in the lung, local expression of the homeostatic chemokines CXCL12, CXCL13, CCL19 and CCL21 (chapter 1, section 1.4) were studied. These chemokines are normally expressed in secondary lymphoid organs such as spleen, where they control placement of lymphocytes (Cyster 1999). However, recent studies have shown that expression of homeostatic chemokines can be induced in non-lymphoid tissue such as lungs upon viral infection like Influenza and to be involved in formation of inducible bronchus-associated lymphoid tissue (iBALT), where its formation is essential for initiating local B and T cell responses to influenza (Rangel-Moreno *et al.* 2007).

To investigate if CXCL13 expression is induced after RSV infection, mice were infected with RSV (A2 strain) at various time points, including time day 0 (non-infected), 1, 2, 4, 7 and 8 (chapter 2, section 2.3). Firstly, CXCL13 mRNA was measured by RT-PCR. Non-infected mice expressed CXCL13 mRNA at day 0 (fold expression relative to control= 0.086) indicating that CXCL13 expression occurs in the lung in the absence of visible infection. However, after RSV infection CXCL13 mRNA expression was increased significantly on day 1 (1.56, P=0.001) and day 7 (0.92, P=0.001) in comparison to UV RSV control at day 1 (0.20) and day 7 (0.18) (Figure 5. 25 A).

To confirm not only CXCL13 mRNA expression was increased following RSV infection, CXCL13 protein (Figure 5.25.B) was measured by ELISA. CXCL13 protein was expressed in control mice at day 0 (mean 271 pg/ml). However, after RSV infection CXCL13 protein was significantly increased at day 1 (mean 774 pg/ml, P=0.0001), day 2 (516 pg/ml, P=0.005) and day 7 (359 pg/ml, P=0.0002) in comparison to UV RSV control on day 1 (334 pg/ml), day 2 (290 pg/ml) and day 7 (242 pg/ml). There was a correlation between the CXCL13 mRNA and protein expressions, both were increased significantly at day 1, 2 and 7 after RSV infection (Figure 5.25.A-B).

Moreover, expression of the CXCL13 protein was further confirmed by immunofluorescence staining of mice lung sections, which has also showed strong positive staining for CXCL13 at day 1 (Figure 5.31), day 2 (Figure 5.33) and day 7 (Figure 5.37) after RSV infection relative to non-infected mice at day 0 (Figure 5.30) and RSV UV control at the same time points, at day 1 (Figure 5.32), day 2 (Figure 5.34) and day 7 (Figure 5.38). The CXCL13 protein was accumulated near airway and epithelium at day 1 (Figure 5.31), day 2 (Figure 5.33) and day 7 (Figure 5.37).

Furthermore, increased expression of CXCL13 mRNA and protein was associated with RSV infection at day 1, 2 but not at day 4, where RSV has reached the highest levels and CXCL13 mRNA and protein declined. In addition, there was no evidence of RSV by RT-PCR at day 7 (Figure 4.16), although CXCL13 mRNA and protein were increased significantly after RSV infection.

5.3.7.2. RSV infection of BALB/c mice significantly induced infliltration or recruitment of B cells

CXCL13 is known to act as B lymphocyte chemoattractant (Gunn *et al.* 1998) and to determine if B cells were recruited into mouse lungs following RSV infection lung sections were stained with the B cell specific marker anti-CD20, which has already been tested in mouse spleen tissue as positive control (Figure 5.41).

Control mice day 0 (Figure 5.42) showed positive staining of B cells accumulated in aggregates. In addition, precence of B cells (CD19) was detected in the lungs of normal mice and their numbers were decreased after depetion of CXCL13 (Rangel-Moreno *et al.* 2007) . However, it could be possible that those mice were exposed to some pathogens before treatment in the animal house. In addition, mouse lung sections showed strong positive staining of B cells (anti-CD20) after RSV infection at day 1 (Figure 5.43), day 2 (Figure 5.45), day 4 (5.47), day 7 (5.49) and day 8 (5.51) relative to UV RSV control at the same time points on day 1 (5.44), day 2 (Figure 5.46), day 4 (Figure 5.48), day 7 (Figure 5.50) and day 8 (Figure 5.52).

To further confirm increased numbers of B cells, they (Figure 5.53) were measured quantitatively using FACS analysis. B cells numbers increased significantly after RSV infection at day 6 and 8 (10×10^5 and 8.5×10^5 respectively) in comparison to UV RSV control at day 6 (4.3×10^5) and day 8 (4.8×10^5).

Taken together, increased expression of the CXCL13 protein is associated with increased presence of B-cell aggregates at day 1, day 2 and day 7 after RSV infection relative to UV RSV control at the same time points, which suggested that CXCL13 recruited B cells into the lung. Although CXCL13 increased significantly on day 1, 2 and 7 but not on day 4, B cells were observed in mouse lung sections at day 4 following RSV infection and increased in day 6 and 8 after RSV infection. Thus, it could be possible that these B cells were recruited into the lung at the early stage of RSV infection by CXCL13 at day 1 and 2. However, to ensure that CXCL13 was responsible for the recruitment of B cells into the lung, mice should be targeted with anti-CXCL13 prior to RSV infection, and we could stain for CXCL13 expressed by B cells in the lung (Chapter 6.3).

5.3.7.3. RSV infection of BALB/c mice did not significantly increase expression of CXCL12, CCL19 and CCL21 mRNA or protein

It has been reported that CXCL12 (Chapter 1.4) can act as a chemoattractant for memory B cells that express CXCR4 (Fleige *et al.* 2014; Okada *et al.* 2002). To determine if CXCL12 is induced following RSV infection, mice were infected with RSV (A2 strain) at different time points, including day 0 (non-infected), 1, 2, 4, 7 and 8. CXCL12 protein (Figure 5.26) was expressed in non-infected mice at day 0 (mean= 1387 pg/ml) indicating that CXCL12 expression occurs in the lung in the absence of visible infection. However, after RSV infection there was no significant increase of CXCL12 protein at day 1, day 2, day 4, day 7 and day 8 in comparison to UV RSV control at the same time points. Thus, it could be possible that expression of CXCL12 protein was normally intracellular and released during inflammation. However, this could also be irrelevant. In addition, it has been shown that epithelium and alveolar macrophages may be the primary source of CXCL12 in the lungs of LPS- injured mice (Petty *et al.* 2007).

Thus, to test if CXCL12 was responsible or not for the recruitment of B cells after RSV infection, we could treat mice with anti-CXCL12 prior to RSV infection and monitor the kinetics of CXCL12 following RSV infection and observe if B cells migrated to the lungs after RSV infection.

Furthermore, CCL19 protein (Figure 5.27) was also expressed in non-infected mice at day 0 (mean 1387 pg/ml) and there was no was no significant increase after RSV infection at day 1, 2, 4, 7 and 8 compared to UV RSV control. Similarly, CCL21 protein was expressed in non-infected mice at day 0 (mean 684 pg/ml) and there was no significant increase flowing RSV infection at day 1, 2, 4, 7 and 8 compared to UV RSV control (Figure 5.28).

Although CCL19 and CCL21 were expressed normally in the lung and there was no significant increase after RSV infection; this could indicate that they are not active in recruiting cells to the airway in RSV disease. To fully understand their role in RSV infection, we should do further studies to determine if CCL19 or CCL21 are released from intracellular stores during infection and are active in the recruitment of lymphocytes. In this regard, it has been shown that RSV infection of DCs resulted in decreased expression of CCR7 and inefficient migration of DC to the lymphatic tissue, which then may contribute to reduce adaptive responses to RSV (Le Nouen *et al.* 2011). CCL19 is secreted by fibroblastic reticular cells present in the lymph node and CCL21 is secreted from fibroblastic reticular cells and high endothelial venules (HEVs), and both are constitutively expressed by stromal cells within the T-cell zones in the secondary lymphoid tissue (Brühl *et al.* 2008; Link *et al.* 2007) (chapter 1, section 1.4)

In contrast to RSV, influenza infection has been reported to induce increased expression of CCL19 and CCL21 (Moyron-Quiroz *et al.* 2004). Taken together, these findings suggest that RSV infection may not be fully responsible for recruitment of T cell response during infection. Furthermore, it could be possible that these chemokines may be induced at later time points after RSV infection.

5.3.7.4. T cells response is absent following RSV infection

Immunofluorescence staining of mouse lung tissue sections showed near absence of T cells (anti-CD3) following RSV infection in comparison to RSV UV control (Figure 5.55 and Figure 5.56). However, it could be possible that the antibody used (anti-CD3) was not good enough to stain T cells in the airways and further work is required, by use of other antibodies to confirm these preliminary results. This could be achieved by staining for CD8 or CD4 in the lung, as well as counting T cells by

FACS. From the work of other studies discussed (Chapter 1.1.5.2.1) presence of T cells would have been expected in the airway. Presence of T cells in the human lung following RSV infection is however controversial. Histological analysis of infants with fatal cases of RSV showed few CD4 and CD8 T cells in the lung (Welliver *et al.* 2007). Moreover, histological tissue of infants who died due to severe RSV infection showed prominent presence of B cells and near absence of CD3+ T cells, which suggests that B cell activation in the lungs during severe infection could be T cell-independent (Borchers *et al.* 2013; Reed *et al.* 2009). However, it could be possible that these children died because they did not develop a proper T cells response and in contrast, another study detected virus-specific CD8 T cells in the bronchial alveolar lavage and peripheral blood of infants after RSV infection (Heidema *et al.* 2007).

5.3.8. Summary

Homeostatic chemokines, including CXCL12, CXCL13, CCL19 and CCL21 were expressed normally in mouse lungs, which indicated that their expression occurs in the lung in the absence of visible infection. However, after RSV infection only CXCL13 mRNA and protein were significantly increased at day 1, 2 and 7 compared to UV RSV control. Expression of CXCL13 was further confirmed by the immunofluorescence staining of mouse lung sections that showed positive staining for CXCL13 after RSV infection at day 1, 2 and 7. In addition, CXCL13 was accumulated in aggregates near the airway at day 1, 2 and 7.

Lung sections showed strong positive staining of B cells (anti-CD20 positive cells). B accumulation also appears to be associated with expression of CXCL13. Moreover, from work described in (chapter 4, 4.17) the BAFF protein was also significantly expressed at high levels at these time points (Figure 4.1.5.3). These findings suggest that CXCL13 may be directly responsible for B cell recruitment into the lung and supports the role of BAFF in promoting airway B cell differentiation.

5.3.9. Summary of the strength of staining of RSV, BAFF, CXCL13, B and T cells and possibility of inflammatory cells

Arbitrary scale such as (-, +, ++, +++, ++++) was used to indicate and evalute the strength of staining of RSV, BAFF, CXCL13, B cell (CD19) and Inflammatory cells (Table 5.1) after RSV infection and UV-treaed RSV at day 0,1,2,4,7 and 8.

			BAFF	CXCL13	B cell	T cell	Inflammatory cells
Day 0	RSV UV-RSV	- -	+ +	+ +	+ +	+	- -
Day 1	RSV UV-RSV	++ -	++++ +	++++ +	++ +	- -	++ +
Day 2	RSV UV-RSV	+++ -	++++ +	++++ +	+++ +	- -	+++ +
Day 4	RSV UV-RSV	++++ -	++ +	++ +	++++ +	- -	+++ +
Day 7	RSV UV-RSV	- -	++++ +	+++ +	++++ +	- -	+++ +
Day 8	RSV UV-RSV	- -	+++ +	+ +	+++ +	- -	+++

Table 5.1. Summary represents the strength of staining of RSV, BAFF, CXCL13 and B cells and possibility of inflammatory cells.

CHAPTER 6. GENERAL DISCUSSION

6.1. RSV infection induced significant expression of BAFF and CXCL13, but not APRIL, CXCL12, CCL19 and CCL21

In vitro, BEAS-2B cells were used to mimic RSV infection of human epithelial cells and to determine if the airway epithelium can support effective immune response, in particular B cell responses through production of B cell growth factors, including BAFF and APRIL during RSV infection. Firstly, RSV F protein can be recognized through TLR4 expressed at the cell surface of the airway epithelial cells (Kurt-Jones *et al.* 2000). In addition, RSV products during replication, such as dsRNA can be also recognized by intracellular TLR3 by respiratory epithelial cells (Rudd *et al.*

2006). After recognition, this leads to triggering of an innate antiviral response, including IFN-β (Chapter 1.1.5.1.2).

From the *in vitro* experiments described in chapter 3 RSV infection of BEAS-2B cells induced significant increased expression of both BAFF mRNA and protein, but not those of APRIL. In addition, increased RSV titre resulted in increased BAFF expression. Furthermore, stimulated BEAS-2B cells with IFN-β induced significant expression of BAFF mRNA and protein. BAFF mRNA reached highest levels at 12h and declined significantly at 48h after either RSV infection or IFN-β stimulation, which suggested that BAFF protein is released at this time point where it has been measured in the culture supernatant (Figure 3.5).

Western blot analysis of BEAS-2B cells showed that resting epithelial cells expressed membrane BAFF and mRNA whose expression peaked at 12h after RSV infection and decreased at 24h. Taken together, these observations suggest that soluble BAFF (17kD) was cleaved from the membrane-bound form (31kD) and released into the culture supernatant of BEAS-2B cells. This is then detected by ELISA at 48hours after infection (Figure 3.11.A-B).

In addition, neutralizing of IFN-β has led to reduced significant expression of BAFF mRNA and protein, which suggests that BAFF production through RSV infection, is dependent on production of IFN-β from the infected cells (Figure 3.10.1-2) and IFN-β is a potent stimulator of BAFF expression.

To further understand the production of BAFF and APRIL, *in vivo*, BALB/c mice were infected with RSV (chapter 4). BAFF mRNA and protein but not APRIL were significantly increased after RSV infection relative to UV-RSV control and there were two peaks of BAFF protein expression, at day 2 and 7 (Figure 4.17).

Although BAFF expression has been shown to be IFN-β dependent in *in vitro* experiments, it remains to be shown that BAFF induction is interferon dependent *in vivo*. To test this we could inhibit IFN-β in mice prior to RSV infection and observe if production of BAFF is dependent on IFN-β at day 2 and 7 after RSV challenge.

Western blot analysis of homogenised lung tissue showed that resting epithelial cells BEAS-2B cells expressed membrane BAFF, and non-infected mice at day 0 expressed slightly membrane BAFF and soluble BAFF was detected at day 1, 2, 4

and 7.These suggested that soluble BAFF (20kD) was cleaved from the membrane-bound (34kD) and released into the supernatant of cells where it has been measured by murine BAFF ELISA (Figure 4.17).

Human respiratory syncytial virus can re-infect asymptomatically throughout life without significant antigenic change, suggestive of incomplete or short-lived immunity. In contrast, re-infection by influenza A virus largely depends on antigenic change, suggestive of more complete immunity (Le Nouen *et al.* 2011).

It has been shown that neutralizing both BAFF and APRIL in Influenza infection reduced the percentage and total number of Ab-secreting cells, including virus-specific Ab-secreting cells, in lungs and bone marrow (BM) and were associated with a significant reduction in the antiviral serum IgG, as well as virus-specific IgG and IgA in the BAL and targeting BAFF alone did not affect antiviral antibody production, which suggested that APRIL and but not BAFF alone, regulates ASC survival in response to influenza virus infection (Wolf *et al.* 2011).

It could be possible that APRIL may be induced at later time points after RSV infection such as day 14, 25 and 35 day. To further understand this process behind this mechanism of antibody regulation it may be possible to block APRIL alone and see if the survival of B cells will be affected since the study above targeted BAFF and APRIL or BAFF alone, but not APRIL alone. Thus, it could be possible that influenza infection induces APRIL expression and therefore increased survival of long lived plasma cells since APRIL binds with BCMA expressed on the plasma cells (O'Connor *et al.* 2004), whereas RSV does not induce APRIL and for this reason no strong adaptive immune response has been made for the RSV, which then is allowing re-infection again.

Furthermore, to evaluate the potential role of the airway epithelium in supporting the adaptive immune response through recruitment of B and T cells, homeostatic chemokines CXCL12, CXCL13, CCL19 and CCL21 (chapter 1, section 1.4) were investigated both *in vitro* and *in vivo*. It has been shown that expression of homeostatic chemokines can be induced in non-lymphoid tissue such as lung upon viral infection such as influenza and to be involved in formation of iBALT, where its formation is essential for initiating local B and T cells responses to influenza (Rangel-Moreno *et al.* 2007).

In vitro there was no expression of these chemokines in RSV infected of BEAS-2B cells. However, in animal model only CXCL13 mRNA and protein expression were increased significantly after RSV infection, not CXCL12, CCL19 or CCL21. This indicates that airway epithelium is not the main source of these chemokine and there could be other potential sources.

CXCL12, CCL19 and CCL21 did not increase in expression following RSV infection relative to UV RSV control. Whist it is possible that an active form is released perhaps from stored cytokines, this could indicate that these were not active in the recruitment of lymphocytes during RSV infection and could be active in other viral infections such as influenza infection, which has been reported to induce increased expression of CXCL12, CCL19 and CCL21 that resulted in induced effective immune response (Moyron-Quiroz *et al.* 2004). To fully understand their role in RSV infection, we should do further studies to determine if the CCL19 or CCL21 are released from intracellular stores during infection and are active in the recruitment of lymphocytes. Considered together, these findings suggest that RSV infection may not fully recruit T cells during infection. However, it could be possible that these chemokines may be induced at later time points after RSV infection, such as day 14, 25 and 35 day.

CXCL13 is known to act as B lymphocyte chemoattractant (Gunn *et al.* 1998) and to determine if B cells were recruited into mouse lungs following RSV infection, mouse lung sections were stained with the B cell specific marker anti-CD20.

Control mice day 0 (Figure 5.42) showed positive staining of B cells which accumulated in aggregates and this could be possible if those mice were exposed to some pathogens before use in this study. In addition, mouse lung sections showed strong positive staining of B cells relative to UV RSV control in days 1, 2, 4, 7 and 8. In addition, B cell numbers were also increased significantly after RSV infection at day 6 and 8 relative to UV RSV control at the same time points (Figure 5.53). This indicates and clearly demonstrates that increased B cell number in the airway at least up to day 8 is a feature of this model of RSV infection.

Taken together, increased expression of the CXCL13 protein is associated with the presence and increased number of B-cell aggregates at day, 1 day 2 and day 7 after RSV infection relative to the UV RSV control at the same time points, which suggest

that CXCL13 could recruit B cells into the lung. To test this, we could then target CXCL13 before RSV infection and examine how many B cells are in the lung and also determine certain features of these B cells. Furthermore, from chapter 4 (Figure 4.17) BAFF protein levels were also increased significantly at these time points. Considering the findings together, this raises the possibility that CXCL13 may be directly responsible for B cell recruitment into the lung and the possible role of the local BAFF produced by epithelium in promoting airway B cell differentiation.

6.2. Proposed model of airway immune response to RSV

Based on the work described in this thesis using both the BEAS2B cell line and animal model, the following model of how the immune response of the airway epithelium to RSV infection may influence the adaptive immunity to RSV and possibly other viral infections (Figure 6.1) has been described.

Firstly, RSV is recognized by the epithelial cells either by TLR4 or TLR3 (Kurt-Jones *et al.* 2000; Rudd *et al.* 2006); this triggers the antiviral response, including IFN-β. In turn this induces cleavage of soluble BAFF from the membrane bound form expressed on the epithelial cell surface. This is supported by my observation that neutralizing IFN-β resulted in reduced BAFF expression by infected BEAS2B cells, which indicates that BAFF production in BEAS-2B cells through RSV infection is IFN-β dependent (Chapter 3), fact also confirmed by the results of western blot analysis shown in Chapters 3 and 4 looking at the molecular weight of BAFF present. Consistent with *in vitro* experiments, the BAFF mRNA and protein were also significantly increased after RSV infection in *in vivo* (chapter 4), but it remains to be shown that BAFF induction is interferon dependent *in vivo*.

This model proposes that at least one activity of BAFF in the airway is to support B cell survival and that B cells are both present and increased in number in the lung during RSV infection, as shown in chapter 4 and 5.

The stimulus for B cell recruitment was suggested to be homeostatic chemokines such as CXCL12, CXCL13, CCL19 and CCL21. BEAS-2B cells infected with RSV did not express CXCL12, CXCL13, CCL19 and CCL21, which suggested that there are other potential sources rather than airway epithelium that express these chemokines during RSV infection *in vivo*.

From the animal model, only CXCL13 increased significantly after RSV infection at day 1, 2 and 7, whereas CXCL12, CCL19 and CCL21 did not increase after RSV infection. It is possible that these chemokines are not active in RSV infection but have been shown to be active in other viral infection such as influenza (Rangel-Moreno *et al.* 2007).

CXCL13 is known to act as a B cell chemoattractant. The examination of the mouse lung sections showed strong positive staining of B cells that appeared accumulated in aggregates at later time points.

Taken together, these findings suggest that CXCL13 may be directly responsible for B cells recruitment into the lung and the possible role of local BAFF expression in promoting airway B cell differentiation and survival. Although these suggestions must be further confirmed experimentally, from the experiment carried out in chapter three BAFF derived from RSV infected BEAS-2B cells increased B cell survival (Figure 3.14).

Moreover, I would expect to observe proper and organised iBALT structure localized in the lung following RSV infection and specific B and T cells areas and associated follicular dendritic cells. However, only CXCL13 was increased and detected in mouse lung sections following RSV infection relative to UV RSV control. Examination of later time points might show if fully organised iBALT is formed in response to RSV infection or if the lack of increased expression of CXCL12, CCL19 and CCL21 at least at these early time points does not facilitate formation of typical iBALT. The outcome of iBALT formation is production of specific antibodies as it occurs in the response to influenza (Moyron-Quiroz *et al.* 2004).

In contrast to influenza, immunity to RSV is not long lasting. This could be as a result of incomplete formation of iBALT or insufficient signals from APRIL that could mediate long lived B cell responses through engagement with BCMA expressed on the cell surface of plasma cells.

To test these possibilities fully, extending the time points analysed would be useful and to determine if APRIL or CXCL12, CCL19 and CCL21 can be subsequently increased. BAFF expression is a common feature in respiratory infection and not

specific for RSV (McNamara *et al.* 2013) and it is likely that the response suggested here to RSV is equally likely against other respiratory pathogens.

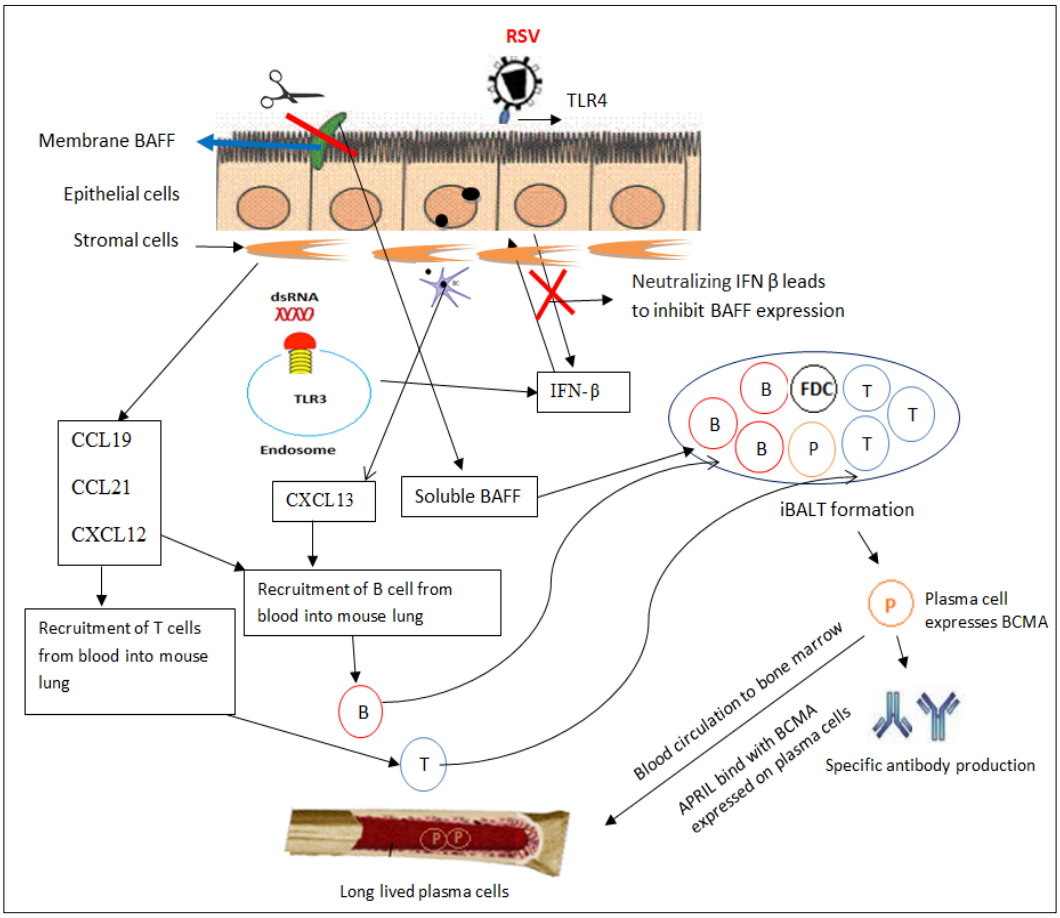

Figure 6.1. Proposed model of airway epithelium immune response to RSV infection

Resting epithelial cells express membrane BAFF. RSV is recognized by TLR 4 expressed at the cell surface of airway epithelial cells or intracellular TLR3 and the outcome of this interaction leads to induced antiviral response, such as IFN-β, that induces soluble BAFF expression after cleaved from the cells surface. Local soluble BAFF increased B cell survival and differentiation. DCs are the main source of CXCL13 that can recruit B cells from the peripheral blood into the lung. Stroma cells may also express other chemokines such as CCL19, CXCL12 and CCL21 that recruit T-cells or B cells from the peripheral blood into the lung. The iBALT formation is dependent on the complex interactions between a number of cell types including activated DCs and stromal cells through the release of these chemokines, where B and T cells are recruited to the site and often organized into distinct zones where the specific antibody is produced. Interaction of APRIL with plasma cells express BCMA may increase their long lived survival in the bone marrow.

6.3. Future directions

Building on previous findings the results also suggest a number of further avenues for investigation. In Chapter 3 it was demonstrated that RSV infected epithelia cell supernatants which contain BAFF support B cell survival. Further work is required to investigate whether that was mediated by BAFF or not by neutralizing BAFF or blocking its receptors, including BAFF-R, TACI and BCMA.

From Chapter 4, the animal model of human RSV infection, the BAFF protein increased significantly after RSV infection and there were two peaks of BAFF response, at day 2 and 7. From *in vitro* experiments, BAFF production after RSV infection is IFN-β dependent. Thus, to determine if this is also IFN-β mediated at day 2 or 7 in mice following RSV infection, further work is required either through neutralizing IFN-β prior to RSV infection and to measure IFN-β mRNA by RT-CR or protein by ELISA.

In addition, to investigate the role of BAFF in supporting B cells differentiation in mouse lungs, we could then inhibit BAFF during RSV infection and determine the B cells response. Furthermore, from Chapter 5 it was shown that CXCL13, which is known to act as B cell chemoattractant, was the only lymphoid chemokine that increased significantly following RSV infection of mice. Further work is required to evaluate if CXCL13 was responsible in recruiting B cells from the peripheral blood into the mouse lung, then we could target CXCL13 before RSV infection and examine how many B cells are in the lung. Moreover, extending the time points of RSV infection in mice more than 8 days would also be useful to achieve better understanding about kinetics of BAFF and APRIL in addition to CXCL12, CXCL13, CCL19 and CCL21 that may be increased at later time points after RSV infection.

REFERENCES

Agency HP. Laboratory reports received by HPA Colindale of infections due to respiratory syncytial virus, England and Wales (2013) [Online], Available from: http://www.hpa.org.uk/webc/HPAwebFile/HPAweb_C/1194947411794 (Accessed: 06.08.2013).

Aherne, W., Bird, T., Court, S.D.M., Gardner, P.S. & McQuillin, J. (1970) 'Pathological changes in virus infections of the lower respiratory tract in children', *Journal of Clinical Pathology*, vol. 23, no. 1, pp. 7-18.

Aloisi, F. & Pujol-Borrell, R. (2006) 'Lymphoid neogenesis in chronic inflammatory diseases', *Nat Rev Immunol*, vol. 6, no. 3, pp. 205-217.

Amanna, I.J., Clise-Dwyer, K., Nashold, F.E., Hoag, K.A. & Hayes, C.E. (2001) 'Cutting Edge: A/WySnJ Transitional B Cells Overexpress the Chromosome 15 Proapoptotic Blk Gene and Succumb to Premature Apoptosis', *The Journal of Immunology*, vol. 167, no. 11, pp. 6069-6072.

Anderson, L.J., Hierholzer, J.C., Tsou, C., Hendry, R.M., Fernie, B.F., Stone, Y. & McIntosh, K. (1985) 'Antigenic Characterization of Respiratory Syncytial Virus Strains with Monoclonal Antibodies', *Journal of Infectious Diseases*, vol. 151, no. 4, pp. 626-633.

Ansel, K.M., McHeyzer-Williams, L.J., Ngo, V.N., McHeyzer-Williams, M.G. & Cyster, J.G. (1999) 'In Vivo–Activated Cd4 T Cells Upregulate Cxc Chemokine Receptor 5 and Reprogram Their Response to Lymphoid Chemokines', *The Journal of Experimental Medicine*, vol. 190, no. 8, pp. 1123-1134.

Bals, R. & Hiemstra, P.S. (2004) 'Innate immunity in the lung: how epithelial cells fight against respiratory pathogens', *European Respiratory Journal*, vol. 23, no. 2, pp. 327-333.

Becker, S., Quay, J. & Soukup, J. (1991) 'Cytokine (tumor necrosis factor, IL-6, and IL-8) production by respiratory syncytial virus-infected human alveolar macrophages', *The Journal of Immunology*, vol. 147, no. 12, pp. 4307-4312.

Becker, S. & Soukup, J.M. (1999) 'Airway Epithelial Cell-Induced Activation of Monocytes and Eosinophils in Respiratory Syncytial Viral Infection', *Immunobiology*, vol. 201, no. 1, pp. 88-106.

Bleul, C.C., Fuhlbrigge, R.C., Casasnovas, J.M., Aiuti, A. & Springer, T.A. (1996) 'A highly efficacious lymphocyte chemoattractant, stromal cell-derived factor 1 (SDF-1)', *J Exp Med*, vol. 184, no. 3, pp. 1101-1109.

Blount, R.E., Jr., Morris, J.A. & Savage, R.E. (1956) 'Recovery of cytopathogenic agent from chimpanzees with coryza', *Proc Soc Exp Biol Med*, vol. 92, no. 3, pp. 544-549.

Bojarska-Junak, A., Hus, I., Chocholska, S., Wąsik-Szczepanek, E., Sieklucka, M., Dmoszyńska, A. & Roliński, J. (2009) 'BAFF and APRIL expression in B-cell chronic lymphocytic leukemia: Correlation with biological and clinical features', *Leukemia Research*, vol. 33, no. 10, pp. 1319-1327.

Borchers, A., Chang, C., Gershwin, M.E. & Gershwin, L. (2013) 'Respiratory Syncytial Virus—A Comprehensive Review', *Clinical Reviews in Allergy & Immunology*, vol. 45, no. 3, pp. 331-379.

Bossen, C. & Schneider, P. (2006) 'BAFF, APRIL and their receptors: Structure, function and signaling', *Seminars in Immunology*, vol. 18, no. 5, pp. 263-275.

Brandenburg, A.H., Groen, J., van Steensel-Moll, H.A., Claas, E.C., Rothbarth, P.H., Neijens, H.J. & Osterhaus, A.D. (1997) 'Respiratory syncytial virus specific serum antibodies in infants under six months of age: limited serological response upon infection', *J Med Virol*, vol. 52, no. 1, pp. 97-104.

Brandenburg, A.H., Kleinjan, A., van het Land, B., Moll, H.A., Timmerman, H.H., de Swart, R.L., Neijens, H.J., Fokkens, W. & Osterhaus, A.D.M.E. (2000) 'Type 1-like immune response is found in children with respiratory syncytial virus infection regardless of clinical severity', *Journal of Medical Virology*, vol. 62, no. 2, pp. 267-277.

Bricks, L.F. (2001) 'Prevention of respiratory syncytial virus infections', *Revista do Hospital das Clínicas*, vol. 56, pp. 79-90.

Brühl, H., Mack, M., Niedermeier, M., Lochbaum, D., Schölmerich, J. & Straub, R.H. (2008) 'Functional expression of the chemokine receptor CCR7 on fibroblast-like synoviocytes', *Rheumatology*, vol. 47, no. 12, pp. 1771-1774.

Cardenas, S., Auais, A. & Piedimonte, G. (2005) 'Palivizumab in the prophylaxis of respiratory syncytial virus infection', *Expert Review of Anti-infective Therapy*, vol. 3, no. 5, pp. 719-726.

Castigli, E., Scott, S., Dedeoglu, F., Bryce, P., Jabara, H., Bhan, A.K., Mizoguchi, E. & Geha, R.S. (2004) 'Impaired IgA class switching in APRIL-deficient mice', *Proc Natl Acad Sci U S A*, vol. 101, no. 11, pp. 3903-3908.

Castigli, E., Wilson, S.A., Garibyan, L., Rachid, R., Bonilla, F., Schneider, L. & Geha, R.S. (2005a) 'TACI is mutant in common variable immunodeficiency and IgA deficiency', *Nat Genet*, vol. 37, no. 8, pp. 829-834.

Castigli, E., Wilson, S.A., Scott, S., Dedeoglu, F., Xu, S., Lam, K.-P., Bram, R.J., Jabara, H. & Geha, R.S. (2005b) 'TACI and BAFF-R mediate isotype switching in B cells', *The Journal of Experimental Medicine*, vol. 201, no. 1, pp. 35-39.

Chang, J. & Braciale, T.J. (2002) 'Respiratory syncytial virus infection suppresses lung CD8+ T-cell effector activity and peripheral CD8+ T-cell memory in the respiratory tract', *Nat Med*, vol. 8, no. 1, pp. 54-60.

Chanock, R., Roizman, B. & Myers, R. (1957) 'Recovery from infants with respiratory illness of a virus related to chimpanzee coryza agent (CCA): Isolation, properties and characterization', *American Journal of Epidemiology*, vol. 66, no. 3, pp. 281-290.

Chaudhuri, J. & Alt, F.W. (2004) 'Class-switch recombination: interplay of transcription, DNA deamination and DNA repair', *Nat Rev Immunol*, vol. 4, no. 7, pp. 541-552.

Collins, P.L. & Graham, B.S. (2008) 'Viral and Host Factors in Human Respiratory Syncytial Virus Pathogenesis', *J Virol*, vol. 82, no. 5, pp. 2040-2055.

Cols, M., Barra, C.M., He, B., Puga, I., Xu, W., Chiu, A., Tam, W., Knowles, D.M., Dillon, S.R., Leonard, J.P., Furman, R.R., Chen, K. & Cerutti, A. (2012) 'Stromal Endothelial Cells Establish a Bidirectional Crosstalk with Chronic Lymphocytic Leukemia Cells through the TNF-Related Factors BAFF, APRIL, and CD40L', *J Immunol*, vol. 188, no. 12, pp. 6071-6083.

Connors, M., Giese, N.A., Kulkarni, A.B., Firestone, C.Y., Morse, H.C. & Murphy, B.R. (1994) 'Enhanced pulmonary histopathology induced by respiratory syncytial virus (RSV) challenge of formalin-inactivated RSV-immunized BALB/c mice is abrogated by depletion of interleukin-4 (IL-4) and IL-10', *Journal of Virology*, vol. 68, no. 8, pp. 5321-5325.

Craxton, A., Draves, K.E., Gruppi, A. & Clark, E.A. (2005) 'BAFF regulates B cell survival by downregulating the BH3-only family member Bim via the ERK

pathway', *The Journal of Experimental Medicine*, vol. 202, no. 10, pp. 1363-1374.

Cyster, J.G. (1999) 'Chemokines and Cell Migration in Secondary Lymphoid Organs', *Science*, vol. 286, no. 5447, pp. 2098-2102.

Dall'Era, M. & Wofsy, D. (2010) 'Connective tissue diseases: Belimumab for systemic lupus erythematosus: breaking through?', *Nat Rev Rheumatol*, vol. 6, no. 3, pp. 124-125.

Dalrymple, N.A. & Mackow, E.R. (2012) 'Endothelial cells elicit immune-enhancing responses to dengue virus infection', *J Virol*, vol. 86, no. 12, pp. 6408-6415.

Daridon, C., Devauchelle, V., Hutin, P., Le Berre, R., Martins-Carvalho, C., Bendaoud, B., Dueymes, M., Saraux, A., Youinou, P. & Pers, J.O. (2007) 'Aberrant expression of BAFF by B lymphocytes infiltrating the salivary glands of patients with primary Sjogren's syndrome', *Arthritis and rheumatism*, vol. 56, no. 4, pp. 1134-1144.

Daridon, C., Youinou, P. & Pers, J.O. (2008) 'BAFF, APRIL, TWE-PRIL: who's who?', *Autoimmun Rev*, vol. 7, no. 4, pp. 267-271.

DeVincenzo, J.P., Wilkinson, T., Vaishnaw, A., Cehelsky, J., Meyers, R., Nochur, S., Harrison, L., Meeking, P., Mann, A., Moane, E., Oxford, J., Pareek, R., Moore, R., Walsh, E., Studholme, R., Dorsett, P., Alvarez, R. & Lambkin-Williams, R. (2010) 'Viral Load Drives Disease in Humans Experimentally Infected with Respiratory Syncytial Virus', *American Journal of Respiratory and Critical Care Medicine*, vol. 182, no. 10, pp. 1305-1314.

Dewhurst-Maridor, G., Simonet, V., Bornand, J.E., Nicod, L.P. & Pache, J.C. (2004) 'Development of a quantitative TaqMan RT-PCR for respiratory syncytial virus', *Journal of Virological Methods*, vol. 120, no. 1, pp. 41-49.

Dillon, S.R., Gross, J.A., Ansell, S.M. & Novak, A.J. (2006) 'An APRIL to remember: novel TNF ligands as therapeutic targets', *Nat Rev Drug Discov*, vol. 5, no. 3, pp. 235-246.

Do, R.K.G., Hatada, E., Lee, H., Tourigny, M.R., Hilbert, D. & Chen-Kiang, S. (2000) 'Attenuation of Apoptosis Underlies B Lymphocyte Stimulator Enhancement of Humoral Immune Response', *The Journal of Experimental Medicine*, vol. 192, no. 7, pp. 953-964.

Domachowske, J.B. & Rosenberg, H.F. (1999) 'Respiratory Syncytial Virus Infection: Immune Response, Immunopathogenesis, and Treatment', *Clinical Microbiology Reviews*, vol. 12, no. 2, pp. 298-309.

Ebisuno, Y., Tanaka, T., Kanemitsu, N., Kanda, H., Yamaguchi, K., Kaisho, T., Akira, S. & Miyasaka, M. (2003) 'Cutting Edge: The B Cell Chemokine CXC Chemokine Ligand 13/B Lymphocyte Chemoattractant Is Expressed in the High Endothelial Venules of Lymph Nodes and Peyer's Patches and Affects B Cell Trafficking Across High Endothelial Venules', *The Journal of Immunology*, vol. 171, no. 4, pp. 1642-1646.

Electron micrograph of respiratory syncytial virus (RSV) virion at a cell membrane (2014) [Online], Available from: http://www.wadsworth.org/divisions/infdis/virology/rsv.htm (Accessed: 14 /04).

Everard, M.L., Swarbrick, A., Wrightham, M., McIntyre, J., Dunkley, C., James, P.D., Sewell, H.F. & Milner, A.D. (1994) 'Analysis of cells obtained by bronchial lavage of infants with respiratory syncytial virus infection', *Archives of Disease in Childhood*, vol. 71, no. 5, pp. 428-432.

Falsey, A.R., Hennessey, P.A., Formica, M.A., Cox, C. & Walsh, E.E. (2005) 'Respiratory Syncytial Virus Infection in Elderly and High-Risk Adults', *New England Journal of Medicine*, vol. 352, no. 17, pp. 1749-1759.

Falsey, A.R., Singh, H.K. & Walsh, E.E. (2006) 'Serum antibody decay in adults following natural respiratory syncytial virus infection', *Journal of Medical Virology*, vol. 78, no. 11, pp. 1493-1497.

Falsey, A.R. & Walsh, E.E. (1998) 'Relationship of serum antibody to risk of respiratory syncytial virus infection in elderly adults', *J Infect Dis*, vol. 177, no. 2, pp. 463-466.

Falsey, A.R. & Walsh, E.E. (2005) 'Respiratory syncytial virus infection in elderly adults', *Drugs Aging*, vol. 22, no. 7, pp. 577-587.

Fearns, R. & Collins, P.L. (1999) 'Model for polymerase access to the overlapped L gene of respiratory syncytial virus', *J Virol*, vol. 73, no. 1, pp. 388-397.

Fernandez, E.J. & Lolis, E. (2002) 'Structure, function, and inhibition of chemokines', *Annu Rev Pharmacol Toxicol*, vol. 42, pp. 469-499.

Fiedler, M.A., Wernke-Dollries, K. & Stark, J.M. (1995) 'Respiratory syncytial virus increases IL-8 gene expression and protein release in A549 cells', *Am J Physiol*, vol. 269, no. 6 Pt 1, pp. L865-872.

Fishaut, M., Tubergen, D. & McIntosh, K. (1980) 'Cellular response to respiratory viruses with particular reference to children with disorders of cell-mediated immunity', *The Journal of Pediatrics*, vol. 96, no. 2, pp. 179-186.

Fleige, H., Ravens, S., Moschovakis, G.L., Bölter, J., Willenzon, S., Sutter, G., Häussler, S., Kalinke, U., Prinz, I. & Förster, R. (2014) 'IL-17–induced CXCL12 recruits B cells and induces follicle formation in BALT in the absence of differentiated FDCs', *The Journal of Experimental Medicine*, vol. 211, no. 4, pp. 643-651.

Fonceca, A.M., Flanagan, B.F., Trinick, R., Smyth, R.L. & McNamara, P.S. (2012) 'Primary airway epithelial cultures from children are highly permissive to respiratory syncytial virus infection', *Thorax*, vol. 67, no. 1, pp. 42-48.

Foo, S.Y. & Phipps, S. (2010) 'Regulation of inducible BALT formation and contribution to immunity and pathology', *Mucosal Immunol*, vol. 3, no. 6, pp. 537-544.

Forster, R., Emrich, T., Kremmer, E. & Lipp, M. (1994) 'Expression of the G-protein--coupled receptor BLR1 defines mature, recirculating B cells and a subset of T-helper memory cells', *Blood*, vol. 84, no. 3, pp. 830-840.

Fulton, R.B., Meyerholz, D.K. & Varga, S.M. (2010) 'Foxp3+ CD4 Regulatory T Cells Limit Pulmonary Immunopathology by Modulating the CD8 T Cell Response during Respiratory Syncytial Virus Infection', *The Journal of Immunology*, vol. 185, no. 4, pp. 2382-2392.

Garofalo, R.P., Patti, J., Hintz, K.A., Hill, V., Ogra, P.L. & Welliver, R.C. (2001) 'Macrophage Inflammatory Protein-1α (Not T Helper Type 2 Cytokines) Is Associated with Severe Forms of Respiratory Syncytial Virus Bronchiolitis', *Journal of Infectious Diseases*, vol. 184, no. 4, pp. 393-399.

Gavin, A.L., Duong, B., Skog, P., Aït-Azzouzene, D., Greaves, D.R., Scott, M.L. & Nemazee, D. (2005) 'ΔBAFF, a Splice Isoform of BAFF, Opposes Full-Length BAFF Activity In Vivo in Transgenic Mouse Models', *The Journal of Immunology*, vol. 175, no. 1, pp. 319-328.

Ghildyal, R., Hartley, C., Varrasso, A., Meanger, J., Voelker, D.R., Anders, E.M. & Mills, J. (1999) 'Surfactant Protein A Binds to the Fusion Glycoprotein of

Respiratory Syncytial Virus and Neutralizes Virion Infectivity', *Journal of Infectious Diseases*, vol. 180, no. 6, pp. 2009-2013.

Glezen, W.P., Taber, L.H., Frank, A.L. & Kasel, J.A. (1986) 'Risk of primary infection and reinfection with respiratory syncytial virus', *Am J Dis Child*, vol. 140, no. 6, pp. 543-546.

Gonzalez-Reyes, L., Ruiz-Arguello, M.B., Garcia-Barreno, B., Calder, L., Lopez, J.A., Albar, J.P., Skehel, J.J., Wiley, D.C. & Melero, J.A. (2001) 'Cleavage of the human respiratory syncytial virus fusion protein at two distinct sites is required for activation of membrane fusion', *Proc Natl Acad Sci U S A*, vol. 98, no. 17, pp. 9859-9864.

González, P.A., Prado, C.E., Leiva, E.D., Carreño, L.J., Bueno, S.M., Riedel, C.A. & Kalergis, A.M. (2008) 'Respiratory syncytial virus impairs T cell activation by preventing synapse assembly with dendritic cells', *Proceedings of the National Academy of Sciences*, vol. 105, no. 39, pp. 14999-15004.

Graham, B.S., Bunton, L.A., Rowland, J., Wright, P.F. & Karzon, D.T. (1991a) 'Respiratory syncytial virus infection in anti-mu-treated mice', *Journal of Virology*, vol. 65, no. 9, pp. 4936-4942.

Graham, B.S., Bunton, L.A., Wright, P.F. & Karzon, D.T. (1991b) 'Role of T lymphocyte subsets in the pathogenesis of primary infection and rechallenge with respiratory syncytial virus in mice', *J Clin Invest*, vol. 88, no. 3, pp. 1026-1033.

Groothuis, J., Hoopes, J.M. & Jessie, V.H. (2011) 'Prevention of serious respiratory syncytial virus-related illness. I: Disease pathogenesis and early attempts at prevention', *Advances in Therapy*, vol. 28, no. 2, pp. 91-109.

Gross, J.A., Johnston, J., Mudri, S., Enselman, R., Dillon, S.R., Madden, K., Xu, W., Parrish-Novak, J., Foster, D., Lofton-Day, C., Moore, M., Littau, A., Grossman, A., Haugen, H., Foley, K., Blumberg, H., Harrison, K., Kindsvogel, W. & Clegg, C.H. (2000) 'TACI and BCMA are receptors for a TNF homologue implicated in B-cell autoimmune disease', *Nature*, vol. 404, no. 6781, pp. 995-999.

Guillot, L., Le Goffic, R., Bloch, S., Escriou, N., Akira, S., Chignard, M. & Si-Tahar, M. (2005) 'Involvement of Toll-like Receptor 3 in the Immune Response of Lung Epithelial Cells to Double-stranded RNA and Influenza A Virus', *Journal of Biological Chemistry*, vol. 280, no. 7, pp. 5571-5580.

Gunn, M.D., Kyuwa, S., Tam, C., Kakiuchi, T., Matsuzawa, A., Williams, L.T. & Nakano, H. (1999) 'Mice Lacking Expression of Secondary Lymphoid Organ Chemokine Have Defects in Lymphocyte Homing and Dendritic Cell Localization', *The Journal of Experimental Medicine*, vol. 189, no. 3, pp. 451-460.

Gunn, M.D., Ngo, V.N., Ansel, K.M., Ekland, E.H., Cyster, J.G. & Williams, L.T. (1998) 'A B-cell-homing chemokine made in lymphoid follicles activates Burkitt's lymphoma receptor-1', *Nature*, vol. 391, no. 6669, pp. 799-803.

Hacking, D. & Hull, J. (2002) 'Respiratory Syncytial Virus—Viral Biology and the Host Response', *Journal of Infection*, vol. 45, no. 1, pp. 18-24.

Haeberle, H.A., Kuziel, W.A., Dieterich, H.-J., Casola, A., Gatalica, Z. & Garofalo, R.P. (2001) 'Inducible Expression of Inflammatory Chemokines in Respiratory Syncytial Virus-Infected Mice: Role of MIP-1α in Lung Pathology', *Journal of Virology*, vol. 75, no. 2, pp. 878-890.

Hahne, M., Kataoka, T., Schröter, M., Hofmann, K., Irmler, M., Bodmer, J.-L., Schneider, P., Bornand, T., Holler, N., French, L.E., Sordat, B., Rimoldi, D. & Tschopp, J. (1998) 'APRIL, a New Ligand of the Tumor Necrosis Factor Family, Stimulates Tumor Cell Growth', *The Journal of Experimental Medicine*, vol. 188, no. 6, pp. 1185-1190.

Haiat, S., Billard, C., Quiney, C., Ajchenbaum-Cymbalista, F. & Kolb, J.-P. (2006) 'Role of BAFF and APRIL in human B-cell chronic lymphocytic leukaemia', *Immunology*, vol. 118, no. 3, pp. 281-292.

Hall, C.B. (2001) 'Respiratory Syncytial Virus and Parainfluenza Virus', *New England Journal of Medicine*, vol. 344, no. 25, pp. 1917-1928.

Hall, C.B., Weinberg, G.A., Iwane, M.K., Blumkin, A.K., Edwards, K.M., Staat, M.A., Auinger, P., Griffin, M.R., Poehling, K.A., Erdman, D., Grijalva, C.G., Zhu, Y. & Szilagyi, P. (2009) 'The Burden of Respiratory Syncytial Virus Infection in Young Children', *New England Journal of Medicine*, vol. 360, no. 6, pp. 588-598.

Harcourt, J., Alvarez, R., Jones, L.P., Henderson, C., Anderson, L.J. & Tripp, R.A. (2006) 'Respiratory Syncytial Virus G Protein and G Protein CX3C Motif Adversely Affect CX3CR1+ T Cell Responses', *The Journal of Immunology*, vol. 176, no. 3, pp. 1600-1608.

Harrison, A.M., Bonville, C.A., Rosenberg, H.F. & Domachowske, J.B. (1999) 'Respiratory Syncytical Virus–induced Chemokine Expression in the Lower Airways', *American Journal of Respiratory and Critical Care Medicine*, vol. 159, no. 6, pp. 1918-1924.

He, B., Raab-Traub, N., Casali, P. & Cerutti, A. (2003) 'EBV-encoded latent membrane protein 1 cooperates with BAFF/BLyS and APRIL to induce T cell-independent Ig heavy chain class switching', *J Immunol*, vol. 171, no. 10, pp. 5215-5224.

Heidema, J., Lukens, M.V., van Maren, W.W.C., van Dijk, M.E.A., Otten, H.G., van Vught, A.J., van der Werff, D.B.M., van Gestel, S.J.P., Semple, M.G., Smyth, R.L., Kimpen, J.L.L. & van Bleek, G.M. (2007) 'CD8+ T Cell Responses in Bronchoalveolar Lavage Fluid and Peripheral Blood Mononuclear Cells of Infants with Severe Primary Respiratory Syncytial Virus Infections', *The Journal of Immunology*, vol. 179, no. 12, pp. 8410-8417.

Hickling, T.P., Bright, H., Wing, K., Gower, D., Martin, S.L., Sim, R.B. & Malhotra, R. (1999) 'A recombinant trimeric surfactant protein D carbohydrate recognition domain inhibits respiratory syncytial virus infection in vitro and in vivo', *Eur J Immunol*, vol. 29, no. 11, pp. 3478-3484.

Hickling, T.P., Malhotra, R., Bright, H., McDowell, W., Blair, E.D. & Sim, R.B. (2000) 'Lung surfactant protein A provides a route of entry for respiratory syncytial virus into host cells', *Viral Immunol*, vol. 13, no. 1, pp. 125-135.

Hsu, B.L., Harless, S.M., Lindsley, R.C., Hilbert, D.M. & Cancro, M.P. (2002) 'Cutting Edge: BLyS Enables Survival of Transitional and Mature B Cells Through Distinct Mediators', *The Journal of Immunology*, vol. 168, no. 12, pp. 5993-5996.

Huard, B., Arlettaz, L., Ambrose, C., Kindler, V., Mauri, D., Roosnek, E., Tschopp, J., Schneider, P. & French, L.E. (2004) 'BAFF production by antigen-presenting cells provides T cell co-stimulation', *Int Immunol*, vol. 16, no. 3, pp. 467-475.

Huard, B., McKee, T., Bosshard, C., Durual, S., xE, phane, Matthes, T., Myit, S., Donze, O., Frossard, C., Chizzolini, C., Favre, C., Zubler, R., Guyot, J.P., Schneider, P. & Roosnek, E. (2008) 'APRIL secreted by neutrophils binds to

heparan sulfate proteoglycans to create plasma cell niches in human mucosa', *The Journal of Clinical Investigation*, vol. 118, no. 8, pp. 2887-2895.

Huard, B., Schneider, P., Mauri, D., Tschopp, J. & French, L.E. (2001) 'T Cell Costimulation by the TNF Ligand BAFF', *The Journal of Immunology*, vol. 167, no. 11, pp. 6225-6231.

Huard, B., Tran, N.L., Benkhoucha, M., Manzin-Lorenzi, C. & Santiago-Raber, M.L. (2012) 'Selective APRIL blockade delays systemic lupus erythematosus in mouse', *PLoS One*, vol. 7, no. 2, p. e31837.

Hunt, D., Huppertz, H., Jiang, H. & Petty, R. (1994) 'Studies of human cord blood dendritic cells: evidence for functional immaturity', *Blood*, vol. 84, no. 12, pp. 4333-4343.

Hymowitz, S.G., Patel, D.R., Wallweber, H.J.A., Runyon, S., Yan, M., Yin, J., Shriver, S.K., Gordon, N.C., Pan, B., Skelton, N.J., Kelley, R.F. & Starovasnik, M.A. (2005) 'Structures of APRIL-Receptor Complexes: like bcma, taci employs only a single cysteine-rich domain for high affinity ligand binding', *Journal of Biological Chemistry*, vol. 280, no. 8, pp. 7218-7227.

Ittah, M., Miceli-Richard, C., Gottenberg, J.-E., Sellam, J., Lepajolec, C. & Mariette, X. (2009) 'B-cell-activating factor expressions in salivary epithelial cells after dsRNA virus infection depends on RNA-activated protein kinase activation', *European Journal of Immunology*, vol. 39, no. 5, pp. 1271-1279.

Ittah, M., Miceli-Richard, C., Lebon, P., Pallier, C., Lepajolec, C. & Mariette, X. (2011) 'Induction of B cell-activating factor by viral infection is a general phenomenon, but the types of viruses and mechanisms depend on cell type', *J Innate Immun*, vol. 3, no. 2, pp. 200-207.

Ivashkiv, L.B. & Donlin, L.T. (2014) 'Regulation of type I interferon responses', *Nat Rev Immunol*, vol. 14, no. 1, pp. 36-49.

Janeway, C. (2001) *Immunobiology five*, Garland Pub.

Jaovisidha, P., Peeples, M.E., Brees, A.A., Carpenter, L.R. & Moy, J.N. (1999) 'Respiratory Syncytial Virus Stimulates Neutrophil Degranulation and Chemokine Release', *The Journal of Immunology*, vol. 163, no. 5, pp. 2816-2820.

Johnson, J.E., Gonzales, R.A., Olson, S.J., Wright, P.F. & Graham, B.S. (2006) 'The histopathology of fatal untreated human respiratory syncytial virus infection', *Mod Pathol*, vol. 20, no. 1, pp. 108-119.

Johnson, J.E., Gonzales, R.A., Olson, S.J., Wright, P.F. & Graham, B.S. (2007) 'The histopathology of fatal untreated human respiratory syncytial virus infection', *Mod Pathol*, vol. 20, no. 1, pp. 108-119.

Jorquera, P.A., Oakley, K.E. & Tripp, R.A. (2013) 'Advances in and the potential of vaccines for respiratory syncytial virus', *Expert Review of Respiratory Medicine*, vol. 7, no. 4, pp. 411-427.

Kallal, L.E., Hartigan, A.J., Hogaboam, C.M., Schaller, M.A. & Lukacs, N.W. (2010) 'Inefficient Lymph Node Sensitization during Respiratory Viral Infection Promotes IL-17–Mediated Lung Pathology', *The Journal of Immunology*, vol. 185, no. 7, pp. 4137-4147.

Kamphuis, T., Meijerhof, T., Stegmann, T., Lederhofer, J., Wilschut, J. & de Haan, A. (2012) 'Immunogenicity and protective capacity of a virosomal respiratory syncytial virus vaccine adjuvanted with monophosphoryl lipid A in mice', *PLoS One*, vol. 7, no. 5, p. e36812.

Kapikian, A.Z., Mitchell, R.H., Chanock, R.M., Shvedoff, R.A. & Stewart, C.E. (1969) 'An epidemiologic study of altered clinical reactivity to respiratory syncytial (RS) virus infection in children previously vaccinated with an inactivated RS virus vaccine', *Am J Epidemiol*, vol. 89, no. 4, pp. 405-421.

Kärre, K. (2002) 'NK Cells, MHC Class I Molecules and the Missing Self', *Scandinavian Journal of Immunology*, vol. 55, no. 3, pp. 221-228.

Kasel, J.A., Walsh, E.E., Frank, A.L., Baxter, B.D., Taber, L.H. & Glezen, W.P. (1987) 'Relation of serum antibody to glycoproteins of respiratory syncytial virus with immunity to infection in children', *Viral Immunol*, vol. 1, no. 3, pp. 199-205.

Kato, A., Hulse, K.E., Tan, B.K. & Schleimer, R.P. (2013) 'B-lymphocyte lineage cells and the respiratory system', *Journal of Allergy and Clinical Immunology*, vol. 131, no. 4, pp. 933-957.

Kato, A., Truong-Tran, A.Q., Scott, A.L., Matsumoto, K. & Schleimer, R.P. (2006) 'Airway Epithelial Cells Produce B Cell-Activating Factor of TNF Family by an IFN-β-Dependent Mechanism', *The Journal of Immunology*, vol. 177, no. 10, pp. 7164-7172.

Kato, A., Xiao, H., Chustz, R.T., Liu, M.C. & Schleimer, R.P. (2009) 'Local release of B cell–activating factor of the TNF family after segmental allergen

challenge of allergic subjects', *Journal of Allergy and Clinical Immunology*, vol. 123, no. 2, pp. 369-375.e362.

Katze, M.G., He, Y. & Gale, M. (2002) 'Viruses and interferon: a fight for supremacy', *Nat Rev Immunol*, vol. 2, no. 9, pp. 675-687.

Kelly, K., Manos, E., Jensen, G., Nadauld, L. & Jones, D.A. (2000) 'APRIL/TRDL-1, a tumor necrosis factor-like ligand, stimulates cell death', *Cancer Research*, vol. 60, no. 4, pp. 1021-1027.

Kern, C., Cornuel, J.F., Billard, C., Tang, R., Rouillard, D., Stenou, V., Defrance, T., Ajchenbaum-Cymbalista, F., Simonin, P.Y., Feldblum, S. & Kolb, J.P. (2004) 'Involvement of BAFF and APRIL in the resistance to apoptosis of B-CLL through an autocrine pathway', *Blood*, vol. 103, no. 2, pp. 679-688.

Kim, H.W., Canchola, J.G., Brandt, C.D., Pyles, G., Chanock, R.M., Jensen, K. & Parrott, R.H. (1969) 'Respiratory syncytial virus disease in infants despite prior administration of antigenic inactivated vaccine', *Am J Epidemiol*, vol. 89, no. 4, pp. 422-434.

Kim, T.H. & Lee, H.K. (2014) 'Innate immune recognition of respiratory syncytial virus infection', *BMB Rep*.

Klein, U. & Dalla-Favera, R. (2008) 'Germinal centres: role in B-cell physiology and malignancy', *Nat Rev Immunol*, vol. 8, no. 1, pp. 22-33.

Kolfschoten, G.M., Pradet-Balade, B., Hahne, M. & Medema, J.P. (2003) 'TWE-PRIL; a fusion protein of TWEAK and APRIL', *Biochemical Pharmacology*, vol. 66, no. 8, pp. 1427-1432.

Kotelkin, A., Belyakov, I.M., Yang, L., Berzofsky, J.A., Collins, P.L. & Bukreyev, A. (2006) 'The NS2 protein of human respiratory syncytial virus suppresses the cytotoxic T-cell response as a consequence of suppressing the type I interferon response', *J Virol*, vol. 80, no. 12, pp. 5958-5967.

Koyama, T., Tsukamoto, H., Miyagi, Y., Himeji, D., Otsuka, J., Miyagawa, H., Harada, M. & Horiuchi, T. (2005) 'Raised serum APRIL levels in patients with systemic lupus erythematosus', *Annals of the Rheumatic Diseases*, vol. 64, no. 7, pp. 1065-1067.

Kumar, H., Kawai, T. & Akira, S. (2009) 'Toll-like receptors and innate immunity', *Biochemical and Biophysical Research Communications*, vol. 388, no. 4, pp. 621-625.

Kurt-Jones, E.A., Popova, L., Kwinn, L., Haynes, L.M., Jones, L.P., Tripp, R.A., Walsh, E.E., Freeman, M.W., Golenbock, D.T., Anderson, L.J. & Finberg, R.W. (2000) 'Pattern recognition receptors TLR4 and CD14 mediate response to respiratory syncytial virus', *Nature Immunology*, vol. 1, no. 5, pp. 398-401.

Lahiri, A., Pochard, P., Le Pottier, L., Tobón, G.J., Bendaoud, B., Youinou, P. & Pers, J.-O. (2012) 'The complexity of the BAFF TNF-family members: Implications for autoimmunity', *J Autoimmun*, vol. 39, no. 3, pp. 189-198.

Lavie, F., Miceli-Richard, C., Ittah, M., Sellam, J., Gottenberg, J.E. & Mariette, X. (2008) 'B-cell Activating Factor of the Tumour Necrosis Factor Family Expression in Blood Monocytes and T Cells from Patients with Primary Sjögren's Syndrome', *Scandinavian Journal of Immunology*, vol. 67, no. 2, pp. 185-192.

Lavie, F., Miceli-Richard, C., Quillard, J., Roux, S., Leclerc, P. & Mariette, X. (2004) 'Expression of BAFF (BLyS) in T cells infiltrating labial salivary glands from patients with Sjögren's syndrome', *The Journal of Pathology*, vol. 202, no. 4, pp. 496-502.

Lay, M.K., González, P.A., León, M.A., Céspedes, P.F., Bueno, S.M., Riedel, C.A. & Kalergis, A.M. (2013) 'Advances in understanding respiratory syncytial virus infection in airway epithelial cells and consequential effects on the immune response', *Microbes and Infection*, vol. 15, no. 3, pp. 230-242.

Le Nouen, C., Hillyer, P., Winter, C.C., McCarty, T., Rabin, R.L., Collins, P.L. & Buchholz, U.J. (2011) 'Low CCR7-mediated migration of human monocyte derived dendritic cells in response to human respiratory syncytial virus and human metapneumovirus', *PLoS Pathog*, vol. 7, no. 6, p. e1002105.

Legg, J.P., Hussain, I.R., Warner, J.A., Johnston, S.L. & Warner, J.O. (2003) 'Type 1 and Type 2 Cytokine Imbalance in Acute Respiratory Syncytial Virus Bronchiolitis', *American Journal of Respiratory and Critical Care Medicine*, vol. 168, no. 6, pp. 633-639.

Lesley, R., Xu, Y., Kalled, S.L., Hess, D.M., Schwab, S.R., Shu, H.B. & Cyster, J.G. (2004) 'Reduced competitiveness of autoantigen-engaged B cells due to increased dependence on BAFF', *Immunity*, vol. 20, no. 4, pp. 441-453.

Levine, A.M. & Whitsett, J.A. (2001) 'Pulmonary collectins and innate host defense of the lung', *Microbes and Infection*, vol. 3, no. 2, pp. 161-166.

Li, F., Zhu, H., Sun, R., Wei, H. & Tian, Z. (2012) 'Natural Killer Cells Are Involved in Acute Lung Immune Injury Caused by Respiratory Syncytial Virus Infection', *Journal of Virology*, vol. 86, no. 4, pp. 2251-2258.

Li, Z., Xu, J., Patel, J., Fuentes, S., Lin, Y., Anderson, D., Sakamoto, K., Wang, L.-F. & He, B. (2011) 'Function of the Small Hydrophobic Protein of J Paramyxovirus', *Journal of Virology*, vol. 85, no. 1, pp. 32-42.

Lied, G.A. & Berstad, A. (2011) 'Functional and Clinical Aspects of the B-Cell-Activating Factor (BAFF): A Narrative Review', *Scandinavian Journal of Immunology*, vol. 73, no. 1, pp. 1-7.

Link, A., Vogt, T.K., Favre, S., Britschgi, M.R., Acha-Orbea, H., Hinz, B., Cyster, J.G. & Luther, S.A. (2007) 'Fibroblastic reticular cells in lymph nodes regulate the homeostasis of naive T cells', *Nat Immunol*, vol. 8, no. 11, pp. 1255-1265.

Litinskiy, M.B., Nardelli, B., Hilbert, D.M., He, B., Schaffer, A., Casali, P. & Cerutti, A. (2002) 'DCs induce CD40-independent immunoglobulin class switching through BLyS and APRIL', *Nat Immunol*, vol. 3, no. 9, pp. 822-829.

Liu, X.Q., Stacey, K.J., Horne-Debets, J.M., Cridland, J.A., Fischer, K., Narum, D., Mackay, F., Pierce, S.K. & Wykes, M.N. (2012) 'Malaria infection alters the expression of B-cell activating factor resulting in diminished memory antibody responses and survival', *Eur J Immunol*, vol. 42, no. 12, pp. 3291-3301.

Liu, Y., Xu, L., Opalka, N., Kappler, J., Shu, H.-B. & Zhang, G. (2002) 'Crystal Structure of sTALL-1 Reveals a Virus-like Assembly of TNF Family Ligands', *Cell*, vol. 108, no. 3, pp. 383-394.

Lopez-Fraga, M., Fernandez, R., Albar, J.P. & Hahne, M. (2001) 'Biologically active APRIL is secreted following intracellular processing in the Golgi apparatus by furin convertase', *EMBO Rep*, vol. 2, no. 10, pp. 945-951.

Luhrmann, A., Tschernig, T. & Pabst, R. (2002) 'Stimulation of bronchus-associated lymphoid tissue in rats by repeated inhalation of aerosolized lipopeptide MALP-2', *Pathobiology*, vol. 70, no. 5, pp. 266-269.

Luther, S.A., Tang, H.L., Hyman, P.L., Farr, A.G. & Cyster, J.G. (2000) 'Coexpression of the chemokines ELC and SLC by T zone stromal cells and

deletion of the ELC gene in the plt/plt mouse', *Proceedings of the National Academy of Sciences*, vol. 97, no. 23, pp. 12694-12699.

Mackay, F. & Ambrose, C. (2003) 'The TNF family members BAFF and APRIL: the growing complexity', *Cytokine Growth Factor Rev*, vol. 14, no. 3-4, pp. 311-324.

Mackay, F. & Browning, J.L. (2002) 'BAFF: A fundamental survival factor for B cells', *Nat Rev Immunol*, vol. 2, no. 7, pp. 465-475.

Mackay, F., Figgett, W.A., Saulep, D., Lepage, M. & Hibbs, M.L. (2010) 'B-cell stage and context-dependent requirements for survival signals from BAFF and the B-cell receptor', *Immunological Reviews*, vol. 237, no. 1, pp. 205-225.

Mackay, F. & Leung, H. (2006) 'The role of the BAFF/APRIL system on T cell function', *Seminars in Immunology*, vol. 18, no. 5, pp. 284-289.

Mackay, F. & Schneider, P. (2009) 'Cracking the BAFF code', *Nat Rev Immunol*, vol. 9, no. 7, pp. 491-502.

Mackay, F., Schneider, P., Rennert, P. & Browning, J. (2003) 'BAFF AND APRIL: a tutorial on B cell survival', *Annu Rev Immunol*, vol. 21, pp. 231-264.

Mackay, F., Silveira, P. & Brink, R. (2007) 'B cells and the BAFF/APRIL axis: fast-forward on autoimmunity and signaling', *Curr Opin Immunol*, vol. 19, pp. 327 - 336.

Marrack, P., Kappler, J. & Mitchell, T. (1999) 'Type I Interferons Keep Activated T Cells Alive', *The Journal of Experimental Medicine*, vol. 189, no. 3, pp. 521-530.

McNamara, P.S., Flanagan, B.F., Hart, C.A. & Smyth, R.L. (2005) 'Production of Chemokines in the Lungs of Infants with Severe Respiratory Syncytial Virus Bronchiolitis', *Journal of Infectious Diseases*, vol. 191, no. 8, pp. 1225-1232.

McNamara, P.S., Fonceca, A.M., Howarth, D., Correia, J.B., Slupsky, J.R., Trinick, R.E., Al Turaiki, W., Smyth, R.L. & Flanagan, B.F. (2013) 'Respiratory syncytial virus infection of airway epithelial cells, in vivo and in vitro, supports pulmonary antibody responses by inducing expression of the B cell differentiation factor BAFF', *Thorax*, vol. 68, no. 1, pp. 76-81.

McNamara, P.S. & Smyth, R.L. (2002) 'The pathogenesis of respiratory syncytial virus disease in childhood', *British Medical Bulletin*, vol. 61, no. 1, pp. 13-28.

Mellow, T.E., Murphy, P.C., Carson, J.L., Noah, T.L., Zhang, L. & Pickles, R.J. (2004) 'The effect of respiratory synctial virus on chemokine release by differentiated airway epithelium', *Exp Lung Res*, vol. 30, no. 1, pp. 43-57.

Meurman, O., Waris, M. & Hedman, K. (1992) 'Immunoglobulin G antibody avidity in patients with respiratory syncytial virus infection', *J Clin Microbiol*, vol. 30, no. 6, pp. 1479-1484.

Moghaddam, A., Olszewska, W., Wang, B., Tregoning, J.S., Helson, R., Sattentau, Q.J. & Openshaw, P.J.M. (2006) 'A potential molecular mechanism for hypersensitivity caused by formalin-inactivated vaccines', *Nat Med*, vol. 12, no. 8, pp. 905-907.

Moore, P.A., Belvedere, O., Orr, A., Pieri, K., LaFleur, D.W., Feng, P., Soppet, D., Charters, M., Gentz, R., Parmelee, D., Li, Y.L., Galperina, O., Giri, J., Roschke, V., Nardelli, B., Carrell, J., Sosnovtseva, S., Greenfield, W., Ruben, S.M., Olsen, H.S., Fikes, J. & Hilbert, D.M. (1999) 'BLyS: Member of the tumor necrosis factor family and B lymphocyte stimulator', *Science*, vol. 285, no. 5425, pp. 260-263.

Moyron-Quiroz, J.E., Rangel-Moreno, J., Kusser, K., Hartson, L., Sprague, F., Goodrich, S., Woodland, D.L., Lund, F.E. & Randall, T.D. (2004) 'Role of inducible bronchus associated lymphoid tissue (iBALT) in respiratory immunity', *Nat Med*, vol. 10, no. 9, pp. 927-934.

Mukherjee, S., Lindell, D.M., Berlin, A.A., Morris, S.B., Shanley, T.P., Hershenson, M.B. & Lukacs, N.W. (2011) 'IL-17–Induced Pulmonary Pathogenesis during Respiratory Viral Infection and Exacerbation of Allergic Disease', *The American Journal of Pathology*, vol. 179, no. 1, pp. 248-258.

Mukherjee, S. & Lukacs, N. (2013) Innate Immune Responses to Respiratory Syncytial Virus Infection, in L.J. Anderson & B.S. Graham (eds), *Challenges and Opportunities for Respiratory Syncytial Virus Vaccines*, vol. 372, Springer Berlin Heidelberg, pp. 139-154.

Mukhopadhyay, A., Ni, J., Zhai, Y.F., Yu, G.L. & Aggarwal, B.B. (1999) 'Identification and characterization of a novel cytokine, THANK, a (T)under-barNF (H)under-baromologue that activates (A)under-barpoptosis, nuclear factor-kappa B, and c-Jun NH2-terminal (K)under-barinase', *Journal of Biological Chemistry*, vol. 274, no. 23, pp. 15978-15981.

Murphy, B.R., Graham, B.S., Prince, G.A., Walsh, E.E., Chanock, R.M., Karzon, D.T. & Wright, P.F. (1986) 'Serum and nasal-wash immunoglobulin G and A antibody response of infants and children to respiratory syncytial virus F and G glycoproteins following primary infection', *J Clin Microbiol*, vol. 23, no. 6, pp. 1009-1014.

Nair, H., Brooks, W.A., Katz, M., Roca, A., Berkley, J.A., Madhi, S.A., Simmerman, J.M., Gordon, A., Sato, M., Howie, S., Krishnan, A., Ope, M., Lindblade, K.A., Carosone-Link, P., Lucero, M., Ochieng, W., Kamimoto, L., Dueger, E., Bhat, N., Vong, S., Theodoratou, E., Chittaganpitch, M., Chimah, O., Balmaseda, A., Buchy, P., Harris, E., Evans, V., Katayose, M., Gaur, B., O'Callaghan-Gordo, C., Goswami, D., Arvelo, W., Venter, M., Briese, T., Tokarz, R., Widdowson, M.-A., Mounts, A.W., Breiman, R.F., Feikin, D.R., Klugman, K.P., Olsen, S.J., Gessner, B.D., Wright, P.F., Rudan, I., Broor, S., Simões, E.A.F. & Campbell, H. (2011) 'Global burden of respiratory infections due to seasonal influenza in young children: a systematic review and meta-analysis', *The Lancet*, vol. 378, no. 9807, pp. 1917-1930.

Nardelli, B., Belvedere, O., Roschke, V., Moore, P.A., Olsen, H.S., Migone, T.S., Sosnovtseva, S., Carrell, J.A., Feng, P., Giri, J.G. & Hilbert, D.M. (2001) 'Synthesis and release of B-lymphocyte stimulator from myeloid cells', *Blood*, vol. 97, no. 1, pp. 198-204.

Ng, L.G., Sutherland, A.P., Newton, R., Qian, F., Cachero, T.G., Scott, M.L., Thompson, J.S., Wheway, J., Chtanova, T., Groom, J., Sutton, I.J., Xin, C., Tangye, S.G., Kalled, S.L., Mackay, F. & Mackay, C.R. (2004) 'B cell-activating factor belonging to the TNF family (BAFF)-R is the principal BAFF receptor facilitating BAFF costimulation of circulating T and B cells', *J Immunol*, vol. 173, no. 2, pp. 807-817.

Ngo, V.N., Lucy Tang, H. & Cyster, J.G. (1998) 'Epstein-Barr Virus–induced Molecule 1 Ligand Chemokine Is Expressed by Dendritic Cells in Lymphoid Tissues and Strongly Attracts Naive T Cells and Activated B Cells', *The Journal of Experimental Medicine*, vol. 188, no. 1, pp. 181-191.

O'Connor, B.P., Raman, V.S., Erickson, L.D., Cook, W.J., Weaver, L.K., Ahonen, C., Lin, L.-L., Mantchev, G.T., Bram, R.J. & Noelle, R.J. (2004) 'BCMA Is

Essential for the Survival of Long-lived Bone Marrow Plasma Cells', *The Journal of Experimental Medicine*, vol. 199, no. 1, pp. 91-98.

Ogasawara, K., Hida, S., Weng, Y., Saiura, A., Sato, K., Takayanagi, H., Sakaguchi, S., Yokochi, T., Kodama, T., Naitoh, M., De Martino, J.A. & Taniguchi, T. (2002) 'Requirement of the IFN-α/β-induced CXCR3 chemokine signalling for CD8+ T cell activation', *Genes to Cells*, vol. 7, no. 3, pp. 309-320.

Okada, T., Ngo, V.N., Ekland, E.H., Förster, R., Lipp, M., Littman, D.R. & Cyster, J.G. (2002) 'Chemokine Requirements for B Cell Entry to Lymph Nodes and Peyer's Patches', *The Journal of Experimental Medicine*, vol. 196, no. 1, pp. 65-75.

Oliveira, T.F., Freitas, G.R., Ribeiro, L.Z., Yokosawa, J., Siqueira, M.M., Portes, S.A., Silveira, H.L., Calegari, T., Costa, L., Mantese, O.C. & Queiroz, D.A. (2008) 'Prevalence and clinical aspects of respiratory syncytial virus A and B groups in children seen at Hospital de Clinicas of Uberlandia, MG, Brazil', *Memorias do Instituto Oswaldo Cruz*, vol. 103, no. 5, pp. 417-422.

Openshaw, P. (2013) The Mouse Model of Respiratory Syncytial Virus Disease, in L.J. Anderson & B.S. Graham (eds), *Challenges and Opportunities for Respiratory Syncytial Virus Vaccines*, vol. 372, Springer Berlin Heidelberg, pp. 359-369.

Oshansky, C.M., Zhang, W., Moore, E. & Tripp, R.A. (2009) 'The host response and molecular pathogenesis associated with respiratory syncytial virus infection', *Future Microbiol*, vol. 4, no. 3, pp. 279-297.

Ostler, T., Davidson, W. & Ehl, S. (2002) 'Virus clearance and immunopathology by CD8 during infection with respiratory syncytial virus are mediated by IFN-γ ', *European Journal of Immunology*, vol. 32, no. 8, pp. 2117-2123.

Ouyang, W., Kolls, J.K. & Zheng, Y. (2008) 'The biological functions of T helper 17 cell effector cytokines in inflammation', *Immunity*, vol. 28, no. 4, pp. 454-467.

Petty, J.M., Sueblinvong, V., Lenox, C.C., Jones, C.C., Cosgrove, G.P., Cool, C.D., Rai, P.R., Brown, K.K., Weiss, D.J., Poynter, M.E. & Suratt, B.T. (2007) 'Pulmonary Stromal-Derived Factor-1 Expression and Effect on Neutrophil Recruitment during Acute Lung Injury', *The Journal of Immunology*, vol. 178, no. 12, pp. 8148-8157.

Pribul, P.K., Harker, J., Wang, B., Wang, H., Tregoning, J.S., Schwarze, J. & Openshaw, P.J.M. (2008) 'Alveolar Macrophages Are a Major Determinant of Early Responses to Viral Lung Infection but Do Not Influence Subsequent Disease Development', *Journal of Virology*, vol. 82, no. 9, pp. 4441-4448.

Prober, C.G. & Sullender, W.M. (1999) 'Advances in prevention of respiratory syncytial virus infections', *The Journal of Pediatrics*, vol. 135, no. 5, pp. 546-558.

Ramaswamy, M., Shi, L., Varga, S.M., Barik, S., Behlke, M.A. & Look, D.C. (2006) 'Respiratory syncytial virus nonstructural protein 2 specifically inhibits type I interferon signal transduction', *Virology*, vol. 344, no. 2, pp. 328-339.

Rangel-Moreno, J., Carragher, D.M., de la Luz Garcia-Hernandez, M., Hwang, J.Y., Kusser, K., Hartson, L., Kolls, J.K., Khader, S.A. & Randall, T.D. (2011) 'The development of inducible bronchus-associated lymphoid tissue depends on IL-17', *Nat Immunol*, vol. 12, no. 7, pp. 639-646.

Rangel-Moreno, J., Moyron-Quiroz, J., Kusser, K., Hartson, L., Nakano, H. & Randall, T.D. (2005) 'Role of CXC Chemokine Ligand 13, CC Chemokine Ligand (CCL) 19, and CCL21 in the Organization and Function of Nasal-Associated Lymphoid Tissue', *The Journal of Immunology*, vol. 175, no. 8, pp. 4904-4913.

Rangel-Moreno, J., Moyron-Quiroz, J.E., Hartson, L., Kusser, K. & Randall, T.D. (2007) 'Pulmonary expression of CXC chemokine ligand 13, CC chemokine ligand 19, and CC chemokine ligand 21 is essential for local immunity to influenza', *Proc Natl Acad Sci U S A*, vol. 104, no. 25, pp. 10577-10582.

Reed, J.L., Brewah, Y.A., Delaney, T., Welliver, T., Burwell, T., Benjamin, E., Kuta, E., Kozhich, A., McKinney, L., Suzich, J., Kiener, P.A., Avendano, L., Velozo, L., Humbles, A., Welliver, R.C. & Coyle, A.J. (2008) 'Macrophage Impairment Underlies Airway Occlusion in Primary Respiratory Syncytial Virus Bronchiolitis', *Journal of Infectious Diseases*, vol. 198, no. 12, pp. 1783-1793.

Reed, J.L., Welliver, T.P., Sims, G.P., McKinney, L., Velozo, L., Avendano, L., Hintz, K., Luma, J., Coyle, A.J. & Welliver, R.C., Sr. (2009) 'Innate immune signals modulate antiviral and polyreactive antibody responses during severe respiratory syncytial virus infection', *J Infect Dis*, vol. 199, no. 8, pp. 1128-1138.

Reijmers, R.M., Groen, R.W., Kuil, A., Weijer, K., Kimberley, F.C., Medema, J.P., van Kuppevelt, T.H., Li, J.P., Spaargaren, M. & Pals, S.T. (2011) 'Disruption of heparan sulfate proteoglycan conformation perturbs B-cell maturation and APRIL-mediated plasma cell survival', *Blood*, vol. 117, no. 23, pp. 6162-6171.

Richert, L.E., Harmsen, A.L., Rynda-Apple, A., Wiley, J.A., Servid, A.E., Douglas, T. & Harmsen, A.G. (2013) 'Inducible bronchus-associated lymphoid tissue (iBALT) synergizes with local lymph nodes during antiviral CD4+ T cell responses', *Lymphat Res Biol*, vol. 11, no. 4, pp. 196-202.

Rodriguez, B., Valdez, H., Freimuth, W., Butler, T., Asaad, R. & Lederman, M.M. (2003) 'Plasma levels of B-lymphocyte stimulator increase with HIV disease progression', *Aids*, vol. 17, no. 13, pp. 1983-1985.

Roman M., Calhoun, W., Hinton, K., AvendaÑO, L., Simon, V., Escobar, A., Gaggero, A. & DÍAz, P. (1997) 'Respiratory Syncytial Virus Infection in Infants Is Associated with Predominant Th-2-like Response', *American Journal of Respiratory and Critical Care Medicine*, vol. 156, no. 1, pp. 190-195.

Ronni, T., Matikainen, S., Sareneva, T., Melen, K., Pirhonen, J., Keskinen, P. & Julkunen, I. (1997) 'Regulation of IFN-alpha/beta, MxA, 2',5'-oligoadenylate synthetase, and HLA gene expression in influenza A-infected human lung epithelial cells', *The Journal of Immunology*, vol. 158, no. 5, pp. 2363-2374.

Roschke, V., Sosnovtseva, S., Ward, C.D., Hong, J.S., Smith, R., Albert, V., Stohl, W., Baker, K.P., Ullrich, S., Nardelli, B., Hilbert, D.M. & Migone, T.-S. (2002) 'BLyS and APRIL Form Biologically Active Heterotrimers That Are Expressed in Patients with Systemic Immune-Based Rheumatic Diseases', *The Journal of Immunology*, vol. 169, no. 8, pp. 4314-4321.

Rosenberg, H.F., Dyer, K.D. & Domachowske, J.B. (2009) 'Respiratory viruses and eosinophils: Exploring the connections', *Antiviral Research*, vol. 83, no. 1, pp. 1-9.

Rosendahl Huber, S., van Beek, J., de Jonge, J., Luytjes, W. & van Baarle, D. (2014) 'T Cell Responses to Viral Infections - Opportunities for Peptide Vaccination', *Front Immunol*, vol. 5, p. 171.

Rudd, B.D., Smit, J.J., Flavell, R.A., Alexopoulou, L., Schaller, M.A., Gruber, A., Berlin, A.A. & Lukacs, N.W. (2006) 'Deletion of TLR3 Alters the Pulmonary

Immune Environment and Mucus Production during Respiratory Syncytial Virus Infection', *The Journal of Immunology*, vol. 176, no. 3, pp. 1937-1942.

Rutigliano, J.A. & Graham, B.S. (2004) 'Prolonged Production of TNF-α Exacerbates Illness during Respiratory Syncytial Virus Infection', *The Journal of Immunology*, vol. 173, no. 5, pp. 3408-3417.

Saeki, H., Wu, M.T., Olasz, E. & Hwang, S.T. (2000) 'A migratory population of skin-derived dendritic cells expresses CXCR5, responds to B lymphocyte chemoattractant in vitro, and co-localizes to B cell zones in lymph nodes in vivo', *Eur J Immunol*, vol. 30, no. 10, pp. 2808-2814.

Sano, H., Nagai, K., Tsutsumi, H. & Kuroki, Y. (2003) 'Lactoferrin and surfactant protein A exhibit distinct binding specificity to F protein and differently modulate respiratory syncytial virus infection', *European Journal of Immunology*, vol. 33, no. 10, pp. 2894-2902.

Scapini, P., Nardelli, B., Nadali, G., Calzetti, F., Pizzolo, G., Montecucco, C. & Cassatella, M.A. (2003) 'G-CSF–stimulated Neutrophils Are a Prominent Source of Functional BLyS', *The Journal of Experimental Medicine*, vol. 197, no. 3, pp. 297-302.

Schlender, J., Walliser, G., Fricke, J. & Conzelmann, K.K. (2002) 'Respiratory syncytial virus fusion protein mediates inhibition of mitogen-induced T-cell proliferation by contact', *J Virol*, vol. 76, no. 3, pp. 1163-1170.

Schneider, P. (2010) The Beautiful Structures of BAFF, APRIL, and Their Receptors, in M.P. Cancro (ed.), *BLyS Ligands and Receptors*, Humana Press, pp. 1-18.

Schneider, P., MacKay, F., Steiner, V., Hofmann, K., Bodmer, J.-L., Holler, N., Ambrose, C., Lawton, P., Bixler, S., Acha-Orbea, H., Valmori, D., Romero, P., Werner-Favre, C., Zubler, R.H., Browning, J.L. & Tschopp, J. (1999) 'BAFF, a Novel Ligand of the Tumor Necrosis Factor Family, Stimulates B Cell Growth', *The Journal of Experimental Medicine*, vol. 189, no. 11, pp. 1747-1756.

Schulz, C., Farkas, L., Wolf, K., KrÄTzel, K., Eissner, G. & Pfeifer, M. (2002) 'Differences in LPS-Induced Activation of Bronchial Epithelial Cells (BEAS-2B) and Type II-Like Pneumocytes (A-549)', *Scandinavian Journal of Immunology*, vol. 56, no. 3, pp. 294-302.

Schutte, B.C. & McCray, P.B. (2002) 'β-Defensins in lung host defense', *Annual Review of Physiology*, vol. 64, no. 1, pp. 709-748.

Shu, H.B., Hu, W.H. & Johnson, H. (1999) 'TALL-1 is a novel member of the TNF family that is down-regulated by mitogens', *Journal of Leukocyte Biology*, vol. 65, no. 5, pp. 680-683.

Singleton, R., Etchart, N., Hou, S. & Hyland, L. (2003) 'Inability to evoke a long-lasting protective immune response to respiratory syncytial virus infection in mice correlates with ineffective nasal antibody responses', *J Virol*, vol. 77, no. 21, pp. 11303-11311.

Spann, K.M., Tran, K.-C., Chi, B., Rabin, R.L. & Collins, P.L. (2004) 'Suppression of the Induction of Alpha, Beta, and Gamma Interferons by the NS1 and NS2 Proteins of Human Respiratory Syncytial Virus in Human Epithelial Cells and Macrophages', *Journal of Virology*, vol. 78, no. 8, pp. 4363-4369.

Spann, K.M., Tran, K.C. & Collins, P.L. (2005) 'Effects of Nonstructural Proteins NS1 and NS2 of Human Respiratory Syncytial Virus on Interferon Regulatory Factor 3, NF-κB, and Proinflammatory Cytokines', *Journal of Virology*, vol. 79, no. 9, pp. 5353-5362.

Stavnezer, J. & Amemiya, C.T. (2004) 'Evolution of isotype switching', *Seminars in Immunology*, vol. 16, no. 4, pp. 257-275.

Stein, J.V., Lopez-Fraga, M., Elustondo, F.A., Carvalho-Pinto, C.E., Rodriguez, D., Gomez-Caro, R., De Jong, J., Martinez, A.C., Medema, J.P. & Hahne, M. (2002) 'APRIL modulates B and T cell immunity', *J Clin Invest*, vol. 109, no. 12, pp. 1587-1598.

Tangye, S. & Fulcher, D. (2010) The Role of BAFF and APRIL in Regulating Human B-Cell Behaviour: Implications for Disease Pathogenesis, in M.P. Cancro (ed.), *BLyS Ligands and Receptors*, Humana Press, pp. 195-220.

Tangye, S.G., Bryant, V.L., Cuss, A.K. & Good, K.L. (2006) 'BAFF, APRIL and human B cell disorders', *Seminars in Immunology*, vol. 18, no. 5, pp. 305-317.

Taylor, G., Stott, E.J., Hughes, M. & Collins, A.P. (1984) 'Respiratory syncytial virus infection in mice', *Infection and Immunity*, vol. 43, no. 2, pp. 649-655.

Tekkanat, K.K., Maassab, H.F., Cho, D.S., Lai, J.J., John, A., Berlin, A., Kaplan, M.H. & Lukacs, N.W. (2001) 'IL-13-Induced Airway Hyperreactivity During

Respiratory Syncytial Virus Infection Is STAT6 Dependent', *The Journal of Immunology*, vol. 166, no. 5, pp. 3542-3548.

Teng, M.N., Whitehead, S.S. & Collins, P.L. (2001) 'Contribution of the Respiratory Syncytial Virus G Glycoprotein and Its Secreted and Membrane-Bound Forms to Virus Replication in Vitro and in Vivo', *Virology*, vol. 289, no. 2, pp. 283-296.

Thomas, L.H., Friedland, J.S., Sharland, M. & Becker, S. (1998) 'Respiratory Syncytial Virus-Induced RANTES Production from Human Bronchial Epithelial Cells Is Dependent on Nuclear Factor-κB Nuclear Binding and Is Inhibited by Adenovirus-Mediated Expression of Inhibitor of κBα', *The Journal of Immunology*, vol. 161, no. 2, pp. 1007-1016.

Toubi, E., Gordon, S., Kessel, A., Rosner, I., Rozenbaum, M., Shoenfeld, Y. & Zuckerman, E. (2006) 'Elevated serum B-Lymphocyte activating factor (BAFF) in chronic hepatitis C virus infection: association with autoimmunity', *J Autoimmun*, vol. 27, no. 2, pp. 134-139.

Treml, J., Hao, Y., Stadanlick, J. & Cancro, M. (2009) 'The BLyS Family: Toward a Molecular Understanding of B Cell Homeostasis', *Cell Biochemistry and Biophysics*, vol. 53, no. 1, pp. 1-16.

Trento, A., Viegas, M., Galiano, M., Videla, C., Carballal, G., Mistchenko, A.S. & Melero, J.A. (2006) 'Natural History of Human Respiratory Syncytial Virus Inferred from Phylogenetic Analysis of the Attachment (G) Glycoprotein with a 60-Nucleotide Duplication', *Journal of Virology*, vol. 80, no. 2, pp. 975-984.

Trinchieri, G. (2010) 'Type I interferon: friend or foe?', *The Journal of Experimental Medicine*, vol. 207, no. 10, pp. 2053-2063.

Tripp, R.A., Jones, L.P., Haynes, L.M., Zheng, H., Murphy, P.M. & Anderson, L.J. (2001) 'CX3C chemokine mimicry by respiratory syncytial virus G glycoprotein', *Nat Immunol*, vol. 2, no. 8, pp. 732-738.

Trombetta, E.S. & Mellman, I. (2005) 'CELL BIOLOGY OF ANTIGEN PROCESSING IN VITRO AND IN VIVO', *Annual Review of Immunology*, vol. 23, no. 1, pp. 975-1028.

Tulic, M.K., Hurrelbrink, R.J., Prêle, C.M., Laing, I.A., Upham, J.W., Le Souef, P., Sly, P.D. & Holt, P.G. (2007) 'TLR4 polymorphisms mediate impaired

responses to respiratory syncytial virus and lipopolysaccharide', *Journal of Immunology*, vol. 179, no. 1, pp. 132-140.

van der Strate, B.W.A., Postma, D.S., Brandsma, C.-A., Melgert, B.N., Luinge, M.A., Geerlings, M., Hylkema, M.N., van den Berg, A., Timens, W. & Kerstjens, H.A.M. (2006) 'Cigarette Smoke–induced Emphysema', *American Journal of Respiratory and Critical Care Medicine*, vol. 173, no. 7, pp. 751-758.

van Drunen Littel-van den Hurk, S. & Watkiss, E.R. (2012) 'Pathogenesis of respiratory syncytial virus', *Current Opinion in Virology*, vol. 2, no. 3, pp. 300-305.

Vareille, M., Kieninger, E., Edwards, M.R. & Regamey, N. (2011) 'The Airway Epithelium: Soldier in the Fight against Respiratory Viruses', *Clinical Microbiology Reviews*, vol. 24, no. 1, pp. 210-229.

Varga, S. & Braciale, T. (2013) The Adaptive Immune Response to Respiratory Syncytial Virus, in L.J. Anderson & B.S. Graham (eds), *Challenges and Opportunities for Respiratory Syncytial Virus Vaccines*, vol. 372, Springer Berlin Heidelberg, pp. 155-171.

Vicario, M., Blanchard, C., Stringer, K.F., Collins, M.H., Mingler, M.K., Ahrens, A., Putnam, P.E., Abonia, J.P., Santos, J. & Rothenberg, M.E. (2010) 'Local B cells and IgE production in the oesophageal mucosa in eosinophilic oesophagitis', *Gut*, vol. 59, no. 01, pp. 12-20.

Vincent, F.B., Saulep-Easton, D., Figgett, W.A., Fairfax, K.A. & Mackay, F. (2013) 'The BAFF/APRIL system: emerging functions beyond B cell biology and autoimmunity', *Cytokine Growth Factor Rev*, vol. 24, no. 3, pp. 203-215.

Vora, K.A., Wang, L.C., Rao, S.P., Liu, Z.-Y., Majeau, G.R., Cutler, A.H., Hochman, P.S., Scott, M.L. & Kalled, S.L. (2003) 'Cutting Edge: Germinal Centers Formed in the Absence of B Cell-Activating Factor Belonging to the TNF Family Exhibit Impaired Maturation and Function', *The Journal of Immunology*, vol. 171, no. 2, pp. 547-551.

Walsh, E. & Falsey, A.R. (2004) 'Humoral and Mucosal Immunity in Protection from Natural Respiratory Syncytial Virus Infection in Adults', *Journal of Infectious Diseases*, vol. 190, no. 2, pp. 373-378.

Wang, H., Marsters, S.A., Baker, T., Chan, B., Lee, W.P., Fu, L., Tumas, D., Yan, M., Dixit, V.M., Ashkenazi, A. & Grewal, I.S. (2001) 'TACI-ligand

interactions are required for T cell activation and collagen-induced arthritis in mice', *Nat Immunol*, vol. 2, no. 7, pp. 632-637.

Wang, S.-Z. & Forsyth, K.D. (2000) 'The interaction of neutrophils with respiratory epithelial cells in viral infection', *Respirology*, vol. 5, no. 1, pp. 1-9.

Wang, X., Yuling, H., Yanping, J., Xinti, T., Yaofang, Y., Feng, Y., Ruijin, X., Li, W., Lang, C., Jingyi, L., Zhiqing, T., Jingping, O., Bing, X., Li, Q., Chang, A.E., Sun, Z., Youxin, J. & Jinquan, T. (2007) 'CCL19 and CXCL13 Synergistically Regulate Interaction between B Cell Acute Lymphocytic Leukemia CD23+CD5+ B Cells and CD8+ T Cells', *The Journal of Immunology*, vol. 179, no. 5, pp. 2880-2888.

Waris, M.E., Tsou, C., Erdman, D.D., Zaki, S.R. & Anderson, L.J. (1996) 'Respiratory synctial virus infection in BALB/c mice previously immunized with formalin-inactivated virus induces enhanced pulmonary inflammatory response with a predominant Th2-like cytokine pattern', *Journal of Virology*, vol. 70, no. 5, pp. 2852-2860.

Wark, P.A.B., Johnston, S.L., Bucchieri, F., Powell, R., Puddicombe, S., Laza-Stanca, V., Holgate, S.T. & Davies, D.E. (2005) 'Asthmatic bronchial epithelial cells have a deficient innate immune response to infection with rhinovirus', *The Journal of Experimental Medicine*, vol. 201, no. 6, pp. 937-947.

Welliver, R., Sr. (2008) 'The Immune Response to Respiratory Syncytial Virus Infection: Friend or Foe?', *Clinical Reviews in Allergy & Immunology*, vol. 34, no. 2, pp. 163-173.

Welliver, T.P., Garofalo, R.P., Hosakote, Y., Hintz, K.H., Avendano, L., Sanchez, K., Velozo, L., Jafri, H., Chavez-Bueno, S., Ogra, P.L., McKinney, L., Reed, J.L. & Welliver, R.C. (2007) 'Severe Human Lower Respiratory Tract Illness Caused by Respiratory Syncytial Virus and Influenza Virus Is Characterized by the Absence of Pulmonary Cytotoxic Lymphocyte Responses', *Journal of Infectious Diseases*, vol. 195, no. 8, pp. 1126-1136.

Wiley, J.A., Richert, L.E., Swain, S.D., Harmsen, A., Barnard, D.L., Randall, T.D., Jutila, M., Douglas, T., Broomell, C., Young, M. & Harmsen, A. (2009) 'Inducible bronchus-associated lymphoid tissue elicited by a protein cage nanoparticle enhances protection in mice against diverse respiratory viruses', *PLoS One*, vol. 4, no. 9, p. e7142.

Wolf, A.I., Mozdzanowska, K., Quinn, W.J., 3rd, Metzgar, M., Williams, K.L., Caton, A.J., Meffre, E., Bram, R.J., Erickson, L.D., Allman, D., Cancro, M.P. & Erikson, J. (2011) 'Protective antiviral antibody responses in a mouse model of influenza virus infection require TACI', *J Clin Invest*, vol. 121, no. 10, pp. 3954-3964.

Wood, P. (2011) *Understanding Immunology*, Prentice Hall/Pearson.

Wu, M.-T. & Hwang, S.T. (2002) 'CXCR5-Transduced Bone Marrow-Derived Dendritic Cells Traffic to B Cell Zones of Lymph Nodes and Modify Antigen-Specific Immune Responses', *The Journal of Immunology*, vol. 168, no. 10, pp. 5096-5102.

Xiao, Y., Motomura, S., Deyev, V. & Podack, E.R. (2011) 'TNF superfamily member 13, APRIL, inhibits allergic lung inflammation', *European Journal of Immunology*, vol. 41, no. 1, pp. 164-171.

Yamaguchi, N., Fujimori, Y., Fujibayashi, Y., Kasumoto, I., Okamura, H., Nakanishi, K. & Hara, H. (2005) 'Interferon-gamma production by human cord blood monocyte-derived dendritic cells', *Annals of Hematology*, vol. 84, no. 7, pp. 423-428.

Yu, G., Boone, T., Delaney, J., Hawkins, N., Kelley, M., Ramakrishnan, M., McCabe, S., Qiu, W.R., Kornuc, M., Xia, X.Z., Guo, J., Stolina, M., Boyle, W.J., Sarosi, I., Hsu, H., Senaldi, G. & Theill, L.E. (2000) 'APRIL and TALL-I and receptors BCMA and TACI: system for regulating humoral immunity', *Nat Immunol*, vol. 1, no. 3, pp. 252-256.

Yu, P., Wang, Y., Chin, R.K., Martinez-Pomares, L., Gordon, S., Kosco-Vibois, M.H., Cyster, J. & Fu, Y.-X. (2002) 'B Cells Control the Migration of a Subset of Dendritic Cells into B Cell Follicles Via CXC Chemokine Ligand 13 in a Lymphotoxin-Dependent Fashion', *The Journal of Immunology*, vol. 168, no. 10, pp. 5117-5123.

Zajac, A.J. & Harrington, L.E. (2008) Immune Response to Viruses: Cell-Mediated Immunity, in B.W.J. Mahy & M.H.V.V. Regenmortel (eds), *Encyclopedia of Virology (Third Edition)*, Academic Press, Oxford, pp. 70-77.

Zheng, S., De, B.P., Choudhary, S., Comhair, S.A.A., Goggans, T., Slee, R., Williams, B.R.G., Pilewski, J., Haque, S.J. & Erzurum, S.C. (2003) 'Impaired Innate Host Defense Causes Susceptibility to Respiratory Virus Infections in Cystic Fibrosis', *Immunity*, vol. 18, no. 5, pp. 619-630.

Zhukovsky, E.A., Lee, J.-O., Villegas, M., Chan, C., Chu, S. & Mroske, C. (2004) 'TNF ligands (communication arising): Is TALL-1 a trimer or a virus-like cluster?', *Nature*, vol. 427, no. 6973, pp. 413-414.

Zlotnik, A., Burkhardt, A.M. & Homey, B. (2011) 'Homeostatic chemokine receptors and organ-specific metastasis', *Nat Rev Immunol*, vol. 11, no. 9, pp. 597-606.

Zlotnik, A., Morales, J. & Hedrick, J.A. (1999) 'Recent advances in chemokines and chemokine receptors', *Crit Rev Immunol*, vol. 19, no. 1, pp. 1-47.

APPENDIX

- **Published abstracts**

W. Alturaiki, A. Fonceca, C. Broughton, P. S. McNamara & B. F. Flanagan (2011). *Inflammatory cytokine induced expression of* of BAFF and APRIL by BEAS-2B airway epithelial cells**. (**British Society for Immunology Congress, Liverpool, UK from 5-8 December 2011). Blackwell Publishing Ltd, Immunology, **137** (Suppl. 1), 185_772.

W. Alturaiki, A. Fonceca, C. Broughton, P. S. McNamara & B. F. Flanagan (2012). *In vitro*, RSV infection of BEAS-2B airway epithelial cells induced expression of BAFF and APRIL. (European Congress of Immunology 5-8 September 2012 Glasgow, UK). Immunology, 137 issue (Suppl. 1), P0090

W. Alturaiki, A. McFarlane, P. Fitch, J. Slupsky, P. McNamara, J. Schwarze & B. Flanagan (2013). B cell differentiation factor BAFF and chemokine CXCL13 are expressed in a murine model of human respiratory syncytial virus infection. (British Society for Immunology Congress, Liverpool, UK from 2-5 December 2013). Immunology, 140, issue (Suppl.1), December 2013

W. Alturaiki, A. McFarlane, P. Fitch, J. Slupsky, P. McNamara, J. Schwarze & B. Flanagan (2013). Expression of the B cell differentiation factor BAFF and chemokine CXCL13 in a murine model of human respiratory syncytial virus infection. (European Respiratory Society Annual Congressin 7-11 September 2013 Barcelona, Spain). European Respiratory Journal.P3880

- **Paper published**

McNamara, P.S., Fonceca, A.M., Howarth, D., Correia, J.B., Slupsky, J.R., Trinick, R.E., Al Turaiki, W., Smyth, R.L. & Flanagan, B.F. (2013) 'Respiratory syncytial virus infection of airway epithelial cells, in vivo and in vitro, supports pulmonary antibody responses by inducing expression of the B cell differentiation factor BAFF', *Thorax*, vol. 68, no. 1, pp. 76-81.